Computational Design Analysis of Height Scenarios in Residential High-rise under BENG 2020

Stephanie Moumdjian
4907663

Computational Design Analysis of Height Scenarios in Residential High-rise under BENG 2020

July 8th, 2020

Author
Stephanie Moumdjian | 4907663

Main Mentor
Dr. Michela Turrin
AE+T | Design Informatics

Second Mentor
Dr. Regina Bokel
AE+T | Building Physics

Delegate of the Board of Examiners
Dr. Diego Andres Sepulveda Carmona
Ir. Huib Plomp

MSc. Architecture, Urbanism, and Building Sciences
Building Technology Track

TU Delft

Abstract

In the Netherlands, the building sector accounts for more than one third of the total primary energy consumption. In response, new regulations, BENG 2020, are implemented and applied to all new constructions as of the 1st of July 2020. Regarding the high-rise typology that is known for its extensive energy consumption, those regulations present a constraint to its height increment. Despite being a potential solution to the shortage in the housing sector, residential apartment high-rises still make up for a minimal part of the country's skyline. The aim of this research is to investigate whether the regulations turn into a limitation to the target height despite the implementation of optimal design solutions.

The performance of a building is an outcome of the environmental conditions, the context, the early stage and the facade design. Under the large number of possible combinations, and being interrelated, the impact of different design scenarios of a residential high-rise in the temperate climate are evaluated regarding the energy performance, the energy loads and the user's thermal comfort. With a computational methodology of work using parametric modeling in Grasshopper, energy simulation in plug-ins and modeFRONTIER platform, the setting of an integrated workflow provides the tool for the exploration and optimization of the parameters.

Based on the near-optimal final design, a gradual height increment is performed on the residential high-rise that is marked by limitations at two different levels under both of the primary fossil usage BENG 2 with 49.25 kWh/m2 and the energy generation BENG 3 with 40.2%. To serve the high-rise typology in achieving the target height of 160 meters, amendments to those regulations are proposed according to the building's volume, envelope surface and height. Based on the optimization results, additional design guidelines are provided to serve architects in achieving a closer ranking to the BENG indicators for residential high-rises.

Key words: computational design, optimization, parametric design, high-rise; BENG, residential, facade design, temperate climate

Acknowledgement

As my two years master program at TuDelft comes to an end, I have been exposed to a lot of experiences in both the cultural and educational environment. I am grateful for all the knowledge grabbed that will serve me in my personal and professional life.

Working on this thesis has been the best part of the master as I have pushed my limits and developed new skills related to the architectural industry. This whole process would not have been possible without the contribution and help of many people to whom I am very grateful.

I would like to firstly thank my first mentor Dr. Michela Turrin who fascinated me with her knowledge in Design Informatics since I met her which motivated me to dive deeper in the optimization world that turned into a passion eventually. You have been very supportive and informative in finding solutions, guiding me in tasks and reaching the outcome of this research. I am also glad to have Dr. Regina Bokel as my second mentor during the whole process. Your expertise in the Building Physics field provided me with very constructive feedback and helped me acquire a new approach for observing and analyzing information under a different angle. Thank you both for the unconditional help and guidance through this journey. It has been an honor to be under both of your tutorships.

Special thanks to the ESTECO company providing me with a license for modeFRONTIER, during the coronavirus outbreak that affected my work process, and the instant response from the help center for all the technical issues during the last months.

I would like to mainly thank my parents, Jacques and Patricia, who gave me the great opportunity to study at this university, believing in me and accomplish all the goals I have set in my life. Thank you for putting me as a priority in your life and supporting me through the hard times. Last but not least, I would like to thank my family away from home; Kiana, Grammatiki, Iro and Qiao for being present for each other, socially and mentally, and surviving the stressful moments.

An invaluable thank to a special person, Micheal Douglas, for being the main motivation in my decision to come to TuDelft, and pushing my limits by asking myself

“ What would Micheal do in this situation ? ”

Contents

1 Introduction

Urbanization

By 2030, around 60% of the world's population is expected to live in urban areas. By 2050, this number is predicted to reach 80% (Ali & Al-Khodmany, 2012). With an increase of the urban population, the demand in the housing sector will keep growing exponentially. Providing accommodation to supply such large demand is one of the main challenges that urban cities will face in the near future, if not already happening. In the Netherlands, the housing supply is currently short (Ministerie van Algemene Zaken, 2015). Constructing horizontally in the Dutch landscape is being more and more limited due to restrictions on the land availability, environmental and health purpose, where the necessity of building vertically and upward should be reconsidered (Ali & Al-Khodmany, 2012).

Energy Use of High-rises

With the increasing housing demand, and the lack of supply in the Netherlands, the development of tall buildings can respond to the growth of the urban population. Perceived as energy consuming and non-environmental friendly, the trend of high-rises is still a very unpopular sector in the Dutch skyline. Studies have shown an increase in the CO_2 emissions of 67% in the shift from a low-rise (for ≤ 5 storeys) to a high-rise (> 10 storeys) due to a rise in the mean electricity and fossil fuel use by 77% and 20% respectively, translating into a gradual growth of 2.4% and 2.9% respectively for each additional storey (Godoy-Shimizu et al., 2018).

Regulations in the Netherlands

The Netherlands has implemented a new plan to regulate the energy consumption of the building sector. As of 2020, all new constructions should meet the BENG regulation that involves 3 requirements related to the energy demand and energy generation. Many complaints have been raised stating the lack of feasibility to reach considerable height in a building under those regulations benchmarks.

Thus, this problem requires the investigation on the performance of a residential high-rise in the Netherlands under BENG 2020 regulations, leading to the following research question:

Research Question

RQ. Based on computational optimization, to which extent are BENG regulations a constraint to the construction of a residential high-rise in the Netherlands, and eventually what amendments can be proposed to adapt the desired height to the performance?

Sub-questions will help answer this question and reach the goal:

SQ.1. Where does the limit in height increment of a residential high-rise stand until the BENG regulations are no longer satisfied?

SQ.2. Then, which of the 3 BENG regulations is responsible for this limitation in height increment?

SQ.3. How does the energy performance of the residential high-rise vary in relation to addition of floors, and how does it affect the BENG indicators?

SQ.4. What amendments can be proposed to improve the BENG regulations to achieve the desired high-rise height?

Methodology

First, from the background information, the problem statement and the main research question are defined with sub-questions. Part of the literature review highlights the nZEB and BENG 2020 regulations to be applied in the Netherlands, specifically on the high-rise typology. Under the current situation of the housing sector shortage, the focus is shifted on the residential function and led to addressing the design of an apartment high-rise.

Following, from the Dutch building decree RVO and regulations, the referential apartment plan layout used in the Netherlands is selected, as well as the target height of the high-rise according to its skyline, to conduct the application phase of this research.

Prior to selecting parameters, the climatic factors are analyzed from peer reviewed journal papers and academic research projects in order to establish a relationship between the design parameters that should be evaluated and their impact on the performance of a high-rise. Part of those parameters are related to the early design stage and others to the facade. Their variable ranges and benchmarks are then set according to literature information, the Dutch building regulations Bouwbesluit as well as the user's comfort.

In the application phase, with the platform of Grasshopper, and several plug-ins such as Honeybee and Ladybug, an integrated workflow is created consisting of several parts; the building parametric modeling, the parameters and variables, the simulation and the energy data calculation, additionally to the design exploration and the optimization of the multi-objective design within modeFRONTIERv2019. The workflow serves as the tool to analyze the high-rise performance in parallel to the height increment and under the changing micro-climate conditions. The outcome provides a gap filling knowledge of the relationship between the parameters, their impacts on one another, and the building performance.

In the first part of the research, the early design stage parameters, involving the geometry compactness and the orientation, are evaluated according to the energy performance, BENG regulations and comfort level, on the total high-rise height. In the second phase, the impact of the site context on the building performance and the regulations is evaluated by using different surrounding heights. Lastly, the envelope parameters are assessed from which the window-to-wall ratio, glazing types, shading systems and energy generating system. The parameters variables are tested according to the target height of the residential high-rise in regard of the BENG requirements and the user's comfort.

The outcome of this study indicates the different energy loads performance in parallel to the height increment, as well as the maximum height of the high-rise that can be reached under the BENG benchmarks which occur at different levels. To respond to these constraints, suggestions of amendments of the BENG are proposed in relation to the building's height to serve the high-rise typology. Additional guidelines are developed, based on the optimization results for the early design stage, the façade parameters and the site context to achieve closed ranking to the BENG 2020.

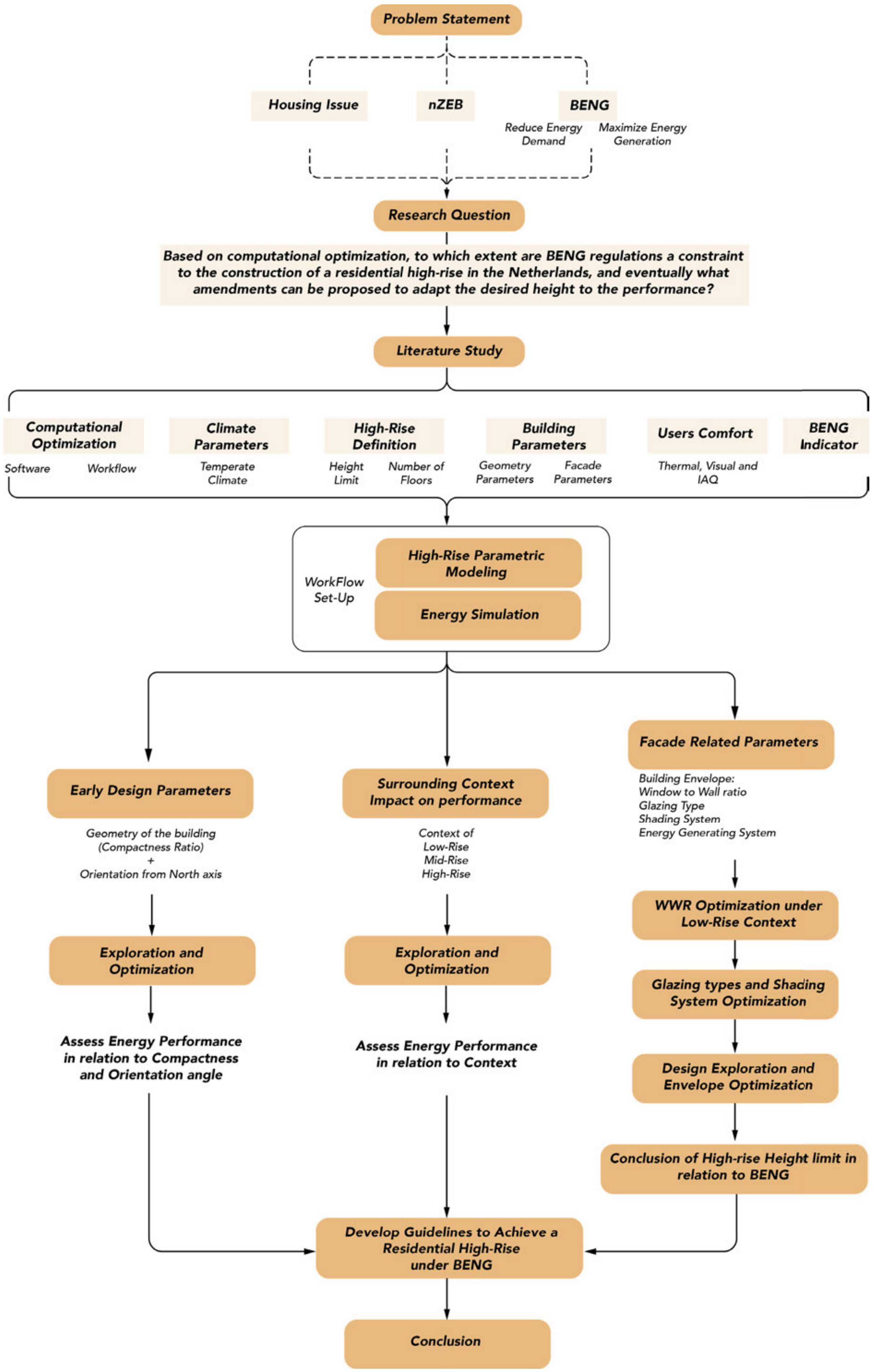

Figure 1 *Scheme of research methodology*

2 Literature Review

2.1. Regulations in the Netherlands: nZEB & BENG

Buildings account for around 40% of energy consumption in Europe, and for 36% of the CO2 emissions (European Commission, 2020). Around 80 to 90% of which is associated with the operational energy of the building, compared to its initial embodied energy estimated to only 10 to 20% (Ramesh, Prakash, & Shukla, 2010).

In the Netherlands, the building sector alone accounts for around one third of the total primary energy. According to the Netherlands Central Bureau of Statistics CBS 2019, natural gas and electricity make up for most of the usage (CBS, 2019), required for the indoor comfort through heating, cooling, ventilation, water heating and electrical devices (Mlecnik, 2013).

Facing the high energy consumption of the building industry, the necessity to shift all construction to "Nearly Zero Energy Buildings (nZEB)" is initiated by the European Energy Performance of Buildings Directive (EPBD).

In response, each European country established its own regulations to comply with a new generation of nZEB buildings starting from 2020. Therefore, in the Netherlands, a new plan of requirements was launched; the BENG 2020 which stands for "Nearly Zero Energy Buildings'', translated from the Dutch "Bijna Energieneutrale Gebouwen" (RVO, 2019).

2.1.1. nZEB General Requirements

The nZEB is defined as a building of high energy performance that utilizes mostly renewable energy resources, from on-site or nearby sources, to make up for the low energy demand (European Commission, 2020). Despite the introduction of these principles, the EDPB does not set a plan of benchmarks or limitations of energy performance to designate a nZEB. Thus, the Netherlands has launched its own regulations to meet the nZEB plan, known as BENG.

2.1.2. BENG Regulations

In previous years, the Energy Performance Coefficient (EPC) was used to evaluate the building's energy performance in the Netherlands (RVO, 2019).

With the established BENG regulations, both residential and commercial buildings that hold the license from the 1st of July 2020 should comply with the new set of benchmarks (RVO, 2019). Due to climate change, higher outside temperatures are being used to determine the building's performance and the benchmarks, necessitating the application of a new method (NTA 8800) that is adapted to the climate data of 2018 (RVO, 2019).

The plan is based on the Trias Energetica concept introduced in 1996 by Lysen (RVO, 2019). It is a 3-step strategy referred to as a guide when designing energy efficient buildings. Its model follows the following chronological order (Figure 2):

1. Limit the energy demand, by avoiding the use of energy with efficient method

2. Use renewable energy sources in the place of finite (primary) fossil energy

3. Use those finite (primary) energy sources efficiently

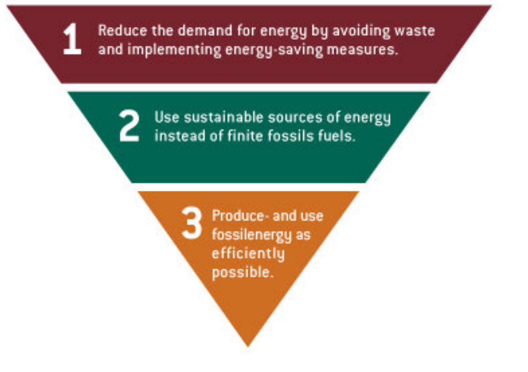

Figure 2 *Trias Energetica Strategy (Source: Eurima, 2019)*

Following this strategy, 3 BENG indicators are defined according to the building function (RVO, 2019). For a residential apartment, the requirements of the energy performance are reported in Table 1.

The BENG 1 implies a reduction of the energy demand by setting the maximum amount of energy for heating and cooling to be used, expressed in kWh per usable area (m²) per year (kWh/m².yr). This indicator depends on the shape of the building, thus the compactness, calculated by the ratio of the Loss Surface Area (A_{ls}) to the Usable Floor Area (A_g). In addition to the shape, it takes into consideration the orientation, and the envelope design that includes the glazing ratio, the insulation properties, the airtightness and thermal bridges. Aside, the values of BENG 1 are given for a "neutral" ventilation system (RVO, 2019).

As for BENG 2, it indicates the maximum allowed primary (finite) fossil energy to be used in an efficient and smart way, expressed in kWh per usable area (m²) per year (kWh/m².yr), and only if really needed, otherwise, it should be compensated by the renewable energy sources. The primary fossil energy consists of the sum of energy for heating, cooling, electrical lighting, ventilation and water heating. For the case of a residential function, the energy generated by PV panels or other sources is deducted from the primary energy use.
Contrary to the calculation of the energy demand of BENG 1, the primary fossil energy use of BENG 2 includes system losses (such as pipe losses during heating), auxiliary energy (such as pumps) and the efficiency of the energy generators (such as the central heating boiler) (RVO, 2019).

Housing Function	BENG 1 Energy Demand [kWh/m².yr]	BENG 2 Primary Fossil Energy Use [kWh/m².yr]	BENG 3 Share of Renewable Energy [%]
Residential Building	If $A_{ls}/A_g \leq 1.83$ BENG 1 ≤ 65	≤ 50	≥ 40
	If $1.83 < A_{ls}/A_g \leq 3.0$ BENG 1 ≤ 55 + 30 *(A_{ls}/A_g -1.5)		
	If $A_{ls}/A_g > 3.0$ BENG 1 ≤ 100 + 50 *(A_{ls}/A_g -3.0)		

Table 1 *BENG indicators for the residential apartment function (Source: RVO, 2019 adapted and translated from the Dutch version of BENG-eisen voor woongebouw appartementen)*

The last indicator BENG 3 indicates the minimum amount of renewable energy to be produced to meet the building energy demand, expressed in (%). The share of renewable energy is determined by dividing the amount of renewable energy by the total sum of both the renewable energy and primary fossil energy use (RVO, 2019).

Referring to Graph 1, the benchmark of BENG 1 is related to the design decision of the building geometry, where less compact shapes are provided with a larger margin of energy demand. However, the determination of BENG 2 and BENG 3 values do not adapt to either the geometry nor the height.

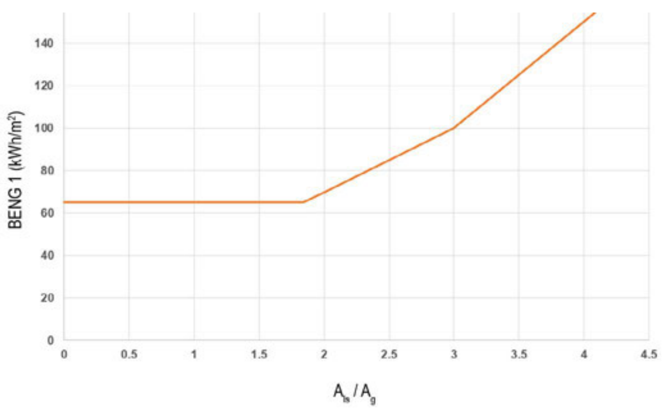

Graph 1 *Relationship between BENG 1 and the ratio of A_{ls}/A_g*

TO-Juli

Due to the increasing risk of overheating during the summer period, and to provide satisfactory comfort, a maximum allowable indoor temperature of 26°C is set to minimize the cooling demand of BENG 1 (RVO, 2019). According to NTA 8800, the TO-juli (TO hours) should not exceed a total of 450 hours per year of an indoor temperature above 26°C for the entire household.

2.1.3. Review of BENG and its implementation

With the implementation of those regulations, part of the building industry is affected. It was found in practice that the benchmarks present limitations to the construction of certain building types, such as high-rise, specifically located in dense urban areas.

A letter concerning the draft decision amending the 2012 Building Decree for new nZEB constructions requested the reconsideration of some of the indicators values being unsuitable to the housing sector (De minister van Binnenlandse Zaken en Koninkrijksrelaties, 2019). Quote on quote, it was stated, "In addition, high buildings were found not to meet the BENG 3 requirement (the share of renewable energy)" (translated from Dutch) (De minister van Binnenlandse Zaken en Koninkrijksrelaties, 2019).

Based on further research done by Peutz (2018) and Mobius Consult (2017), only part of these constraints were supported by making the requirement for BENG 1 partly dependent on the geometry ratio. However, most of the data are related to low and mid-rises, leaving a questionable gap about the performance of high-rises, and the other indicators values.

2.1.4. Previous Research and Results

Compared to low-rises, it is harder for high-rises to fit and meet the requirement of energy generation of BENG 3 as the surface area of the roof is relatively small, despite the presence of the facade (Raji et al., 2017). Also, the calculation method of the indicators are related, where a change in BENG 3 indicator always leads to a variation of the BENG 2 indicator.

Following the strategy of the Trias Energetica and the BENG indicators orders, the improvement of the energy performance refers to minimizing the energy demand prior to the implementation of renewable energy. Considering that the BENG 1 indicator implies the passive design strategy, and the BENG 3 indicator revolves around active design solutions, those two indicators should be designed and analyzed simultaneously to result in the most efficient solution.
As an example, the energy performance can differ drastically when balancing the provided area on the facade to balance between the glazing-to-wall ratio and the energy generating system. One allows more natural daylight to the internal space while risking overheating, whereas the other generates renewable energy on site, if given enough surface area. Thus, the optimization methodology allows the balance between both passive and active related parameters to reach an integrated approach to maximize energy performance.

In a previous research on the energy performance of a nZEB residential high-rise in the Netherlands, an optimization of the facade was carried out on a case study to verify the requirements of the BENG regulations. The resulting data, shown in Table 2, were extracted from a floor in the lower part, at 25 meters high, and a floor from the upper part at 130 meter. As a result, the BENG 1 indicator was met in both floors in around 75% of cases. However, both of the indicators BENG 2 and BENG 3 have not been reached at any level. The values of the BENG 2 are above the maximum recommendation of 50 kWh.m².yr, whereas the energy generation of the BENG 3 indicator is under the minimum required 40%.

	BENG 1 ≤ 70 kWh/m².yr	BENG 2 ≤ 50 kWh/m².yr	BENG 3 ≥ 40 %
Results at 25 m Lower Part	48 - 81 (89% of cases)	62 - 91	0 - 15
Results at 130 m Upper Part	52 - 89 (74% of cases)	65 - 95	0 - 14

Table 2 *Results from a study of a nearly zero-energy residential high-rise in the Netherlands (Source: Marginean, C. M., 2019)*

2.2. High-Rise

2.2.1. Introduction

The high-rise trend has led many countries into a competition aiming for the tallest structure. Meanwhile, in urban cities, this motive emerged with the population growth and urbanization process (Ekici, Kazanasmaz, Turrin, Tasgetiren, & Sariyildiz, 2019). There are contradicting opinions concerning the high-rise typology.

On the one hand, most criticism is due to its impact on the environment with its extensive energy consumption and operational cost, categorizing it as unappealing in the built environment from the public (Ali & Al-Khodmany, 2012).
On the other hand, assuming a similar urban plot, a taller structure can provide a higher rentable area than a low-rise, if it reaches an effective amount of floors. In the same order of ideas, facing the population growth occurring in urban zones, the demand for maximizing the population density per ratio of land area has become a primary necessity.

Given the contradicted perspective on high-rises, part of this research's interest is based on achieving an energy conscious design of a tall building, by providing on the one hand an efficient amount of floors to respond to demand for housing, therefore achieving a high density per ratio, and on the other hand, reducing its energy consumption to comply with the BENG requirements.

2.2.2. Standard Definition

There is not a universal standard for the exact amount of floor or height to categorize the typology as a Tall Building or Skyscraper (CTBUH, 2019). Under the standards of the Council on Tall Buildings and Urban Habitat (CTBUH), many criteria are taken into consideration for the classification.

Height Relative to Context
Depending on the context, a 14-story building is perceived as tall when surrounded by low-rises, such as in suburbs and European cities. However, the same building is not considered as tall if relocated in a city such as Dubai or Hong Kong with higher urban norm (CTBUH, 2019).

Figure 3 *Height relative to context in tall building (source: CTBUH, 2019)*

Also, considering the number of floors can lead to confusion as the total height depends on the floor-to -floor height. Therefore, the CTBUH (2019) considers a "tall building" threshold of a minimum of 14 stories, or above 50 meters in height.

Supertall and Megatall Buildings
Furthermore, the CTBUH classifies sub-groups for tall buildings, where a "supertall" is achieved from 300 meters and above, and a "megatall" from 600 meters (CTBUH, 2019).

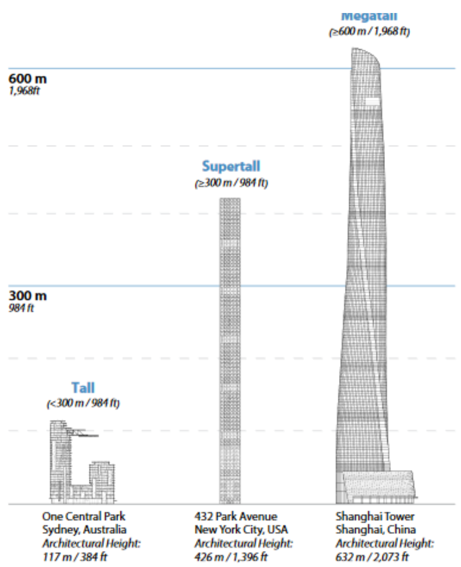

Figure 4 *Classification of buildings by their height (Source: CTBUH, 2019)*

2.2.3. Definition in the Netherlands

In the Netherlands, according to the Dutch Building Regulations, article 2.128, a building is defined as a high-rise above the height of 70 meters (Bouwbesluit, 2012).

For a low-rise, it is considered under five storeys, which does not require any lift usage (Davies & Jokiniemi, 2008). For a mid-rise, the range of floors varies between five and ten storeys included (Designing Buildings Wiki, 2019).

2.2.4. High-Rise in the Netherlands

Currently, the high-rise trend affected a very minimal part of the skyline in the Netherlands compared to other countries. In the last 10 years, since 2009, only 18 tall buildings emerged, presenting an average of around 2 contracts per year (CTBUH, 2019).

As of today, there are 48 buildings in the Netherlands above 100 m that can be defined as high-rises, 5 of which above 150 m height mostly located in Rotterdam (CTBUH, 2019). The tallest Dutch building has a limit of around 165 meters, with the highest residential building of 158.4 meters (Table 3).

Considering the presented definitions and the height of the tallest structures in the Netherlands, this study will be based on the design of a high-rise up to 160 meters, of an average number of 48 floors.

6	Rembrandt Tower	Amsterdam (NL)	150	492	35	1995	composite	office
5	De Rotterdam	Rotterdam (NL)	151.3	496	45	2013	concrete	office / residential / hotel
4	Gebouw Delftse Poort 1	Rotterdam (NL)	151.4	497	41	1991		office
3	Montevideo	Rotterdam (NL)	152.3	500	43	2005	composite	residential
2	New Orleans	Rotterdam (NL)	158.4	520	46	2010	concrete	residential
1	Maastoren	Rotterdam (NL)	164.8	541	44	2010	concrete	office

Table 3 *Ranking of High-Rises in the Netherlands by height (Source: CTBUH, 2019)*

2.3. Housing Sector in the Netherlands

2.3.1. Social Housing Situation

Since 2009, the rental demand for housing has exceeded the supply in the Netherlands (Graph 3 and Table 4) (Ministerie van Algemene Zaken, 2015). Although the supply has scarcely increased in 2012, the demand has drastically surpassed it, strengthening the gap.

It is expected for the housing market to undergo the fastest growing period in the upcoming years due to the rise of households (Graph 2). Under those circumstances, the shortage of dwelling is estimated to reach 300.000 in the near future (Ministerie van Algemene Zaken, 2015).

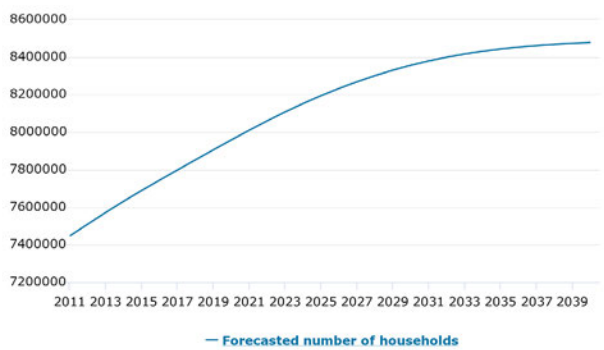

Graph 2 *Forecasted number of households demand in the Netherlands between 2011 and 2039 (Source: Ministerie van Algemene Zaken, 2015)*

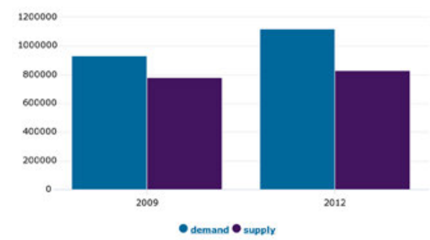

Graph 3 *Demand and supply in the rental market in 2009 and 2012 in the Netherlands (Source: Ministerie van Algemene Zaken, 2015)*

Demand and supply in the rental market

	demand	supply
2009	932000	781000
2012	1120000	828000

Table 4 *Demand and supply in the rental market in 2009 and 2012 in the Netherlands (Source: Ministerie van Algemene Zaken, 2015)*

2.3.2. User's Comfort

The major benchmarks of this study are related to the BENG regulations. While enhancing the energy performance of the building, it is essential to satisfy the user's comfort who will spend around 80% of the time indoors. The comfort is evaluated according to the indoor environment quality IEQ that consists of the indoor air quality (IAQ) (Diagram 1), acoustics, thermal comfort and visual comfort (Chen, Yang & Sun, 2016). As this study investigates energy related factors, the acoustical criteria is not taken into consideration.

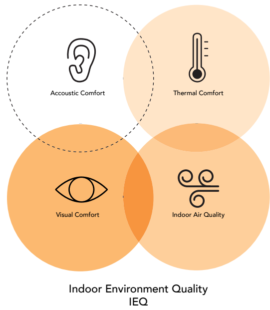

Diagram 1 *The four types of comfort of the IEQ Indoor Environment Quality*

Thermal Environment

The indoor air temperature is an indicator of the user's thermal comfort. Recommendations of the average temperature are presented as a range of acceptable zones, with lower and upper value respectively for winter and summer seasons. The range of temperature might differ from a regulation to another, with a variation of +/- 1 °C.

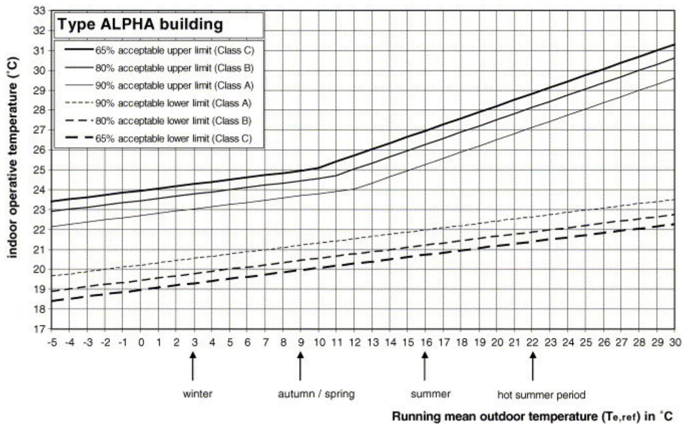

Graph 4 *Adaptive comfort temperature limits as a function of the running mean outdoor temperature for different levels of acceptance. These values are valid for buildings with a high degree of adaptive capabilities (Source: Van der Linden et al., 2006)*

To predict the general thermal sensation and degree of discomfort of the users, there are 2 indicators used according to the international standard EN ISO 7730. First, the Predicted Mean Vote PMV that defines the mean value of thermal votes of a group of people under the same environmental conditions. The second indicator used is the Predicted Percentage of Dissatisfied PPD that indicates the number of people that are thermally dissatisfied, which stands outside the limits of comfort, either feeling too cold or too warm (BPIE, 2015). The category II, in Table 5, defines the normal range of expectations for a newly designed building (EN15251, 2006). According to the European Standards EN 15251, different categories of PPD and PMV are provided in relation to 6 thermal parameters (clothing, activity level, air and mean radiant temperature, air velocity and humidity) (Table 6).

Category	Explanation
I	High level of expectation and is recommended for spaces occupied by very sensitive and fragile persons with special requirements like handicapped, sick, very young children and elderly persons
II	Normal level of expectation and should be used for new buildings and renovations
III	An acceptable, moderate level of expectation and may be used for existing buildings
IV	Values outside the criteria for the above categories. This category should only be accepted for a limited part of the year

Table 5 *Description of the different categories of comfort use (Source: EN 15251, 2006)*

Category	Thermal state of the body as a whole	
	PPD %	Predicted Mean Vote
I	< 6	-0.2 < PMV < + 0.2
II	**< 10**	**-0.5 < PMV < + 0.5**
III	< 15	-0.7 < PMV < + 0.7
IV	> 15	PMV<-0.7; or +0,7<PMV

Table 6 *Recommended categories for thermal state design of the user's comfort (Source: EN 15251, 2006)*

The European Standards EN 15251 recommends a range of temperature for a comfortable indoor environment of minimum heating set point of 20°C and a maximum cooling set point of 26°C (Table 7). In summer, a temperature up to 27°C is still perceived comfortable, while for winter as low as 18°C (Table 8). However, according to the Dutch regulations, the indoor temperature for summer should be limited to 26°C to reduce overheating risk.

Type of building/ space	Category	Operative temperature °C	
		Minimum for heating (winter season), ~ 1,0 clo	Maximum for cooling (summer season), ~ 0,5 clo
Residential buildings: living spaces (bed rooms, drawing room, kitchen etc)	I	21,0	25,5
	II	**20,0**	**26,0**
Sedentary ~ 1,2 met	III	18,0	27,0

Table 7 *Recommended indoor temperature for design and ventilation system (Source: EN 15251, 2006)*

Type of building or space	Category	Temperature range for heating, °C	Temperature range for cooling, °C
		Clothing ~ 1,0 clo	Clothing ~ 0,5 clo
Residential buildings, living spaces (bed room's living rooms etc.)	I	21,0 -25,0	23,5 - 25,5
Sedentary activity ~1,2 met	**II**	**20,0-25,0**	**23,0 - 26,0**
	III	18,0- 25,0	22,0 - 27,0

Table 8 *Temperature ranges for hourly calculation of cooling and heating energy for indoor environment (Source: EN 15251, 2006)*

Ventilation

According to Dutch building decree Bouwbesluit (2012) article 3.29, NEN 1087, minimum ventilation requirements are implemented for new residential buildings with 0.7 dm^3/s per m^2 of continuous ventilation, and a minimum of 7 l/s for occupied rooms for longer periods. Some values are based on the room function and others expressed with the floor area (Table 9).

For the European Standards EN 15251, it recommends an airflow of 7 l/s/person (Table 10). During unoccupy, the minimum ventilation rate is between 0.05 and 0.1 $l/s.m^2$ (if no value is mentioned on the national level) (EN, 15251, 2006).

Function / Space	Ventilation Rate
Kitchen	minimum of 21 dm^3/s
Living Room	0.7 dm^3/s per m^2 floor space minimum of 7 dm^3/s
Bedroom	0.9 dm^3/s per m^2 floor space minimum of 7 dm^3/s
Bathroom	minimum of 14 dm^3/s
Toilet	minimum of 7 dm^3/s
Circulation Area	minimum of 0.5 dm^3/s per m^2
Storage	minimum of 10 dm^3/s per m^2

Table 9 *Requirement of ventilation rates by room function according to the Bouwbesluit, 2012, NEN 1087 (Source: Rijksoverheid, 2012)*

Category	Air change rate [1]		Living room and bedrooms, mainly outdoor air flow		Exhaust air flow, l/s		
	$l/s,m^2$ (1)	ach	l/s, pers[2] (2)	$l/s/m^2$ (3)	Kitchen (4a)	Bathrooms (4b)	Toilets (4)
I	0,49	0,7	10	1,4	28	20	14
II	0,42	0,6	7	1,0	20	15	10
III	0,35	0,5	4	0,6	14	10	7

Table 10 *Ventilation and airflow ratesfor the residences under continuous operation during occupied hours (Source: EN 15251, 2006)*

Relative Air Velocity

As for the supply of fresh air (air velocity), a maximum value is required by the Bouwbesluit 2012 to avoid draughts. it should not exceed 0.2 m/s in the living zone of a residential area, according to NEN 1087 (Rijksoverheid, 2012).

Relative Humidity Level

The European Standards EN 15251 (2006) recommends a humidity range for a comfortable category of minimum 25% and maximum 60% (Table 11).

Type of building/space	Category	Design relative humidity for dehumidification, %	Design relative humidity for humidification, %
Spaces where humidity criteria are set by human occupancy. Special spaces (museums, churches etc) may require other limits	I	50	30
	II	60	25
	III	70	20
	IV	> 70	< 20

Table 11 *Recommended humidity level of an occupied space with and without humidification system (Source: EN 15251, 2006)*

Visual Comfort

Providing adequate amount of daylight is important to comply with the user's visual comfort, but also, to save a potential amount of energy by reducing electric lighting demand. Adequate amount of daylight is considered achieved if the target illuminance level is distributed across the mentioned fraction of the space area.

According to the European Standards EN17037, for a minimum recommendation of daylight provided through vertical openings, the target illuminance measured on the plane surface should be equal to 300 lux, with a minimum of 50% of the total space and for at least 50% of the occupancy time (Table 12).

According to the Dutch building degree, article 3.74, a minimum of 10% of the total floor area should be covered with natural daylight in residential buildings with a minimum of 0.5 m² (Bouwbesluit, 2012).

Level of recommendation for vertical and inclined daylight opening	Target illuminance E_T lx	Fraction of space for target level $F_{plane,\%}$	Minimum target illuminance E_{TM} lx	Fraction of space for minimum target level $F_{plane,\%}$	Fraction of daylight hours $F_{time,\%}$
Minimum	300	50 %	100	95 %	50 %
Medium	500	50 %	300	95 %	50 %
High	750	50 %	500	95 %	50 %

Table 12 *Recommendations of daylight provision by daylight openings in vertical and inclined surface (Source: EN 17037, 2006)*

2.3.3. Residential Occupants Requirement

There are 2 types of energy use in the building consumption; the building related and the user-related. Building related energy use involves the common space heating, cooling, ventilation and lighting. The user related usage is defined by the activity level occurring in the house such as cooking, water consumption, electrical equipment and other appliances (Guerra-Santin et al. 2018).

First, from the user's related consumption, the artificial lighting responds to the visual need when there is a lack of daylight availability or access. It contributes to around 14% of the total household consumption. The LenteAkkoord (2019) suggests replacing conventional lighting equipment with LED systems that are more energy efficient in order to reduce the BENG 1 and 2 indicators (LenteAkkoord, 2019). The lighting equipment has 2 indicators on which to base the simulation; the required amount of illuminance for the comfort of the user expressed in lux and the heat gains in W/m^2 that causes additional internal heat.

The schedule to be implemented will be based on the time of the day that the room is suggested to be occupied. In addition, powering the household equipment and other appliances related to each room will also be included and based on their consumption amount in Watt (W).

2.4. Parameters for the Optimization of a Nearly Zero Energy High-Rise Building

From previous research, it is shown that tall buildings are more energy consuming than low-rises (Godoy-Shimizu et al., 2018). In the design of a high-rise, the performance is related to both the external factors and design parameters in regard to the height. Several studies indicate the advantages of passive strategy of parameters such as the building layout, the building geometry, the envelope thermophysics and air-tightness (Chen, Yang & Sun, 2016). Aside from the building design, external factors were observed to have a significant impact on the performance such as the environmental conditions and the urban context.

2.4.1. Environmental Parameters (in relation to a High-Rise)

Moving into a taller structure, the microclimate conditions of wind speed, temperature range and the exposure to the sun gradually differ with altitude. Those factors influence primary decision making of the architectural design, as well as engineering decisions (Godoy-Shimizu et al., 2018).
As the height expands, the energy consumption increases to adapt to the varying conditions of the thermal and visual comfort (Ekici, Kazanasmaz, Turrin, Tasgetiren, & Sariyildiz, 2019), where overexposure to direct sunlight, higher wind pressure and temperature difference occur in upper floors, leading to different lighting, heating and cooling demand from bottom levels.

Temperature Variation

The external air temperature fluctuates between the lower and the upper part of the building. With altitude, the temperature range tends to drop gradually. Some weather data suggest a decrease of 1.2°C per 100 meters (National Weather Service, 2019) while others indicate an average of 0.7°C per 100 meters (Engineering Toolbox, 2003). The rate of decrease is not uniform, but rather related to the sky forecast under different seasons, time of the day and the location.

Therefore, the treatment of the building design geometry and envelope should be adapted to the variation to result in similar indoor quality. For example, the insulation in the upper floors requires a higher R-value than if the lower part is treated. Not only the external envelope gets affected, but also the embedded systems for ventilation, cooling and heating (Hamilton et al. 2017).

Wind Pressure

The wind speed increases with the building's elevation (Figure 5), noting that the magnitude of the change is also related to the urban context (CIBSE, 2006). Usually, wind moves from high to low pressure air zones, therefore the wind speed near the ground is lower because of the presence of obstacles such as buildings and other structures that block the flow (Marugg, 2018).

The change of wind flows influences the energy consumption. In taller structures, it has been shown that there is a relationship between the increase of gas consumption and the increase of wind shear (Hamilton et al. 2017). In fact, there is pressure differentials from the higher wind speed at the upper part of a high-rise related to the air tightness attribute of the envelope that controls the indoor temperature and drafts (Ali & Al-Khodmany, 2012), leading to higher infiltration rates through the building envelope.

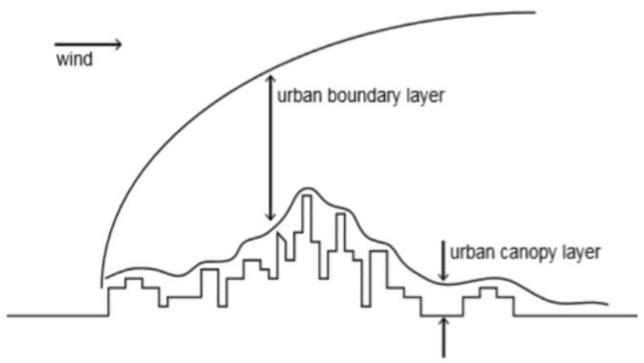

Figure 5 *Effect of the urban boundary and canopy layer on the wind speed and flow (Source: Marugg, 2018)*

Direct Sun and Daylight

In high-rises, the greater access to daylight and sun loads in upper part, due to less over-shading, plays an important role in the overall performance of the building, as well as the user's comfort needs (Ekici, Kazanasmaz, Turrin, Tasgetiren, & Sariyildiz, 2019).
As shown in previous research, Godoy-Shimizu et al. demonstrate that, on the one hand, under constant variables of parameters, when the height extends, the amount of natural daylight increase, leading to a reduction for the need of artificial lighting in the envelope perimeter zone, only if other factors, interfering with the visual comfort, do not require the need to control blinds or shading system such as excess glare, solar gains or privacy reasons (Godoy-Shimizu et al., 2018). On the other hand, the advantages from the reduction of energy expenses on artificial light are counterbalanced by an increase in electricity and fossil fuel demand for cooling in response to the higher solar gains exposing the indoor space to risk of overheating (Godoy-Shimizu et al., 2018).

However, other factors interfere in the complexity of design decisions such as the urban context, the building's geometry, the envelope design and materials properties (Ekici, Kazanasmaz, Turrin, Tasgetiren, & Sariyildiz, 2019), where the building height relative to the surroundings is decisive for the amount of daylight and solar gains that can access the facade (Godoy-Shimizu et al., 2018). The interrelation between all the parameters leads to complexity for design decision taking, facing a wide range of design alternatives (Ekici, Kazanasmaz, Turrin, Tasgetiren, & Sariyildiz, 2019).

2.4.2. Urban Parameters (in relation to a High-Rise)

Under different urban conditions, the building's behaviour adjusts to any modification. Tall structures cast a wider range of shadow on their surroundings, thus blocking sunlight and incoming wind flow to their neighborhood.

Site Surroundings Conditions

The character of the urban area determines the relative height of a building in relation to its surroundings. The presence of tall neighboring buildings will result in overshadowing of the facades, obstructing the incoming winds, or blocking direct sunlight, as the opposite is true in place of a low-rise. Also, nearby obstruction can affect the lower part of the geometry, half of it or the total building's facade. Therefore the lower and upper part are subjected to different conditions.

As observed in a case study by Ellis and Torcellini (2005), the total heating and cooling demand in a rectangle shaped office high-rise, located in Manhattan, increases between the lowest and highest floors. Under several site settings, the main factor affecting this increase in energy consumption was the overshadowing from the surroundings. Moreover, some studies showed that the height counts for a 2.5 variation in the energy use of a building, compared to 2.0 variation from other systems or users behavior. This same study showed that the urban context led to a 10% variation in the energy performance of the building (Godoy-Shimizu et al., 2018).

Future Urban Developments

As the surrounding buildings to the site impact considerably its energy outcome, any ongoing change in the urban fabric, such as the demolition of an old edifice or the erection of a neighboring high-rise, will impact the performance of the building along its lifetime.

The majority of studies done on high-rises do not take into account any variation of the building geometry or its envelope when transitioning from bottom to top floors. In response to the context's height, the design decision will differ between the ground level and the highest level (Ekici, Kazanasmaz, Turrin, Tasgetiren, & Sariyildiz, 2019). Therefore, in adaptation to the external conditions, a design solution in the lower floor will not be optimal at all levels of the high-rise. Also, the selection of the site environment is critical, and its interactions with many other parameter variables should be underlined (Chen, Yang & Sun, 2016).

2.5. Building Geometry Parameters

For the early stage design, decisions are taken for larger scale parameters, tackling the building's geometry in relation to its environment, and involving 3 main parameters; the compactness ratio, the orientation and the floor plan layout.

2.5.1. Compactness Ratio

The compactness of a building is defined by the ratio of the external surface (envelope area) to the total volume (Raji et al. 2017). Studies have shown that as the relative compactness increases, the annual energy consumption decreases, under hot and cold climate conditions (Raji et al. 2017). In a study by Raji et al. (2017), the energy efficient compact ratio observed was a 1:1 and 3:1 ratio, respectively squarish and rectangular plan.

Being directly related to the envelope area, most study results indicate that the compactness correlates negatively with the glazing ratio (WWR) because less surface is available for opening. This variation has a potential impact on heat transfer, solar gains, daylight, natural ventilation and infiltration (Godoy-Shimizu et al., 2018). Thus, facing the constraint to use lower window-to-wall ratio, the glazing properties should adjust to the heat gain and lighting needs (Godoy-Shimizu et al., 2018).
Also, the available envelope area results from the compactness ratio, thus the potential of the energy generation from the facade is affected.

2.5.2. Orientation

The orientation of a building defines the amount of sun exposure on the different facades. Depending on the angle, it can maximize the solar energy production by increasing the exposure to solar irradiance. This is in the advantage of the BENG 3 indicator, to allow a higher energy production from the energy generating systems of the facade. In other cases, it can minimize the cooling loads by avoiding large exposure to solar radiation, as well as reduce artificial lighting dependency by allowing more natural daylight. In a study conducted on high-rises, the amount of daylight availability in relation to the height is shown to be mainly determined by the orientation and the surrounding buildings (Godoy-Shimizu et al., 2018). Depending on the goal, orienting the building in a certain direction can impact its performance while considering other parameters such as the floor plan layout, the compactness and the envelope's features.

2.5.3. Floor Plan Layout

Another parameter involved in the building geometry is the floor plan layout that directly affects the building shape, and vice versa. It influences the amount of heat gain and heat loss through the envelope. Several factors of the floor plan layout can be investigated: the geometry type, the depth of the plan, the plan ratio to wall (floor height), the distribution of functions and the occupancy.

Rectilinear shapes have a greater envelope area exposure to sun load in comparison to circular or elliptical form. On the contrary, curved shape buildings, known as aerodynamic, can minimize the wind turbulence and assist the natural ventilation. Effectively, the wind can flow around the envelope from any direction, without being obstructed by sharp corners or edges (Raji et al. 2017).

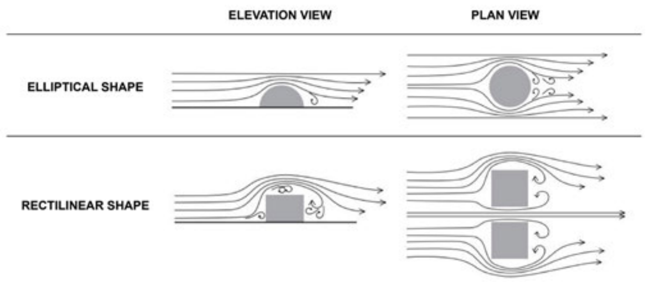

Diagram 2 *Effect of an elliptical and rectilinear geometry on the aerodynamic of the building (Source: Ching, 2014)*

In addition, the depth of the plan can negatively impact the amount of natural daylight accessing the space, resulting in non-homogeneous distribution of light. Most studies define optimal range of depth between 6 to 8 m from the external facade (Raji et al. 2017). With passive strategy, the daylight distribution can reach a greater depth by increasing the floor height, the window ratio, selecting the right type of glazing and adding external light shelves (Ekici, Kazanasmaz, Turrin, Tasgetiren, & Sariyildiz, 2019).

In addition to its impact on the daylight, the net floor height affects the heating demand when it increases the total volume of the space. According to Bouwbesluit 2012, article 4.1, in the Netherlands, the minimum allowed floor height is 2.6 meters above the floor surface (Rijksoverheid, 2012).

Regarding the distribution of the functions among the plan layout, the requirements of each room are mixed in the design of a high-rise (Ekici, Kazanasmaz, Turrin, Tasgetiren, & Sariyildiz, 2019), and thus, it can impact the energy consumption if a certain room requires an adequate amount of daylight, but a lower exposure to solar loads.

In a study conducted on households in the Netherlands, the increase of the energy consumption between 2000 and 2017 is mostly due to an increase in the size of the house, more dwellings and the change in the lifestyle of the occupants involving more appliances (Graph 5). To compensate, the implementation of energy saving solutions led to a reduction of 5.05 Mtoe (Odysee, 2020).

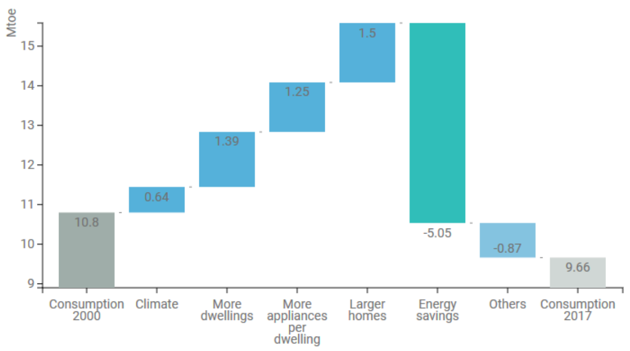

Graph 5 *Main factors of the energy consumption variation in households between the yearly period of 2000 and 2017 (Source: Odysee, 2020)*

2.6. Design Strategies Consideration for the Parameters

Achieving the concept of nearly zero-energy, by reducing the energy demand, facilitates the replacement of the dependence on finite fossil sources by renewable energy (Mlecnik, 2013).

To do so, energy-efficient strategies, such as climate-responsive designs, can be implemented through energy conservation, distribution, buffering, recovery and storage (Figure 6). Thus, natural resources are exploited such as the sun, wind, water, earth and sky, in addition to less common sources of energy recovered from waste flow (Looman, 2017). In application, indoor temperature can be conserved to reduce heating loads. Also, to provide a cooler space by preventing overheating during summer, it is possible to reduce solar heat gains and promote natural ventilation that is also beneficial to constantly replace fresh air for a healthy and comfortable indoor environment.

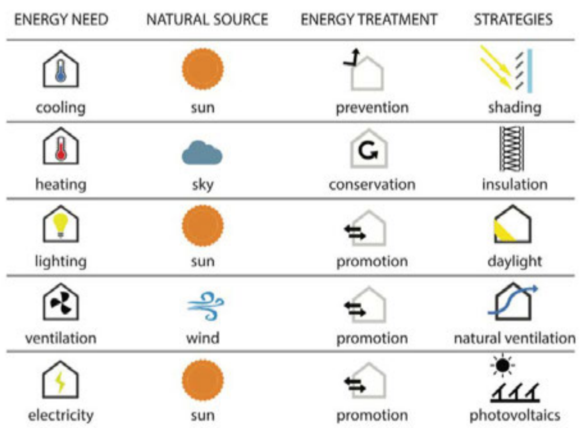

Figure 6 *Elements of climate responsive architecture (Source: Looman, 2017)*

2.7. Facade Parameters

Additionally to the building geometry, the facade plays a major role in the design of a nearly zero energy high-rise. In fact, it is the median layer between the indoor and outdoor environment where energy and heat transfer occurs. Regarding its parameters, the selection is based on the previously mentioned strategies ("2.6. Design Strategies Consideration for the Parameters") achieved in the passive house concept (Figure 7) for a temperate climate.

Firstly, the materials should incorporate high insulating properties, such as low heat transfer coefficient U-value, to ensure less heat lost during cold periods through the facade. Similarly, the glazing type properties should avoid heat transfer while allowing daylight into the internal space. To conserve the indoor temperature, the airtightness of the envelope can prevent unwanted air leakage and heat loss, that also occur through thermal bridges in connection, edges and joints. Lastly, with at least 75% of recovered heat loss from the exhaust air, considerable energy saving can be saved from the selection of the ventilation system while maintaining a comfortable indoor air quality (Passive House Institute, 2015).

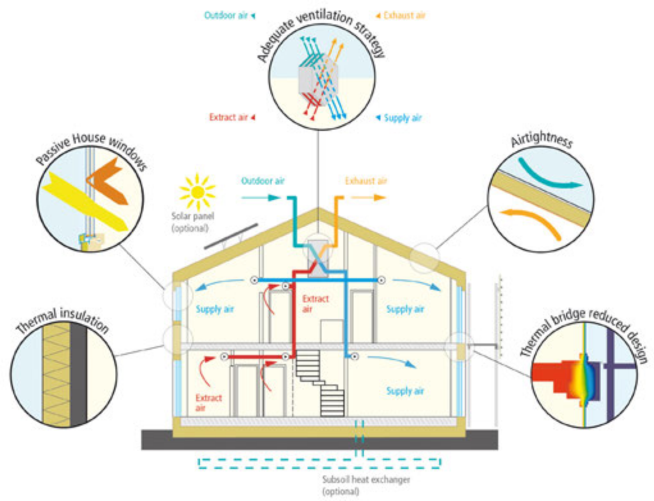

Figure 7 *The 5 principles of a Passive House Design (Source: Passive House Institute, 2015)*

2.7.1. Facade Typology

This study addresses the design of a residential high-rise in which a commonly single-skin facade is applied. In fact, its function distribution in the plan layout and user's needs do not come hand in hand with the design of a double-skin facade that presents many disadvantages with higher costs, fire safety, maintenance, reduction in usable space, overheating issues, daylight availability and viewing comfort. Therefore, the single-skin system is selected for this research.

2.7.2. Window-to-Wall Ratio

From the parameters of the facade, the window distribution area is highly correlated to the energy performance of the building (Chen, Yang & Sun, 2016). In fact, it defines the amount of daylight entering the space, and thus, affects the dependence on artificial lighting. Similarly, the heating and cooling demand are related to the window size, where an enlargement of glazing provides more surface for heat transfer. Depending on the envelope area, an exceeding ratio minimizes the available surface to be used for the installation of energy generating systems such as PV or BIPV cells.

In a temperate climate, for an equal distribution of windows on all orientations (North, South, East, West), most studies state that the efficient WWR ratio ranges between 20% and 30% for narrow and deep plan design (Raji et al. 2017), and between 30% to 50% depending on the thermal performance of the external envelope.

However, there is not a single optimal window ratio that can be applied on all sides and floors of the building. In fact, each facade has a different exposure angle and duration to the sun, in addition to different exposure to the micro-climate conditions differing between the lower and upper floors. For example on the South orientation, the higher the ratio (above 30%) the higher the cooling load which is amplified in the top floors under the drop of air temperature. Thus, the WWR in the upper floors should be reduced where also the exposure to the direct sun is higher (Godoy-Shimizu et al., 2018).

Due to the several factors to consider, it is therefore more efficient to have a different WWR distribution on each facade, and per floor level, that adapts to the environmental conditions, and the surrounding height if obstruction occurs. Nevertheless, in addition to its ratio, the glazing type is another parameter affecting the opening area, with its insulating properties and material type.

2.7.3. Thermal Properties

Regarding the regulations, in BENG 1, the sum of the heating and cooling are affected by heat loss. In BENG 2, the required fossil energy that compensates for heat losses is taken into consideration, and in some cases, in the cold demand. As for BENG 3, it is calculated by the result of BENG 2 (LenteAkkoord, 2019). Thus, to comply with the regulations, potential energy savings can be achieved with passive solutions by providing a well-insulated shell.

In a report provided by Harm Valk, the two main factors that were shown to have the greatest influence on BENG 1 are the R-values of the envelope and the ventilation system (LenteAkkoord, 2019). The lower the external wall and the glazing type insulation properties, the higher the heat requirement, specifically in lower parts of a building, where the sun exposure in winter period is lower.

The building skin can outperform the external climate conditions by selecting the materials thermal properties accordingly (Table 13), even when less favourable to achieve a comfortable indoor environment (Schittich, 2006). Among its properties, three energy-related features translate the material capacity to transfer heat.

	U-value	g-value	Diminution factor	Transmit-tance
Summer, clear skies	high	low	low	high
Summer, overcast	high	n/a	n/a	high
Summer, night	high	n/a	n/a	low
Winter, clear skies	low	high	high	high
Winter, overcast	low	n/a	n/a	high
Winter, night	low	n/a	n/a	low

Table 13 *Requirements of the facade parameters in relation to the external environmental conditions (Source: Schittich, 2006)*

For the thermal conductivity (Lambda λ), expressed in W/m.K, it measures how easily the heat moves across the material, independently of its thickness. The lower the value, the slower the flow of the heat, resulting in a better insulator (Table 14).

Type of insulation	Nominal density (kg/m^3)	Mean Temperature (°C)	Thermal Conductivity (W/mK) at nominal density
Glass mineral wool	10-200	10	0.037-0.031
Rock mineral wool	20-200	10	0.033-0.034
Expanded polystyrene (EPS)	15-30	10	0.038-0.033
Extruded polystyrene (XPS)	28-45	10	0.027-0.026
Phenolic foam	35-60	10	0.018-0.022
Polyisocyanurate foam (PIR)	32-50	10	0.023
Polyurethane foam (PUR)	35-50	10	0.023
Cork	112	10	0.038
Exfoliated vermiculate	109	10	0.066

Table 14 *Typical thermal conductivity values for a variety of insulation products (Source: AEA, 2010)*

The thermal resistance (R-value), expressed in m².K/W, defines the resistance to heat flow through the material for a given surface. This indicator is commonly used to define the opaque parts of the facade such as external walls. For a multi-layered material, the total R-value of the wall is the result of each layer's thermal resistance added together. A higher value indicates a better insulating performance. However, the R-value only includes the conduction, disregarding the convection and radiation.

The thermal transmittance (U-value), in W/m².K, indicates the amount of heat that can travel through the material. The lower the value, the less heat transfer occurs through the material and the greater the effectiveness of the insulating properties. Contrary to the R-value, the U-value includes the three heat movements; conduction, convection and radiation.

According to the Bowbesluit 2012, article 5.3, NEN 1068, the external envelope should have a thermal resistance (R-value) of minimum 3.5 m².K/W (Rijksoverheid, 2012). As for windows, doors and frames, the maximum thermal transmittance U-value should be 1.65 W/Km2 (Rijksoverheid, 2012). The Lente Akkoord (2019) is an initiative from the government that suggests starting point values for R-values of the floor, wall, and roof respectively of 5, 7 and 8 m2.K/W (LenteAkkoord, 2019).

According to the Nederlands Vlaamse Bouwfysica Vereniging 2018, the following Table 15 suggests the range of thermal insulation R-values for non-transparent façade parts, involving all external, structural and internal space separation, to minimize heat loss during winter period when most of the energy loss occurs. The ranges were adapted according to the Ducth building decree, Bouwbesluit (NVBV, 2018). For this study, the "basic quality level" insulating properties of the external shell, floor and roof will be used as fixed values to provide a good thermal performance of the envelope.

Thermal Insulation	Quality level		
	Basic	Good	Excellent
Non-Transparent Parts	$R_{c;Floor}$ ≥ 3,5 m2K/W $R_{c;Facade}$ ≥ 4,5 m2K/W $R_{c;Roof}$ ≥ 6,0 m2K/W	$R_{c;Floor}$ ≥ 4,5 m2K/W $R_{c;Facade}$ ≥ 6,5 m2K/W $R_{c;Roof}$ ≥ 8,0 m2K/W	$R_{c;Floor}$ ≥ 5,5 m2K/W $R_{c;Facade}$ ≥ 8,5 m2K/W $R_{c;Roof}$ ≥ 10,0 m2K/W

Table 15 *Categorized Levels for the Thermal Insulation of Non-transparent Facade Parts*
(Source: Adapted and translated from the Dutch version of the Nederlands Vlaamse Bouwfysica Vereniging NVBV, 2018)

2.7.4. Glazing Type

The glazing type parameter comes hand in hand with the window-to-wall ratio. Together, the outcome should enhance the daylight factor and provide views to the exterior, while conserving indoor temperatures. Therefore, several characteristics are considered in the selection of the glazing type, from which the aforementioned U-value (paragraph 2.6.3), g-value and the VLT.

According to the regulations of NVBV (2018), achieving a "good" level of thermal quality is indicated by a maximum U-value of 1.65 W/m^{2}K for the transparent parts of the facade (Table 16).

Thermal Insulation	Quality level		
	Basic	Good	Excellent
Transparent Parts	$U_{w;Maximum}$ ≤ 2,20 W/m2K $U_{w;Average}$ ≤ 1,65 W/m2K	$U_{w;Maximum}$ ≤ 1,65 W/m2K $U_{w;Average}$ ≤ 1,20 W/m2K	$U_{w;Maxiumum}$ ≤ 1,1 W/m2K $U_{w;Average}$ ≤ 0,8 W/m2K

Table 16 *Categorized Levels for the Thermal Insulation of Transparent Facade Parts*
(Source: Adapted and translated from the Dutch version of the Nederlands Vlaamse Bouwfysica Vereniging NVBV, 2018)

To reach lower U-value and reduce heat loss, multi-panes, such as double-glazing and triple-glazing profiles, are built with a gap in between each consecutive pane. To further enhance the insulating property, gas-filled gaps with air, argon or krypton can improve the overall U-value of the final product. The normal range of a double-pane insulated glass, and argon filled, can reach 1.2 W/m².K. The investment of a triple glazing with krypton gas filling can reduce the range to 0.6 W/m².K (Schittich, 2006).

In the temperate climate, on the one hand, minimizing heat loss through glass during winter should be prioritized with a lower U-value to conserve indoor heat. On the other hand, passive heat gains can be desired to allow heat in and reduce the heating demand with a higher U-value (Raji et al. 2017). However, it can lead to overheating in the summer period and uncontrolled heat transfer during winter.

Another property of the glazing is the solar energy transmission coefficient, g-value. It represents the amount of solar radiation (for wavelength between 320 and 2500 nm) that can transpass through transparent or translucent elements (Schittich, 2006). Commonly, for a double glazing insulated glass the g-value reaches 60%, and can be reduced to 50% when using a triple-glazing layer. Adding solar selective coatings can further reduce its value, with 40% for a double-pane glass (Schittich, 2006).

Regarding the optical properties of the glass, the visible transmittance (VT or Tvis) refers to the fraction (value between 0 and 1) of visible light of the spectrum passing through the material. It is affected by the glazing type, the number of layer panes and the coating (Commercial Windows, 2019). For an uncoated clear glass, the VT value is higher, whereas it decreases considerably for tinted glass combined with highly reflective coatings. Thus, a double glazing has a lower VT when a Low-E coating is added, and the value decreases if a tint is added (Commercial Windows, 2019).

Some glazing types can be selective of solar radiation to reduce heat transfer (Table 17). Balancing between the heat transfer and daylight requires spectrally selective coatings to control visible light entrance, infrared and ultraviolet. In a temperate climate, Low-E coatings can minimize thermal transfer between the internal and external environment by rejecting solar heat gain during summer and reducing heat loss during winter, while allowing at all times for the visible light to pass through the glazing.

Glazing Type	Composition	U-value [W/m²K]	g-value [-]	VLT [%]
Standard Double Glazing	4/12/4 mm Air fill	2.7	0.76	-
Double Glazing HR 3% Emission	4/15/4 mm Argon fill	1.1	0.62	80
Double Glazing HR	6/15/6 mm Argon fill	1.1	0.56	77
Double Glazing HR	6/15/4 mm Argon fill	1	0.28	60
Double Glazing Low-E on Outer Pan	4/12/4 mm Krypton fill	0.9	0.47	75
Triple Glazing HR	6/12/4/12/4 mm Argon fill	0.7	0.5	69
Triple Glazing HR	4/12/4/12/4 mm Krypton fill	0.6	0.5	-
Triple Glazing HR	4/12/4/12/4 mm Argon fill	0.5	0.7	72

Table 17 *Comparison of glazing systems by properties of U-value, g-value and VLT (Source: Looman, 2017)*

2.7.5. Shading System

The design of the shading systems should be based on the sun position and exposure of the facade throughout the day. The system can be either external or internal to the envelope layer.

The advantage of an external shading is its capacity to block sun radiation at an earlier stage, and therefore preventing heat transfer during hot seasons. Although it can reduce unwanted thermal transfer, it is more prone to the high wind speed in upper floors of a high-rise, and presents greater risk to the pedestrian safety and damages.
Another solution is to provide an internal system, secured from the wind and requiring less maintenance. In this case, it can lead to more cooling demand due to the greenhouse effect occurring in the created cavity (Raji et al. 2017). However, for both types, it obstructs the user's view and the access to natural daylight that can increase the dependence on artificial lighting.

Providing dynamic control to the system presents advantages in balancing between the indoor environment and saving energy in cooling, while increasing the visual comfort. The additional control can be implemented with conditions of an increase in the indoor air temperature, reaching the cooling set point, under a high exposure of the glazing surface to sun radiation.

Additional properties of the shading system of the color and material selection affect the solar gains with the total g-value (Table 18). The material determines the total amount of heat transfer by the sum transmitted and absorbed by the fabric (velux, 2020). White color has a lower absorption which is effective in minimizing heat transfer, but also, in reducing the amount transmitted from an external to an internal environment (Mandalaki and Tsoutsos, 2020). The transmittance is measured for an index of 0 to 1 according to EN 14501. The lower the value, the less radiation is transferred through the fabric (Designing Buildings Wiki, 2019). Lastly, emissivity is another property to the shading as it can control the amount of heat absorbed. A higher emissivity value indicates that the absorbed radiation is reflected back in the external environment instead of the indoor space, resulting in a reduction of overheating for the summer period (Designing Buildings Wiki, 2019).

Moreover, the shading system can act as a thermal storage and contribute to unwanted heat transfer if positioned internally to the glazing, contrary to an external system in which the air flow minimizes transfer (Mandalaki and Tsoutsos, 2020).

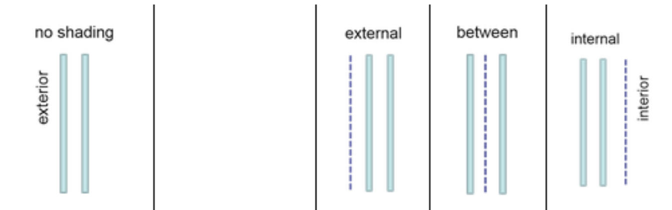

Glazing g-value	Fabric	Resultant g-value of shading and glazing		
0.64	black-black	0.04	0.24	0.57
0.64	white-white	0.12	0.17	0.29
0.28	metallized		0.08	0.11

Table 18 *Comparison of the total g-value for shading solutions in different positions (Source: Hunter Douglas Architectural, 2020)*

2.7.6. Ventilation System

To ensure a comfortable indoor environment quality, a good ventilation system should provide the right balance of fresh air in a space and its regular replacement. This fresh air can be entirely or partially incoming from outside. Prior to the implementation of the ventilation system, it is important to ensure a highly airtight envelope, as unwanted air leaks result in uncontrolled air flow through the space. In this case, it presents constant unwanted natural ventilation, which is different from the allowed one by opening windows or from a mechanical system.

The choice of the ventilation system affects the BENG results. Not only on the outcome of the indicator BENG 1, which is calculated for a fixed ventilation system, but also BENG 2 is affected in addition to the outcome of the TOjuli (LenteAkkoord, 2019).

First, natural ventilation NV provides fresh air from the outdoors and should be used adequately through operating windows of the facade, during occupancy. Regarding the environmental conditions, it operates when the outdoor air temperature range is below the minimum indoor temperature of 20 °C and not under the heating set back of 18 °C to not result in an unwanted drop of temperature in the internal space (paragraph 2.3.2 "User's Comfort"). Also, the outdoor air should not exceed the maximum cooling set back of 27°C, when the indoor temperature reaches 26°C (Wood & Salib, 2012). This can minimize cooling and heating load in response to a temperature difference.

Alternative solutions are available to provide appropriate ventilation such as mechanical ventilation MV. This system is more energy saving in consumption, as well as it minimizes the amount of heat loss that occurs when opening windows. In order to meet the BENG requirements, the LenteAkkoord (2019) suggests the implementation of either a C-System (natural supply with mechanical exhaust) or a D-system (mechanical ventilation system).

As this study is based on a high-rise, and nor a low-rise or single family-house, the combination of both natural ventilation and mechanical ventilation, known as hybrid or mixed-mode system, is in favor of the changing micro-climate conditions in respect to the height. In high-rises, extreme weather conditions in upper floors with higher wind speed and lower temperature can prevent the use of natural ventilation on a daily basis.

Based on the passive house concept, additional energy saving can be implemented in a MVHR mechanical ventilation with heat recovery, where mechanical exhaust and supply can provide an efficiency up to 95% for the satisfaction of the user's comfort (Passive House Institute, 2015). Previous studies on temperate climate have shown considerable advantages in prioritizing a heat recovery ventilation to standard mechanical exhaust or natural ventilation, with significant reduction of the primary energy, CO_2 emissions and household energy consumption (Konstantinou, 2014).

Increasing the air exchange rate to improve the indoor air quality can lead to more energy consumption. In response, it can be compensated by a heat recovery system (Diagram 3). Usually, the air exhaust carries energy considered as wasted. Thus, the MVHR system can minimize the energy cost by recollecting around 95% of this energy loss through the exhaust air flow with a heat exchanger that can heat or cool the supplied (incoming) fresh air (Passive House Institute, 2015). In extremely hot conditions, the reverse strategy is possible. Incoming heated air from the outside can be pre-cooled before entering the rooms (International Passive House Association, 2019).

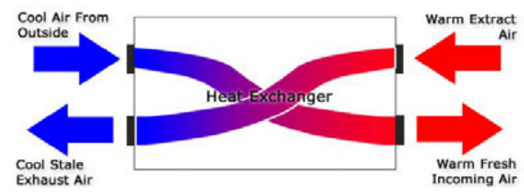

Diagram 3 *Heat recovery system principles (Source: Nash, 2013)*

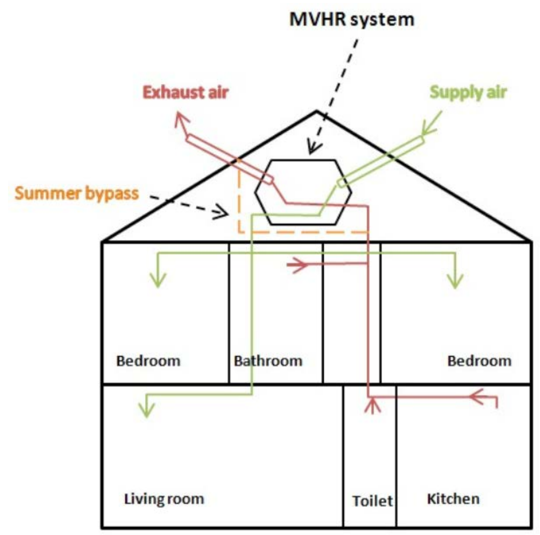

Diagram 4 *Schematic representation of the MVHR system (Source: Nash, 2013)*

2.7.7. Cooling & Heating

Heating & Water Heating

Heating is required to ensure the thermal comfort of the user for the internal temperature of the space, as well as supplying hot water. In the Netherlands, space heating represents 70% of the total consumption of households, followed by water heating, electrical lighting and appliances, with lastly cooking consumption (Graph 6) (European Environment Agency, 2012). These results imply that a reduction in space heating demand can provide great achievement in energy saving.

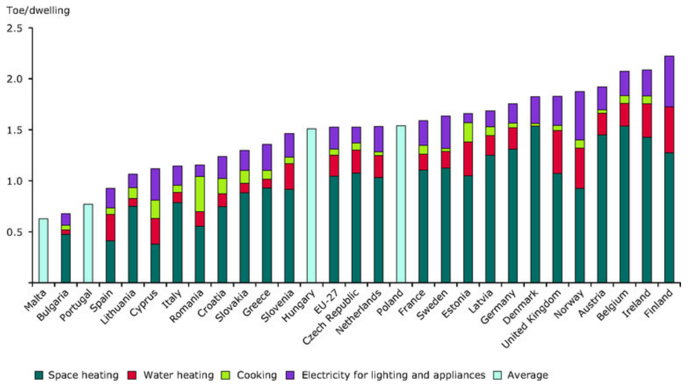

Graph 6 *Ratio of energy consumption by end users divided by the number of permanently occupied dwelling (Source: European Environment Agency, 2012)*

In high-rises, heating can be an obstacle if the goal is to reduce energy demand, and sustain the heat demand only by renewable energy. Seeking for renewable energy to guarantee a heating source is essential to achieve the share of the BENG 3 indicator. If the energy source for heating is not supplied by renewable energy (net zero percent renewable), then BENG 3 is hardly or not at all achievable (LenteAkkoord, 2019).

Therefore, options for a heat generating system in high-rises are presented such as heat pumps. The LenteAkkoord states that the 40% prescribed of BENG 3 is easily achievable through the use of a heat pump where ground heat or other ambient heat sources counts as renewable energy (LenteAkkoord, 2019). This system can generate hot water for hydronic heating systems and for domestic water heating usage. On average, a person consumes around 61 litre of hot water per day in a household in the Netherlands (Vewin, 2016), consisting partly for showering, dishwasher and washing (Appendix A, Table 3).

Heat pumps transfer heat from the source by means of electrical or thermal energy at a high temperature to different areas of the house. Most commonly for residential buildings, hydronic systems are used by transferring hot water as a heat source from the heat generator to the heating systems in the apartment (emitters/end point) with either radiators, convectors or floor heating systems (Konstantinou, 2014).
The source of heat can originate from the ground with either a GSHP ground source heat pump or geothermal energy (Konstantinou, 2014), which is in favor of a temperate climate such as the Netherlands, where the heating seasons are relatively short. There are several types of geothermal energy systems, consisting of applying pipes at deeper depth underground to use the available heat energy. A borehole thermal energy storage BTES is usually designed with U-shaped pipes, and transfers the heat via conduction. It is more convenient in the case of small scale projects (Pellegrini et al., 2019). In the case of larger buildings, such as high-rises, an aquifer thermal energy storage, ATES, can respond to greater demand (Pellegrini et al., 2019). It consists of using the groundwater by the means of two or more wells. During the summer period, groundwater from the cold given well can be provided which in results will use the extracted heat to warm up the groundwater in the second well up to temperature between 15 and 18 °C, and reaching 50 and 60 °C depending on its usage with the heat pump system. Similarly, during winter, the stored heat is used in addition to a heat pump, while extracting the cold temperature to store groundwater at lower temperature down to 5 to 8 °C (Pellegrini et al., 2019).

Cooling

In the temperate climate of the Netherlands, cooling does not account for the largest fraction of the energy consumption in households (Graph 2.4). However, during extreme heat periods, in order to avoid increasing the cooling energy demand, limiting the high range of temperature is essential to regulate the indoor temperature, when the cooling set point temperature above 24°C is reached.

As already mentioned previously, the passive strategy through the natural ventilation of window opening can provide an air flow to cool down the indoor air temperature. However, as previously mentioned, in the design of a high-rise, making use of the natural ventilation can be restrictive when the weather conditions do not allow it. In this case, the use of a mechanical cooling system is required aside from the passive strategy.

As previously presented, the heat pumps that are employed for heating can be used in a reversible functioning for cooling. The provided cool air is supplied through inlets in the ceiling or, in the case of a floor-system, through the pipes. Most commonly, for air-conditioning systems the energy source for cooling can be either through an electric pump when the refrigerant plant is used, or through the pumps by means of air, or water in hydronic systems (Konstantinou, 2014). Water is more effective than air by serving as a thermal mass, and can save more energy when combined with the Dedicated Outdoor Air Systems (DOAS) compared to HVAC systems (Xiang, Zhao, Liu & Jiang, 2020). In this case, it requires less amount of time to cool the indoor environment.

In order to determine the efficiency of a system, the coefficient of performance COP is used to indicate the heating efficiency (calculated for the emitters and circuit, with the boiler), and the energy efficiency ratio EER is used for the cooling (Office of Energy Efficiency & Renewable Energy, n.d.). Providing low temperature is possible with a EER coefficient reaching value around 14 or 15, as for the heating COP, the higher the temperature of the water heated, the lower the COP (Industrial Heat Pumps, 2020). Depending if an air, water or other liquid heat pump system is used, a COP of 3.5 can provide the high temperature of heating for the household (RVO, 2020).
Regarding the domestic water heating, according to NEN 1006, it should be within a range of 55 to 60 °C. In this case, the use of the heat pump allows to keep the high temperature, by minimizing any loss through its transfer. Thus, the COP of the appliance needed can be lowered (LenteAkkoord, 2019), down to 2.5 depending on the selected heat pump.

2.7.8. Air Tightness

Air tightness of the envelope prevents the infiltration of air, moisture and heat transfer through cracks, leaks and non-tight openings (Sherman & Chan, 2004). In the case of high-rises, it is important to avoid pressure differential from the incoming high winds in upper floors. In addition to energy saving, the permeability to air ensures a better indoor air quality. A decreasing exchange of air between the internal and external environment requires the implementation of an adequate ventilation system to provide fresh air in the space, and reduce heat loss rate that affects the cooling and heating demand. In the Netherlands, according to NEN 2687: 1989, the design of an energy efficient building, class 2, is characterized by a good quality of air tightness that should be between 0.3 and 0.6 dm3/s.m^2 (Nieman, 2020).

2.7.9. Energy Generating System

The exploitation of the sun source is mostly known under the form of a PV photovoltaic system which produces energy from converting solar radiation. This energy supply contributes to the share of renewable energy of BENG 3. In addition to the roof surface, using the available facades area for incorporating PVs can enhance the annual outcome under specific orientation. This strategy involves placing those panels in place of standard cladding on the remaining surface from the glazing ratio on the facades (Schittich, 2006).

Areas that are prone to be shaded during a major time of the day should be avoided as it can compromise with other parameters function, such as additional windows for lighting. According to the sun position and exposure of a facade orientation, PV system is expected to show more efficiency on the South, East and West facade. In Northern Europe, studies have shown that on the South oriented facade, under an angle of 30°, the PV efficiency can reach its highest performance where most radiation occurs during mid-day (Konstantinou, 2014). In comparison, the East and West facades present effective peak time respectively during the morning and afternoon in the summer period, and a lower generation in winter due to shorter days. However, the North facade has the lower exposure to the sun which can turn in a poor investment.

Although usually positioned on the roof, its potential is reduced on this surface when the building's height expands vertically, such as in high-rises. In a study by Hachem, Athienitis, & Fazio (2013), the ratio of the available generating area to the total used floor area is inversely proportional to the amount of floors in the residential building (Graph 7).

Graph 7 *Relation between the south facing roof area of gable roof and the total floor area for all studied apartment buildings (Source: Hachem, Athienitis, & Fazio, 2013)*

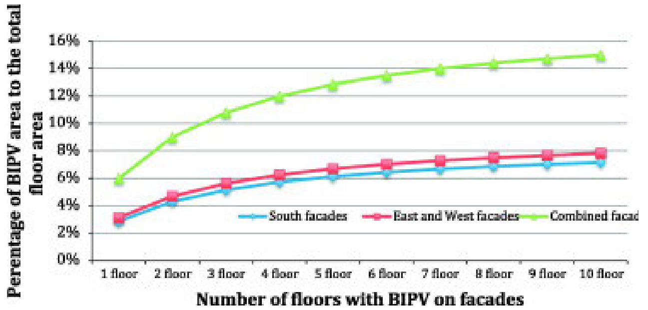

Graph 8 *Relation between BIPV area covering South, East and West façades, and the total floor area for apartment buildings (Source: Hachem, Athienitis, & Fazio, 2013)*

Advanced geometric solutions for the facade, such as folded-plate, sizes, tilting and angle orientation, can increase the production, as well as incorporating PV in shading devices. A study has shown an increase of the potential of 250% on South facade when additional design considerations were implemented (Hachem, Athienitis, & Fazio, 2013). Their study indicates that the ratio of BIPV area to total roof area in an apartment building decreases with height extension, while the ratio of BIPV area to total facade area increases (Graph 8) (Hachem, Athienitis, & Fazio, 2013).

There are many types of PV cells of different performance and efficiency. The most common ones are the crystalline silicons consisting of polycrystalline category, efficiency between 13 and 16%, and monocrystalline of higher efficiency between 15 and 20% but higher price range (Konstantinou, Ćuković Ignjatović & Zbašnik-Senegačnik, 2018). Another category is thin-film PV panels of an efficiency varying between 11-13%. During recent years, some tests showed its efficiency increasing to 25% (Energysage, 2019). This category regroups 4 different types based on the cells material; Amorphous silicon (a-Si) (21%), Cadmium telluride (CdTe) (18.7%), Copper indium gallium selenide (CIS/CIGS) (22.4%) and Gallium Arsenide (GaAs) (28.9%) (Energysage, 2019). Other types of PV cells are available on the market providing a larger efficiency (Green, et al., 2018):

- Multijunction cell GaInP/GaAs (Soitec): 46.0 ± 2.2 %
- GaInP/GaAs/GaInAs (Microlink ELO): 37.8 ± 1.4 %
- Cell (III-V) GaInAsP/GaInAs (NREL) : 32.6 ± 1.4 %
- III-V cell GaAs (thin film cell): 29.1 ± 0.6 %
- III-V cell InP (crystalline cell) (NREL): 24.2 ± 0.5 %
- Silicon Si Monocrystalline (Kaneka): 26.7 ± 0.5 %
- Silicone Si Multicrystalline (FhG-ISE) : 22.3 ± 0.4 %

A more advanced form of PVs is CPV Concentrating Photovoltaics panels with an efficiency that is beyond common flat-plate PV in which cost-effective concentrating optics are used to minimize the cell area (Table 19). They can also be provided with two-axis tracking which increases the concentration of sunlight by a factor of 300 to 1000 such as in high concentration PV, HCPV. In 2015, a CPV efficiency of 38.9% was designed, and above 30% for commercial CPV using fresnel lenses and mirrors for the optical elements (NREL, 2017).

An alternative to PV panels is building-integrated photovoltaic panels BIPV. They are similar in the modules with additional integration into the building envelope which can replace regular materials and components (cladding, roofing and shading devices). Therefore, it presents advantages as the cost is reduced by providing double functions into a single element; building envelope material and energy generating systems. In addition, BIPVs can be designed as semi-transparent elements on the facade allowing partial light into the internal space.

Cell architecture	Record efficiency (accredited test lab)	Institution	Comments
GaInP/GaAs//GaInAsP/GaInAs [3],[25]	46.0 @ 508 suns (AIST)	Fraunhofer ISE/ Soitec/ CEA	4J, wafer bonding, lattice matched grown on GaAs and InP
GaInP/GaAs/GaInAs/GaInAs [26][27]	45.7% @ 234 suns (NREL)	NREL	4J, inverted metamorphic
GaInP/GaAs/GaInAs [20]	44.4 @ 302 suns (Fraunhofer ISE)	Sharp	3J, inverted metamorphic
GaInP/GaAs/GaInNAs [28]	44.0% @ 942 suns (NREL)	Solar Junction	3J, MBE, lattice matched, dilute nitrides, grown on GaAs
GaInP/Ga(In)As/GaInAs [29][30]	42.6% @ 327 suns (NREL) (40.9% @ 1093 suns)	NREL	3J, inverted metamorphic
	42.4% @ 325 suns (NREL) (41% @ 1000 suns)	Emcore	
GaInP-GaAs-wafer-GaInAs [31]	42.3% @ 406 suns (NREL)	Spire	3J, epi growth lattice matched on front and inverted metamorphic on back of GaAs wafer
GaInP-Ga(In)As-Ge [21]	41.6% @ 364 suns (NREL)	Spectrolab	3J, lattice matched, commercially available
GaInP-GaInAs-Ge [32]	41.1% @ 454 suns (Fraunhofer ISE)	Fraunhofer ISE	3J, upright metamorphic; commercially available from AZUR SPACE, Spectrolab

Table 19 *Summary of record concentrator cell efficiencies above 41% based on III-V multi-junction solar cells (Source: NREL, 2017)*

2.8. Referencial Plan Layout

According to the Dutch building regulations, the following plan layout in Figure 8 depicts a dwelling apartment used by the RVO as a reference in the Netherlands for research related to residential apartments (RVO, 2019).

The surface area of a multi-family dwelling is on average 105 m^2 including all types of residential houses. In addition, it usually consists of two bedrooms, with an average of 3 to 4 occupants per house and a maximal density of 0.2 pers/m^2 (RVO, 2013). Each floor is composed of 6 apartments, located around a central common core used for services, technical and circulation facilities.

Therefore, for this study on the residential function, the layout is selected and adapted to the parameters that will be investigated.

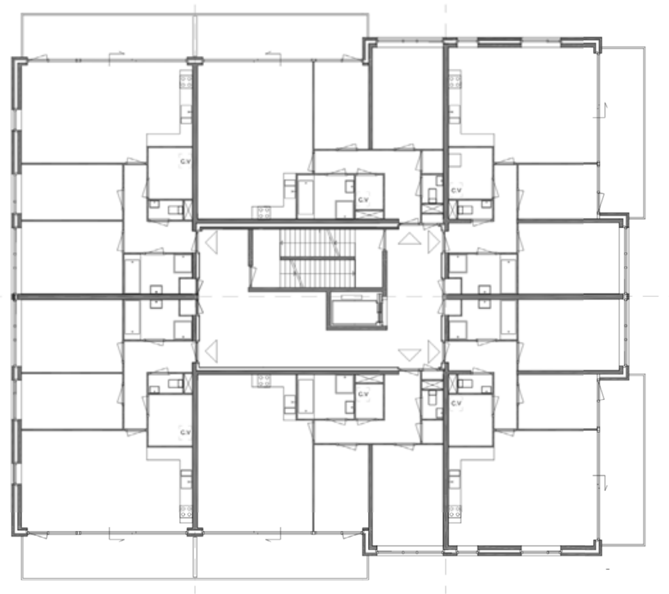

Figure 8 *Typical apartment plan layout according to the referencial Dutch design by RVO (Source: RVO, 2013)*

2.9. Conclusion: Benchmarks and Simulation Parameters

Considering the impact that the micro-climates have on the design of the building parameters, the change in wind speed, temperature fluctuation and sun exposure will be analyzed in respect to high-rise height, with the addition of the implementation of the urban character where different heights of surroundings are inserted.

In regard to the geometry, basic rectilinear polygons are used for the building shape with squarish and rectangular plan layout determined by the compactness adapted from the referential plan (Figure 2.14). For the orientation, the angle ranges from the North axis is applied on the resulting plans. As for the depth of plan and functions distribution, they are defined as constant, to reduce the amount of variables and explore the influence of the compactness and orientation only.

In relation to the envelope design, a highly airtight facade is considered, where the amount of Air Change per Hour ACH should not be exceeded. For the enclosed parts (opaque), its material is designed with fixed insulating R-values, covered with PV panels for energy generation, whereas the transparent part of glazing serves as a variable with properties of U-value, g-value and VLT. Additionally, different shading systems will be analyzed with fixed and dynamic systems.

Lastly, for the ventilation system, a mechanical ventilation system D is selected, with both of the supply and exhaust, presenting the suitability to use heat recovery for energy saving. The natural ventilation will depend on the wind speed, temperature range and the openabe fraction area of the window.

2.9.1. Benchmarks

According to the BENG indicators, the total ratio of Als/Ag is under 1.83 at all given height (Appendix F, Table 7), which indicates a maximum value of 65 kwh/m2 for BENG 1 (Graph 1).

As for BENG 2 and BENG 3, the benchmarks are respectively of 50 kwh/m2 and 40%.

Additionally, the indoor temperature should not exceed the required 26°C of the TOjuli, and, similarly, the thermal comfort should be above 90% throughout the entire year (Diagram 5).

2.9.2. User Requirement

In a residential function, the space is occupied during the 7 days of the week. The schedule of occupancy is defined by 24 hourly values depending on the room function (Appendix B, Table 2). A value of 0 states that the zone is non-occupied, while a value of 1 represents an occupied space for the full hour.

To ensure a comfortable environment along the year, the indoor temperature range for summer should be between 23°C and 26°C, and between 20°C and 25°C during winter (Diagram 6). For a good air quality, the ventilation rates are assigned by function types, with a maximum air velocity of 0.2 m/s. Also, regarding the visual comfort, the space should be lit during the occupancy with 300 lux for at least 10% of the total floor area. Lastly, a resident uses on average 21 litre of hot water daily, and will be calculated for the 20 occupants per floor.

Another part of the user consumption is related to the equipments that are defined for each function by the loads and LED lighting density (W/m²) (Table 20).

Parameters

Prior to the application phase for the optimization, the number of parameters with their variable ranges is a main criteria to consider. A larger number of variables leads to time consuming optimization by increasing the total number of iterations in the design space to evaluate.

To estimate the total iterations, the amount of variables from each parameter should be multiplied together. For example, the window-to-wall ratio has a range between 20% and 90 %, with an incremental range of 10%, for each of the 4 facades of the high-rise.

Benchmarks

BENG Indicators for Residential Apartment

BENG 1	Energy demand	≤ 65 kWh/m².yr
BENG 2	Primary fossil use	≤ 50 kWh/m².yr
BENG 3	Share of renewable energy	≥ 40 %

TOjuli
Indoor temperature < 26 °C

Thermal Comfort > 90%

Diagram 5 *Benchmarks of the BENG regulations with the high-rise characteristics*

User Requirements

Schedule of occupancy
Working Day Schedule (Monday to Friday)
0:00 to 8:00 & 17:00 to 0:00

Weekend Schedule (Saturday & Sunday)
0:00 to 12:00 & 19:00 to 0:00

Thermal Comfort
PPD < 10
- 0.5 < PMV < + 0.5
Thermal Comfort > 90%

Temperature Range Summer (0.5 clo) 23°C - 26°C

Temperature Range Winter (1.0 clo) 20°C - 25°C

Ventilation (during occupancy)
Air flow rate: 7 l/s/person

Per room function

Function / Space	Ventilation Rate
Kitchen	minimum of 21 dm³/s
Living Room	0.7 dm³/s per m² floor space minimum of 7 dm³/s
Bedroom	0.9 dm³/s per m² floor space minimum of 7 dm³/s
Bathroom	minimum of 14 dm³/s
Toilet	minimum of 7 dm³/s
Circulation Area	minimum of 0.5 dm³/s per m²
Storage	minimum of 10 dm³/s per m²

Equipments per room function
Lighting (LED)
Households equipment and appliances

Relative air velocity
Maximum of 0.2 m/s

Daylight
> 300 lux
> 10% of the room area (minimum 0.5 m²)

Hot Water Consumption
61 litre/day/person

Diagram 6 *User comfort requirements and consumption in a household*

Zone	Equipment Load per Area W/m2	Lighting Density per Area W/m2
Kitchen / Living	30 + 5	3
Bedrooms	5	3
Bathroom	5	2
Hall	5	2
Sorage	5	2

Table 20 *Equipment loads and lighting density per function of the apartment in W/m2*

The total number of iterations is 8x8x8x8 = 4096.

The evaluation of all those combinations is unfeasible, considering that each simulation needs 25 minutes.

Therefore, the selection of the parameters ranges is adapted by either adjusting incremental steps for the ranges, reducing the variables to evaluate or disregarding non-relevant parameters.

Total High-Rise Height (meters)	160
Net Floor Height (meters)	3.3
Number of Floors	48
Last Floor Count under 100 meters	30th

Table 21 *Total high-rise geometry characteristics*

Climatic Data

To simulate the environmental conditions of the temperate climate in the Netherlands, the city of Amsterdam is used as the pilot location in this study. The implementation in the workflow is done by inserting the weather file .epw from the year 2018 in both of Ladybug (Sadeghipour Roudsari & Mackey, 2013) and Honeybee (Mackey, 2013) plug-ins.

Geometry Parameters

The total high-rise height is 160 meters, resulting from 48 floors of 3.30 meters net floor height.

For the compactness analysis, the reference plan (Figure 8) is readapted into 3 plan options (Figure 9) of shape factor FS equals to 1.2, 1.46 and 1.66, calculated by dividing the length by the depth.

To assess only varying compactness, all the plans have a constant fixed surface area of 698 m2, a total of 6 apartments per floor, in addition to identical distribution and floor area of each function (Table 22).

The additional orientation parameter will be applied with a range of angle between 0° to 180°, and an incremental step of 20° to reduce the total variables.

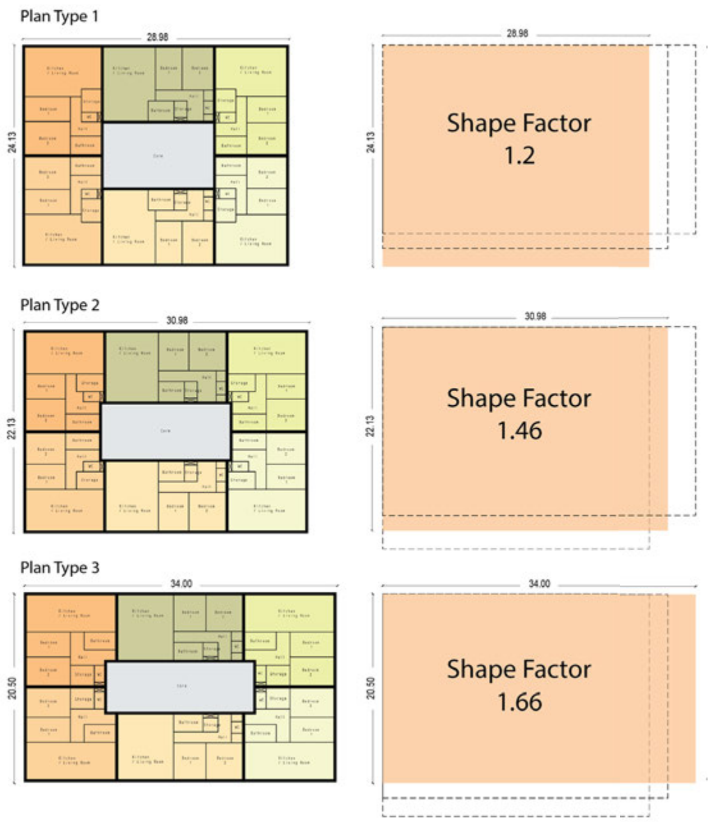

Figure 9 *Overview of the 3 plan types shape factor FS and Layout Distribution*

	Plan Shape	Area per Apartment (m2)	Floor Surface Area (m2)	Apartment per Floor	Occupant per Apartment	Max. Density (pers/m2)	Depth of Plan (m)	Length (m)	Depth (m)	Floor Height (m)	Ratio	Shape Factor SF
Plan Type 1 *Most Compact*	Square	105	698	6	4	0.2	6	28.9	24.13	3.30	1:1	1.2
Plan Type 2		105	698	6	4	0.2	6	31.9	21.85	3.30	2:1	1.46
Plan Type 3 *Least Compact*	Rectangle	105	698	6	4	0.2	6	34	20.5	3.30	3:1	1.66

Table 22 *Characteristics and shape factor of the 3 plan types*

Facade Parameters

For the design of an energy efficient facade, a highly airtight envelope of infiltration rate of 0.6 $dm^3/s.m^2$ is used (Nieman, 2020). In the case of this research, the simulation plug-in of Honeybee uses the air tightness metric with the building volume expressed in "Air changes per hour" ACH rate. For the conversion, the following equation (Raji et al, 2019) is used:

Quantity of fresh air (l/s) = Air change rate (ach) x Room volume (m3) x 1000/3600

With a minimal 14 m² area from the adapted referencial plan, the resulting air tightness corresponds to 0.15 ACH.

For the envelope opaque materials, the insulating properties are set as constant with the basic quality for the R-value of 4.5 m^2.K/W, and for the roof layer 6.0 m^2.K/W. For the non-facade related components, they are fixed values of 0.5 m^2.K/W for the partition walls and 0.8 m^2.K/W for floor/ceilings.

Regarding the transparent parts, 5 different glazing types serves as input variables, each with specific U-value, g-value and VLT (Table 23). The glazings with lower U-value are expected to minimize the heat loss through the facade during winter, by conserving indoor heat, and therefore lead to a decrease of heating loads. A high g-value leads to more solar gains during the summer period and can contribute to higher cooling loads. Therefore, lower values are expected to show more energy saving in cooling loads, but also indicate a better comfort level. Also, a higher VLT is expected to allow more daylight, and minimize the lighting demand.

Additionally to the glazing materials, the opening ratio WWR input is set to a range between 20 and 90%, with an incremental step of 10% (Figure 10). The available area for energy generating systems is related to the amount of left on the facade from the WWR. It is covered with PV panels of 20% efficiency corresponding to the crystalline silicon modules, and are also included on the roof layer with a surface covered at 75%.

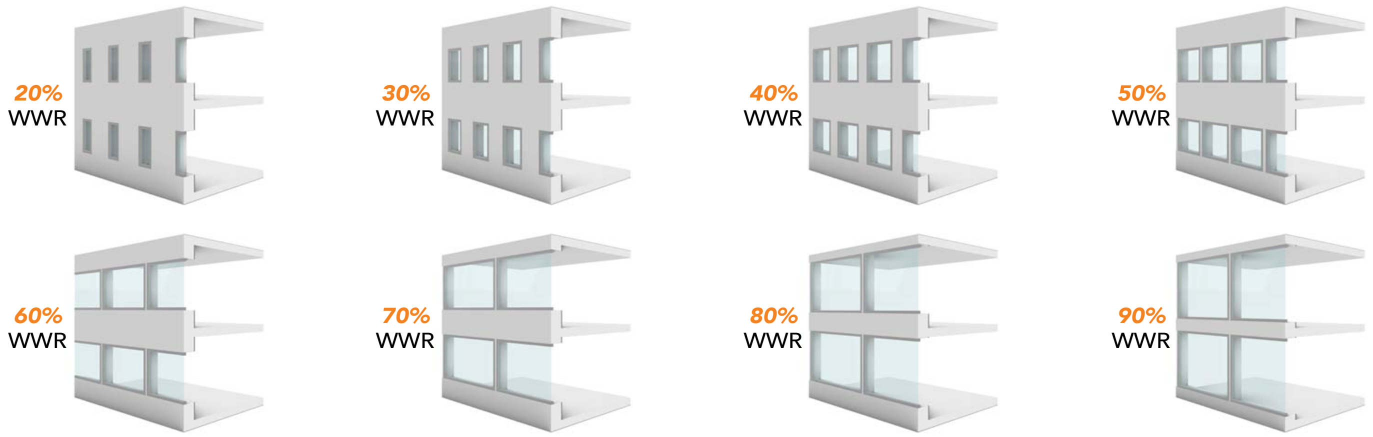

Figure 10 *Inputs for the glazing ratio ranges*

Glazing Type		U-value W/m²K	g-value -	VLT %
Type 1	Double Glazing HR 3% Emission	1.1	0.62	80
Type 2	Double Glazing Low-E	0.9	0.47	75
Type 3	Triple Glazing HR Argon fill 6/12/4/12/4 mm	0.7	0.5	69
Type 4	Triple Glazing HR Krypton Fill 4/12/4/12/4 mm	0.6	0.5	75
Type 5	Triple Glazing HR Argon fill 4/12/4/12/4 mm	0.5	0.7	72

Table 23 *Glazing types with their different characteristic values used for the simulation*

Also, for the facade parameters, 3 different types of shading systems are considered (Figure 11). Among them, 2 types are dynamically controlled; one positioned internally to the glazing, and the other externally.

These roller blinds operate when the indoor temperature exceeds the set point of 23 °C while the solar irradiation on the window is above 300 W/m² (Diagram 9). The internal blind is designed with a light colored fabric (white) of reflectance 60%, transmittance 40%, emissivity 90%, and a g-value of 0.33. The external blind has a medium colored fabric (greyish) of reflectance 20%, transmittance 15%, emissivity 90% , and a g-value of 0.53. The total amount of solar gains depends on the glazing types g-value. However, when positioned

on the external layer of the glass, it can be lower than in the case of an internal position. Both systems are expected to decrease the cooling loads, and increase the lighting loads.

The last type is a 400 mm extruded fin, positioned on the upper part of the windows frame, and mounted with additional PV cells, expected to decrease cooling loads, and generate more energy, but also affect the daylight distribution in the space.

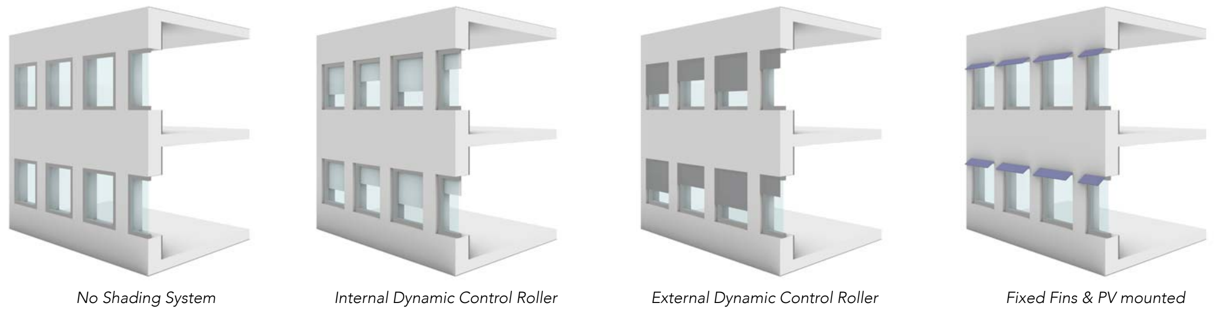

Figure 11 *Inputs for the different types of shading systems geometry*

Ventilation & Cooling/Heating

Regarding the ventilation, it is based on a hybrid system with natural ventilation through operable windows, and a system D mechanical ventilation with heat recovery. Their usage schedule depends on the indoor and outdoor climatic conditions.

The average yearly wind speed, according to the representative city of Amsterdam, is 5.3 m/s, with at highest an average of 7.0 m/s during the month of January (Appendix A, Table 1). For the natural ventilation, the indoor temperature should be within 21°C and 26°C, while 2 external conditions should be met. The wind speed should not exceed the maximum of 7.0 m/s, above which it is too windy, with its increase in speed that occurs with altitude (Diagram 9). Also, the minimum outdoor air temperature should be between 18°C and 27°C (Diagram 7).

As for the mechanical ventilation, the ventilation rates used for each room are set according to the user requirement (Diagram 6), and when the outdoor conditions are unfavorable for natural ventilation. Additionally, for heating and cooling, the set points, respectively of 21°C and 26°C, operate during occupancy, and the setbacks, respectively of 18°C and 28°C, when the space is non-occupied (Diagram 9). The mechanical system has a 95% heat recovery, and the integrated radiant floor system has a heating COP of 3.6 and cooling EER of 15. For the domestic hot water usage, a COP of 3.6 is used in this study, which could be of lower value if considering the high water temperature reaching 55 - 60°C.

Parameters

Climatic Data

Temperate Climate (*epw. file, year 2018*)

Geometry

High-rise Characteristics
Total height: 160 meters
Number of floors: 48 floors
Floor height: 3.30 meters

Plan Shape
Fixed 698 m²
6 apartments per floor
4 persons per apartment

Shape Factor
SF 1.2 (Plan Type 1)
SF 1.46 (Plan Type 2)
SF 1.66 (Plan Type 3)

Orientation Angle from North Axis
Between 0° and 180°
Incremental range of 20°

Facade

Air-tightness (Infiltration Rate)
Hghly airtight facade 0.15 ACH
with consideration of wind speed per height

R-values (Envelope & Partitions)

External Walls	4.5 m².K/W
Roof Layer	6.0 m².K/W
Internal Partition	0.5 m².K/W
Floor/Ceiling	0.8 m².K/W

Glazing Type	**U-value**	**g-value**	**VLT**
Type 1	1.1	0.62	80%
Type 2	0.9	0.47	75%
Type 3	0.7	0.5	69%
Type 4	0.6	0.5	75%
Type 5	0.5	0.7	72%

Window-to-Wall Ratio
Range between 20% and 90%
Incremental step of 10%

Energy Generating System
Facade: PV of Efficiency 20%
Roof covered at 75% with PV of Efficiency 20%

Shading Systems
Type 1
Internally Controlled Roller Blind (white fabric)
• Indoor temperature > 23°C
• Solar irradiation > 300 W/m2
g-value 0.33, *total depend on glazing type*

Type 2
Externally Controlled Roller Blind (grey fabric)
• Indoor temperature > 23°C
• Solar irradiation > 300 W/m2
g-value 0.53, *total depend on glazing type*

Type 3
Externally Extruded Fin (400 mm) mounted with PV

Ventilation & Heating/Cooling

Natural Ventilation
Windows opening: 0.3 fraction of total glazing
Wind speed < 7.0 m/s
Minimum indoor temperature: 21°C
Maximum indoor temperature: 26°C
Minimum outdoor temperature: 18°C
Maximum outdoor temperature: 27°C

Mechanical System
Cooling EER = 15
Heating COP = 3.6
Heat Recovery Efficiency = 95%
Cooling Set point: 26°C
Heating Set point: 20°C

Water Heating
COP = 3.6

Diagram 7 *Parameters to be used as inputs in the simulation and optimization*

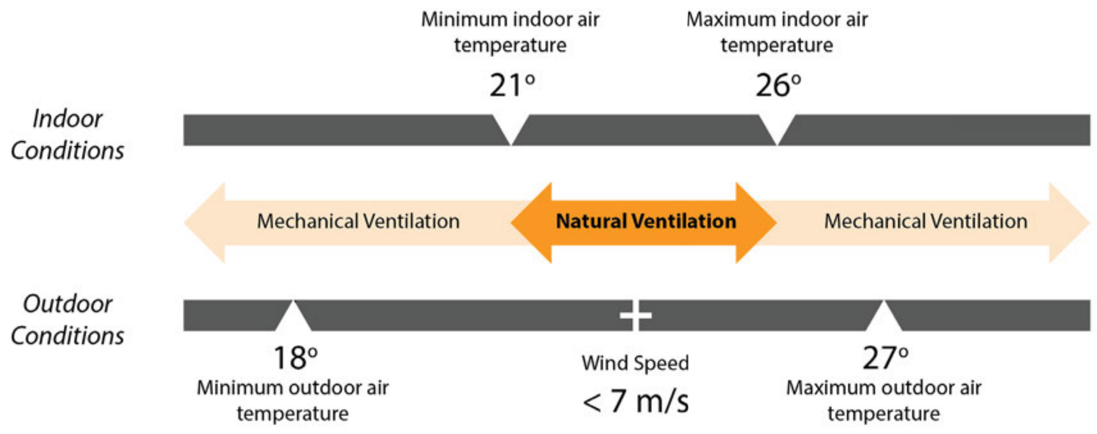

Diagram 8 *Condition diagram of the set points for natural ventilation NV and mechanical ventilation MV*

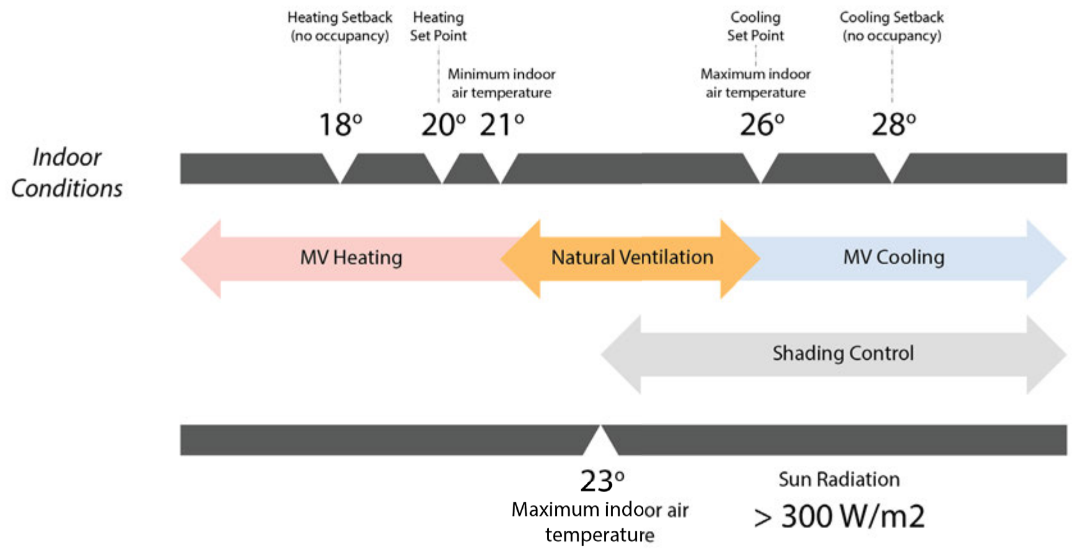

Diagram 9 *Set points scheme for natural ventilation NV, mechanical ventilation MV and shading control*

2.9.3. Micro-Climate Analysis

Among the changing micro-climatic conditions, the temperature fluctuates in parallel to the height, with an acceleration in the wind speed occurring in altitude.

Temperature Fluctuation

The levels located at higher altitude are subjected to a decrease in the air temperature, known as the temperature lapse rate. The annual temperatures recorded for the 4 zones middle floor of 5th, 17th, 29th and 41th are presented in the Graph 9. In fact, from the bottom to the top floors, it is observed that the range of temperature decreases considerably. Lower temperature ranges are recorded at higher altitude, indicating a minimum of -11.78ºC at the 41th floor (level of 135 meters), whereas in the lowest part, indicated by the 5th floor (level of 16.5 meters), the minimal temperature reached is -5.23ºC.

The fluctuation in temperature to which the high-rise is exposed will affect the energy consumption, in which higher heating demand is expected in parallel to the height increment to reach comfortable indoor temperature range.

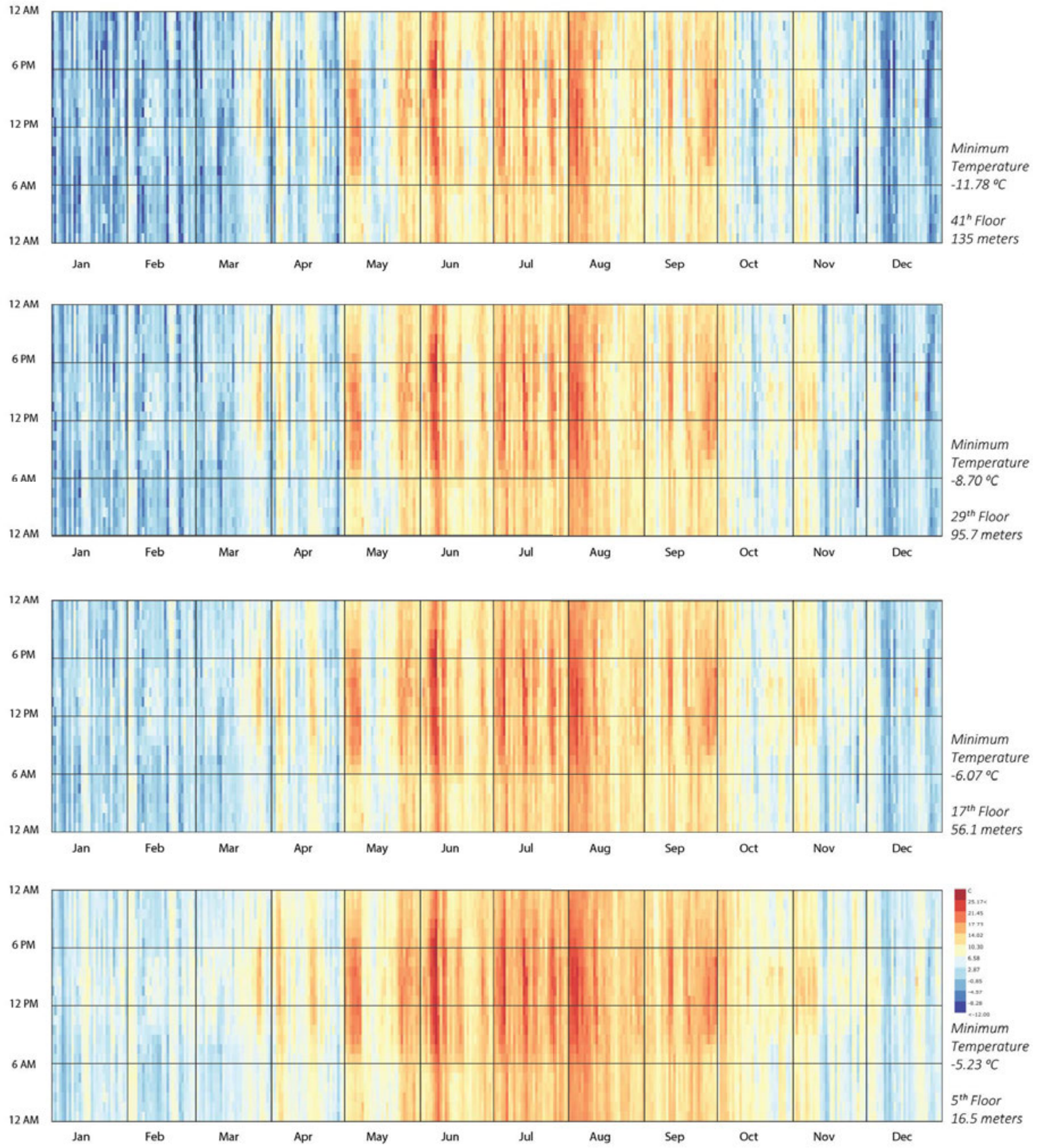

Graph 9 *Outdoor temperature in parallel to height increment for the middle floor of each zone, with the minimal annual recorded temperature, generated by Ladybug (Source: Sadeghipour Roudsari, & Mackey, 2013)*

3 Computational Design & Optimization

"...automation applied to an efficient operation will magnify the efficiency... (and) automation applied to an inefficient operation will magnify the inefficiency."

-Bill Gates

3.1. Computational Workflow

3.1.1. Computational Approach

Architectural Design Optimization (ADO) is the practice of merging parametric design modeling and building performance simulations, aiming at reaching the best performance design solutions in an automated process (Wortmann, 2019).

With the computational methodology, different disciplines are integrated under a single workflow; architecture, facade design and climatic design, by connecting multiple platforms and softwares. To do so, a parametric process is used, where all data are combined, allowing to transfer information in and out and ensure the efficiency of the system. In the process, the design is encoded through the computer language where numerical values refer to parameter variables, geometry and energy data.

3.1.2. Parametric Modeling

Compared to low-rises, the assessment of the energy performance of a high-rise involves more complexity in decision taking where the impact of the surrounding context and micro-climate conditions vary at different levels, additionally to the several interrelated design parameters. Within the advantages of the computational approach, the environmental conditions are simulated by the implementation of weather data extracted from external sources, and in this case, representative of the city of Amsterdam.

For the creation of the workflow, a correct continuity of the data is followed depending on the type of information that needs to be transferred from a sequence to another. Among the integrated data are the high-rise geometry and design parameters, in addition to the energy, daylight and ventilation simulations.

A hierarchical order is employed in the workflow, from small scale to larger scale, i.e. from the floor plan geometry creation to the completion of the high-rise building, and to the integration of the different contextual geometries. The modeling of the single floor is based on the selection of plan layout and includes all the design parameters to assess. The energy simulations are then applied on this single floor. Once all data are checked to ensure that no error occurred, the workflow is extended to the larger scale to generate the totality of the high-rise.

From this point, any modification or alteration in the geometry, parameter ranges or addition of data is automatically updated to the remaining script, providing the instant control of the workflow. Therefore, contrary to a manual methodology of work that demands more labor, the automated process requires less time to alternate between designs, and thus, allows to reach solutions in a faster way. In results, the generated iterations can be instantly visualized and evaluated in regard to the performance of the high-rise design.

3.1.3. Softwares and Plug-in

For the integration of the different disciplines required for this study, the following softwares and plug-in presented in figure 3.01 are selected, and their role in the workflow is described as following:

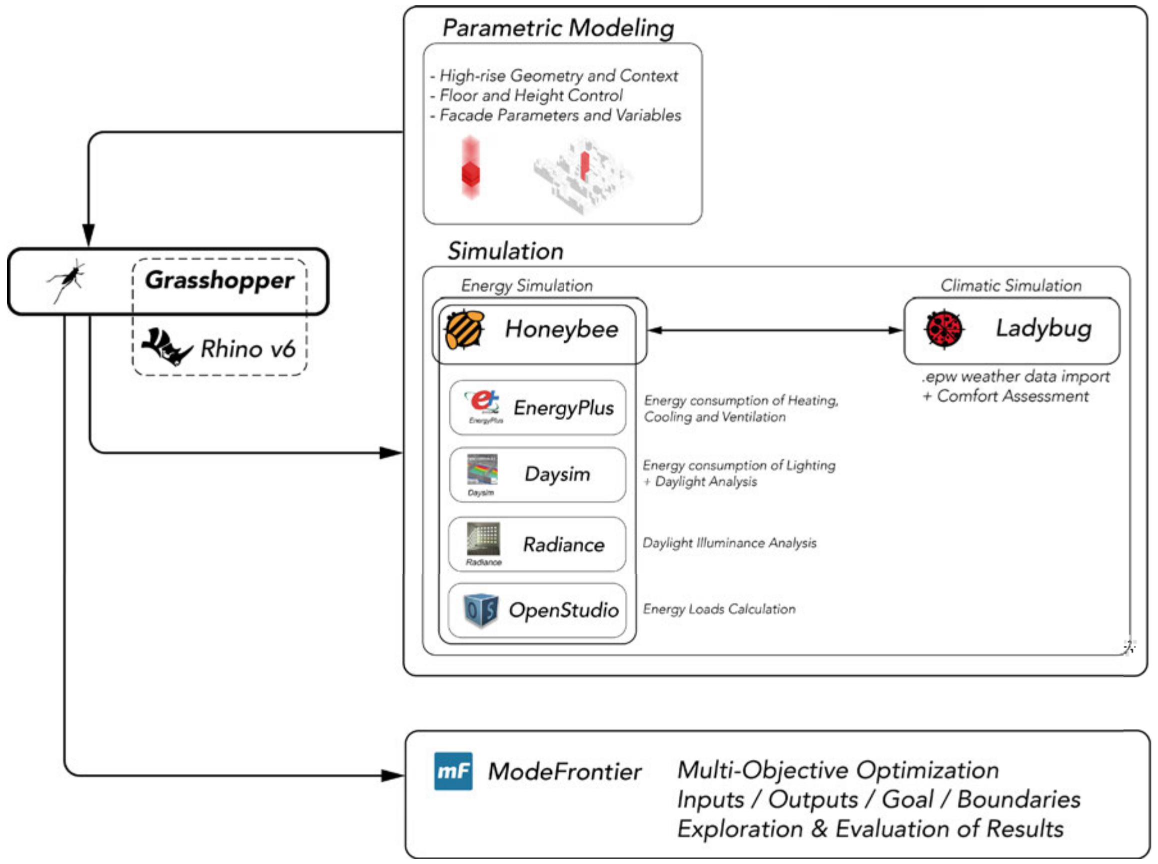

Diagram 11 *Softwares and plug-ins scheme implemented in the workflow*

Grasshopper
Grasshopper is a plug-in platform that runs in the software Rhino v6, mainly used for parametric modeling. In the advantage of designers, Grasshopper is a 3D representative programming environment where all operations are visualized in Rhino. Therefore, all graphs, diagrams and design models are extracted directly from the workflow space. In this research, Grasshopper is used as the node interface to link internal and external platforms into a single design space, from which the plug-ins Ladybug and Honeybee.

Ladybug Plug-in Version 0.0.68 (January_01_2020)
To simulate the climatic and environmental conditions, Ladybug is used to import the weather data (.epw file) of the city of Amsterdam, with a database from the year of 2018 (Onebuilding, 2020), into the Grasshopper workflow. Several environmental analyses of the air temperature and the wind speed relative to the high-rise's height are conducted with graphical representation. Additionally, within the scope of this study, it presents the possibility to model the PV energy generating systems, the heat recovery and domestic water usage. Finally, for the determination of the user's comfort, the PMV, PPD and adaptive comfort are calculated.

Honeybee Plug-in Version 0.0.65 (January_01_2020)
Another plug-in operating within the platform of Grasshopper is Honeybee. It is used for the daylight and thermodynamic modeling that are assessed in the early design stages and the facade features. In this study, Honeybee simulates the energy, comfort and ventilation by connecting to external simulation engines of EnergyPlus and OpenStudio, as well as daylight and lighting simulations by using Radiance and Daysim. As most of its components operate parametrically, the modeling of the opening ratios, glazing types, material properties and dynamic shading devices are done through Honeybee. Also, the different schedules of occupancy, equipment and lighting are defined through it. Also, the energy performance data of consumption and generation are calculated as outputs to be later exported to the optimization platform.

Radiance
Radiance is one of the external simulation engines used in Honeybee for the daylight and lighting simulation giving access to analyze and visualize the design in terms of numerical data and color based images. Within this platform, the scene geometry, floor surface, material properties, lighting schedule, climate conditions (sky conditions) and analysis period are set as inputs. In the case of this research, the calculation is done for a yearly period to meet the requirements for both winter and summer seasons. Thus, the visual comfort is assessed by the daylight factor and the lighting demand.

Daysim
In combination with Radiance, Daysim allows to predict the annual daylight of the design for the indoor visual comfort, where the surrounding buildings and shading devices can be included as context objects to reach more accurate results.

EnergyPlus
EnergyPlus is a thermal simulation engine based on thermodynamic equations rather than graphical results. It is used for a wide range of features in this study. Thermal and energy simulation are analyzed by this platform to calculate the heating and cooling loads. Also, it is possible to implement contextual geometries such as surrounding buildings and shading systems. In addition, the effect of the wind speed and temperature difference in parallel to the height are included in the simulation process which affect the natural ventilation factor (Saroglou, Meir, & Theodosiou, 2017).

OpenStudio
In order to merge all the Radiance-based lighting simulation and EnergyPlus energy simulations in Honeybee, OpenStudio acts as the cross-platform combining all the results together to calculate the outputs for the total lighting, ventilation, heating, cooling loads as well as the energy generated.

modeFRONTIERv2019
The optimization part is conducted externally to Grasshopper, by linking and internalizing the workflow data inputs and outputs in the external platform modeFRONTIER2019 by ESTECO. All of the input parameters ranges to be evaluated are defined, in addition to the objectives and constraints benchmarks. Within the black box of the workflow setting, several optimization algorithms are provided for the exploration and evaluation of the results, as well as tools for visual representation of the design solutions.

3.2. Set-Up of the Workflow

3.2.1. Modeling Phase

Part of the workflow consists of the modeling of the apartment floor with the integration of all the design parameters previously mentioned in "2.9. Conclusion: Benchmarks and Simulation Parameters". Following, the total high-rise geometry is generated from the single floor, with additional zone divisions of the total high-rise and the gradual floor addition. For the contextual analysis, the surrounding is modeled to implement the building on site.

3.2.1. a) Surrounding Context Modeling

For the modeling of the surrounding buildings, the urban location is extracted from Google Map 2020, from a residential area of the city of Rotterdam (Google, 2020) (Appendix H, Figure 1). The layout is first drawn in Autocad 2018 in 2D, then the 3D shapes are generated in Grasshopper.

There are 3 types of surrounding context include; type 0, type 1 and type 2, corresponding respectively to low-rises, mid-rises, and high-rises ("Figure 12 Modeling of the 3 types of surrounding buildings"). The range of values determining the minimum and maximum height that a building in the surrounding can take are based on the number of floors from the definition in "2.2. High-Rise". The total height is calculated for a net floor height of 3.60 meters. Finally, each context can be selected separately depending on the phase of the research being analyzed.

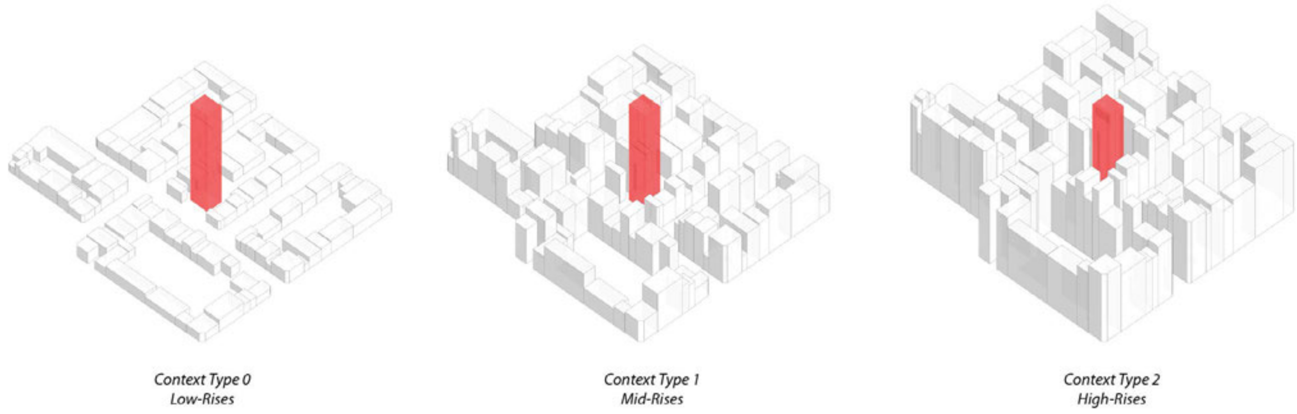

Figure 12 *Modeling of the 3 types of surrounding buildings*

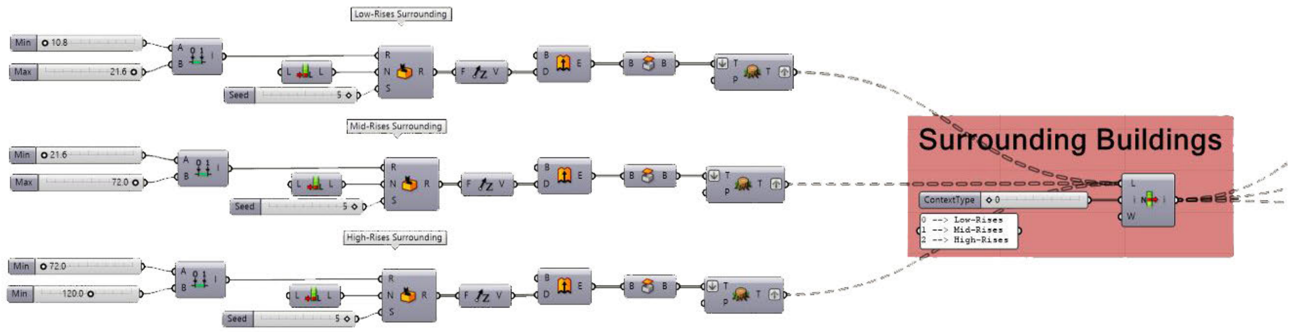

Figure 13 *Part of the workflow of the modeling of the 3 types of contexts (source: Grasshopper)*

3.2.1. b) Apartment Floor Plan Modeling

There are 3 types plans analyzed in this study, with different compactness (Figure 9), which are first drawn in 2D in Autocad 2018. The translation into 3D geometry is done by extruding each room function individually in Rhino v6. To be read by Honeybee, the resulting 3D solids are converted into HBzones (Honeybee Zones) through the component “Honeybee_Mass2Zones” (Figure 16). All the zones of similar functions are assigned in groups for ease of selection, resulting in several groups of zones as following; Kitchen/Living, Bedroom A, Bedroom B, Bathroom, WC, Storage, Hall, Shafts and Core (Figure 17).

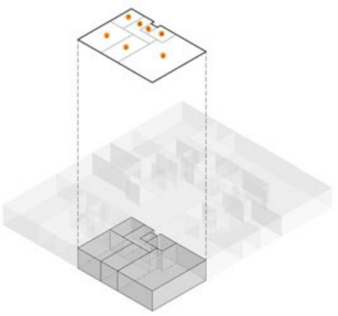

Figure 14 *Overview of the Modeling of a Single Apartment of the total Floor*

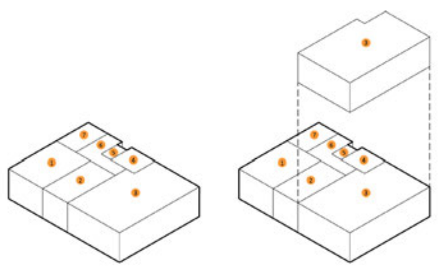

Figure 15 *Modeling of each Zone of the Apartment as a closed 3D Shape*

In addition, each group of zones requires the specification of the “ZonesPrograms” assigned as “MidriseApartment: Apartment” to all functions that require schedule of occupancy, equipment and lighting. However, the core and the shafts are specified as “MidriseApartment: Corridor” where those data are not required.

In Grasshopper, modeling each room independently leads to coplanar internal walls. Therefore, in Honeybee, the component “Honeybee_SolveAdjc” allows to solve the adjacencies between the spaces to determine surface elements and categorize them as external walls, internal walls, floor, ceiling, roof or ground floor. This step ensures that there are no duplicate elements or gaps left between the geometries that can lead to errors during the simulation and the energy performance calculation.

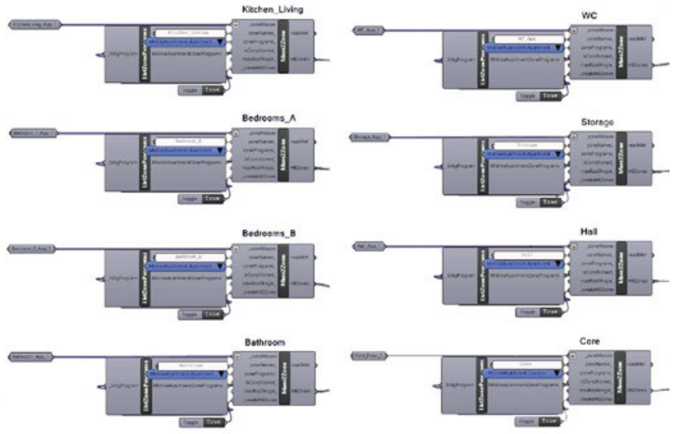

Figure 16 *Part of the workflow for the creation of the HBzones (Source: Honeybee)*

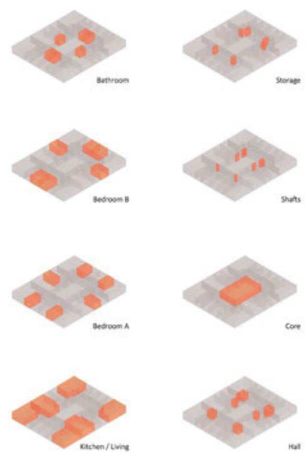

Figure 17 *Group of HBzones categorized by function type (source: Grasshopper)*

Additionally, the labeling is added with the component “Honeybee_LabelZones” which will rename each created zone by its given name in the HBzones creation. In this case, the labeling is done by the function type and are numbered counterclockwise from 0 to 5.

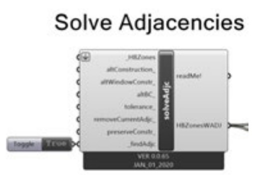

Figure 18 *Part of the workflow for solving adjacencies between the HBzones (source: Honeybee)*

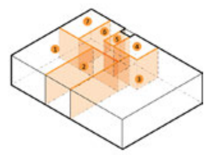

Figure 19 *Solved adjacencies between the HBzones of a single apartment in Honeybee*

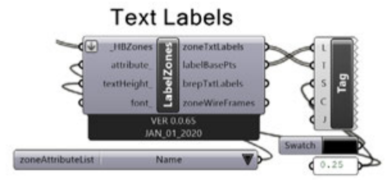

Figure 20 *Part of the workflow for zone labeling by function of the HBzones (source: Honeybee)*

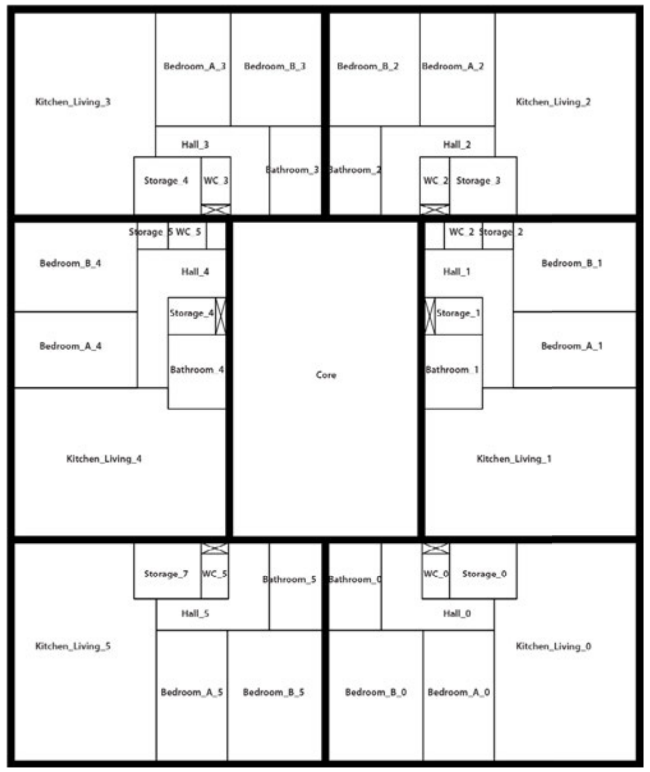

Figure 21 *Plan view of the apartment model with the label zones by function and Nnumbering counterclockwise (source: Grasshopper - Honeybee)*

Adiabatic Boundaries

Adiabatic walls or components are defined as boundaries that prevent all thermal transfer from a space to another. In Honeybee, the component "Honeybee_MakeAdiabaticbyType" is connected to the total HBzones to define the elements to be set as adiabatic boundaries (Figure 22). In this case, floors and ceilings are modeled as adiabatic elements as they are considered to separate well-insulated heated spaces, with floor heating systems integration and intemedian technical level between each storey. Therefore, there is a very minimal thermal transfer between consecutive floors, presenting the advantage to reduce the simulation calculation time.

It is important to note that defining adiabatic boundary to construction elements means that the same boundary condition is applied to both sides of the zone, and not by eliminating heat transfer to a zero-heat flux. However, all other elements with external and internal walls are prone to heat transfer and not defined as adiabatic boundaries.

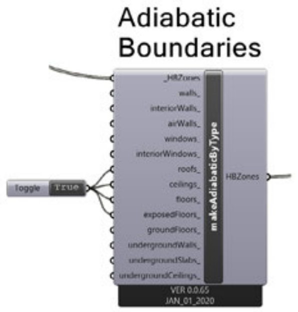

Figure 22 *Setting of adiabatic boundaries between HBzones (source: Honeybee)*

Rotating

Part of this study focuses on analyzing the impact of the orientation of the high-rise from the North axis. Therefore, there are 2 ways of including the rotation of the geometry; either with the component from Grasshopper "Rotate" or from Honeybee "Honeybee_RotateHoneybee". Both methods were tested to check the translation of the information in the workflow.

In results, it was observed that the Grasshopper method leads to error in the following step when the window-to-wall ratio and glazing distribution among the facades are defined. In fact, each facade is identified in Honeybee for facing the North, South, West and East, whereas in Grasshopper the identification of the facade is not included. Thus, it is essential to rotate the floor geometry plan prior to applying the glazing and window distribution to ensure the correct continuity of information flow. The rotation angle range of this study is stretched from 0° to 180°. For the incremental step of 20°, it is later specified in the optimization platform of modeFRONTIER2019.

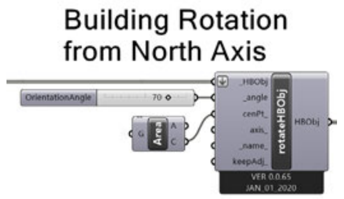

Figure 23 *Part of the workflow for the orientation of the modeled geometry (source: Honeybee)*

Move Floor

Similarly to rotation angle, moving the geometry of the floor plan created is done by adding the component "Honeybee_moveHoneybee". Moving the final created floor geometry serves the control for the height increment, and the modeling of the total high-rise.

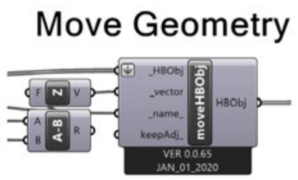

Figure 24 *The positioning of the floor geometry (source: Honeybee)*

Glazing Ratio

For the modeling of the opening, the windows distribution, the ratio per facade orientation and the glazing types are assigned. It is generated in Honeybee with the component "Honeyee_glazingCreator" where several inputs are required as standard to be followed when applying later the window-to-wall ratio. First, the breakup between windows is set to true, to divide large windows into smaller ones for each zone, instead of combining them together. This allows avoiding glazing larger than 2.5 or 3 meters wide as it is not a common practice in residential buildings. The window's height is set to 1.5 meters, with a still height of 0.60 meters underneath. In the case of this research, all those parameters are kept constant and just the ratio is a variable. Note that the visual comfort can be impacted from these glazing features.
The percentage of WWR for each facade orientation, North, West, South and East, is done with the component "Honeybee_GlazingParametersLists". The ratios are set with numbers ranging between 0 and 1, representing the percentage from 0 to 100. In this study, the range is set from 0.2 to 0.9, representing 20% to 90%.

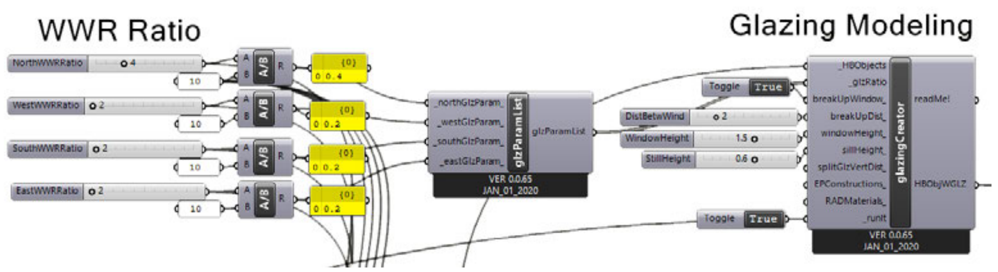

Figure 25 *Part of the workflow for the creation of the opening and window-to-wall ratio (source: Honeybee)*

Glazing Material Properties

The different types of glazing included for this study are defined in Honeybee with the components "Honeybee_EnergyPlusConstruction" and "Honeybee_EnergyPlusWindowMaterial" where the glazing properties are assigned. The properties are assigned for the U-value (W/m2K), the solar heat gain coefficient SHGC (g-value) and the visible transmittance VT (%) according to Table 23.

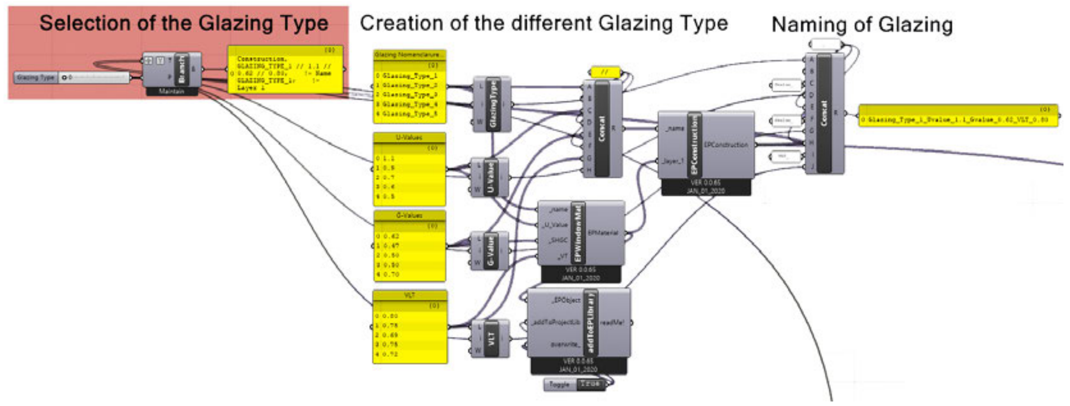

Figure 26 *Part of the workflow for the creation of the glazing types (source: Honeybee)*

Material Creation

The materials properties of all the building components for external wall, roof, internal separation, flooring and ceiling, are created with the component "Honeybee_EnergyPlusConstruction" and "Honeybee_EnergyPlusNoMassMat" where the R-value are assigned according to Figure 27.

Once all the materials and glazing types are created in the Energy Plus database, the building's elements are assigned to their corresponding materials by using the components "Honeybee_setEPZoneConstr" for external envelope and "Honeybee_setEPZoneIntConstr" internal elements.

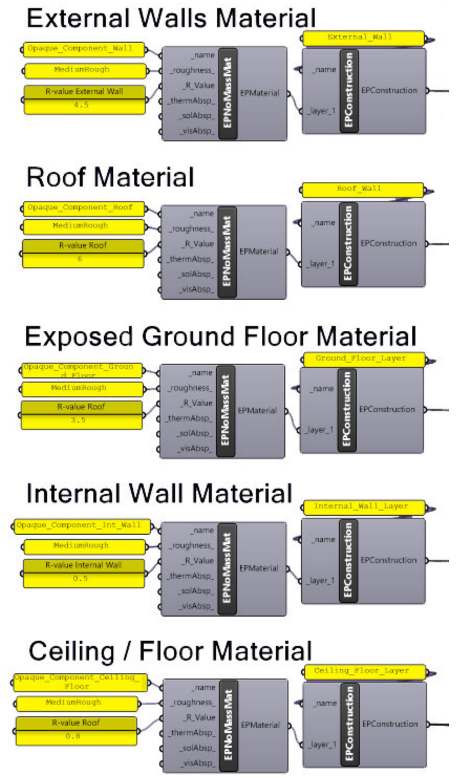

Figure 27 *Part of the workflow for the creation of the materials properties (source: Honeybee)*

Domestic Hot Water

To determine the amount of domestic water heating, the component "Ladybug_ResidentialHotWater" is used to extract the energy load per hour (in kWh) required to heat the domestic hot water consumption for each hour during a year.

As previously stated, in this study it is considered that an average of 4 persons occupy each apartment, resulting in 20 persons in total for 6 apartments per floor. From the literature study, 61 litre per day per person is needed, which results in 445300 litre per year for the total floor apartment. From the resulting value of Ladybug, the result is higher than the estimation with 506422 litre per year, as the consumption for the shower, dishwasher and washing can not be implemented manually but are presented as standard in the plug-in.

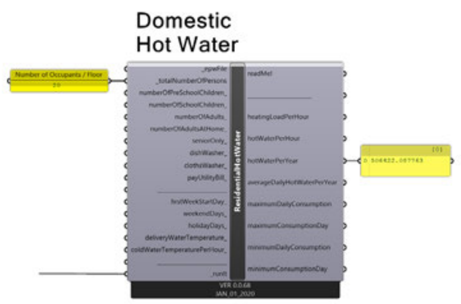

Figure 29 *Part of the workflow for the calculation of domestic hot water (source: Ladybug)*

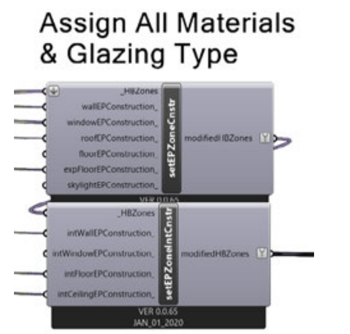

Figure 28 *Part of the workflow for assigning the created materials (source: Honeybee)*

Energy Generation

For energy generation, the photovoltaic panels PV are modeled with the component "Ladybug_ PhotovoltaicSurface" and applied to the remaining surfaces on the facades from the WWR and the roof layer, covering 90% out of the total surface and an efficiency of 20%. As for the mounting type, the configuration is set to insulated back behind the PV, with the presence of the walls. From the outputs, the AC energy per year is calculated in kWh.

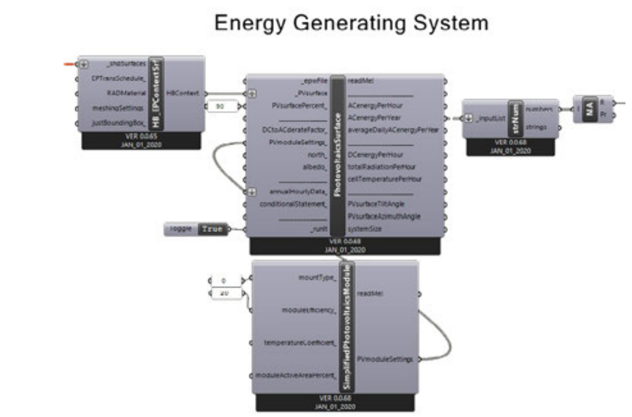

Figure 30 *Part of the workflow for the creation of the PV panels on the facades and the roof in Ladybug (source: Ladybug)*

Shading Devices

The different types of shading systems (Figure 11) are modeled with the component "Honeybee_ EPWindowShade". The properties and dynamic control are assigned according to the parameters in Figure 31. In addition to the 3 types evaluated, the absence of a shading system is added to serve as a reference to compare with the other types.

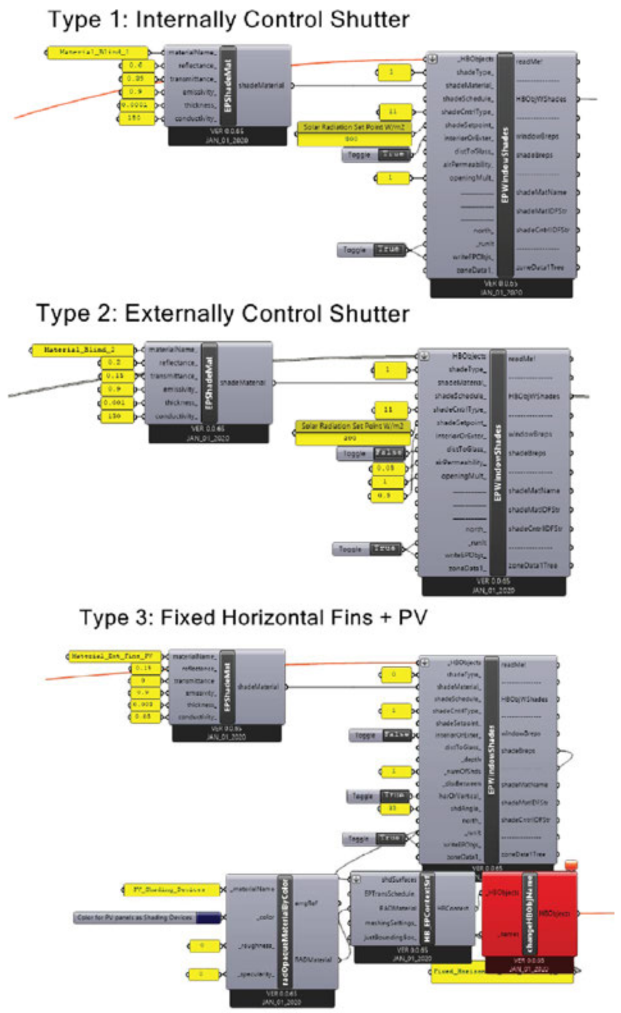

Figure 31 *Part of the workflow for the creation of the shading systems (source: Honeybee)*

3.2.1. c) Total High-Rise Geometry and Zones Modeling

For this research, the total high-rise height consists of 160 meters, indicated by 48 floors. In order to analyze the performance of the building regarding the design parameters and the micro-climate conditions in parallel to the height increment, several analyses are required.

In this case, simulating the 48 floors is time-consuming. Therefore, the modeling of the total high-rise is divided into zones (Table 24), from which the middle floors are extracted to apply the simulation and the optimization, and facilitate the research process. To do so, the accuracy of the results and the calculation time will be compared for 3, 4 and 8 divisions (Figure 46).

	Zone 3	Zone 4	Zone 8
Number of Zones	3	4	8
Total Number of Floors	48	48	48
Floors per Zones	16	12	6
Height of Each Zone	52.8	40	20
Zones < 100 meters	2	2.5	5
Zones > 100 meters	1	1.5	3

Table 24 *Overview of the zones divisions characteristics*

3 Zones		4 Zones		8 Zones	
Zone Number	Middle Floor	Zone Number	Middle Floor	Zone Number	Middle Floor
1	8	1	6	1	3
2	24	2	18	2	9
3	40	3	30	3	15
		4	42	4	21
				5	27
				6	33
				7	39
				8	45

Table 25 *Level of the middle floors extracted from the zones, depending on the amount of division*

3.2.2. Energy and Daylight Simulation

Simulation Set-up

The BENG indicators are provided for a yearly period (Table 1). In this case, the energy and daylight simulations included in this study are performed accordingly in the workflow over an entire year. The total number of 8760 hours is related to the provided data from the weather file (.epw) of Amsterdam, 2018.

Parameter	Value	Unit
Hour of day START	0	Hour
Hour of day END	24	Hour
Breaks whithin the range	0	Hour
days/week	7	Day
hours/days	24	Hour
hours/year	8760	Hour

Table 26 *Period values of simulation and calculation time*

Energy Load and Infiltration Rates

In Energy Plus, several data loads are required for the energy simulation of the HBzones through the component "Honeybee_SetEPZonesLoads". The inputs are added according to the room functions (Figure 32).

First, the equipment load per area (in W/m2) represents the loads of the appliances used in the zones, as well as the lighting density per area (in W/m2), which are LED bulbs in this case. Also, the estimated density per area (in ppl/m2) is defined for the peak occupancy.

The infiltration rate per area facade (in ACH) is required for the zones provided with opening, representing the air infiltration through the facade. As the ventilation per area, it is set according to the rate by function type in Diagram 6.

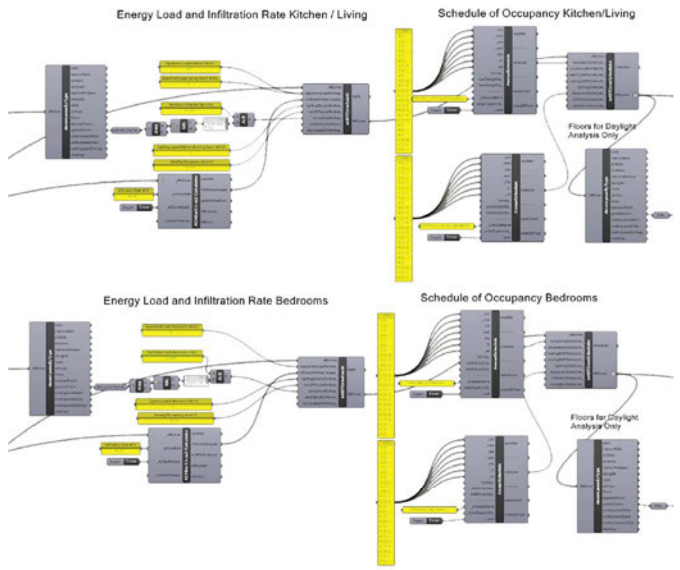

Figure 32 *Workflow for the simulation of the energy load, infiltration rate and occupancy schedule of each HBzones (source: Honeybee)*

Schedule of Occupancy and Equipment

The component "Honeybee_SetEPZonesSchedules" is used to assign the occupancy and equipment schedules for each function (Appendix B, Table 2). In EnergyPlus, any value above 0.2 is considered as occupied.
For the lighting schedule, it is generated from the workflow, only for the zones with openings located on the perimeter of the plan such as the kitchen, living room and bedrooms, according to the result of the daylight analysis. For an average amount of lux under the setpoint of 300 lux, while being occupied, the lighting control recipe of Honeybee will automatically conclude that the artificial lighting system should be turned on to meet the visual comfort of the user. For the spaces occupied during the night, there is no need to provide 300 lux between the period of 21:00 to 7:00, which is inserted in the occupancy inputs of "Honeybee_ ReadAnnualResults". For the rooms without access to daylight, such as the bathroom, WC, hall and storage, the lighting load will be defined by the occupancy schedule assigned for those zones.

Daylight Simulation

The visual comfort of the space is determined in Honeybee by the combination of daylight simulation recipe and artificial lighting control (Figure 33). The daylight simulation is applied to the zones on the envelope perimeter that have access to natural daylight through windows, which in this case are the bedrooms, living and kitchen spaces. The daylight is calculated for a yearly period with the component "Honeybee_ AnnualDaylightRecipe" and applied on the floor surface of the HBzones. The component "Honeybee_ RunDaylightSimulation" is added to the sequence to generate the daylight recipe of the yearly values.

The selected surfaces are divided with "_gridSize" into a mesh grid of points. The simulation uses the grid based analysis to get an annual result of the cumulative radiation values received by each point. Thus, the smaller the grid size, more refined, the greater the amount of points created which increases the calculation time, while it provides more accuracy. Also, the "_distBaseSrf" indicates the distance above the floor surface where the calculation is desired to be run. In this case, the grid size created is of 0.7 meters, with a distance of 0.1 meters above the floor level. Lastly, the "_radParameters" represents the radiance characteristics, presented in the following section.

From this part of the workflow, the daylight factor sDA (%) is calculated for the selected zone to determine whether the visual comfort is satisfied or not, and create the adapted artificial lighting schedules accordingly. The spatial daylight autonomy sDA factor represents the percent of analysis points across the analyzed floor surfaces that meet or exceed the illuminance threshold value of 300 lux for at least 50 % of the analysis period.

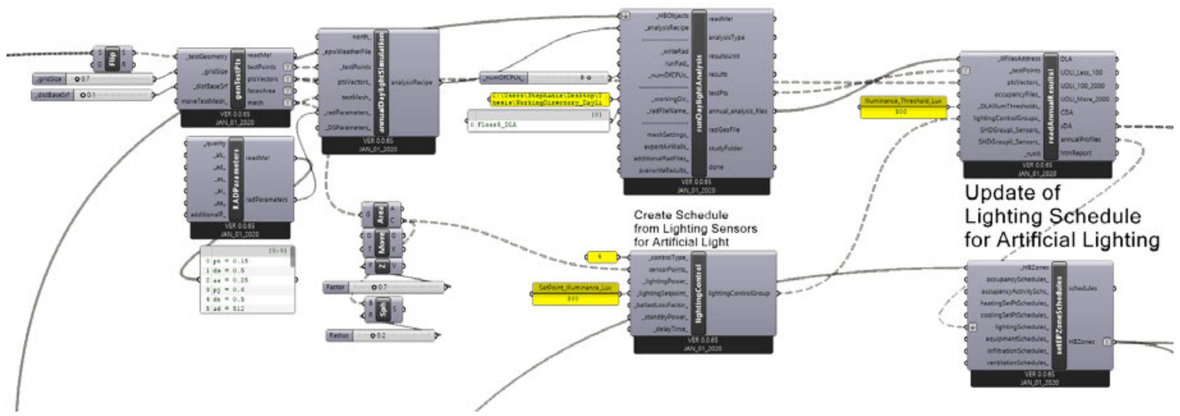

Figure 33 *Part of the workflow for the daylight simulation (source: Honeybee)*

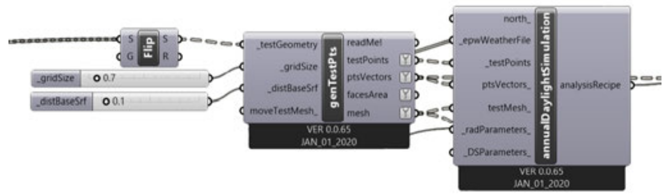

Figure 34 *Part of the workflow for the creation of the test points grid for the daylight simulation (source: Honeybee)*

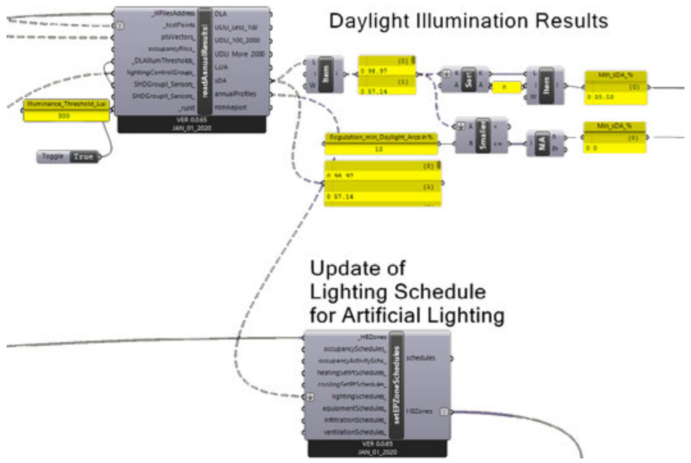

Figure 35 *Part of the workflow for the creation of the artificial lighting schedule based on the daylight simulation (source: Honeybee)*

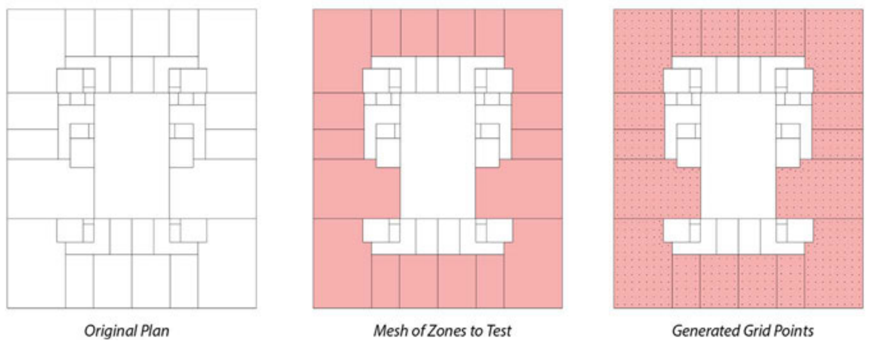

Figure 36 *Creation of the test points grid for the daylight simulation for the HBzones provided with windows (source: Honeybee)*

Artificial Lighting Control

Part of the lighting simulation consists of balancing the available daylight with artificial lighting to generate its usage schedule. It is based on the automatic control of the artificial lighting to meet the visual comfort requirements when the illuminance threshold is not reached, while saving energy. From the test point grid, one sensor point is created in the center of each room at a distance of 0.7 meters above the floor surface. Adding more than one sensor point provides more accuracy as a room with great depth might get a low illuminance level in corners, however the calculation time will increase.
The control type is set to an auto-dimming of the lighting system and switching off based on the occupancy schedule. When the benchmark of 300 lux is not met during occupancy, the artificial lighting is turned on automatically at the given time of day and the schedule is updated accordingly with the component "Honeybee_LightingControlRecipe". If the space is unoccupied, the lighting is switched off.

Daylight Calculation Time

The daylight simulation makes up for most of the calculation time. The process behind the lighting rendering time is based on the radiance parameters. In the component of "Honeybee_RadParameters", default values for ambient parameters are used, Figure 37. From these inputs, there is the quality level that can be set to low, medium or high. In this case, the value is set to 0 for "Low Quality". The "ab" is the ambient bounces, representing the amount of time that the daylight will reflect in the space, the "ad" is the amount of ambient divisions, "as" is the ambient super-samples, "ar" is the ambient resolution and "aa" is the ambient accuracy.

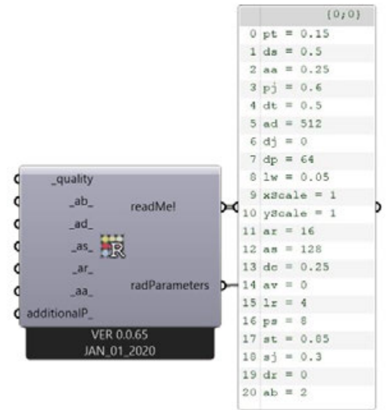

Figure 37 *Default values of the radiance parameters (source: Honeybee)*

In order to reduce calculation time, while achieving close to reality values, several tests are performed by altering those parameters. The results are compared in order to reach the set of values of the rad parameters to validate the daylight part of the workflow. By applying the standard values provided in Table 27, the calculation time increases progressively from "min" values to "max". The "max" settings are disregarded for the -aa and -ar as they require a very expensive amount of time and can disable the optimization process, which can lead to errors. In fact, setting the -aa ambient accuracy to the maximal accuracy value slows down the simulation, while the "max" value of 0 disables the irradiance interpolation algorithms used by Radiance and provides wrong results.

Parameter	Description	Min	Fast	Accur	Very Accur	Max
-ab	ambient bounces	0	0	2	5	8
-aa	ambient accuracy	0.5	0.2	0.15	0.08	0
-ar	ambient resolution	8	32	128	512	0
-ad	ambient divisions	0	32	512	2048	4096
-as	ambient super-samples	0	32	256	512	1024

Table 27 *Ambient parameters values of the radiance setting (source: Jacobs, 2012)*

Radiance Parameters Values

With the highest parameters used for "simulation 6" (Figure 38), the ambient division is set to 2048, ambient accuracy 0.08, ambient resolution, super samples to 512 and ambient bounces to 5. This set of parameters provides "very accurate" results, while presents a disadvantage in the calculation time of 5 minutes, considered above the average compared to other tests of average time of 25 seconds. To compare, the results of simulation 6 is used as the reference test with the highest accuracy.

As observed in figure 3.31, the results of the simulation 4 and 5 indicate a poor distribution of the daylight among the space, due to the cancelation of the ambient bounces set to a value of 0. In both simulations 8 and 9, the ambient bounces of 1 resulted with a poor distribution of the daylight into the depth of the space, where the amount of lux in the internal corners is lower. From the simulation test 1, 2, 3 and 7, the total calculation time is around 25 to 30 seconds which is acceptable for a 5 seconds difference. Therefore, the values are checked according to the reference test 6 to validate the parameters. Out of those results, the closest to the "very accurate" amount of lux is the test number 7 that had resulted with the closest values, and its inputs are used accordingly for the radiant parameters.

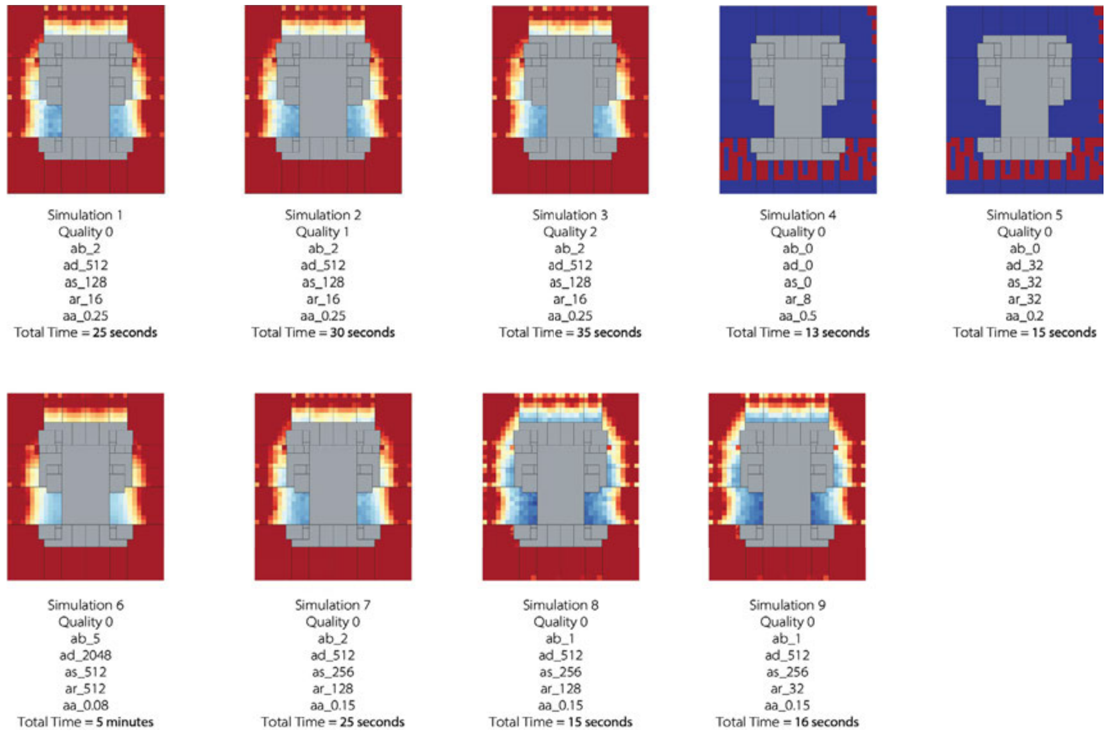

Figure 38 *Results of the daylight simulation tests under different radiance parameters in Honeybee (source: Honeybee)*

Natural Ventilation

Through the plug-in Ladybug, the natural ventilation NV is simulated with the component "Ladybug_ setEPNatVent" depending on the internal and external conditions that need to be met. First, the outdoor temperature has to be within a range of 18°C and 27°C, with a maximum allowable wind speed of 7.0 m/s. For the conditional equations, some Python coding is used for writing equations under the form of "If… Then…".

The outcome indicates values of 0 for "no, the conditions are not met" and values of 1 for "yes, the conditions are met". The result provides a schedule of the total number of hours during the year where the above conditions allow for the NV. Some climatic data needed for this simulation are extracted from the component "Ladybug_WindSpeedCalculator" that indicates the wind speed above ground and direction at the floor level being analyzed. Also, for more accuracy of the urban conditions, the terrain type is set to "City" representing a large city centre, with 50% of buildings above 21m over a distance of at least 2000m upwind. In addition to the external conditions, the indoor temperature needs to be within the range of 21°C and 26°C. The type of natural ventilation is set to "window opening" with a fraction of 0.3 of the total glazing ratio.

If all of the above conditions are met, then natural ventilation is provided. However, in the case that the temperature or the wind speed do not allow for it at a certain time, the mechanical ventilation is activated to make up for the natural ventilation.

Mechanical Ventilation

The mechanical ventilation MV is simulated when the previous conditions for natural ventilation are unfavorable. Thus, from the Python equation, the remaining number of hours corresponds to the activation of the MV, and are translated into a schedule. Note that the alternation between MV and NV is only required for the zones that are provided with direct opening through the facade, which are the kitchen/living and the bedrooms in this case. For the other functions, the ventilation is only based on a mechanical system. With the component "Honeybee_HVACSystem", the HVAC system properties are assigned to those HBzones, requiring the type of HVAC system used, the air, heating and cooling details.

For the HVAC system, the "Radiant Floors + DOAS" is selected, and represents 2 parallel systems. The first one DOAS, dedicated outdoor air system, provides the ventilation from the fresh outdoor air, and the second system represents the radiant heating/cooling system such as the underfloor system. In addition, according to the parameters in Diagram 7, the heat recovery effectiveness is set to 95%, the COP to 3.6 and the EER to 15, as well as the different temperature set points and setbacks.

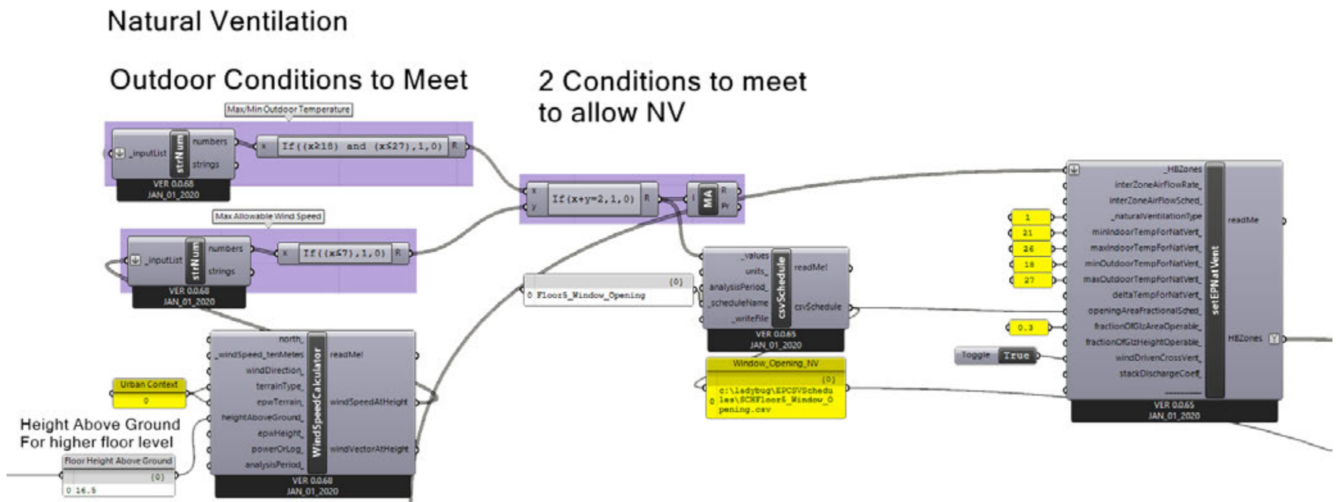

Figure 39 *Part of the workflow for the simulation of the natural ventilation (source: Ladybug)*

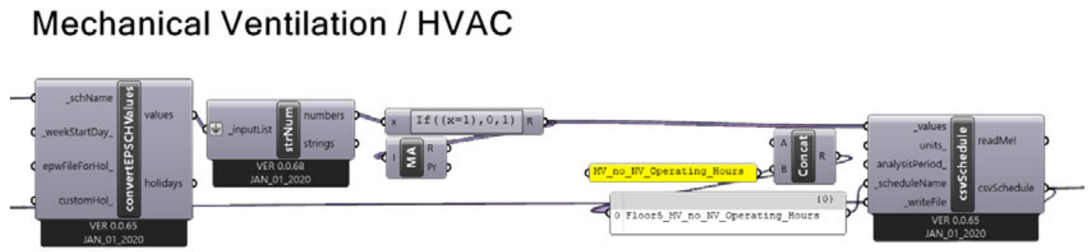

Figure 40 *Part of the workflow for the simulation of the mechanical ventilation (source: Ladybug)*

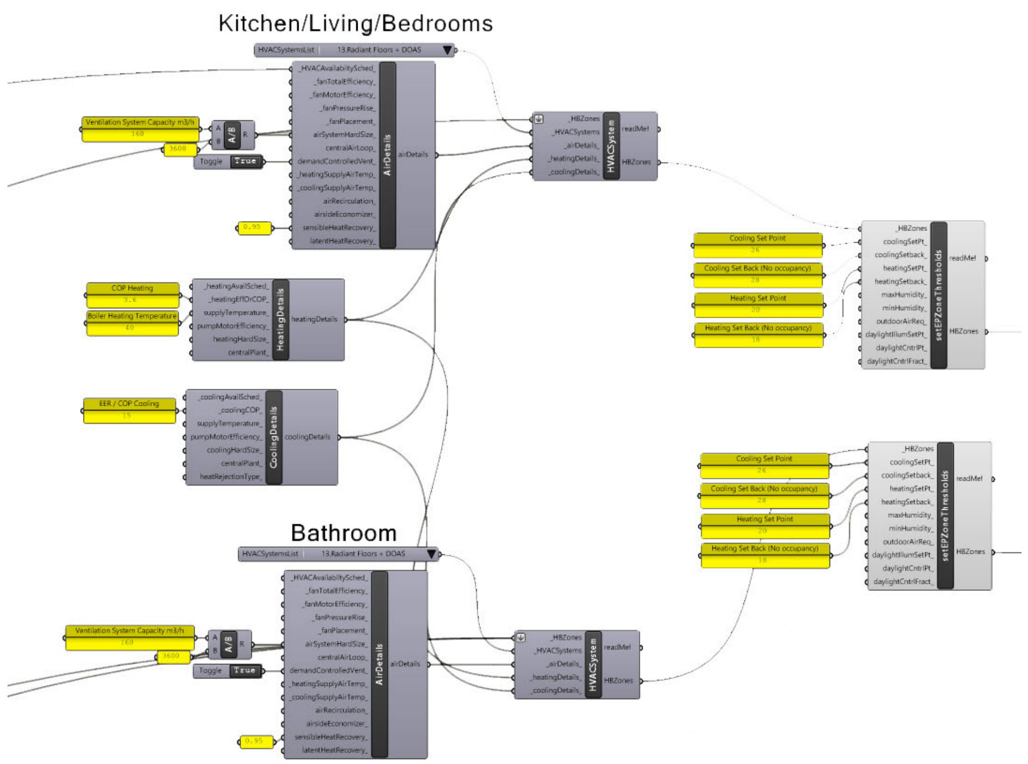

Figure 44 *Part of the workflow for the simulation of the mechanical ventilation and the HVAC system parameters (source: Ladybug)*

3.3. Outputs Extraction

From the outputs required for this research are the different energy loads, the determination of the BENG indicators, as well as comfort related data such as the thermal and visual (Figure 42).

Energy Loads

With the plug-in Open Studio, the heating, cooling and lighting loads (kWh/m²) are calculated over a yearly period consumption. Part of those data such as the cooling and heating are provided by Energy Plus and are determined for the total floor rather than a breakdown by zones function due to the mechanical systems modeled as centralized. The initial values are given in kWh, and then divided by the total floor area (m2) to get the results in kWh/m².

BENG Indicators

The calculation of the 3 BENG indicators is based on their definition in “2.1.2. BENG Regulations”. The total energy demand of BENG 1 is determined by the sum of the heating and cooling loads in kWh/m₂. For the calculation of the primary fossil energy of BENG 2, the energy used for heating, cooling, electrical lighting, ventilation and water heating are added together, and calculated with the COP and EER to include all energy loss through transmission and transfer. Additionally, the renewable energy calculated in BENG 3 is subtracted from its total result which gives the final results of the BENG 2 in kWh/m2. The generated energy of BENG 3, the amount of renewable energy is divided by the total sum of both the renewable energy and primary fossil energy and expressed in percentage %. Also, according to the regulations, for the TOjuli, the maximal indoor temperature recorded on the floor is extracted.

User’s Thermal Comfort

By using the component “Ladybug_Adaptive Comfort Parameters”, the European (EN-15251) standard comfort level is used with a comfort class set to 90 % acceptability of comfort, and an offset of plus or minus of 3°C acceptable.
Part of the benchmarks are related to the thermal comfort of the user, represented by “the percent of time comfortable” calculated for an annual period, during the occupancy schedule. Additional data are extracted such as the percent of time too cold and percent of time too hot.

User’s Visual Comfort

As previously mentioned, the visual comfort is determined by the extraction of the sDA that should be above 10%.

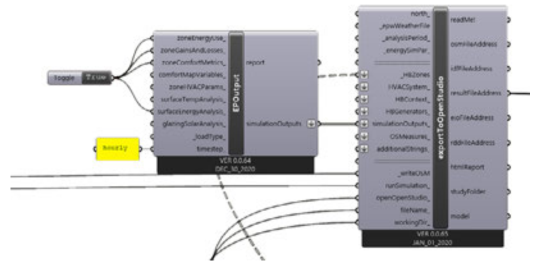

Figure 41 *Part of the workflow for the extraction of outputs (source: OpenStudio)*

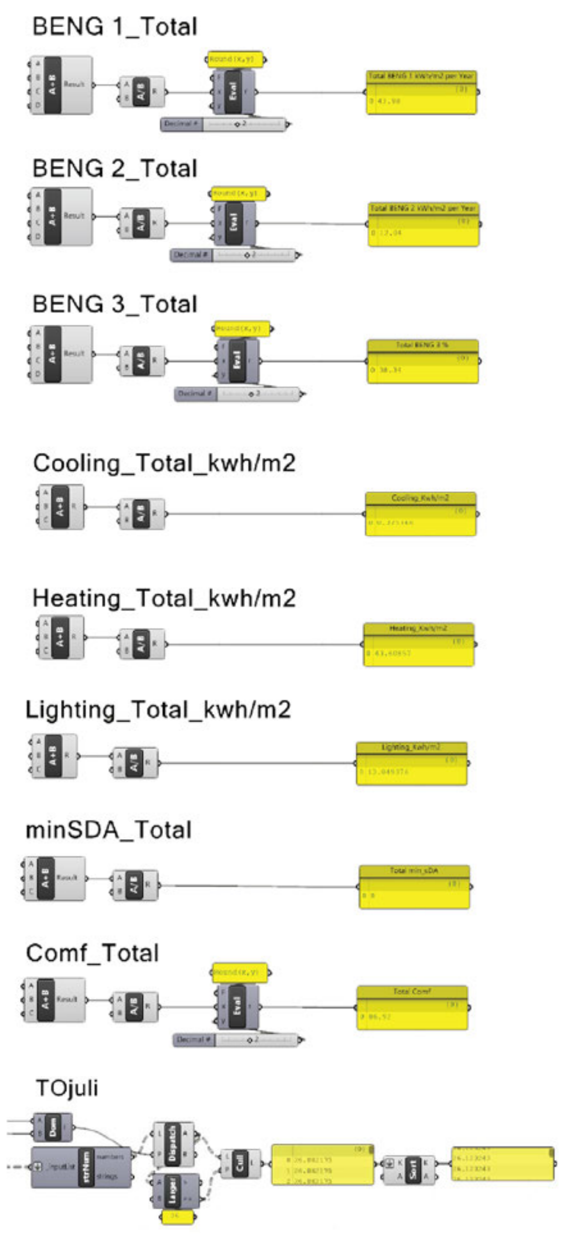

Figure 42 *Part of the workflow for the extraction of outputs (source: Grasshopper)*

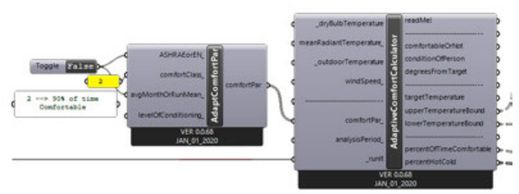

Figure 43 *Part of the workflow for the determination of comfort level and percent of too cold or too hot (source: Ladybug)*

3.4. Optimization Process

3.4.1. Methodology

To proceed with the optimization phase, the previously calculated outputs are extracted from the Grasshopper workflow and transferred to modeFRONTIERv2019 platform. Following, the objectives and constraints of the study are defined according to the benchmarks (Diagram 5). For the objectives, the indicators BENG 1 and 2 are set to be minimized, and BENG 3 to be maximized (Appendix E, Diagram 5). For the constraint, the user’s thermal comfort should provide a minimum of 89% (Appendix E, Diagram 6).
For the optimization process, several criteria should be considered regarding calculation time, methodology and results accuracy. Working with a multi-objective optimization MOO, and several parameters, under a short period of time led to divide the total research into phases. In fact, merging all the parameters into a single phase to run an optimization necessitates a large period of time to calculate, due to the wider design space. Thus, the optimization of the parameters related to the early design and the facade is processed into steps to speed the study, as well as facilitate the analysis of the design impact on the objectives.

3.4.2. Steps of Optimization and Research Process

The total research is organized into 6 main phases (Appendix I, Table 9), organized in a chronological order as each one provides data and end-results to be used for inputs of the following phase:

Phase 0: Assessment of the Zone Divisions
Due to the large amount of time required for the simulation of the total building with 48 floors, the high-rise geometry is divided into 3, 4 and 8 zones, from which the middle floors are extracted to simulate the different height levels and to speed the research process. To assess the division impact, all other parameters are kept constant and the outcome will point out which amount of zones should be selected to ensure high accuracy of the results in the study.

Phase 1: Early Design Stage: Compactness and Orientation
For the early design parameters, with all other parameters kept constant, the effect of the plan geometry compactness is assessed by testing 2 plan layouts of different shape factors. In addition, the orientation angle from the North axis is included in this phase as the total amount of design iterations does not enlarge the design space to be simulated.

Phase 2: Facade Performance under different Surrounding Contexts
In this phase, the energy performance of the lower part of the high-rise is assessed under 3 urban contexts of different height. The window-to-wall ratio of the middle floor (5th floor) of the lower zone of the high-rise is optimized under those low-rises, mid-rises and high-rises surroundings. As an outcome, the impact of the context on the facade treatment design is evaluated in relation to the energy performance regarding the regulation’s benchmarks.

Phase 3: Optimal WWR per level and facade orientation
Under a low-rise context, the WWR of each zone middle floor of the high-rise is optimized by the facade orientation and the height level. Under the changing micro-climate with altitude, the results will indicate, for each facade orientation, whether the ratios tend to increase, decrease or present a constant pattern from the bottom to the top of the building. As an outcome, the best design iterations of each zone are extracted to be used as input in the following Phase 4 to accelerate the process and by reducing the total iterations combinations.

Phase 4: Facade Parameters Optimization
With the resulting iterations of phase 3, the glazing types and shading systems from the facade parameters are applied to the extracted WWR iterations. The outcome provides the near optimal design parameters at the different height to be used for the final phase.

Phase 5: Energy Performance in respect to the Height Increment
To assess the impact of the height increment on the benchmark regulations, a gradual analysis of the floor addition is conducted with the final selected optimized design, in parallel to the energy performance and user’s comfort. The goal is to verify if the regulations present a constraint to the target height, and if so, indicate which indicators are responsible for this limitation.

3.4.3. Criteria for the selection of the algorithm

The selection aims at reaching high accuracy of the results, under a minimal amount of time. First, for the multi-objectives optimization of this research, there are specific types of algorithms that are better at solving many objectives under the constraints such as PilOPT. For that, the searching process for optimal solutions focuses on the area of the design space that is the closest to the objectives. Also, the greater the number of inputs parameters and variable ranges, the longer the time required to evaluate more iterations. Thus, combining different types of algorithms, where some provide initial result databases, and others refine the search closer to those selected designs, is in the advantage of this research methodology.

3.4.4. Optimization Algorithm

Design of Experiments DOE

The DOE Design of Experiments presents several types of algorithms in modeFRONTIER 2019, ranging from random selection, to manual user defined and more. The advantages of using the DOE are a better exploration of the wide range of the design space from a reduced, limited, range of test runs in a short amount of time, instead of running all the possible design variations. For this research, the user-defined DOE and the ULH are used for producing scattered variables values and data.

User-defined

In the user-defined DOE, the created table of experiments is manually defined, where all the variables and combinations are inserted according to the iterations that need to be evaluated, mostly in the case of predefined designs, such as the case of the geometry compactness and the orientation angle of Phase 1. The total number of designs is set in the configurations, and the lower and upper bounds correspond to the inputs ranges.

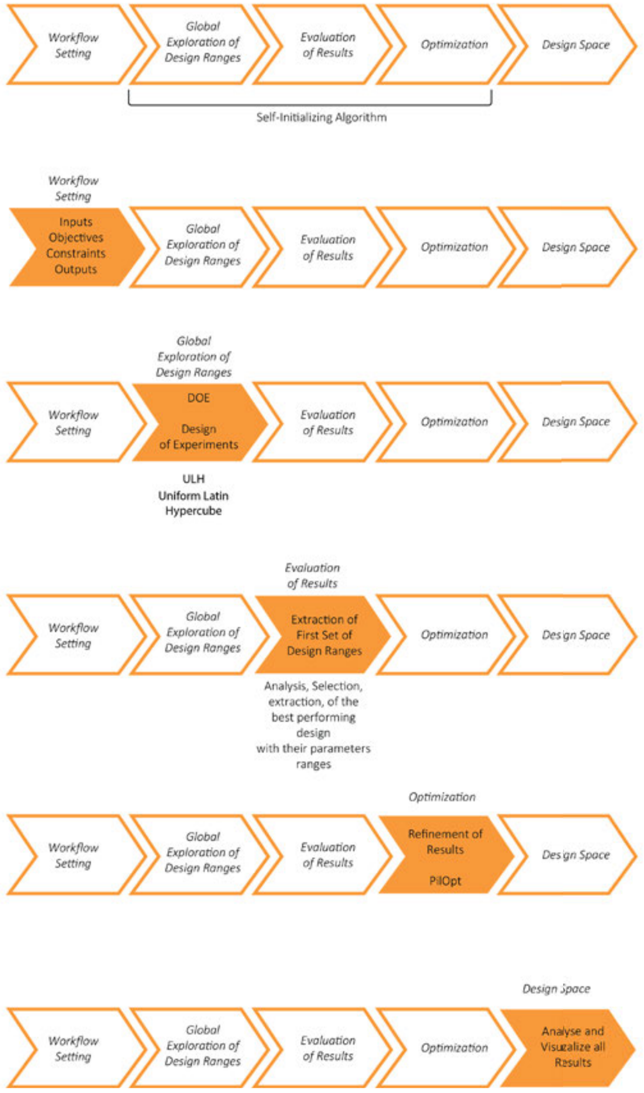

Diagram 12 *Scheme process of the optimization phase by steps*

ULH Uniform Latin Hypercube

With more complexity, for several parameters of many variables, the evaluation of all the iterations can take several days, even weeks, which is unsuitable for the short amount of time available. Therefore, the Uniform Latin Hypercube ULH creates a set of iterations that spread uniformly the variables, with a minimal correlation between variables. The advantage of this space filler algorithm is that it will give a wide range of combinations, without focusing on one depth of the variables ranges, but rather maximizing the distance between the generated designs, without duplications. The resulting primary database is used as the base of the following optimization algorithm. Additionally, the larger the population and size of iterations, the more accurate the results will be, thus it requires more time to calculate.

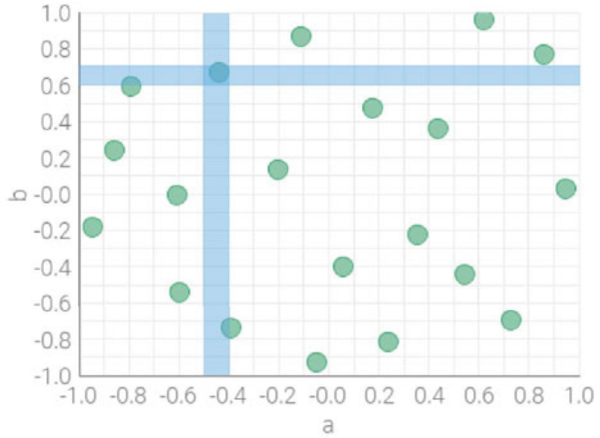

Diagram 13 *Representation of the Uniform Latin Hypercube ULH scattered variables (Source: modeFRONTIER)*

PilOPT

For MOO the PilOPT algorithm allows to focus the search both locally and globally among the variables, leading to a faster strategy to meet the objectives and respond to the given constraints. This algorithm can either work with a "Self-initializing" or "Autonomous" mode. The "Autonomous" mode stops searching for more iterations when the objectives or the Pareto Front has reached a state that cannot be improved anymore, whereas with "Self-Initializing" the number of evaluations is predefined manually. The advantage of the "Self-initializing" is that by setting the amount of evaluations, it is possible to assume the amount of time required for the calculation to be completed contrary to "Autonomous" where it can extend on several days, see even weeks of calculation due to the large amount of variables. As outcomes, by identifying the correlations between the range of variables, PilOPT explores the areas that are the most optimal for the given objectives and constraints, to provide the near-optimal designs.

3.4.5. Pareto Front

For the multi-objective study, the design solutions should satisfy both of the BENG indicators and the user's comfort. Commonly, MOO results are presented as Pareto fronts, where the range of solutions show the tradeoffs between the many objectives, aiming at balancing several goals. It is based on a graphical representation of the set of non-dominated results of the Pareto optimal. Although not all the objectives can be met by a single design, the Pareto front represents the many optimal solutions that are the closest to satisfy all the goals requirement. Those solutions are the dominated ones among all results, having reached certain of the objectives. The optimum set is reached when there is no further improvement possible to be made, unless a certain objective is prioritized over another. However, in the case where there are more than 3 objectives, it is more complex to validate all the results under a single space of the Pareto frontier. The Pareto method assists in the decision taking and development of the design guidelines by identifying the set of potential solutions of the multi-objective optimization problem, which corresponds to the Pareto-efficient designs, instead of the full range of parameters. In modeFRONTIER, the PilOPT algorithm optimizer evaluates the designs iterations, while instantly searching for the optimal designs to be distributed on the Pareto front. The resulting data are either dominating designs or the designs that it finds are neither dominant nor dominated.

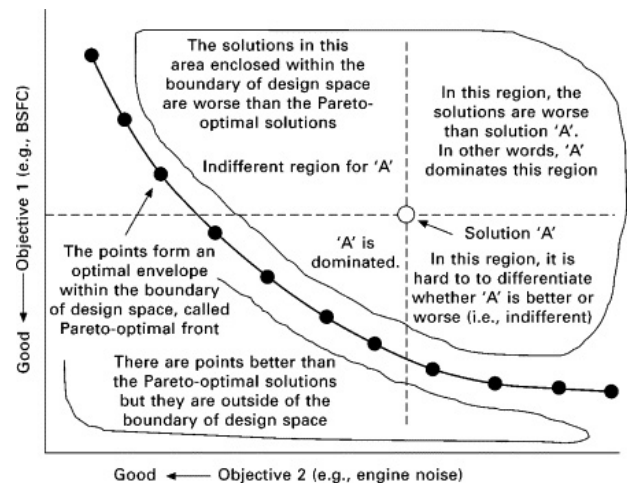

Diagram 14 *Position of the near-optimal designs on the Pareto Front according to objectives (Source: Xin, 2014)*

4 Simulation & Optimization Results

4.1. Climatic Data

The environmental conditions present background information for the design decision regarding the orientation of the building, the tackling of the facade and the analysis of the results according to the objectives.

4.1.1. Environmental Data

In the temperate climate of the Netherlands, the summers are quite cool with an average monthly temperature of 17°C in August (Appendix A, Table 1), and the winters are mild to harsh with an average of 3°C in February (Figure 45).

There is a variation of around 13°C between the average monthly temperature, with a yearly mean average around 10°C (Figure 45). Among the total daylight hours around the year, the total percentage of sunny days is 35%, whereas covered sky days are higher with 65%.

The East, South and West have the highest exposure to solar radiation and direct sun over the year (Diagram 15), above 440 kWh/m2, indicating that on these orientations the mounted PV would result in more efficiency for the energy generation. However, the North has the least exposure, with a maximal annual amount of radiation of 146 kWh/m2.

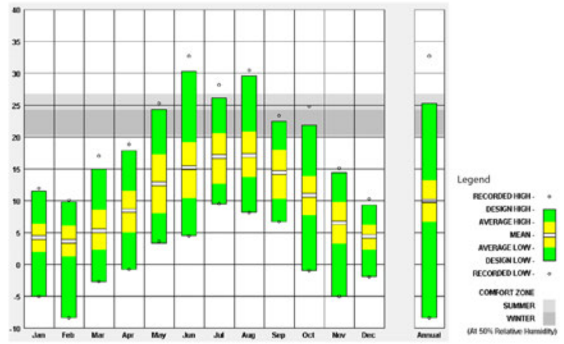

Figure 45 *Average monthly dry bulb temperature range for Amsterdam weather file of 2018 (source: ClimateConsultant 6.0)*

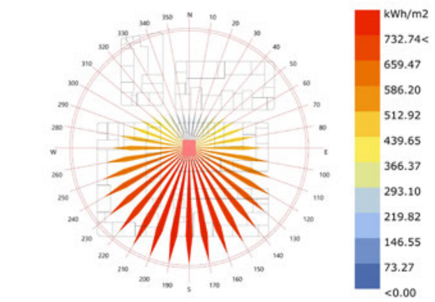

Diagram 15 *Total annual solar radiation rose for the site location (Source: Honeybee / Ladybug)*

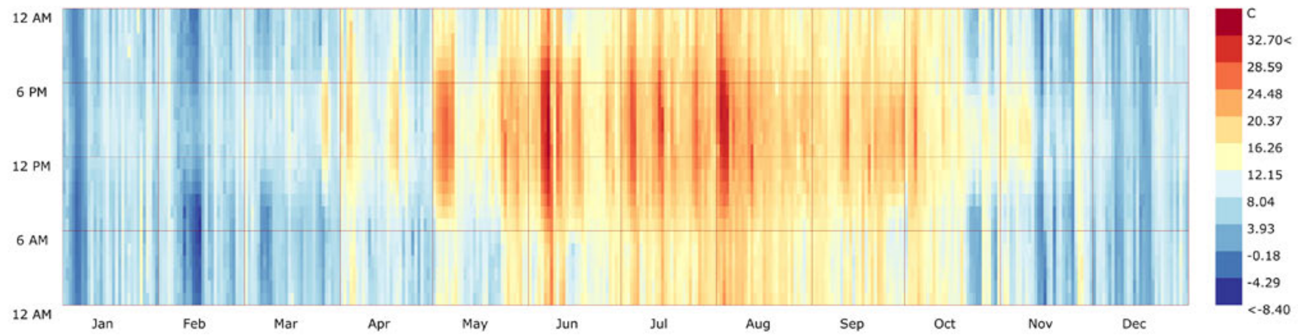

Diagram 16 *Hourly dry bulb temperature for Amsterdam location (Source: Honeybee / Ladybug)*

4.1.2. Ventilation Schedule

According to the internal and external environmental conditions previously mentioned in "2.9.3. Micro-Climate Analysis", a schedule is generated representing the total annual hours during which the natural ventilation is allowed through the opening of windows, as well as the number of hours for the usage of the mechanical systems. The annual schedules are extracted at different height levels of the high-rise on the middle floors of the 4 zones; 5th (at 16.5 meters), 17th (at 56.1 meters), 29th (at 95.7 meters) and 41th (at 135.3 meters), represented in the following Diagram 17.

At the lower zone 1 (5th floor), the mechanical ventilation MV indicates the lowest number of hours 8115 hours, in comparison to a higher allowable natural ventilation NV of 645 hours. As for the next zone 2 (17th floor), the schedule indicates a total of 8398 hours of MV and 361 hours of NV. The third zone 3 (29th floor) presents a total hours of MV of 8490 and NV of 270 hours. The last zone 4, representing the upper part (41th floor), has the highest amount of hours for MV with 8574, whereas the natural ventilation NV is at the minimum with 186 hours.

As observed, from the bottom to the top floors, the number of hours of NV decreases respectively from 645 to 186 hours. In response, the scheduled hours of the mechanical ventilation MV increases respectively from a total of 8115 to 8574 hours. In fact, The floors located in greater altitude are exposed to the wind speed acceleration and the temperature drop which affect the ventilation usage. In fact, it is less possible to open windows and take advantage of the natural ventilation. Thus, with more hours dedicated to mechanical ventilation over the year, a larger demand for its usage affects the energy consumption in upper floors.

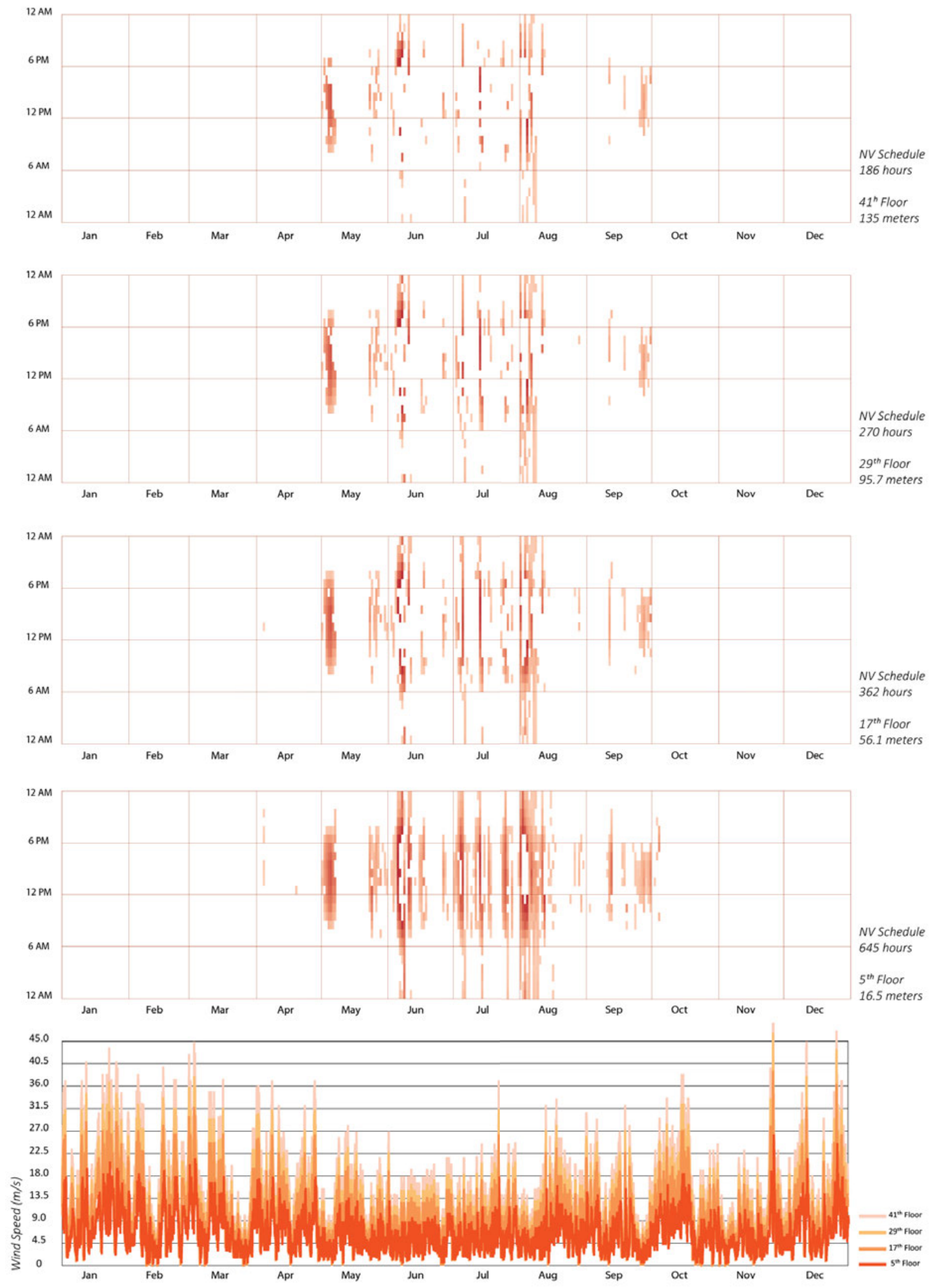

Diagram 17 *Wind speed in parallel to height increment with each zone natural ventilation schedule (Source: Honeybee / Ladybug)*

4.2. Phase 0 : Assessment of the Zone Divisions

Taking into account the 48-storey high-rise, and the high amount of time required to perform several simulations, the selection of several floors at different levels are used to analyze the building performance in parallel to the height. To do so, the total geometry of the building is divided into 3, 4 and 8 zones (Figure 46), from which the middle floors are extracted and then multiplied by the corresponding number of floors in the zone (Table 24). The final results for each zone are added together to represent the entire building.

The decision between 3, 4 or 8 divisions is based on the calculation time required for their simulations, as well as the accuracy of the extracted BENG and comfort values. In this case, all other parameters are kept constant to only provide the impact of divisions. Note that the relevance of the values to the study are disregarded. To compare the results, the following percentage difference formula is used, obtained by dividing the absolute value difference from each column by the average of those two preceding numbers:

$$\text{Percentage Difference} = \frac{|V_1 - V_2|}{(V_1 + V_2)/2} \times 100$$

Between 3 & 4, 3 & 8 and 4 & 8 number of zones, there is a larger range of difference, above 10%, between a division into 3 and 8 zones, whereas between 4 and 8 zones the difference is under 5% (Table 28). The more division applied to the building, the more time is required for the simulation and optimization. Considering the 4 zone-division, 65 minutes is needed in total, whereas with 8 zones it is 110 minutes. Therefore, to ensure a faster process and higher accuracy, the selection of 4 zone-divisions is implemented in this research.

BENG Indicators & Comfort Level	Number of Zones: 3	4	8	Percentage Difference between Zones: 3 & 4	3 & 8	4 & 8
BENG 1 kWh/m2	38.05	35.76	34	6 %	10.6 %	4.9 %
BENG 2 kWh/m2	34.96	33.71	33.58	3.6 %	4 %	0.4 %
BENG 3 %	34.3	34.65	34.72	1 %	1.2 %	0.2 %
Comfort Level %	80.1	79.44	79.74	0.8 %	0.5 %	0.4 %

Table 28 *Results of the BENG indicators and comfort level between different divisions of zone of the high-rise geometry*

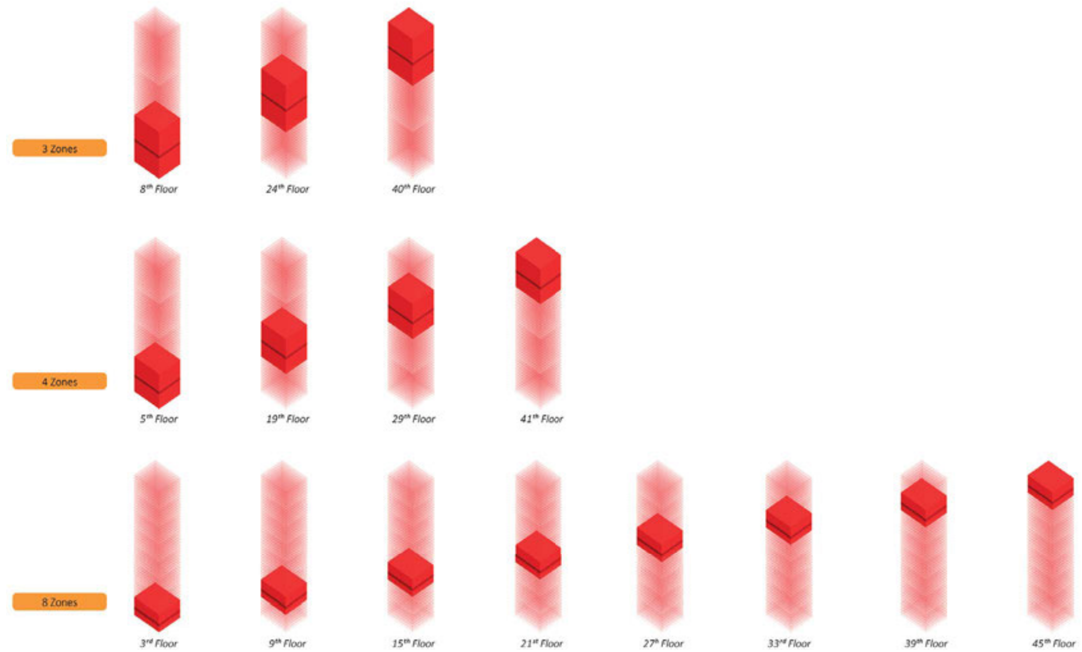

Figure 46 *Representation of the high-rise divided into 3, 4 and 8 zones*

4.3. Phase 1 : Early Design Stage: Compactness and Orientation

From the 3 adapted plan layout for the compactness study (Figure 9), the Plan Type 1 and Plan Type 3, respectively defined by a shape factor SF of 1.2 and 1.66, are selected in priority for this analysis due to the time-demanding of the simulations of the total high-rise. Additionally, the orientation angle is evaluated from the North axis, with its input range indicated in Diagram 18.

From the parameters included in the facade, a constant 40% WWR is used with the glazing type 1 (U-value 1.1 W/m2.K / g-value 0.62 / VLT 80%) and without shading system, as for the context it is represented by the low-rise surroundings.

By the end of the analysis of both plan types 1 and 3, the results presented a large margin of difference. Thus, the intermediate plan type 2 (SF 1.46) is evaluated for the verification and validity of those results.

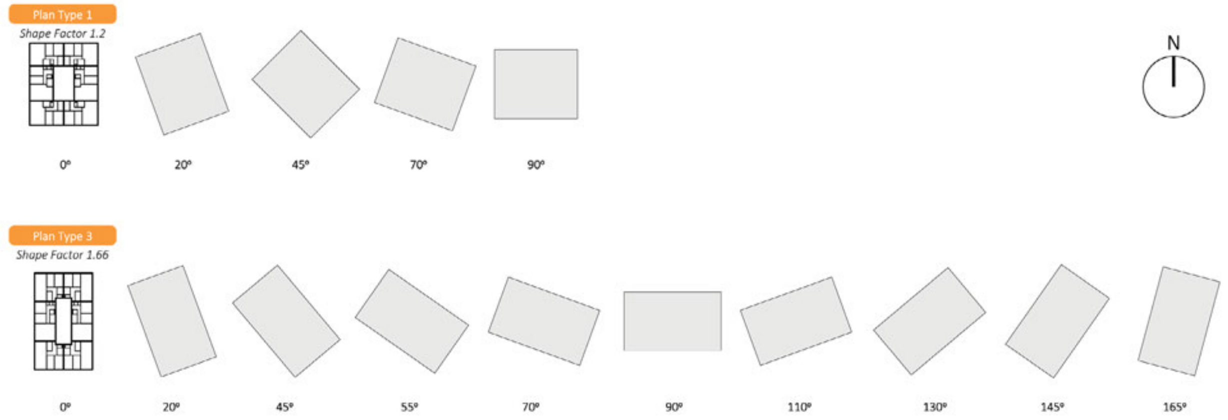

Diagram 18 *Variables tested for the compactness plan layouts and the orientation angle in Phase 1*

Compactness and Orientation Results

The plan type 1 (square shape / FS 1.2) and the plan type 3 (rectangular shape / FS 1.66) are evaluated according to the 3 BENG indicators and the comfort level, under the different orientation angles from the North axis.

Plan Type 1
SF 1.2

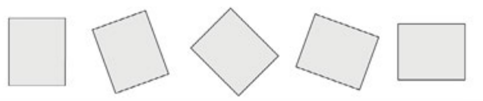

Orientation Angle	0	21	45	71	90
BENG 1 *kWh/m²*	42.3	40.8	36.9	41.0	41.6
BENG 2 *kWh/m²*	77.5	74.5	66.5	74.3	75.7
BENG 3 %	20.6	21.0	22.3	21.0	20.8
Comfort Level %	81.7	81.0	81.4	82.5	81.2
Heating *kWh/m²*	40.7	39.1	35.2	39.3	40.0
Cooling *kWh/m²*	1.6	1.6	1.7	1.6	1.6

Plan Type 3
SF 1.66

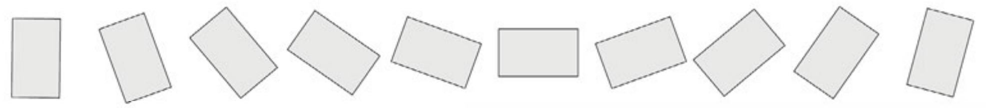

Orientation Angle	0	19	37	55	72	90	110	128	145	164
BENG 1 *kWh/m²*	60.7	64.4	64.5	64.0	66.0	73.2	73.7	71.8	66.9	65.6
BENG 2 *kWh/m²*	119.0	126.4	126.5	125.0	128.9	123.4	144.5	141.0	132.0	131.0
BENG 3 %	20.4	19.5	19.6	19.8	19.5	20.0	18.0	18.3	18.5	18.3
Comfort Level %	81.7	80.1	78.8	80.6	82.7	82.5	81.1	80.5	81.2	80.5
Heating *kWh/m²*	59.0	62.7	62.8	62.3	64.5	61.7	72.1	70.2	65.1	64.0
Cooling *kWh/m²*	1.6	1.7	1.7	1.6	1.5	1.5	1.6	1.6	1.7	1.7

Table 29 *Resulting data of the BENG indicators, comfort level, cooling and heating loads regarding the compactness and orientation angles*

Referring to Table 29, BENG 1 results range between 36.9 and 42.3 kWh/m2 for plan type 1 (average of 39.6 ± 2.7) and between 60.7 and 73.7 kWh/m2 (average of 67.2 ± 6.5) for plan type 3. For BENG 2, the results range between 66.5 and 77.5 kWh/m2 for plan type 1 (average of 72 ± 5.5) and between 119.0 and 144.5 kWh/m2 for plan type 3 (average of 131.8 ± 12.8). As for BENG 3, the range is between 22.3 and 20.6 % for plan type 1 (average of 21.5 ± 0.85) and between 18.0 and 20.4 % for plan type 3 (average of 19.2 ± 1.42).

There is a large disparity between Plan 1 and Plan 3 averages in BENG 1, respectively 39.6 kWh/m2 and 67.2 kWh/m2, and BENG 2, respectively 72 kWh/m2 and 131.8 kWh/m2. However, the performance of both plans in BENG 3 resulted in values at proximity of energy generation, respectively of 21.5% and 19.2%.

Referring to Graph 10, Graph 11, Graph 12, under a similar orientation from the North axis, the plan type 1 (square shape) indicates a better performance in all of the BENG indicators compared to the plan type 3 (rectangular shape), with lower values of BENG 1 and 2, and a slight growth in BENG 3.

Regarding the energy consumption, the cooling loads vary in parallel to the orientation, with the highest demands under 45° and 165° in the rectangular plan, and a peak at 45° in the squarish plan (Graph 14). However, the difference in its consumption is within an absolute difference of 0.3 kWh/m2 which does not present a considerable impact from the orientation.

On the contrary, the heating loads indicate a higher demand in the least compact plan type 3, with a peak in consumption of 72.1 kWh/m2 under an angle of 110°, and a minimal consumption of 59 kWh/m2 at an orientation of 0° (Graph 15).
For the most compact plan type 1, the heating demand is more constant, with a decrease in its consumption to 35.2 kWh/m2 at angle of 45° from the North axis, compared to 40.7 kWh/m2 at angle of 0° (Graph 15).

The comfort level presents a minor variation of 4% absolute difference between the 2 plan types for given orientation angles (Graph 13). In all the designs the comfort is above 78.8%, with the highest levels for both plans at 75°, and additionally at 90° for the rectangle plan. However, the constraint assigned to the comfort requirement in the optimization is set to be above 90%, which is not met in any designs in this phase, expected to be due to the lack of optimization of other parameters regarding the facade design.

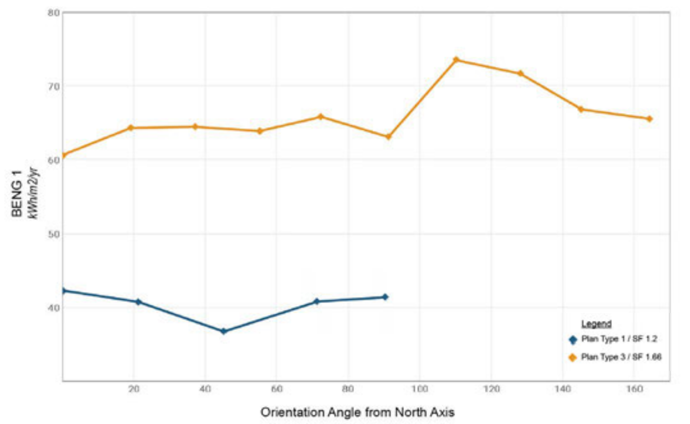

Graph 10 *BENG 1 regarding the orientation angle in plan type 1 and 3*

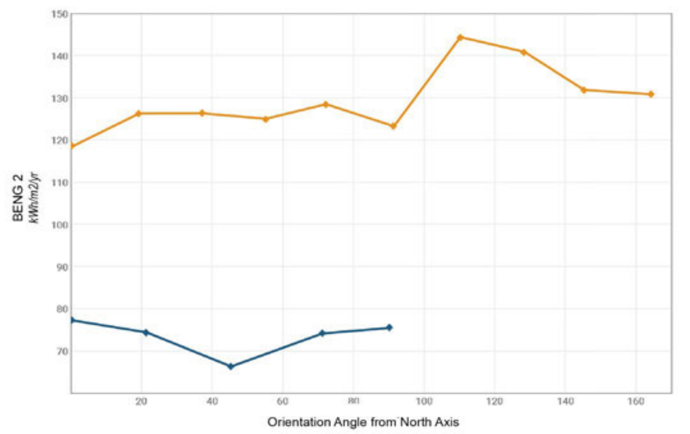

Graph 11 *BENG 2 regarding the orientation angle in plan type 1 and 3*

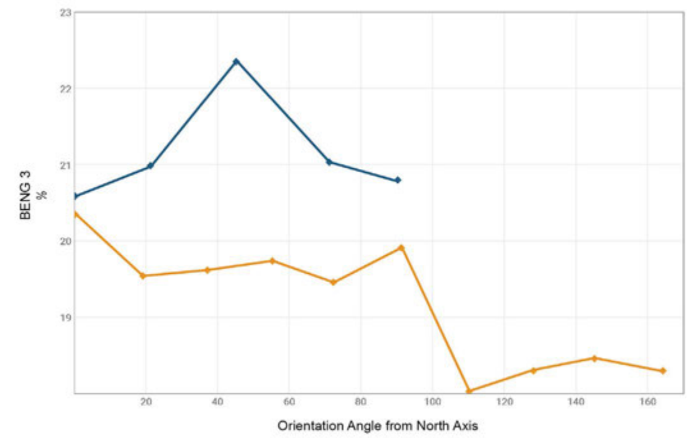

Graph 12 *BENG 3 regarding the orientation angle in plan type 1 and 3*

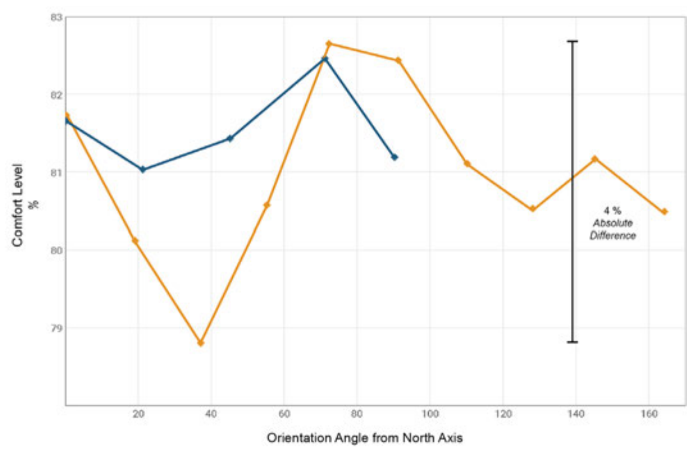

Graph 13 *Comfort regarding the orientation angle in plan type 1 and 3*

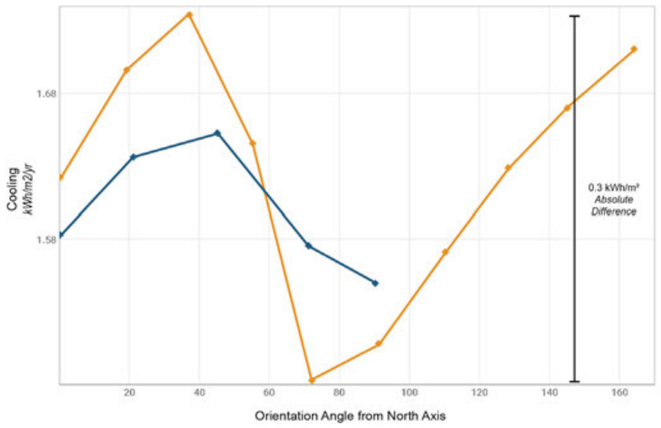

Graph 14 *Cooling loads regarding the orientation angle in plan type 1 and 3*

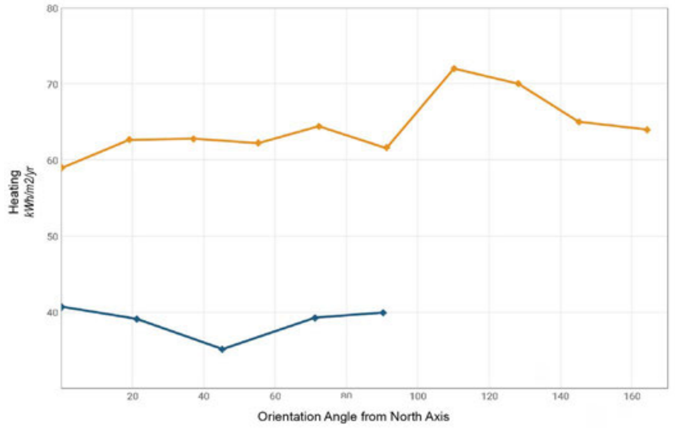

Graph 15 *Heating loads regarding the orientation angle in plan type 1 and 3*

Performance Analysis of Plan Type 1

For the plan type 1 (square shape / SF 1.2), BENG 1 and 2 indicate a poor performance in the designs under angles of 0° and 90°, linked to the increase in the heating loads. In fact, at these orientations, only 3 out of the 4 facades are directly exposed to direct sun, with the North facing facade having a limited access. Therefore, the rooms located on the Northern side of the envelope require a higher heating demand due to less heat gains, in addition to the greater amount of overcasted sky days with lower temperature.

Similarly, at those orientations, BENG 3 results with a poor energy generation due to the inefficiency of the PV mounted on the North, and only 3 facades being used.

On the contrary, when the building is rotated toward 45°, BENG 1 and 2 are minimized, and BENG 3 is maximized. In this case, the building is repositioned toward a more efficient exposure to the sun path where all of the 4 facades receive a certain amount of radiation along the day compared to the previous orientations, allowing for more PV to generate energy. Also, with the balanced distribution of the sun, the heating loads are reduced as all the spaces located on the envelope perimeter are prone to heat gains. Although the cooling loads tend to increase in response, the growth is only 1%, which does not contribute to an increase in the final consumption.

With lower heating, the total energy consumption is reduced for the orientation of 45°. In fact, in the temperate climate, the amount of overheated days over the year counts for less than cold days which necessitates less demand for cooling, but a greater dependence on heating.

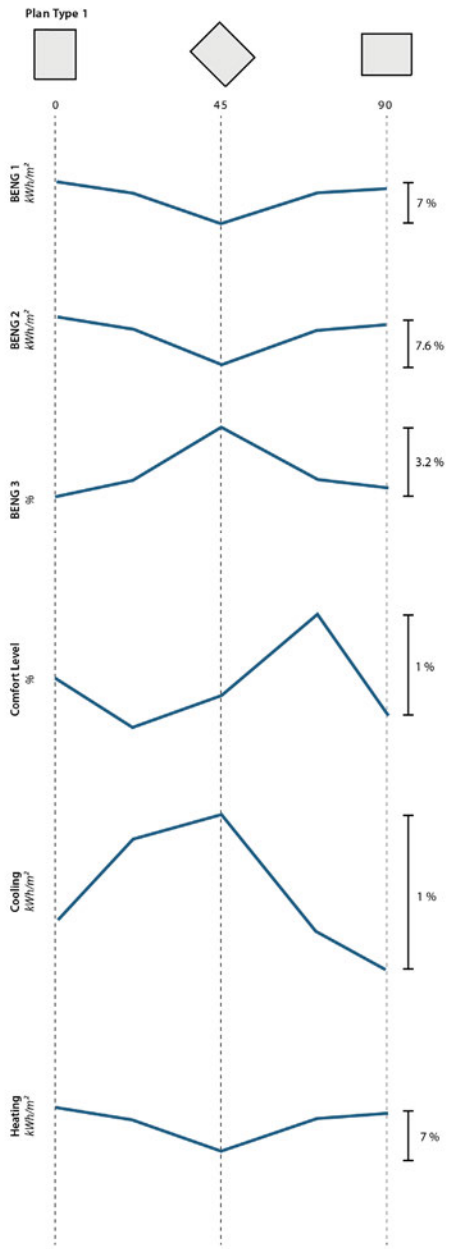

Graph 16 *Results of BENG indicators, comfort level, cooling and heating loads under different orientation angles for plan type 1*

Performance Analysis of Plan Type 3

For the plan type type 3 (rectangular shape / SF 1.66), BENG 1 and BENG 2 indicate higher values between angles of 110° and 145°, with an increase in the heating demand.
In this case, with the shortest side of the rectangle facing the South-West, where most of the sun radiation occurs, the remaining areas located on the envelope perimeter are located on the longest sides and require more heating.

Additionally, the energy generation of BENG 3 is lower due to the presence of the shortest facade facing the direction where most of the sun radiation occurs, resulting in less efficiency from PV panels mounted on the largest facade area.

Between an orientation of 0°, with the long axis parallel to the north-south axis, and 90° when the longest facade is facing the South-West, the designs indicate a better performance in BENG 1 and 2, with lower heating demand.

Having the short facade facing the North on one side, and South on the other, less rooms are located toward the North and require less heating than under 90°. In this case, the internal spaces around the envelope on South, East and West are more prone to overheating risk during the day, mainly in summer. However, the cooling loads indicate an increase of only 1%.

In comparison with the 90° design, the orientation of 0° provides a higher amount of energy generation for BENG 3 because the shortest facade is facing the North with the smallest side of the rectangle.
Between the 45° and 135°, the 4 facades are exposed to sun radiation, but in the case where the longest side is toward SW it is more advantageous for the mounted PV panels.

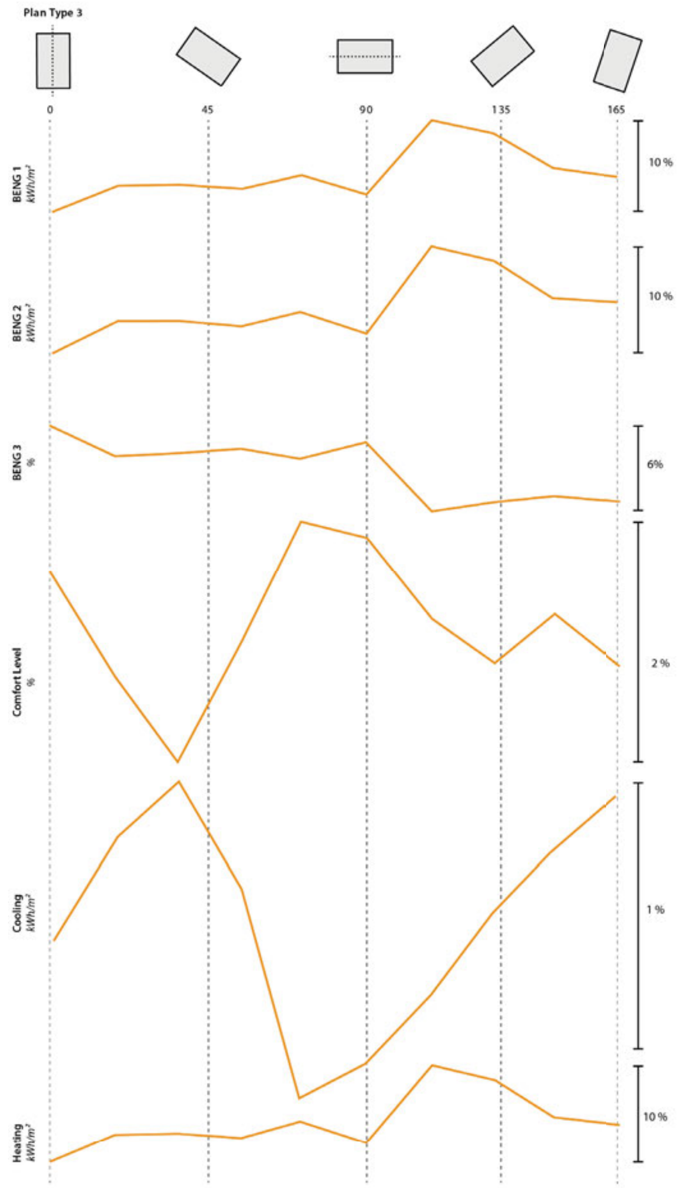

Graph 17 *Results of BENG indicators, comfort level, cooling and heating loads under different orientation angles for plan type 3*

Analysis of the Compactness

First, referring to the parallel coordinates Graph 18, the best performing design in plan type 1 has an orientation angle toward 45° from the North. In this case, BENG 1 and 2 have respectively values of 36.9 kWh/m2 and 66.5 kWh/m2, and BENG 3 of 21%.

For the plan type 3, there are two designs presenting an improvement in the performance. First, the design at 0°, with the long axis parallel to the North, indicates lower BENG 1 and BENG 2, respectively of values 60.7 kWh/m2 and 119.0 kWh/m2, and BENG 3 of 20.4%. As for the design with an orientation of 90°, with the short axis parallel to the North, it has a slightly higher consumption of BENG 1 and BENG 2, respectively 73.2 kWh/m2 and 123.4 kWh/m2, but closer value of BENG 3 of 20%.

In both cases, the best performing designs indicates the lowest heating consumption, which highlights the importance of minimizing the heat demand in the households to reduce the total energy consumption. Thus, in this case, with balanced heat gains to the spaces around the envelope area, the comfort level indicates a higher indoor satisfaction.

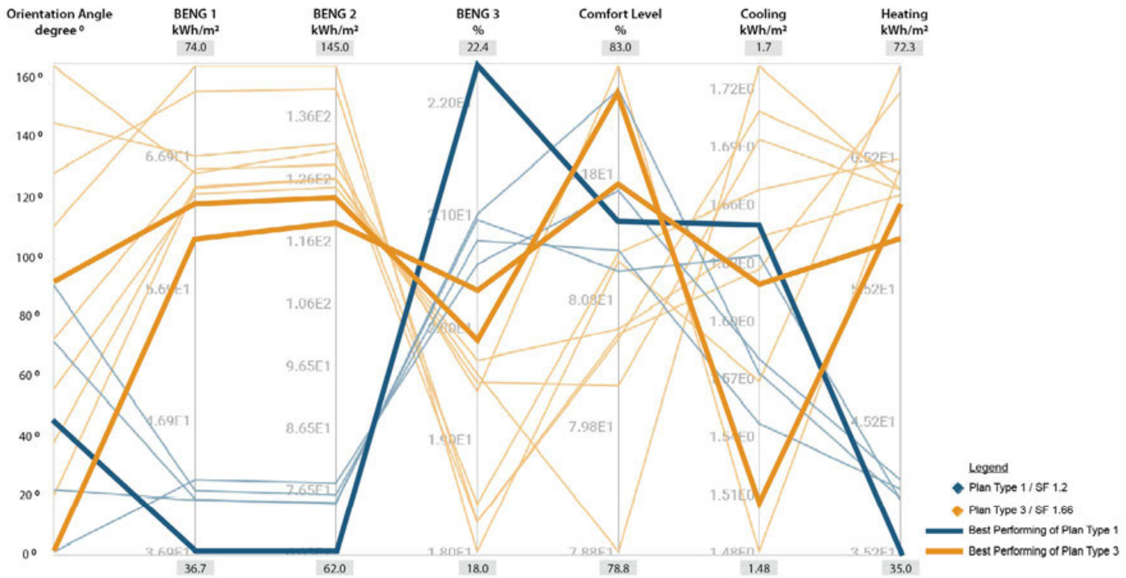

Graph 18 *Parallel coordinates chart representing the plan types 1 and 3, at the different orientation angle, with the BENG indicators, the comfort level and the energy loads*

Regarding the compactness, under similar orientation angles, the most compact plan 1 (square shape / SF 1.2) has shown a better performance in all of the 3 BENG indicators, compared to the plan shape 3 (rectangle shape / SF 1.66). Thus, taking into consideration that the only variable in this case is the shape factor, the square plan has less facade area (16752 m2) exposure to the external environment than the rectangular plan (17280 m2).

Also, considering the constant input of WWR (40%), there is less glazing surface in plan type 1 of 6701 m2, compared to the plan type 3 with 6912 m2 (Table 30). A lower amount of envelope and less glazing minimize the heat gain during summer and heat loss in winter, implying the lower cooling and heating demand respectively.

	One Floor		Total High-Rise	
	Opaque Surface m²	40% Glazing m²	Opaque Surface m²	40% Glazing m²
Plan Type 1 SF 1.2	349	139.6	16752	6701
Plan Type 3 SF 1.66	360	144	17280	6912

Table 30 *Area of Opaque wall and glazing for one floor and total high-rise of each plan*

In conclusion, the most compact shape provides a closer ranking to the BENG regulations. Regarding the orientation, the angle from the North axis depends on the geometry, where a squarish plan (length/width almost equal) performs better at a 45°, and in the case of a longitudinal shape, the longest sides should face the South-West, with angle between 0° and 90° in this case.

Solar gains and thermal comfort

To assess the impact of the compactness on the energy demand in cooling and heating, the solar gains and thermal comfort factors, with the percent of time too cold and too hot for the user, are analyzed for both plan types at an orientation angle of 0° from the North axis, reported in Table 31.

In both plans, the Bedrooms A3, B3, A2 and B2 located on the Northern side (Figure 47 and Figure 48) receive the smallest amount of solar gains, in which the values are close such as in Bedroom B3 with 27.7 and 25.7 kWh/m2 respectively. The location of those rooms is the least exposed to the sun, highlighting the low heat gains and percent of time feeling too hot under 2%. On the other hand, the percent of feeling too cold is above 11% implying the larger heating demand to meet the user's comfort.

As for the zones located on the West side of the plan; Bedroom B4 and A4, and Kitchen/Living_4, the solar gains are slightly higher in plan type 3 such as in the zone KitchenLiving_4 with 70.5 kWh/m2, compared to 66.3 kWh/m2 in plan type 1. Similarly, on the East side, the zones Bedroom A1 and B1, and Kitchen/ Living_1 show a slight increase in the plan type 3.

In fact, the spaces located on the East and West of plan type 3 have a percent of users feeling too hot around 13%, slightly higher than in plan type 1, and a minimal increase in the percent of feeling too cold around 5%. Those rooms have more envelope area and glazing area as previously mentioned in Table 30. Thus, with more facade area exposure to the external environment, more heat gains and heat loss occur through the envelope, implying the increase of the cooling and heating loads.

In the zones Bedroom A5, B5, A0 and B0, facing the South, the annual solar gains are the highest ranging from 88.9 to 106.3 kWh/m2, showing an increase in the percent of users feeling too hot, above 16%. Between plan type 1 and plan type 3, the values are very close, as the plan shape is not elongated on this side under the changing compactness.

On the envelope perimeter, there are 4 zones located on corners. In plan type 3, both Northern corner zones kitchen/Living_2 and kitchen/Living_3 indicate an increase in solar gains. Those rooms have a more longitudinal area with less facade toward the North, and more on the East and West respectively. Whereas, for the two Southern corner zones kitchen/ Living_0 and kitchen/Living_5, the external walls are exposed to solar gains from the West, South and East, indicating higher gains in the plan type 1 where a larger facade ratio is facing the South, and less on the West and East.

In conclusion, the impact of the compactness on the user comfort and solar gains is mainly observed in

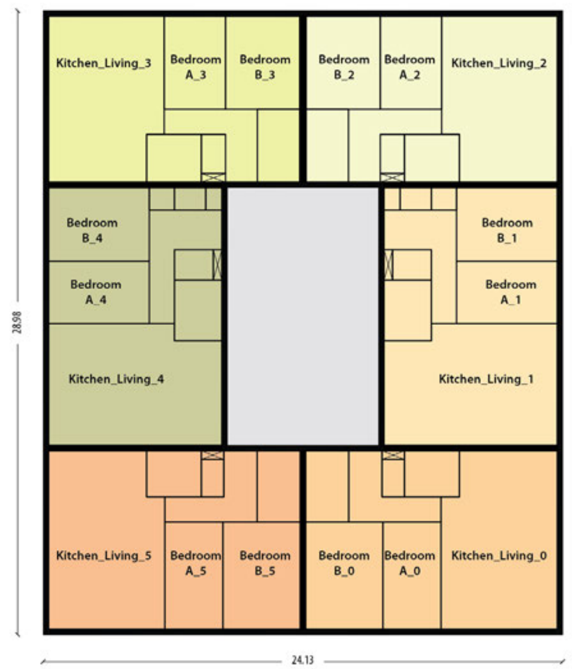

Figure 47 *Plan type 1 layout with zones nomenclature, at an orientation of 0°*

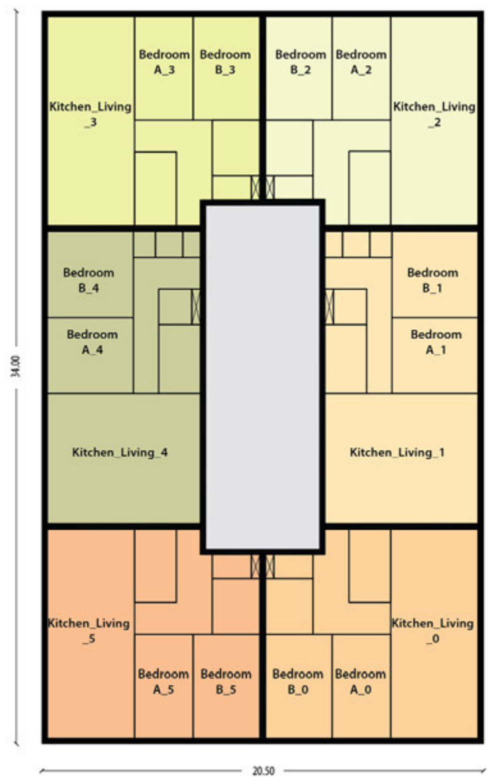

Figure 48 *Plan type 3 layout with zones nomenclature, at an orientation of 0°*

the rooms that are affected by the change in the shape factor; the zones on the East and West, and the corner located zones, which have their external walls surface enlarged, and increasing the exposure to solar gains. Thus, the more compact the shape, the lower the amount of envelope area, and therefore, the glazing ratio is reduced simultaneously. In result, the cooling and heating loads are reduced.

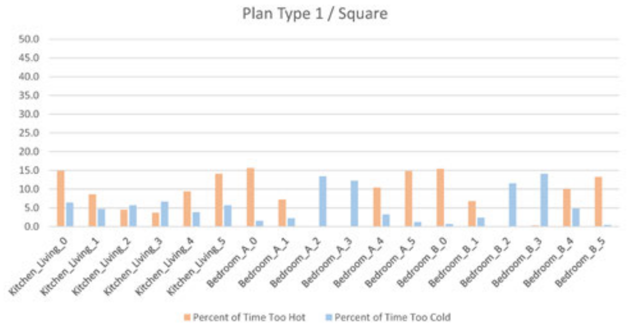

Graph 19 *Percent of time too cold and too hot in the zones of plan type 1*

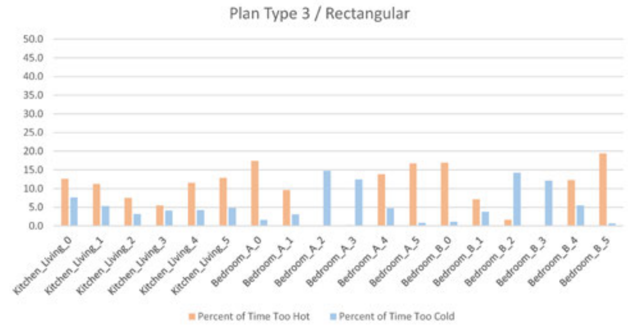

Graph 20 *Percent of time too cold and too hot in the zones of plan type3*

Zone	Plan Type 1			Plan Type 3		
	Solar Gains *kWh/m2*	Percent of Time Too Hot	Percent of Time Too Cold	Solar Gains *kWh/m2*	Percent of Time Too Hot	Percent of Time Too Cold
Kitchen_Living_0	96.8	14.9	6.4	88.5	12.6	7.6
Kitchen_Living_1	61.1	8.6	4.7	64.3	11.2	5.3
Kitchen_Living_2	35.4	4.5	5.7	48.6	7.5	3.2
Kitchen_Living_3	32.0	3.7	6.7	39.0	5.5	4.1
Kitchen_Living_4	66.3	9.4	3.8	70.5	11.5	4.2
Kitchen_Living_5	94.3	14.1	5.7	86.2	12.8	4.8
Bedroom_A_0	93.6	15.6	1.5	91.8	17.4	1.6
Bedroom_A_1	57.4	7.2	2.2	62.6	9.6	3.1
Bedroom_A_2	28.1	0.1	13.4	23.9	0.1	14.7
Bedroom_A_3	29.0	0.0	12.2	23.7	0.2	12.4
Bedroom_A_4	73.1	10.4	3.3	78.3	13.8	4.7
Bedroom_A_5	92.7	14.8	1.2	95.4	16.7	0.8
Bedroom_B_0	99.2	15.4	0.7	101.5	16.9	1.1
Bedroom_B_1	45.4	6.8	2.4	48.4	7.1	3.8
Bedroom_B_2	26.8	0.1	11.5	24.1	1.6	14.2
Bedroom_B_3	27.7	0.3	14.1	25.7	0.0	12.1
Bedroom_B_4	70.4	10.1	4.8	73.6	12.2	5.5
Bedroom_B_5	103.4	13.2	0.4	106.3	19.4	0.7

Table 31 *Results of the comfort level and the solar gain of the envelope area zones of plan type 1 and 3 at an orientation angle of 0 degree from the North Axis (Simulated with Honeybee)*

Results Verification & Reliability

Due to the wide difference in the results between the analyzed plans, further investigation behind the plug-in simulation is done for the verification and reliability of those data, in addition to the evaluation of the intermediate design of plan type 2 (FS 1.46) (Figure 9).

First, the difference in the solar gains between the 2 plans (Table 31), does not account for an increase of 20 kWh/m2 and 41.5 kWh/m2 in BENG 1 and 2 respectively, as the solar gains values are very close, with less than 10 kWh/m2 between similar functions .

Regarding the compactness, the total percentage difference in the envelope area between the plan type 1 (FS 1.2) and the plan type 3 (FS 1.66) is only 3.2 %. This increase in the envelope area is expected to have a minimal impact on the energy consumption. However, from the compared results between the two plans, at an orientation of 0°, BENG 1 indicates a difference of 43 % in performance with an increase of 18.4 kWh/m2 (Graph 21).

On the contrary, the results between plan type 2 (FS 1.46) and plan type 3 (FS 1.66) indicate a difference of 5% in performance with 2.6 kWh/m2 increase in the consumption. The same observation occurs in BENG 2, and the energy loads (Appendix G, Graph 14, 15, 16 and 17).

Moreover, for the energy generation of BENG 3, the results are based on the envelope surface area left for implementation of PV depending on the WWR. In this phase, the glazing ratio is set to a 40% constant. However, in the setting of Honeybee, the resulting amount of glazing area is calculated based on the initial facade area. As the compactness is changing, the glazing size is reduced or enlarged in parallel. Therefore, a smaller shape factor leads to less glazing area, whereas, with larger shape factor, more glazing is modeled. Therefore, it is not possible to consider that the WWR is a constant parameter when the building geometry is a variable.

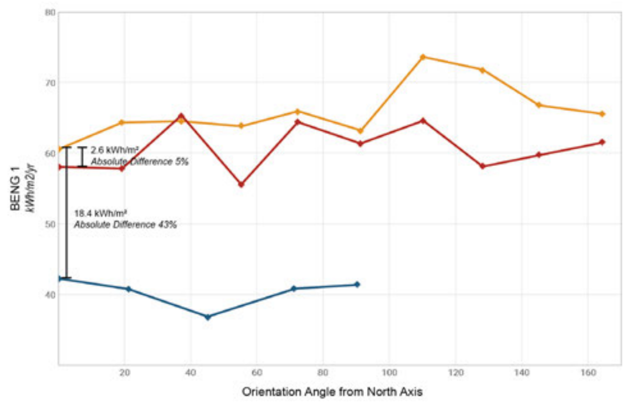

Graph 21 *Results of BENG 1 regarding the orientation angle from the North axis for the 3 types of plan*

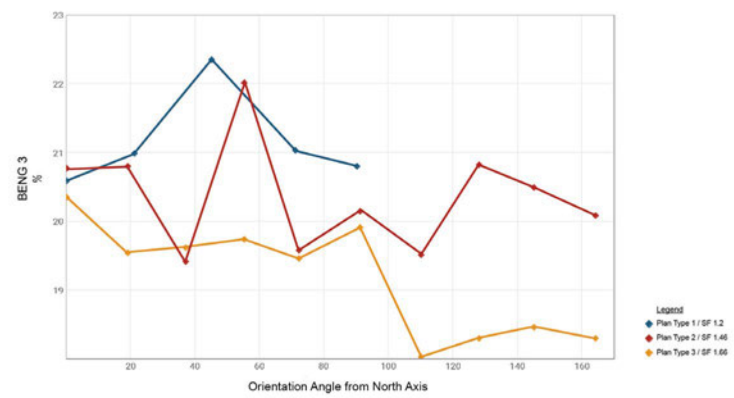

Graph 22 *Results of BENG 3 regarding the orientation angle from the North axis for the 3 types of plan*

With further investigation behind the plug-ins, for the modeling of the multi-zone plan in Honeybee, the number of surface areas between each room should be identical. In the case of plan type 2 and 3, none of the rooms presents this issue (Diagram 19). However, in the plan type 1, all of the kitchen/living corners indicate that there is a mis-match in the surface areas with the adjacent rooms, which lead to different calculation through the walls in the heat leaving from the neighboring rooms and external walls compared to the heat arriving (Diagram 20 and Diagram 21).

Therefore, the heating and cooling loads calculations are affected, and reflected in the large margin of results between plan type 1 and 3 compared to plan type 2 and 3. Thus, the energy loads are expected to be higher in the plan type 1, with an increase in both indicators BENG 1 and 2.

As a consequence, on the one hand, the results of BENG 3 are higher in the plan type 1 of smaller shape factor. On the other hand, with less glazing area provided, there is less amount of heat loss and gain through the envelope compared to other geometry which affects the heating and cooling loads, and BENG 1 and 2.

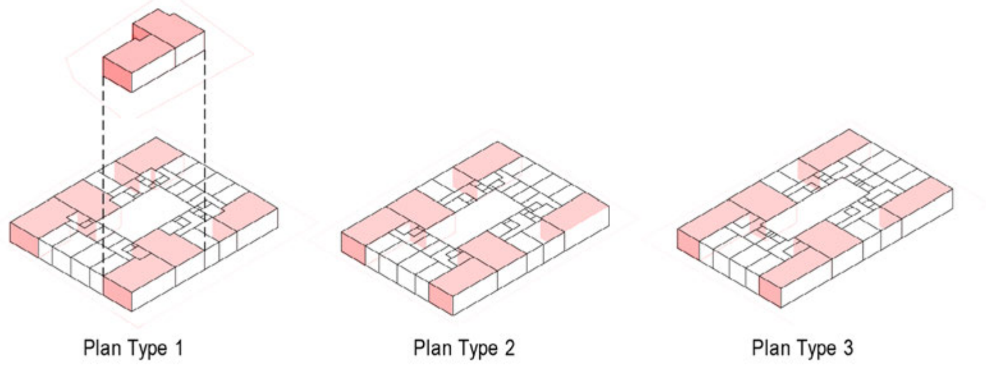

Diagram 19 *Modeling of the 3 designed plan compactness highlighting the zones causing different calculation in Honeybee*

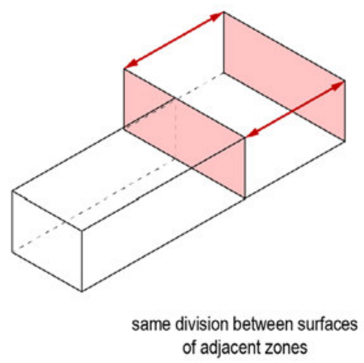

Diagram 20 *Modeling of the 3 designed plan compactness highlighting the zones causing different calculation in Honeybee*

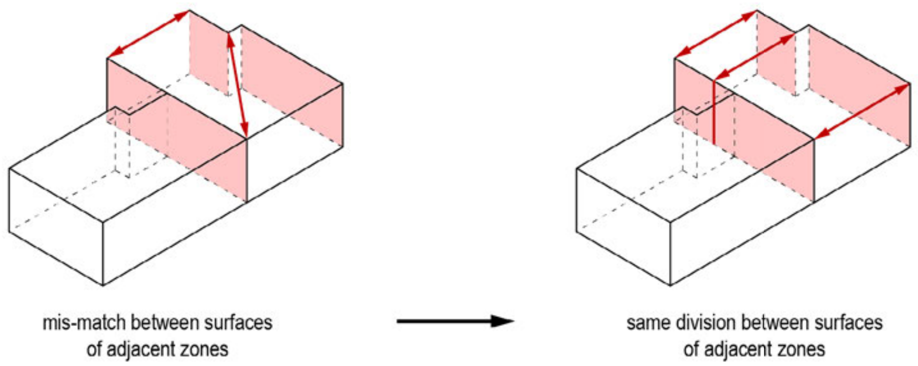

Diagram 21 *Modeling of the 3 designed plan compactness highlighting the zones causing different calculation in Honeybee*

4.4. Phase 2 : Facade Performance under Different Surrounding Contexts

In this phase, the impact of the site context on the energy performance of the residential high-rise is assessed according to the BENG regulations, in addition to the feasibility of the design to still meet the requirements if changes occur in the surroundings on the long term. Designing a high-rise surrounded by low-rise buildings is expected to have different energy performance than if it is facing neighboring structures of higher height. In order to verify this statement, the window-to-wall ratio on each facade is optimized under 3 different scenarios of context; low-rises, mid-rises and high-rises, to observe the context impact on the performance and how it relates to the facade parameter design.

The analysis is conducted on the lower zone of the residential high-rise (5th floor at a level of 16.5 meters) with the most compact geometry under an orientation of 0° from the North axis, and the glazing type 1 (U-value 1.1 W/m2K, g-value 0.62, VLT 80%) without shading system.
In this case, by only considering the lower part of the building, the impact on the BENG regulations will indicate whether the context presents an obstacle in the design of the high-rise from an early stage. If the regulations are not met in the lower part, it will indicate additional constraint to improve the indicators ranking in the remaining floors.

Optimization Algorithms and Methodology

The total amount of iterations and time required for those simulations are calculated to support the selection of the methodology, as following:

Total iterations for each surrounding = 8 x 8 x 8 x 8 = 4096
Total iterations for 3 surroundings = 4096 x 3 = 12288
Time required for each simulation = 25 minutes
Time required for 3 surroundings = 5120 hours = 213 days

Facing the unfeasible amount of time to run all design iterations, the methodology puts in application 2 types of optimization algorithms in modeFRONTIER.

Firstly, a DOE, in this case Uniform Latin Hypercube, space filler, is used to create a first set of results. From the parameter ranges inserted, the design iterations will be created from combining as many different variables of the 4 orientation of WWR, with minimal correlation and duplication, in order to provide a uniform distribution.

The goal is to cover the largest area of the design space, with the smallest amount of experiments, to extract from it the most qualitative data to this study, without using a full factorial DOE. Among the results, the best performing are selected

according to the objectives and constraints that are defined in the modeFRONTIER. Thus, those iterations present WWR ranges that are reduced from the original inputs. This created first set of data is inserted as the base of the search in the second optimization with PilOPT (Graph 23).

After launching several runs of experiments with the ULH in the DOE, PilOPT will exploit those previously created datasets and extract the best designs for the initialization of the optimization. In results, there are 288 near-optimal iterations (Graph 23), which indicate a closer ranking in the BENG objectives and constraints (Graph 24).

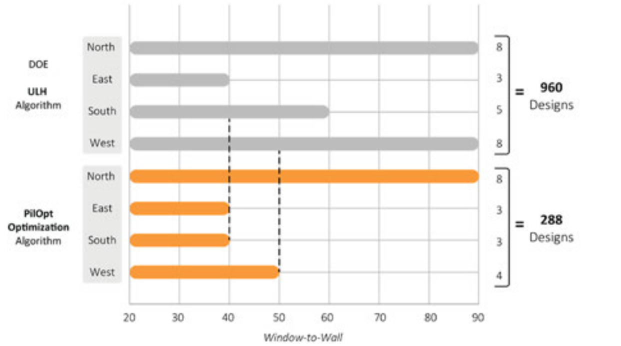

Graph 23 *Results of the WWR ranges with the ULH and PilOPT in low-rise context*

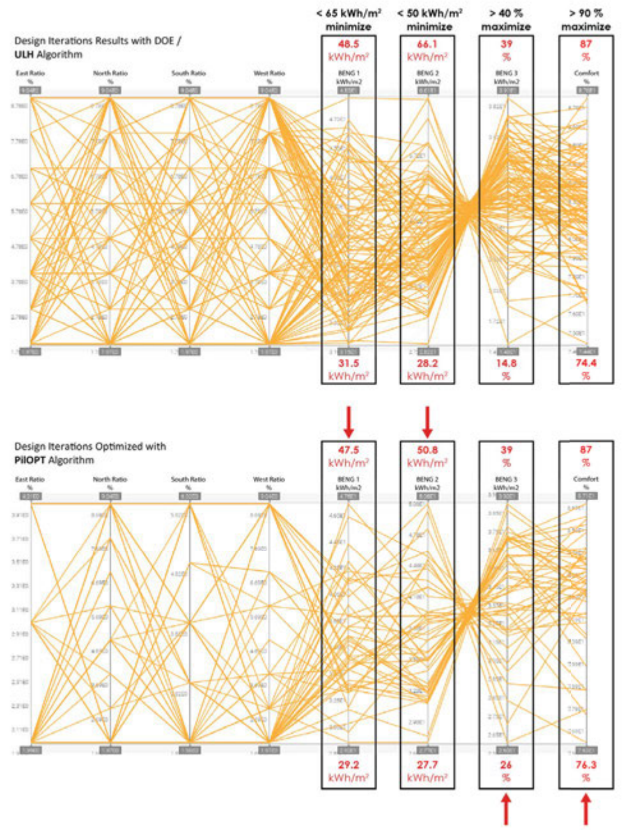

Graph 24 *Parallel coordinates indicating the results ranges according to the objectives and constraints between the ULH and PilOPT optimization algorithm of the WWR with low-rises context*

Correlations

The impact of the surroundings' height on the design performance is reflected in the correlation between the WWR facade orientation, the BENG indicators and the energy loads. Similar relationships between the glazing ratio parameters and energy outputs are observed under the different context, in addition to non-identical patterns (Graph 25).

First, under a low-rise context, the cooling loads indicate a higher positive correlation with the South (+0.753), East (+0.669) and West (+0.440) which highlight that an enlargement of the WWR on those orientations leads to more heat gains due to their high exposure to annual solar radiation of 732 kWh/m2 (Diagram 22). Thus, the glazing on these facades are kept under a ratio of 50% in the optimal ranges (Diagram 23).
However, with higher surroundings, the correlations are less strong, showing negative values in some cases such as with the North (-0.502). With more obstruction of all the facades, and therefore less heat gain, the influence on the cooling demand is similar from all orientations. Therefore, the East and West WWR incorporate more variables up to 90% in the design space compared to the previous upper bound of 40% and 50% respectively.

Concerning the heating loads, under the low-rise context, only the North orientation indicates a positive correlation (+0.473), where the larger the ratio the more heat loss occurs as it is the only facade that is not prone to heat gains in summer. However, under higher surroundings, the correlations become less strong (between +0.100 and +0.400) on all orientations, indicating the equal influence of the WWR parameters on the heating. In fact, enlarging any of the glazing ratio results in heat loss due to the overshadowed facades.

Compared to low-rise context, the lighting loads show a negative correlation on all orientations similarly to the heating and cooling loads, with the lack of access to natural daylight (Graph 25).

Lastly, for the energy generation of BENG 3, in the lower surrounding heights, negative correlations with the South (-0.734) and the East (-0.657) are observed, which indicate that the larger those ratios, the lower the amount of energy generated as less surface is left on the facade to mount PV panels. Therefore, the glazing ratios have optimal ranges between 20 and 40%. On the contrary, with more obstruction in the other surroundings, the correlations become equal on all the orientations, where even the East, West, and North show a relation to BENG 3 highlighting the necessity to benefit from all the facades to maximize energy generation.

Overall, the relationship between facade parameters and the energy outputs becomes less impacted by only a single facade in higher context. In fact, according to the Pearson correlation, the resulting values below ±0.500 imply a medium strength of association. Thus, all orientations have an equal contribution to the objectives of the energy performance and comfort level.

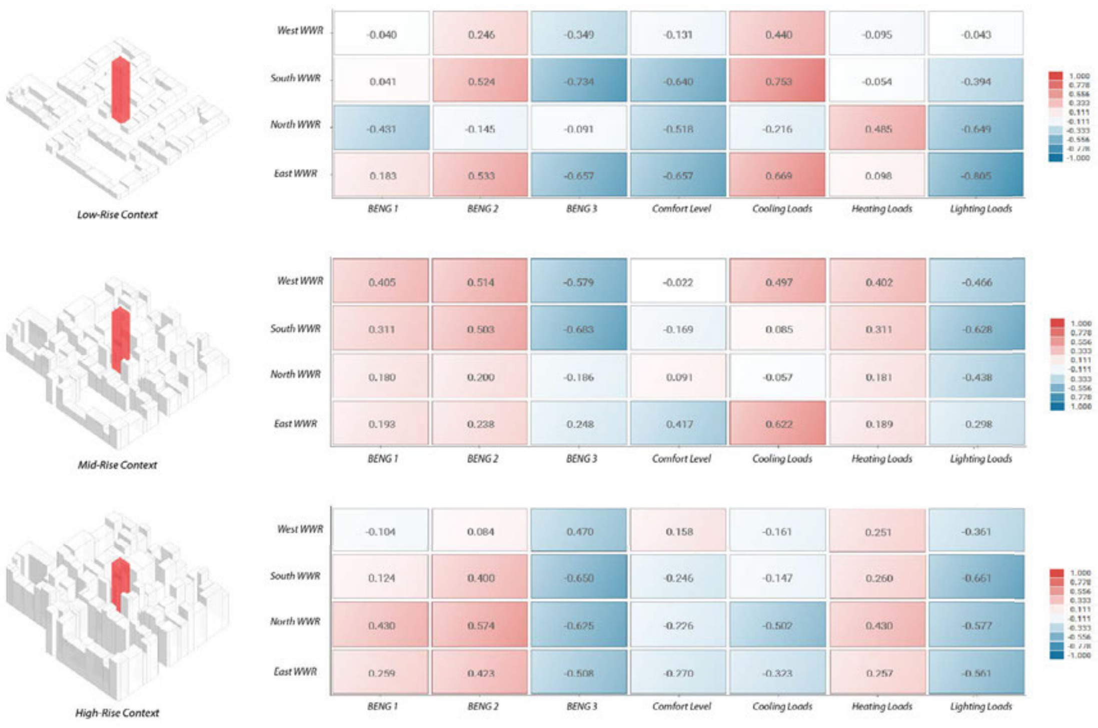

Graph 25 *Correlation chart between the WWR facade orientation, BENG indicators, the user's comfort and the cooling and lighting loads for each of the 3 types of surrounding buildings context*

In the design of a high-rise, the floors above the urban skyline are more exposed to direct solar radiation than the floors at the bottom of the building. Such as the case in this study, the lower zone has been evaluated under the 3 types of context, in which its facades are more overshaded throughout the day when surrounded by mid-rises and high-rises with a reduction of access to solar radiation.

In result, the glazing ratio ranges included a larger amount of variables to achieve similar goals, and thus, leading for a greater percentage area of the total facade. A facade parameter contribution in achieving a certain objective is completely altered considering the urban canopy layer of the context.

Energy performance regarding the Context Height

The performance of the lower zone is evaluated according to the BENG indicators, the comfort level and the loads, under the different contexts.

Referring to the Graph 26, it is observed that BENG 1 energy demand is satisfied under the benchmark of 65 kWh/m2 for the 3 contexts, with only a few iterations above the limit with mid- and high-rises. The total energy demand is lower in the low-rise context, between 31.05 and 44.93 kWh/m2, compared to when surrounded by the mid- and high-rises, 36.4 and 72.33 kWh/m2, indicating a 37% decrease of performance, due to less access to direct sun and daylight.

As for BENG 2, it is only satisfied, under the benchmark of 50 kWh/m2 in some iterations in the low-rise context. With higher surrounding, the performance of the designs decreases by 65%, reaching up to 145.9 kWh/m2.

The resulting bandwidth that appears in the trend between BENG 1 and BENG 2 (Graph 26) is due to the consideration of the heating and cooling loads in the calculation of both indicators. Thus, an increase of the heating loads will appear in both of the energy demand and the primary fossil use.

The relationship between the decrease of performance of BENG 1 and BENG 2, is related partly to the demand of both the cooling and the heating in the households. According to Graph 27, with the low-rise context, there is a lower heating demand between 30.2 to 48.3 kWh/m2, and more cooling consumption between 0.7 to 2.7 kWh/m2. On the contrary, in a mid- and high rise context, scarcely any cooling is needed with its decrease in consumption to under 0.4 kWh/m2. However, there is a larger dependence on heating loads leading to a demand above 36.2 kWh/m2 and up to 72.1 kWh/m2.

In regard to the thermal comfort, the rise of the heating load in taller contexts is required to achieve a similar range of the user's comfort objective within the range of 80 and 87%, where the double of the heating demand is needed (Graph 28) compared to when the floor apartment is surrounded by low-rises. Also, some designs with the low-rise surrounding show a poor indoor comfort under 80% indicating overheating from the solar gains. Similarly, the demand of artificial lighting is more important under higher surroundings (Graph 29) to satisfy the 300 lux illuminance threshold of the visual indoor comfort (Graph 30).

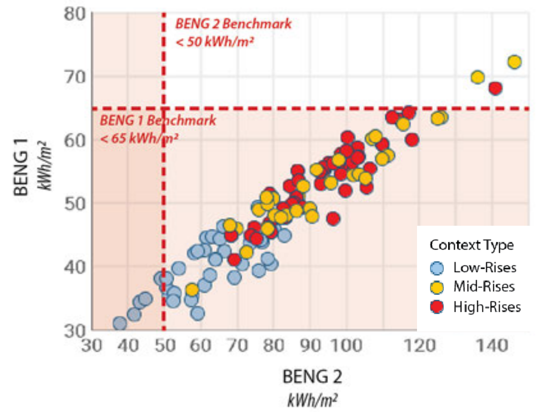

Graph 26 *Designs ranked by surrounding types according to BENG 1 and BENG 2*

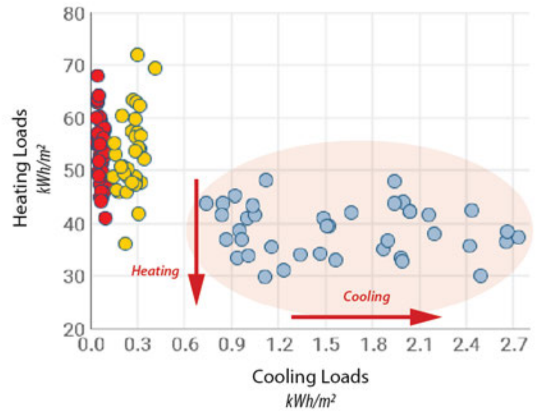

Graph 27 *Designs ranked by surrounding types according to the heating and cooling loads*

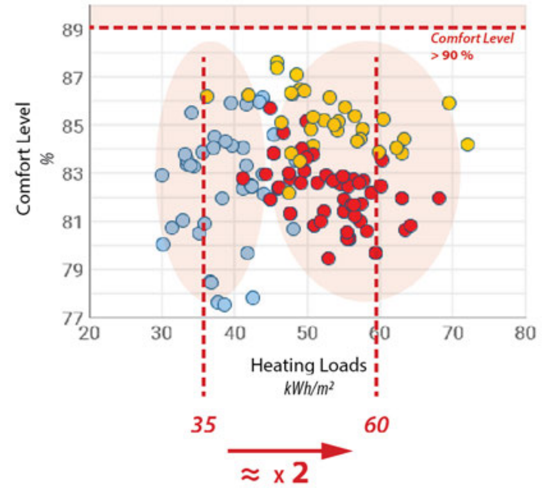

Graph 28 *Designs ranked by surrounding types according to comfort level and heating loads*

To evaluate the results according to the environmental conditions, the geometry of the residential high-rise is implemented in those different contexts. It is observed from the position of the stereographic diagram of the sun-path that the access to direct sun in the lower floors is obstructed from the surrounding buildings of the mid- and high-rise context along a daily and yearly period (Diagram 22). The annual amount of radiation reaching the East, South and West facades is reduced from 420 kWh/m2 to a total of 24.40 kWh/m2, in the transition from lower to higher surroundings respectively.

In results, the minimized exposure to direct sun in the higher context implies less heat gains through the envelope facade, leading to the lower cooling demands from one side, and a higher heating consumption on the other. In addition, the poor access to natural daylight is linked to higher artificial lighting consumption.

Concerning the last indicator, BENG 3 performance is higher in the low-rise context as the facades have a greater exposure to radiation (Graph 31). In results, with a combination of lower WWR, the energy generated indicates values reaching 35.56 % being in proximity to the minimum requirement of 40%, and decreases to 20% energy generation under larger glazing ratio. However, for the higher surrounding, the energy generation is under 20%, with values decreasing to 0%. In this case, the efficiency of the PV panels is too far from meeting the benchmark.

To sum up, the performance of the 3 BENG indicators decreases if the lower part of the residential high-rise is subjected to obstruction. The growth in the energy consumption is mainly due to the higher demand of the heating compared to cooling due to less access to heat gains and sun radiation, with an additional dependence on artificial lighting to make up for the lack of natural daylight. Moreover, the energy generation extracted from the facades is not sufficient, and in response leads to a rise of the primary fossil usage of BENG 2.

In conclusion, in all the contexts there is a compliance with the benchmark of BENG 1 (< 65 kWh/m2). However, the iterations of the higher contexts are too far from the regulations benchmark of BENG 2 (< 50 kWh/m2) and BENG 3 (> 40%), except for some results of the lower context that satisfy BENG 2, and provides an energy generation in proximity of BENG 3 requirement.

The provided result meets the expectation of a decrease in the overall energy performance of the high-rise if changes occur in the urban context or in the presence of obstructions in the site selection. In this case, achieving a good ranking according to BENG regulations presents a greater obstacle if from a starting point the lower part of the high-rise already indicates a poor energy performance, and therefore presents an additional constraint in pursuing the target height.

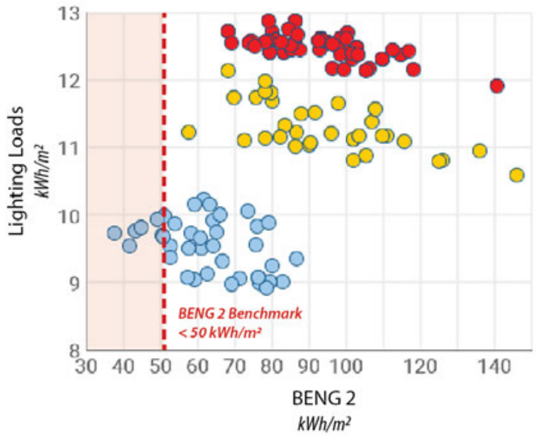

Graph 29 *Designs ranked by surrounding types according to BENG 2 and the lighting loads*

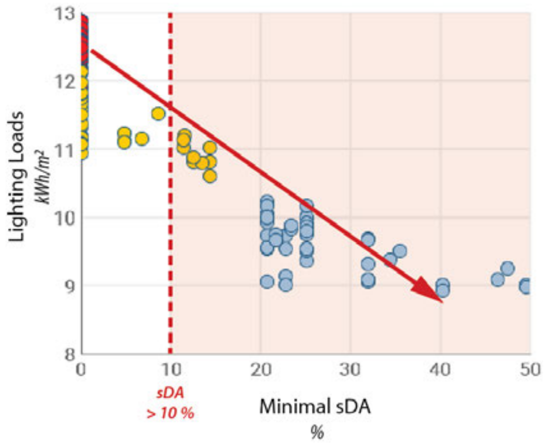

Graph 30 *Designs ranked by surrounding types according to the lighting loads and the minimal sDA*

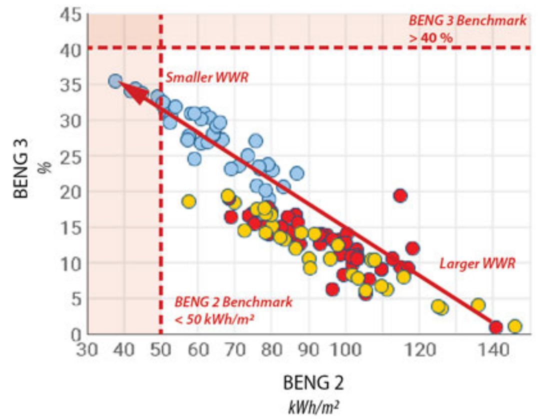

Graph 31 *Designs ranked by surrounding types according to BENG 2 and BENG 3*

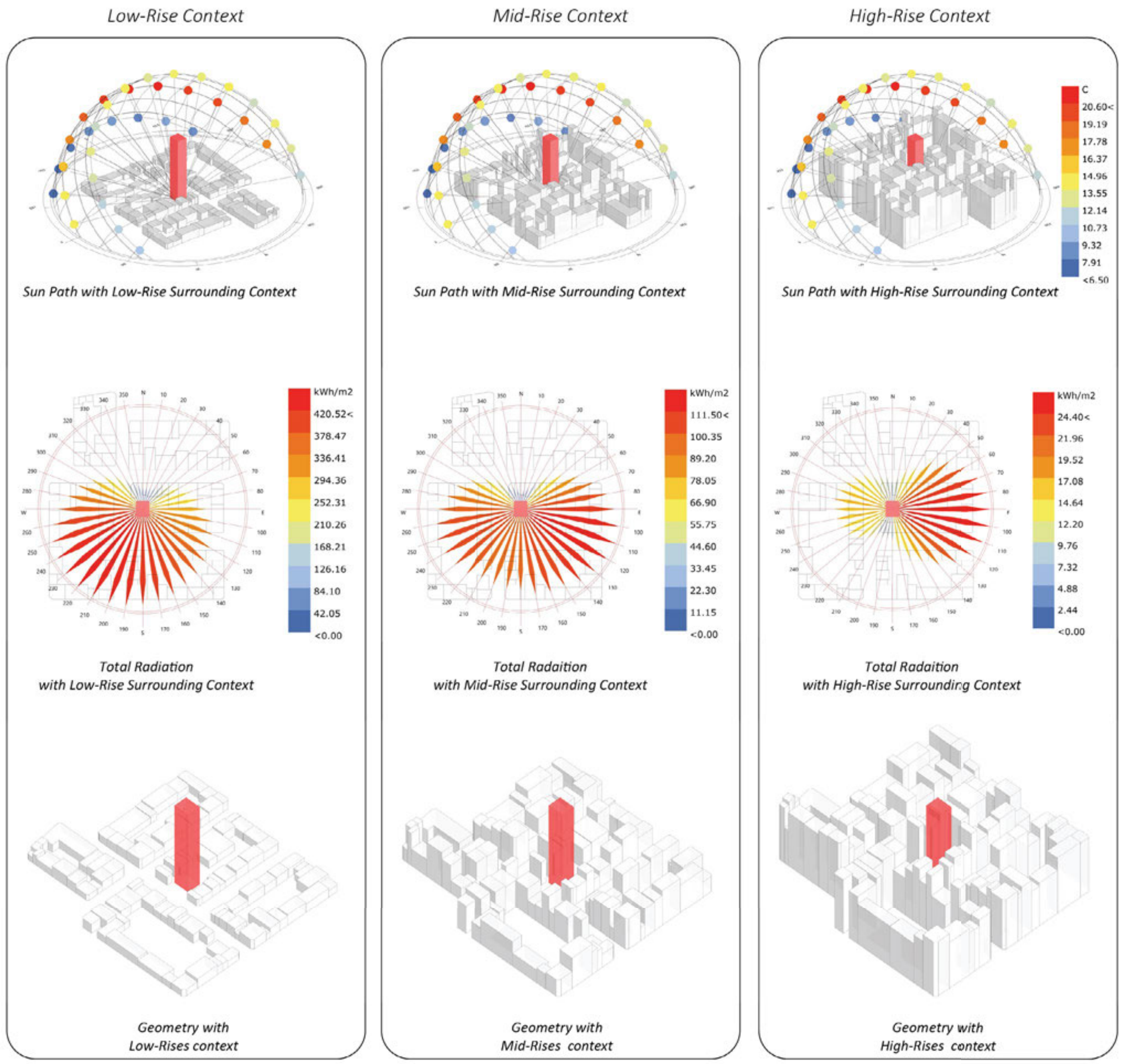

Diagram 22 *Impact of the different surrounding context on the annual solar radiation rose and sun access (Source: Honeybee / Ladybug)*

Context impact on the facade parameters of the WWR

The window-to-wall ratio used as input for the optimization has a variable range between 20% to 90%, with an incremental step of 10%. From the optimization results, the design space provides the range of WWR for which each facade has the most efficient performance according to its orientation, and in this case, according to the surrounding building height.

Under a low-rise context, the indicators of BENG 1, 2 and 3 have resulted within the ranges of 31.0 to 50 kWh/m2, 37.5 and 59.0 kWh/m2 and 19.0 to 35.5 % respectively, and a comfort level between 77.5 to 86.1% (Appendix C, Graph 1).

For higher surrounding buildings, with mid-rises, BENG 1, 2 and 3 are respectively between 36.4 to 72.3 kWh/m2, 57.4 to 145.8 kWh/m2 and 1.07 to 19.4 %, and a comfort level between 82.1 and 87.6% (Appendix C, Graph 2).

As with high-rises surroundings, BENG 1, 2 and 3 are respectively between 41.1 to 68.1 kWh/m2, 68.2 to 140.7 kWh/m2 and 0.91 to 19.5 %, and the comfort level between 79.4 to 85.6 % (Appendix C, Graph 3).

In comparison to the low-rises, the performance of the BENG indicators has decreased considerably when the context canopy is higher, whereas between the mid-rise and high-rises the results are within closer ranges. As for the user's comfort, the level of satisfaction is maintained.

To reach the objectives and constraints in the energy performance and indoor comfort, the WWR ranges under the low-rise surroundings indicate for the North variables from 20 to 90%, for the West 20 to 50%, and for East and South between 20 to 40 %. However, under higher context of the mid-rises and high-rises, a larger amount of variables are incorporated indicating an enlargement of all the glazing ratios to reach similar goals, with all of the East, West and North WWR between 20 to 90%, and the South from 20 to 60% (Diagram 23).

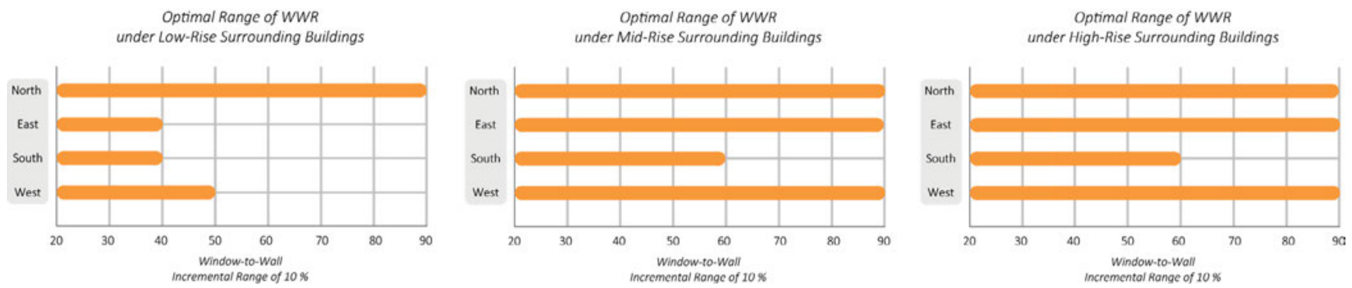

Diagram 23 *Results of the range of WWR (between 20 and 90%) to achieve optimal designs under each of the 3 types of surrounding building context*

Performance evaluation for close WWR iterations

To evaluate the previous performance, similar combinations of WWR parameters are explored among the 3 types of surrounding. From the results, there were no identical iteration matches, which led to select the closest in variables, reported in table 4.06. All the designs overlapping have a similar WWR on South (40%) and West (50%), with the West 30% to 40%, and lastly the North is more varying 40% and 70%.

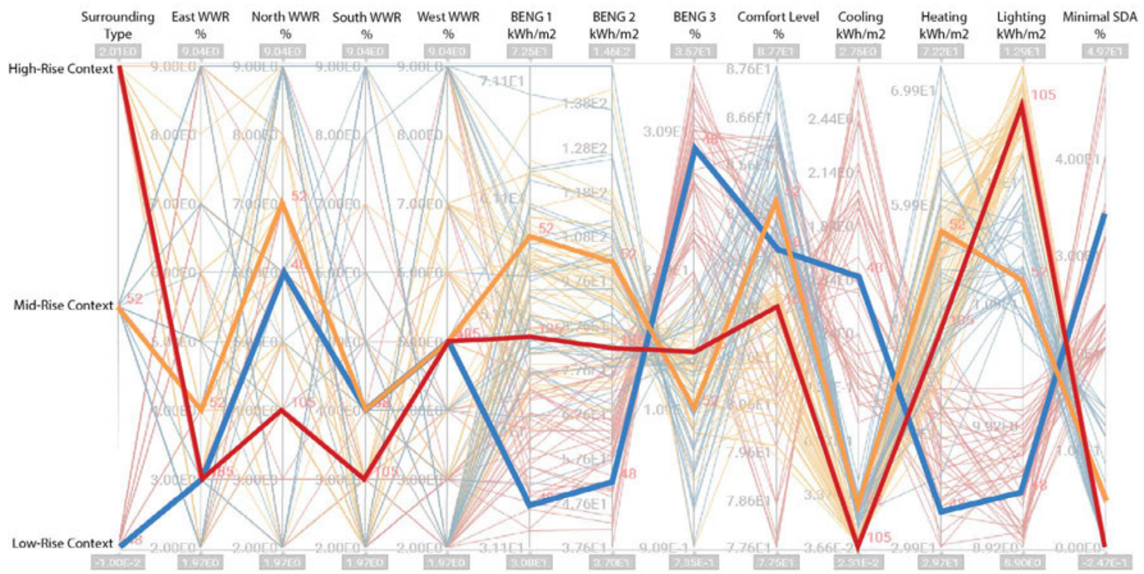

Graph 32 *Parallel Coordinates Chart of the WWR of all the best performing iterations from all the High-rise, Mid-rise and Low-rise Surroundings*

The impact of the context height meets the expectation of the previous observation. Under the different context, with close design iterations of the facade, the performance of the 3 BENG indicators have decreased considerably (Table 32).

	WWR %				BENG				Loads			
	East	North	South	West	BENG1 kWh/m2	BENG 2 kWh/m2	BENG3 %	Comfort Level %	Heating kWh/m2	Cooling kWh/m2	Lighting kWh/m2	mininum sDA %
Low-Rise Context	30	60	40	50	34.6	52.4	29.7	83.7	33.0	1.6	9.3	34.3
Mid-Rise Context	40	70	40	50	57.7	101.8	10.9	84.8	57.5	0.3	11.1	4.7
High-Rise Context	30	40	40	50	49.1	82.4	15.0	82.5	49.1	0.5	12.5	0.0

Table 32 *Results of BENG and energy performance of the 3 design iterations with closest WWR from each context*

On another note, concerning the visual comfort, the spatial daylight autonomy sDA is extracted, which represents the percent of analysis points across the floor surface of a room that either meet or have exceeded the illuminance threshold of 300 lux for at least 50% of the day. In the low-rise context, the minimum sDA reached for a single room is of 34.3% (Graph 32) which is above the 10% of the regulations, however, the visual comfort is not satisfied in the mid-rise with 4.7% being under 10%, and reaching 0% in the high-rise context. Designing for visual comfort is more critical with mid- and high-rises, where there is less room for natural daylight to enter, in addition to the obstructed views. In results, the lighting loads have increased (Figure 49) to compensate for the lack of light access.

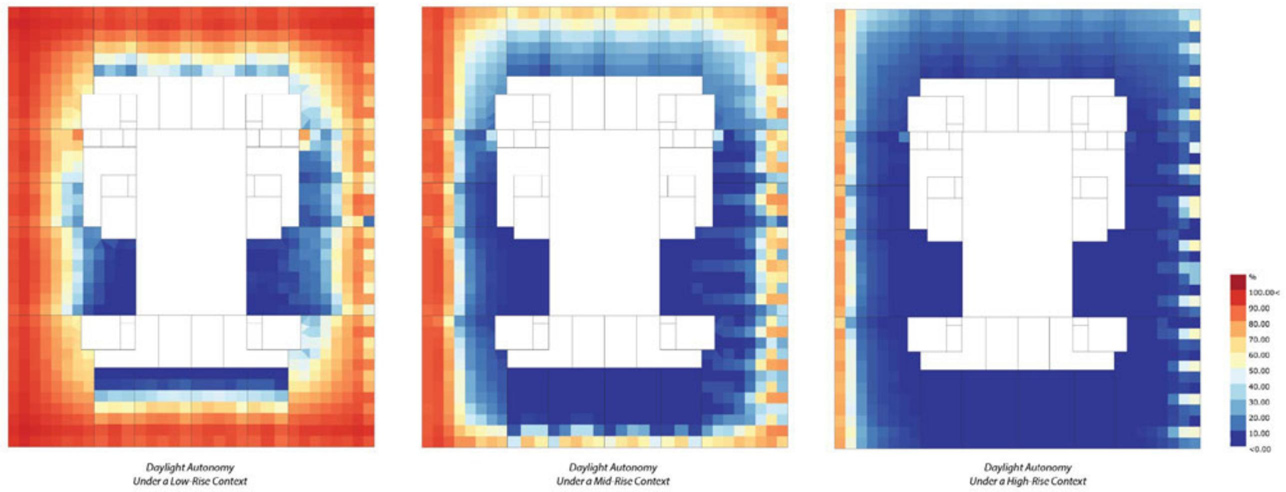

Figure 49 *Annual daylight autonomy DA under the different surrounding contexts showing the amount of time during occupancy when points receives more daylight than the threshold illuminance of 300 lux (Source:*

4.5. Phase 3 Optimal WWR per Level and Facade Orientation

For the 4 middle floors, extracted from the 4 zone-divisions at different levels of the high-rise, the window-to-wall ratio parameter is evaluated according to its facade orientation and the height level of the analyzed floor. With the changing micro-climate conditions with altitude, and the different exposure of each facade to the sun, the outcome of this analysis is expected to provide a scheme of the adaptation of the glazing ratio regarding the environmental conditions in parallel to the height. The optimal ranges will indicate whether the ratios tend to increase, decrease or present a constant pattern from the bottom to the top of the high-rise for each of the 4 facades. Lastly, the resulting optimal ranges will serve as inputs in the following section "4.6. Phase 4: Facade Parameters Optimization" to accelerate the optimization process due to the lack of time to evaluate all the design variables simultaneously.

For this analysis, the design is evaluated under a low-rise surrounding context, with the consideration of other facade related parameters kept as constant; the double glazing type 1 (U-value 1.1 W/m²K, g-value 0.62, VLT 80%) without a shading system.

Prior to the assessment of the glazing ratios, a primary analysis is conducted on the lower zone to to support the selection of the design with different WWR distribution per facade in comparison to using a constant ratio on all floor facades with the following ratio 20%, 30%, 40%, 50%, 60%, 70%, 80% and 90% (Diagram 38). An enlargement in the glazing ratio is expected to increase the internal solar gains and natural daylight, while contributing to more heat loss.

Referring to Diagram 38, designing with constant WWR on all the facades meets the expectations. In the enlargement of the ratios from 20% to 90%, BENG 2 indicates an increase, whereas BENG 3 decreases considerably. Under all the ranges, the indicator of BENG 3 is below the minimum 40%, whereas for BENG 2, the results meet the maximum benchmark of 50 kWh/m² only in the design with ratios of 20% and 30%. However, the energy demand of BENG 1 under 65 kWh/m² is met in all the variables. On another note, the comfort level decreases with an enlargement of the ratio, being under 90% in all cases (Appendix D, Table 4).

Regarding the loads, the lighting usage gradually decreases with larger glazing ratio that provides a better access to natural daylight. However, both the cooling and heating demand increase due to a greater amount of heat loss and gains through the glazing surfaces (Diagram 38). On the one hand, these observations support the approach of designing with different WWR on each facade, where the optimization methodology is required to reach a balance between the energy consumption and the energy generation, while satisfying the thermal dn visual comfort. On the other hand, according to the results and in addition to the literature review on the regulations, among the BENG indicators, the main obstacles in the design of the high-rise typology is in minimizing the fossil fuel usage of BENG 2 (< 50 kWh/m²) and maximizing the energy generation of BENG 3 (> 40%). Thus, the focus of the objectives in the optimization is shifted on both of BENG 2 and 3 as a priority versus BENG 1. To proceed with this approach, the selection of the ratios will be based on the highest correlation with those 2 indicators to extract the most relevant spot areas of the entire design space.

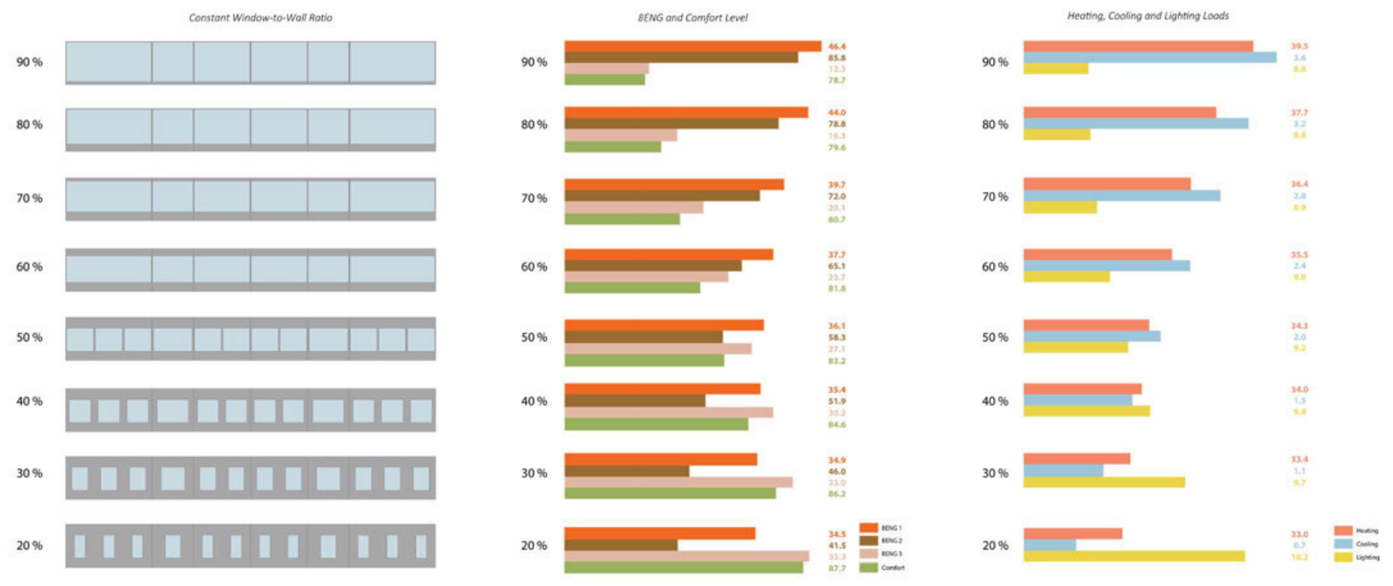

Diagram 38 *Results of BENG and energy loads with constant WWR parameters on all facades*

Results of Zone 1 at the 5th Floor, level of 16.5 m

The relationship between the WWR parameters and the outputs of the energy loads and comfort level are depicted in the correlation Graph 33. For the lowest zone 1 of the high-rise, the East and South WWR are highly correlated to BENG 2, BENG 3 and the comfort level, the West to BENG 3, and the North WWR to BENG 1 and the comfort level.

The negative correlations with the energy generation of BENG 3 indicate that the smaller WWR on the East and South facades provide more surface for the implementation of PVs, and therefore serve the maximization of this objective. Similarly, the smaller ratios indicate a reduction in the final fossil usage energy of BENG 2, where the heating and cooling loads are lower, whereas the artificial lighting tends to be higher due to the low sDA. For the visual comfort, the larger ratios are more advantageous to satisfy the visual comfort. However, thermal comfort is prioritized for its contribution to more energy-saving in this case, and reach closer values to the objectives.

As observed in Graph 33, the smaller the glazing ratios, the lower the resulting values of BENG 2 and the higher is the energy generation of BENG 3. Similarly, in the same order of ideas, with larger ratio, the opposite is true where lower energy generation is resulting, and higher amount of primary fossil usage. Moreover, under smaller ranges of glazing ratio, the sDA is at minimal values, resulting with higher amount of lighting loads. On the contrary, the more satisfactory the visual comfort, the higher the percentage of the sDA, and the less dependance is observed on the artificial lighting from the user.

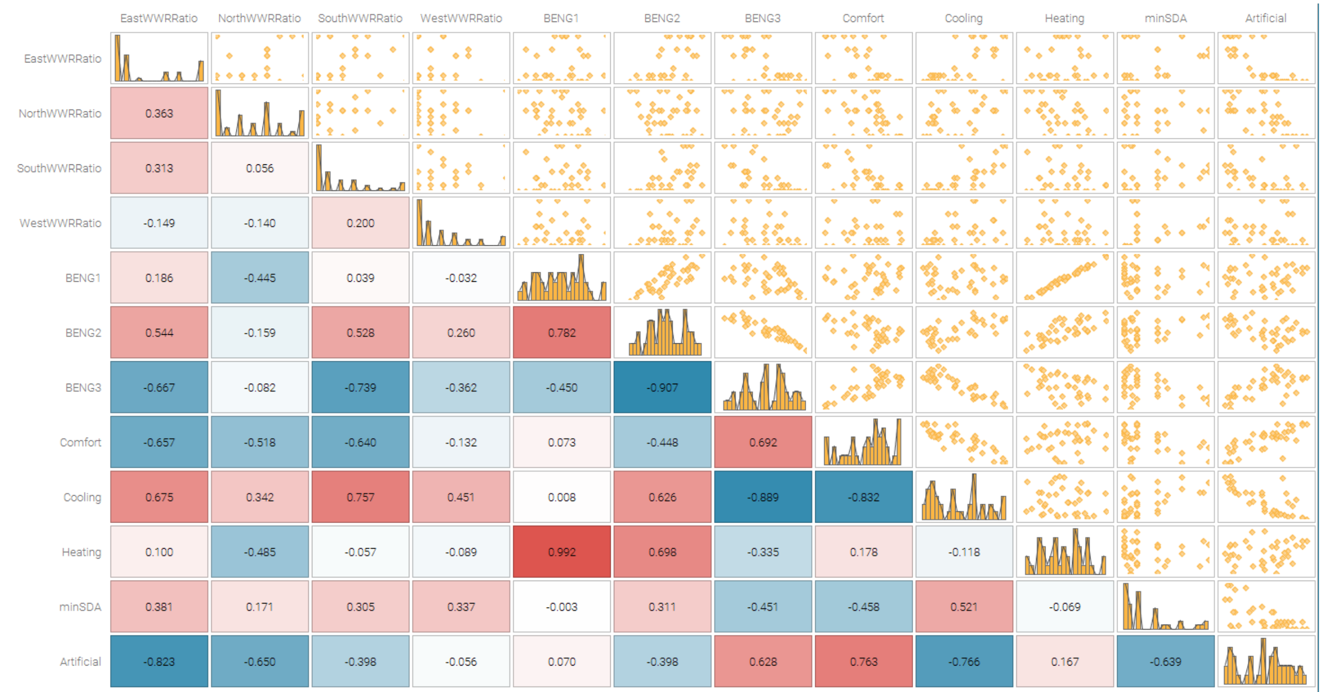

Graph 33 *Scatter matrix of the correlation between the WWR, BENG indicators and the energy outputs at the Zone 1*

Followingly, the parallel coordinates chart provided as a tool in modeFRONTIERv2019 assists in the comparison and selection of the iterations according to the defined objectives. In the Graph 33, the results of zone 1 are evaluated regarding their impact on the energy performance and comfort level. In order to filter out the entire design space into the optimal spot area, the range of BENG 2 is minimized, and BENG 3 maximized. As for BENG 1, it is kept to its extent as it fulfills the requirements in all the results. The resulting designs, from the filtered out parallel coordinates (Graph 34), have combinations of WWR from each facade orientations that achieved a performance the closest to the objectives.

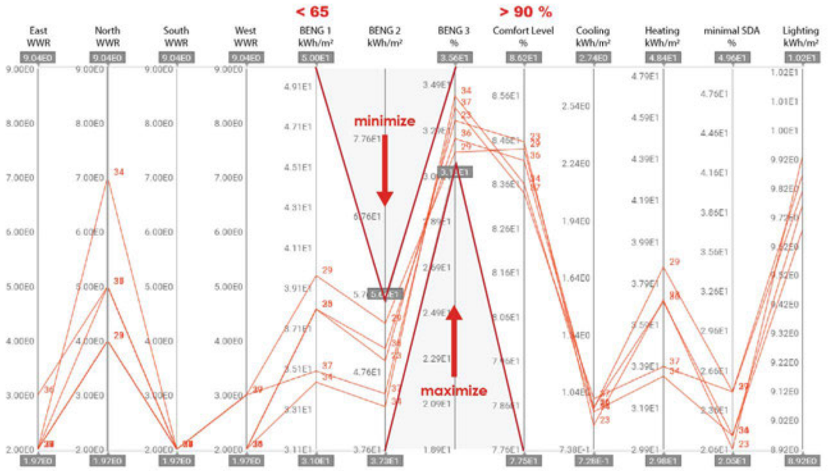

Graph 34 *Parallel coordinates chart of the design iteration selection for zone 1 by adjusting the range toward the objectives*

Moreover, referring to Graph 35, the position of those designs is observed in relation to their near-optimal WWR variables and their rankings regarding the BENG 2 and BENG 3 indicators. In all the cases, the outcome of the WWR per facade provides the lowest values of BENG 2. Similarly for BENG 3, all the iterations indicate the highest range of energy generation.

In the case of this study, the 5 best performing iterations are extracted from the design space (Table 33). The South facade presents a 20% ratio, and the East and West facades both ratios of 20% and 30%.

They all contribute to the objectives of the energy generation from the facades with their highest exposure to sun radiations, and reduction of energy loads by minimizing heat transfer through the facade. As for the North, the ratios indicate a larger range of values with 40%, 50% and 70% as they are more beneficial to increase natural daylight, and reduce lighting loads, and do not present potential to the indicator of BENG 3.

Among those resulting design iterations, the designs indicate a glazing ratio of 20% are considered acceptable in the design of the residential building as long as there is an adequate amount of daylight into the space. The minimal sDA in these cases are above the required 10% for visual comfort according to NEN-EN 17037.

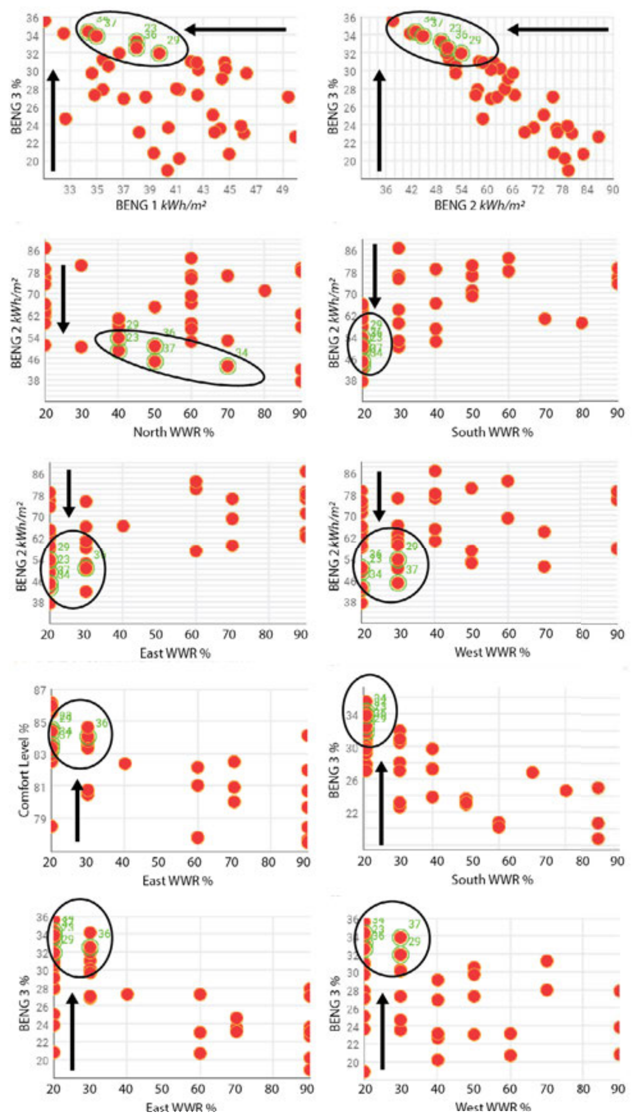

Graph 35 *Scatter diagram representing the proximity of the design iterations WWR of zone 1 regarding energy indicators and comfort level, with a low-rise surrounding context*

To proceed with the selection of the best performing design WWR of zone 2 (17th floor), zone 3 (29th floor) and zone 4 (41th floor), the same methodology used previously for zone 1 is applied by prioritizing the ranking of the iterations variables regarding BENG 2 and BENG 3. The correlations and ranking of their design iterations are reported in Appendix D.

Results of Zone 2 at 17th Floor, level of 56.1 m

For the second zone, the best performing iterations are reported in Table 33.The South and East facades ratio range from 20% to 30%, the North WWR indicates 40%, 50% and 60%, and the West ratio is constant at 20% in all iterations.

Results of Zone 3 at 29th Floor, level of 95.7 m

For the third zone, the selected iterations, reported in Table 33, indicate for the South facade ratio range of 20%, 40% and 50%, the North WWR range between 30% and 60%, the East range between 20% and 30%, and the West ratio values of 20%, 40% and 50%.

Results of Zone 4 at 41th Floor, level of 135.3 m

For the last zone, at the upper part of the high-rise, the provided WWR ranges for the South between 20% and 40%, for the West values of 20% and 30%, the East values of 20%, 30% and 50%, and for the North between 50% and 80%.

ZONE 1	WWR %											
	East	North	South	West	BENG 1 kWh/m2	BENG 2 kWh/m2	BENG 3 %	Comfort Level %	Cooling Loads kWh/m2	Heating Loads kWh/m2	Lighting Loads kWh/m2	minimial sDA %
	20	40	20	20	38.0	49.0	33.3	84.5	0.9	37.1	9.9	21.0
	20	40	20	30	39.7	53.7	32.0	84.4	1.0	38.7	9.8	25.0
	20	70	20	20	34.4	43.0	34.4	84.0	0.9	33.4	9.7	22.0
	30	50	20	20	38.0	51.0	33.0	84.0	1.0	37.0	9.7	22.0
	20	50	20	30	35.0	44.7	33.9	83.3	1.0	34.0	9.8	25.0

ZONE 2	WWR %											
	East	North	South	West	BENG 1 kWh/m2	BENG 2 kWh/m2	BENG 3 %	Comfort Level %	Cooling Loads kWh/m2	Heating Loads kWh/m2	Lighting Loads kWh/m2	minimial sDA %
	20	60	20	20	33.3	40.7	35.0	83.6	1.0	32.4	9.8	21.0
	20	50	20	20	33.3	40.1	35.3	84.5	0.9	32.3	9.9	22.0
	30	40	20	20	32.7	39.5	35.3	84.9	0.9	31.8	9.7	21.0
	20	50	30	20	33.8	42.8	34.2	87.1	1.0	32.9	9.8	22.0
	20	40	20	20	33.2	39.5	35.6	85.4	0.9	32.4	10.0	21.0

ZONE 3	WWR %											
	East	North	South	West	BENG 1 kWh/m2	BENG 2 kWh/m2	BENG 3 %	Comfort Level %	Cooling Loads kWh/m2	Heating Loads kWh/m2	Lighting Loads kWh/m2	minimial sDA %
	30	40	20	50	38.3	55.0	31.0	86.0	1.2	37.1	9.6	35.4
	20	60	40	20	33.5	44.6	33.2	83.9	1.2	32.4	9.7	21.0
	20	50	20	20	38.7	50.8	32.8	83.9	0.9	37.9	9.9	22.0
	20	50	50	20	38.2	55.3	30.4	84.0	1.2	37.0	9.7	22.0
	30	30	20	40	39.9	56.2	30.8	82.6	1.1	39.0	9.7	35.4

ZONE 4	WWR %											
	East	North	South	West	BENG 1 kWh/m2	BENG 2 kWh/m2	BENG 3 %	Comfort Level %	Cooling Loads kWh/m2	Heating Loads kWh/m2	Lighting Loads kWh/m2	minimial sDA %
	30	60	30	20	41.5	60.0	30.0	84.0	1.0	40.5	9.5	22.0
	20	60	30	20	39.5	54.6	31.4	82.0	1.0	38.5	9.7	22.0
	50	80	20	20	39.7	58.0	30.0	81.0	1.3	38.4	9.3	21.0
	20	80	20	20	42.9	60.5	30.4	84.0	0.9	42.0	9.7	21.0
	30	50	40	30	33.0	45.6	32.4	83.5	1.3	31.7	9.5	32.0

Table 33 *Selected design iterations for zones 1, 2, 3 and 4 with the combination of each WWR and energy performance*

On the overall scheme of the high-rise, from the lower to the upper zone, the South, East and West facades have ranges of WWR between 20% and 30% and single iteration presenting 40% and 50%. Those orientations perform better under lower ratios that can increase the energy generations at all levels, while minimizing heat transfer through the transparent components of the facade.

For the North, it includes a larger range of ratio between 30% and 80% (Diagram 24). The enlargement of the WWR on this orientation is related to its lower exposure to solar radiation which does not contribute to maximizing the objective of BENG 3. In this case, it presents a greater potential in satisfying the visual comfort by allowing more daylight into the internal space. However, with smaller openings, less heat is lost through the facade, and can conserve more indoor temperature.

To provide a better insulation of the envelope with the glazing properties and shading systems, all those resulting designs are evaluated in the next step, Phase 4, with additional facade parameters.

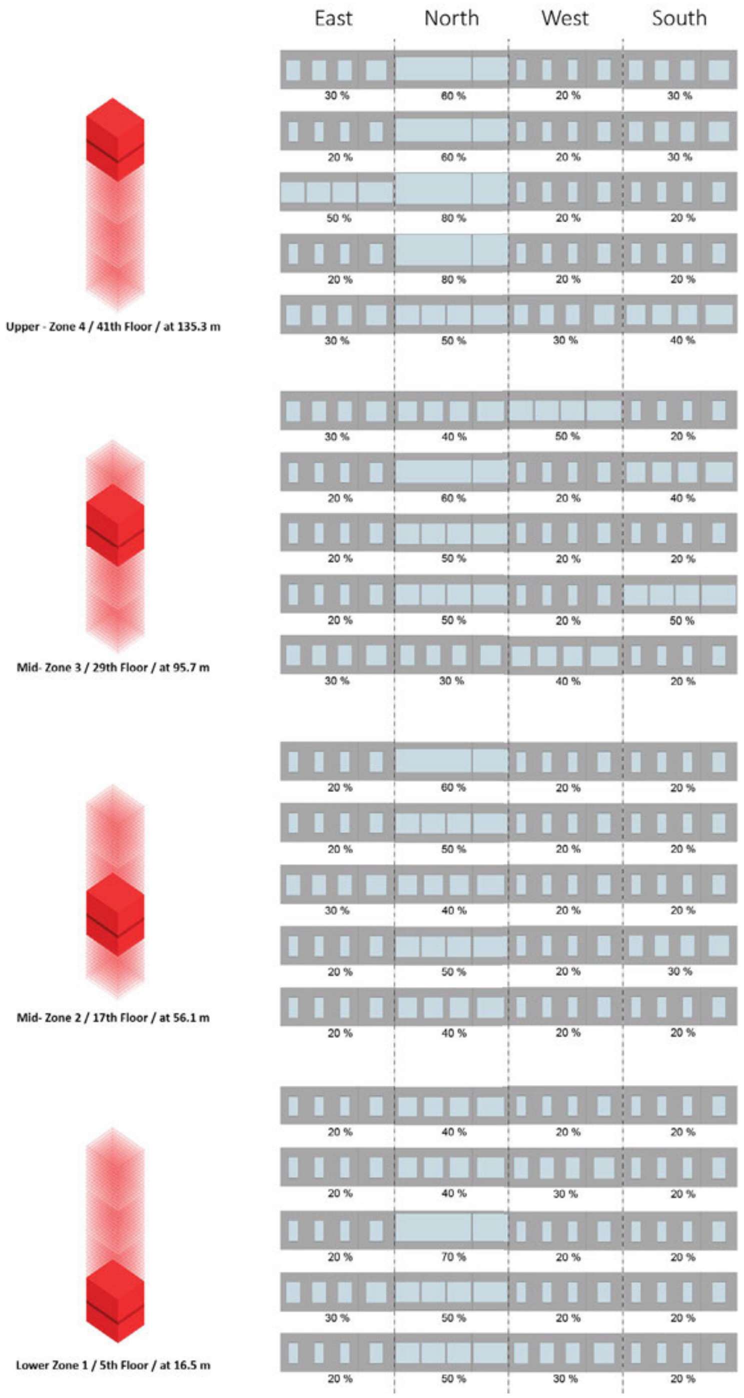

Diagram 24 *Scheme of the resulting optimal iterations of WWR per facade and per zone*

4.6. Phase 4: Facade Parameters Optimization

To proceed with the optimization of the facade, the different glazing types and shading systems parameters are assigned to the resulting design iteration that were extracted from phase 3 with the near-optimal WWR. To evaluate the performance of the parameters properties on the energy and comfort level, the variables are implemented in the workflow setting of modeFRONTIER (Appendix E, Diagram 3).

From those inputs, 5 different glazing types are analyzed, each with specific U-value, g-value and VLT as reported in Table 23. Also, 3 types of shading systems are include (Figure 11) among which 2 types are dynamically controlled systems. However, due to limitations from the Honeybee plug-in used, the effect of the dynamic shading is not taken into consideration in the part of the workflow for the lighting simulation. Thus, the lighting loads results can not be validated, and the glazing property related to the visual transmittance VT is not included in this study, and only the U-value and the g-value are evaluated.

Analysis of the Glazing Properties

For the analysis of the glazing types, only the thermal related properties of U-value and g-value are evaluated.

The glazing types 1, 2 and 3 have the highest U-values, respectively of 1.1, 0.9 and 0.7 W/m2K, and indicate an increase of the heating demand. On the contrary, a decrease in the loads is observed in the performance of both glazing types 4 and 5 that are provided with lower U-values of respectively 0.6 and 0.5 W/m2K (Graph 36), which imply less heat loss and heat gains through the facade. In results, the lower demand leads to a reduction of BENG 2, being closer to the benchmark (< 50 kWh/m2).

Regarding the g-value, it is higher in glazing type 5, of 0.7, compared to all other types, which allows more solar gains into the space. In results, more heat gain occurs under direct sun during summer and leads to higher cooling demand (Graph 37). Followingly, the rise of the indoor temperature resulted with a lower total comfort of the user (Graph 38). Effectively, in this case, the glass reaches higher temperature under the direct sun and acts as a radiant heating surface along the day which becomes a disadvantage during warmer periods with less satisfying indoor comfort although the cooling is activated.

According to Honeybee, the total zone temperature is an average of the surface and the room air temperature, indicating that the room is becoming warmer. In reality, the temperature is warmer next to the glazing surface.

On the other hand, the other types of glazing 1, 2, 3 and 4, have lower g-values 0.62, 0.47, 0.5 and 0.5 respectively. Therefore, the cooling loads are reduced. However, the difference in the demand does not show any considerable impact on BENG 2, as the total cooling loads are lower than the heating, as well as the WWR and the U-value vary in the design iterations.

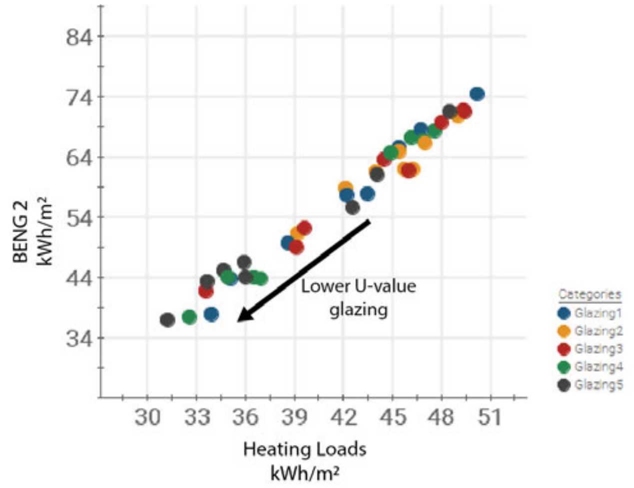

Graph 36 *Designs ranked by glazing types according to BENG 2 and the heating loads*

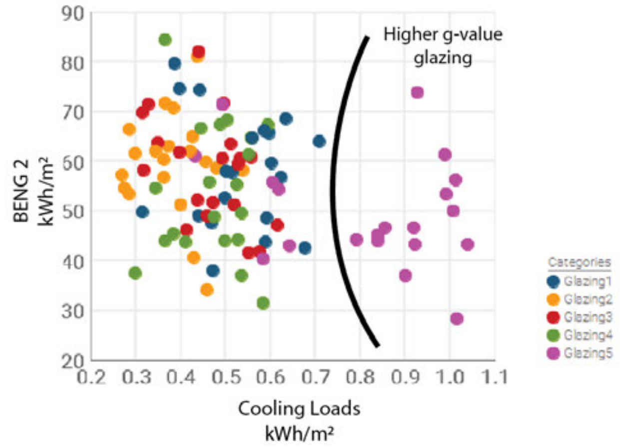

Graph 37 *Designs ranked by glazing types according to BENG 2 and the cooling loads*

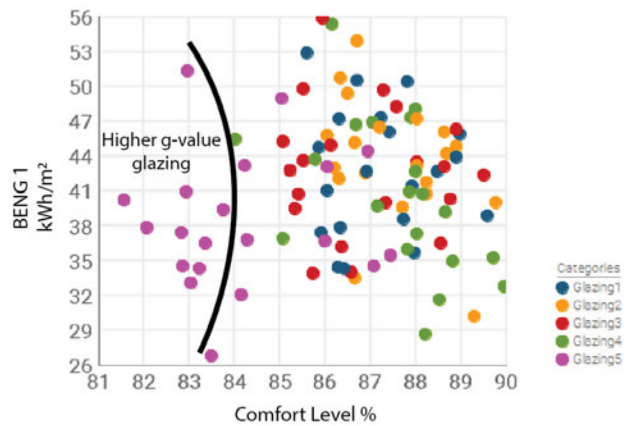

Graph 38 *Designs ranked by glazing types according to BENG 1 and the comfort level*

Analysis of the Shading Systems

The shading elements provide a better performance in the reduction of the cooling loads, depending also on the range of the WWR. Referring to Graph 39, the most efficient in reducing heat gains is the external controlled shutter, compared to both the internal shutter and the external fins where the cooling loads are higher.

The observed variations in the indicator BENG 2 is a result of the combination of the shading systems, with the amount of WWR and the glazing types considered.

Similarly, the comfort level is higher (Graph 40) with the external controlled system as it creates a barrier to solar radiation before entering the internal space where the air in the created cavity is constantly changed in the external environment. On the contrary, the internal shading system acts as a thermal mass by being positioned on the internal layer of the facade with a continuous release of heat leading to less comfort in warmer periods.

Also, the iterations that resulted with a comfort level under 85%, despite the implementation of shading systems, are designed with the glazing type 5 of higher g-value, and therefore contributes to more solar gains, that can be a disadvantage in the presence of the shading system acting as thermal mass too.

For the external fins mounted with PV cells (type 3), it improves the energy generation of BENG 3 above a certain level (Graph 41). However, some design iterations include a WWR that provides a more advantageous surface area on the facade for the mounted PV than the positioning of the extruded fins that contributes to self-shadowing.

According to the literature review, in the design of high-rises, for safety reasons it is less practical to implement overhanging objects at great altitude due to the strong winds. Therefore, although the PV-integrated fins can improve the energy generation, it is disregarded as an option to be used in this study.

Among all the iterations that have been evaluated in the design space, the selection is based on the target objectives to reduce BENG 2 and maximize BENG 3, while satisfying the 90% comfort of the users. Referring to the parallel coordinates Graph 42, the most efficient design that respond to the goals resulted on the WWR iterations of 20% on East, South and West, and 40% on the North, in combination with the glazing type 4 (U-value 0.6 W/m2K, g-value 0.5, VLT 75%) and the externally controlled roller blind (Shading Type 2).

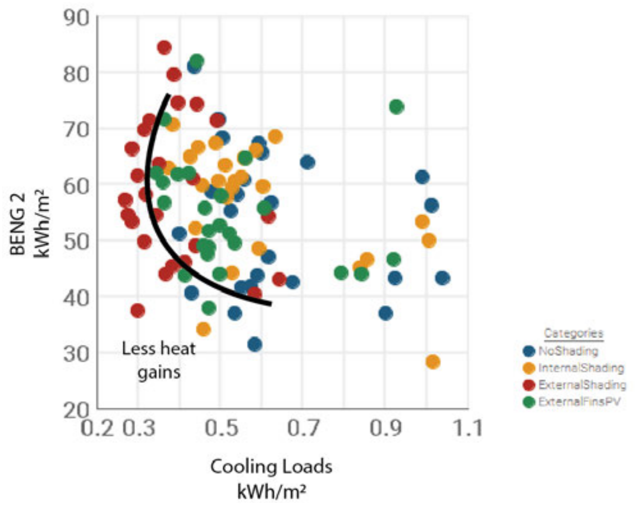

Graph 39 *Designs ranked by shading types according to BENG 2 and the cooling loads*

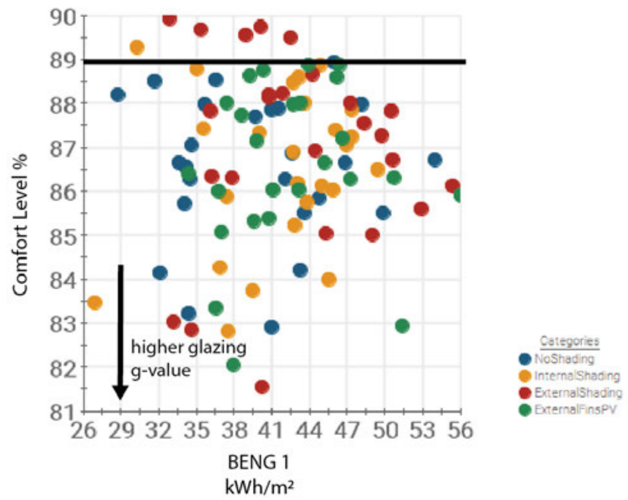

Graph 40 *Designs ranked by shading types according to BENG 1 and the comfort level*

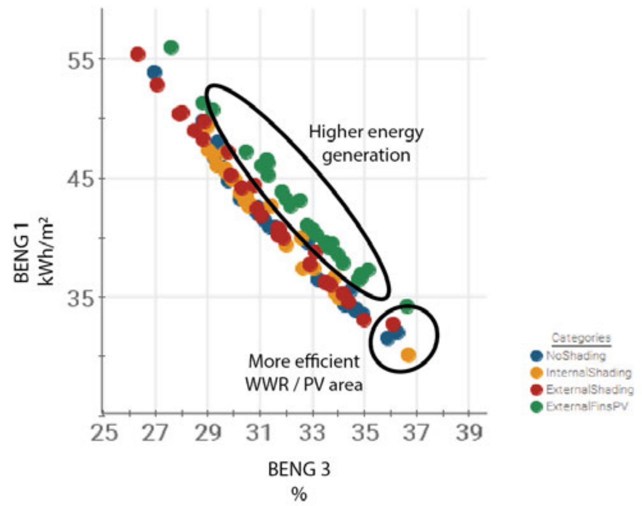

Graph 41 *Designs ranked by shading types according to BENG 1 and BENG 3*

The design presents a reduction of the heating loads, of 32.5 kWh/m2, related to the lower U-value of the selected glazing type, and a reduction of the cooling loads, of 0.29 kWh/m2, resulting from the barrier to heat gains during summer created by the external shutter layer. However, concerning the visual comfort, the sDA is the lowest at 21% for this combination of WWR where 3 facades out of 4 have a 20% ratio. Thus, the artificial lighting indicates an increase in its demand 9.93 kWh/m2.

In result, for the lower zone of the high-rise, the user comfort indicates a satisfaction of 90% (Diagram 28), with a BENG 1, 2 and 3 respectively of 32.8 kWh/m2, 37.6 kWh/m2 and 35%.

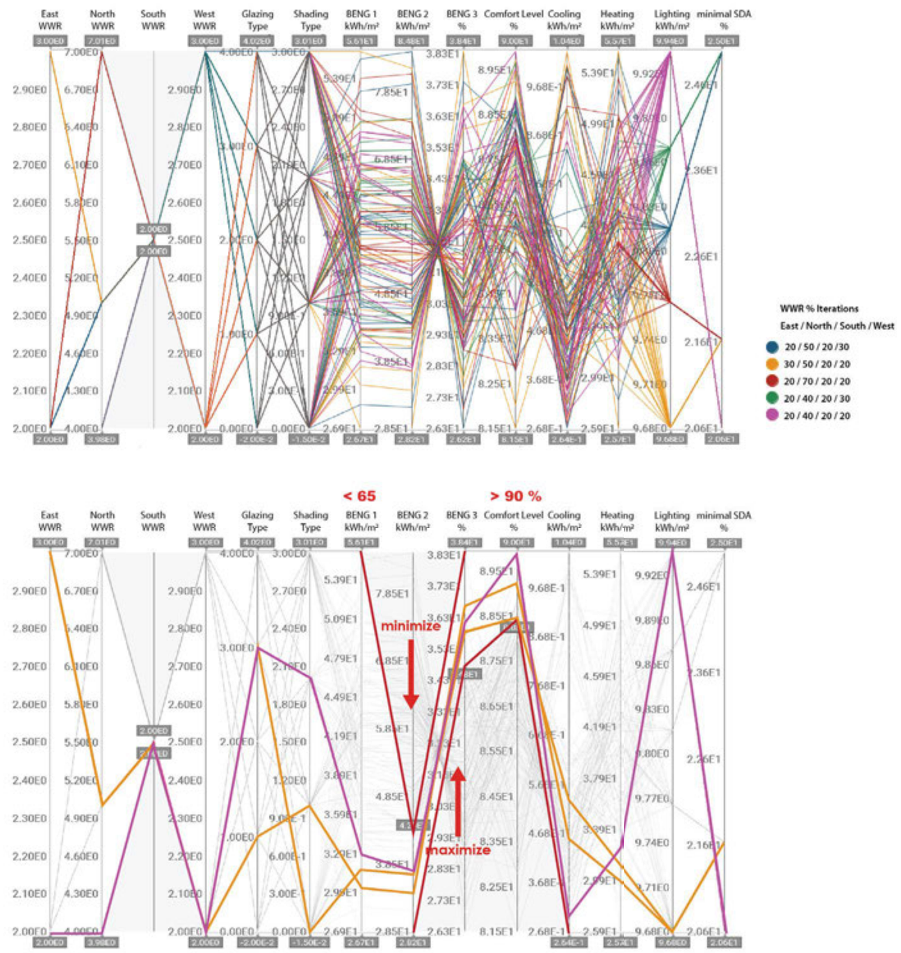

Graph 42 *Parallel coordinates chart of the filtering for the selection of the design according to BENG 2, BENG 3 and the comfort level*

Due to the lack of time to run optimization with all the parameters, to proceed with the selection of the design iterations in the remaining zones of the high-rise, the glazing type 4 and the externally controlled shading system are applied to the WWR iterations of zones 2, 3 and 4. For the selection of the best performing iterations, they are ranked regarding BENG 2 and 3, and their proximity to achieve a high indoor comfort.

For zone 2, the design with the highest comfort level and lowest BENG 2 indicates a WWR of 20% for East, West and South, and 50% for the North (Diagram 27). The selection of the 20% in this case provides a minimal sDA of 20%, which is above the required 10% (NEN-EN 17037). However, the visual comfort is affected with less access to the view to the outdoors. Therefore, in the case where the visual comfort is a more important criteria, higher ratios should be prioritized to the energy performance factors.

As for the next zone 3, the best iteration has shown a lower BENG 2 with a WWR of 30% East, 20% South, 50% West and 40% North (Diagram 26). In this case, the comfort is slightly lower due to the larger range of glazing surface on the West, but the energy performance was prioritized according to the objectives of this study.

For the upper zone 4, the best performing iteration indicates a WWR distribution of 30% for the East and South, 20% for West and 60% for North (Diagram 25). However, the comfort level is not satisfying in this case, and a further optimization might have provided better results.

To observe the scheme of WWR in parallel to height, the best performing iterations of each zone are combined for the final design of the high-rise (Diagram 29), which all include the selection of the glazing type 4, and the externally controlled shading system.

The variation of the facade WWR in parallel to height does not indicate an improvement of the performance of the residential high-rise. In fact, the opening does not show any pattern of enlargement or reduction as the considered floor level rises in altitude.

However, each orientation is identified to a range of variables that provides improvement to the efficiency of the design. For the East, South and West lower glazing ranges have shown to be the most efficient, with variables between 20% to 30%, whereas the North performs better under larger ratios between 40% and 60%.

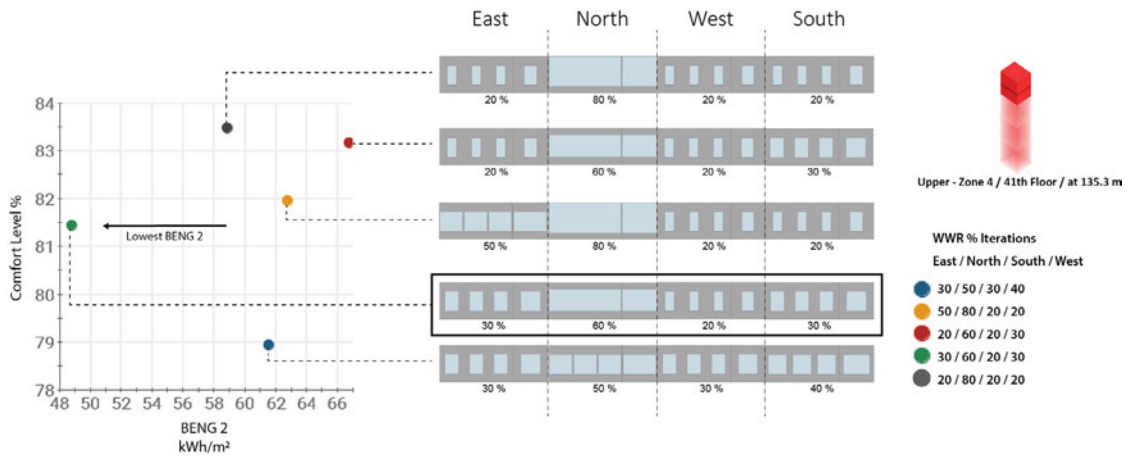

Diagram 25 *Design iterations of zone 4 ranked according to the performance of BENG 2 and the comfort level*

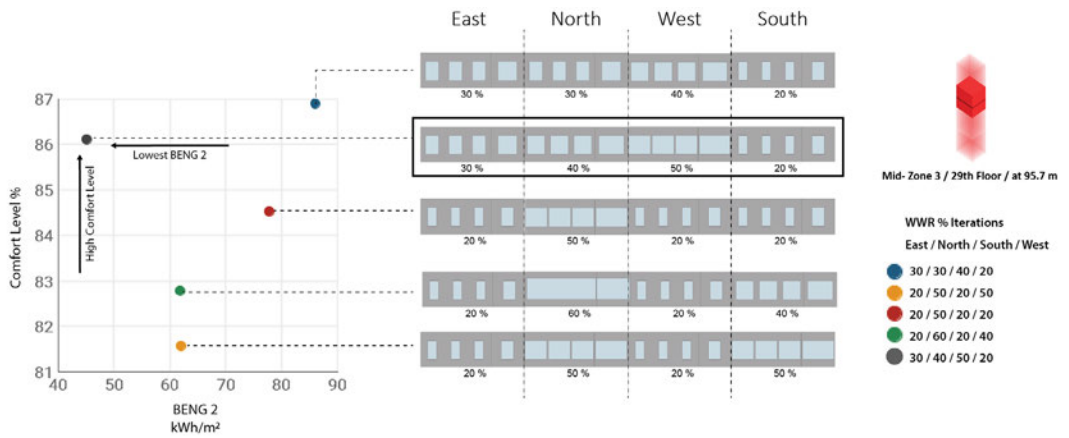

Diagram 26 *Design iterations of zone 3 ranked according to the performance of BENG 2 and the comfort level*

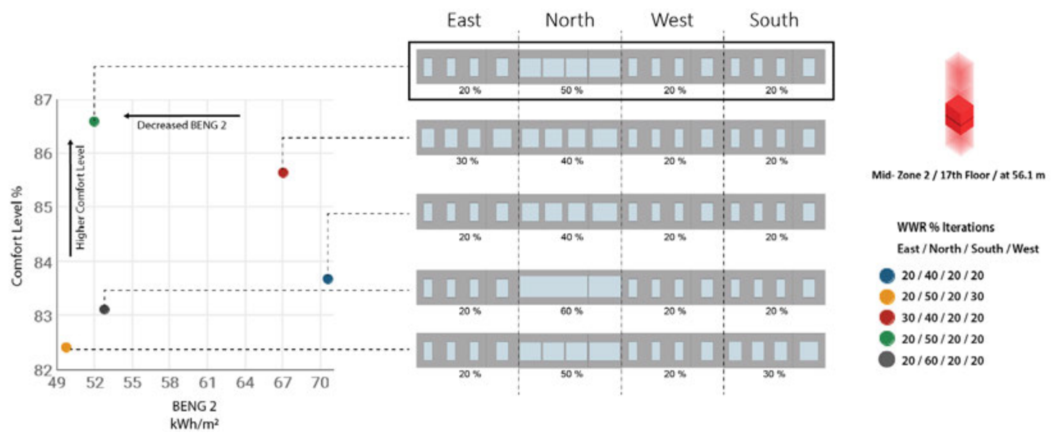

Diagram 27 *Design iterations of zone 2 ranked according to the performance of BENG 2 and the comfort level*

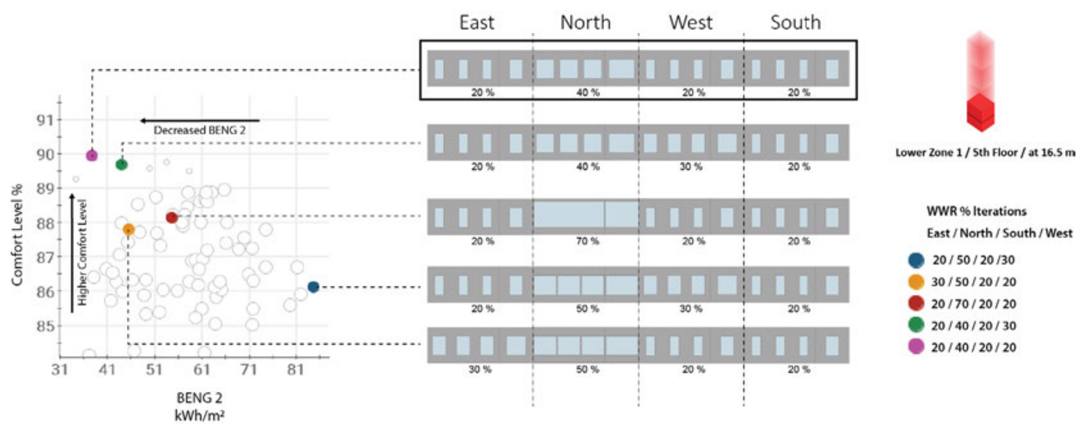

Diagram 28 *Design iterations of zone 1 ranked according to the performance of BENG 2 and the comfort level*

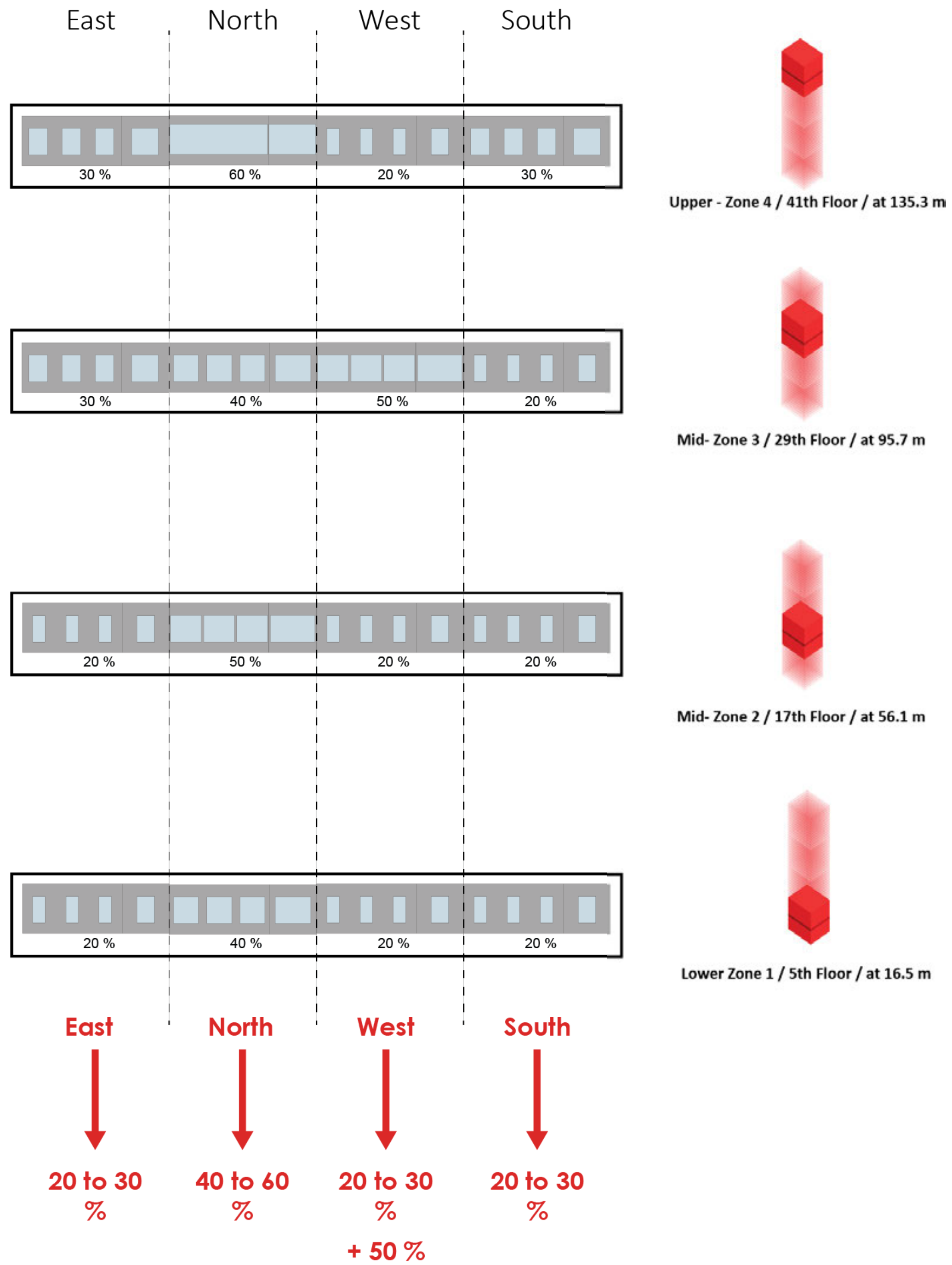

Diagram 29 *Optimal design iterations of each zone, at the different height level, with the range of WWR per orientation*

4.7. Phase 5: Energy Performance in respect to the Height Increment

As the BENG regulations present a constraint to the design of the high-rise typology, mainly located in urban dense areas, the target height is examined to determine the factor behind the restriction. To investigate the impact of the height increment on the performance of the residential high-rise, a gradual addition of the floors, starting from the 2nd floor (level of 6.60 meters) up until the 48th floor (level of 158.4 meters), is conducted on the final design, providing the total mean values of BENG indicators and the comfort level at different levels.

The optimal design results of each zone (Diagram 29) are applied to the final design of the residential high-rise which is inserted into a low-rise surrounding context to simulate the urban area conditions. For the energy generation of BENG 3, the roof layer is a major factor considered in this gradual analysis. It is covered at 75% of its surface area by PV cells with a 20% efficiency.

The benchmarks of BENG 2 and 3 are expected to be satisfied until a certain height, where their limit will be reached under a decrease of the overall performance of the high-rise. Also, in parallel to the height, it is assumed to observe a fluctuation in the energy loads to adapt to the changing micro-climate conditions. To refer to the resulting data of each floor, refer to Appendix F, Table 5.

Height Increment Results

For the three indicators, different trends are observed in parallel to the high-rise height. First, the increment from the lower to the upper floor presents a continuous increase of the energy demand of BENG 1 (Graph 43), from 29.5 kWh/m2 to 48.6 kWh/m2, indicating an overall decrease of 39% in its performance. Regarding the benchmark, the total energy demand is under the required 65 kWh/m2 along the entire high-rise, and tends to get closer if additional floors are added. In the last zone of the high-rise, from the 38th floor and upward, the drop in energy consumption is expected to be due to the resulting optimal design that includes smaller ranges of WWR compared to the preceding floor below it, which minimize heat loss and gains.

The increase of the total energy demand consists of the sum of both the cooling and heating loads. Referring to the Graph 44, there is a similar growth in the trend of BENG 1 and the heating loads in parallel to the floor addition. From the lower to the upper floor, the demand for heating increased from 28.8 kWh/m2 to 48.2 kWh/m2, in which the amplification appears in between the 14th (46.5 meters) and the 30th floor (100 meters).

As for the drop in its demand in the upper zone 4 (from the 38th floor), the optimal glazing WWR is smaller than in zone 3 below it. Thus, with less glazing surface, the area of heat loss through the envelope is minimized, and leads to a lower consumption of heating.

Regarding the micro-climate conditions, according to wind profile calculated with simulations in Ladybug plug-in (Diagram 10), the transition at 100 meters is marked by an acceleration in the wind speed from around 4.0 m/s to above 6.3 m/s, and reaching values of 7.0 m/s at the top of the building geometry. The higher speed is expected to increase the air pressure and air infiltration on the facade, leading to a higher rate of heat loss, in addition to the drop in the outdoor air temperature that occurs in higher altitude (Graph 9).

On the other hand, the cooling loads present more consistency in its demand of average of 1.10 kWh/m2 among all the floors above 20 meters (Graph 45). The lower demand of 0.72 kWh/m2 up to the 6th floor is caused by the facade overshadowing from the presence of the low-rise surroundings and leading to less exposure to solar radiation, and thus, less heat gains.

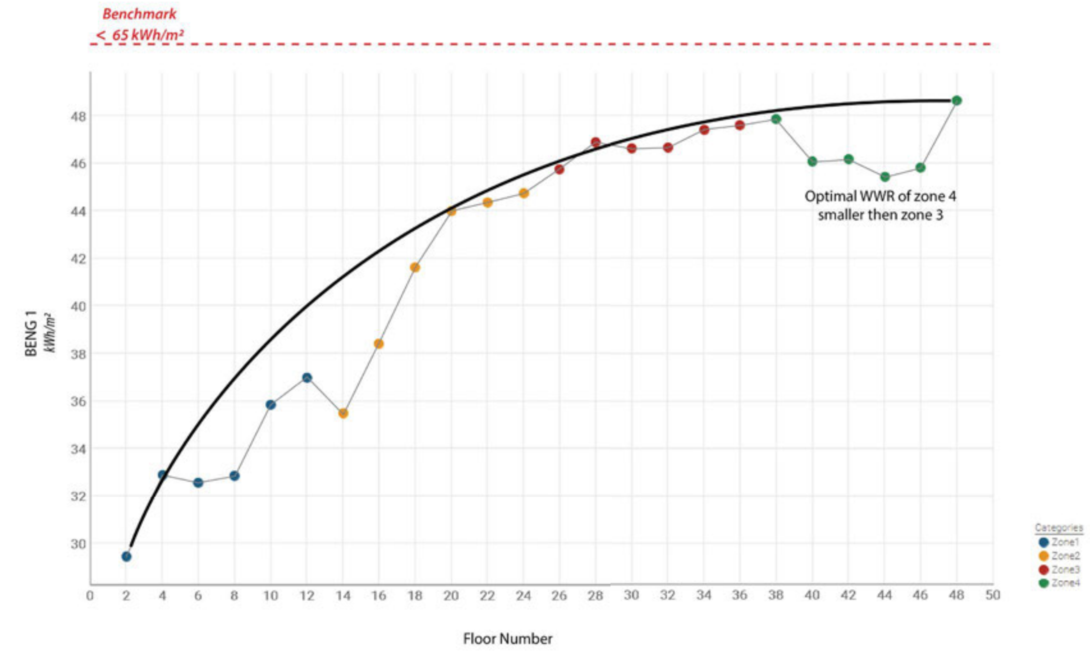

Graph 43 *Relationship between the gradual floor increment of the high-rise and the total energy consumption of BENG 1 regarding its benchmark*

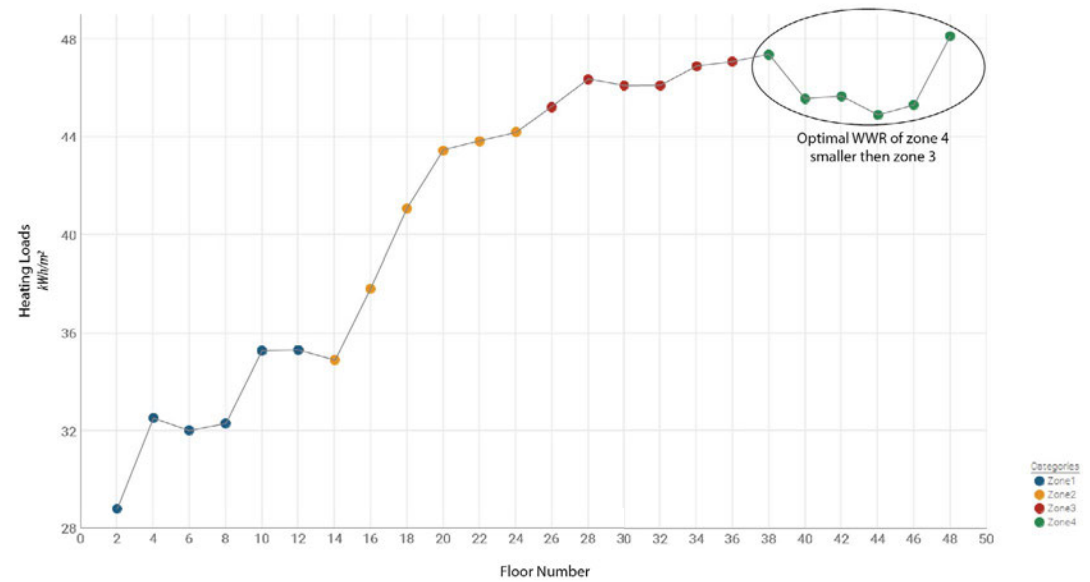

Graph 44 *Relationship between the gradual floor increment of the high-rise and the heating loads*

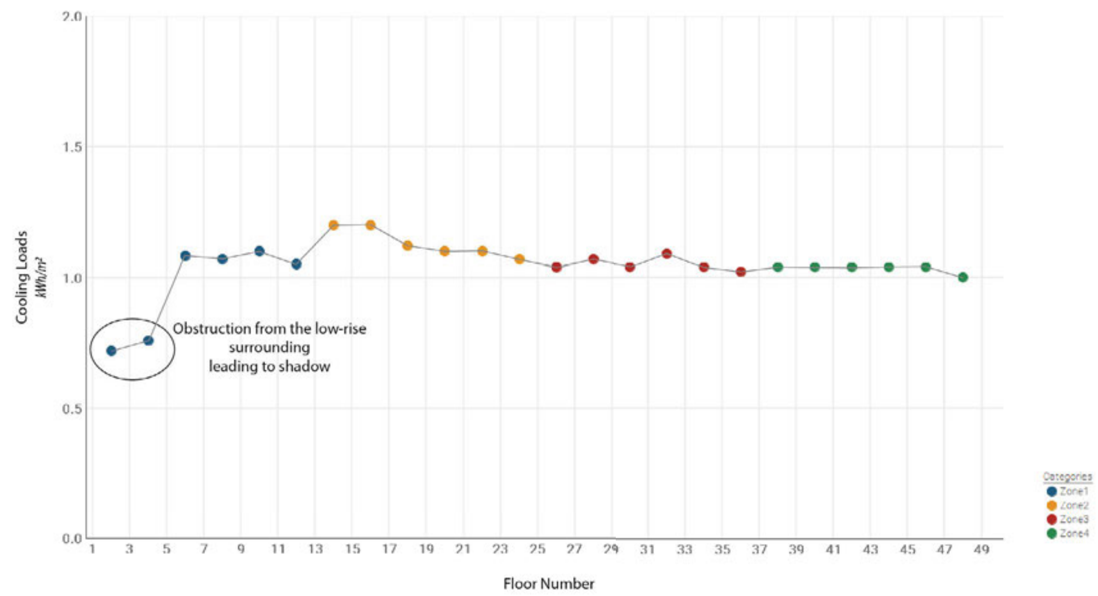

Graph 45 *Relationship between the gradual floor increment of the high-rise and the cooling loads*

Concerning the renewable energy of the indicator BENG 3, three different trends are observed (Graph 46). In the first part, a gradual decline of the trend occurs from 44.7% to 39.8% between the 2nd and 12th floor respectively, followed in a second part by its strong decrease from 39.8% down to 31.7% at 26th floor. Lastly, for all levels above the 26th floor (level of 85.8 meters), a more constant state is observed in the energy generation between 31% and 32%. In total, the performance of this indicator went down by 30% overall.

To establish the relation between the height increment and the reduction in the energy generation efficiency, the indicator of BENG 3 is analyzed according to the ratio of the total PV area implemented on the roof and the facades to the total usable surface area (Appendix F, Graph 13) in respect to the floor level (Graph 47).

Similar trends are observed in the total PV ratio along the increment of the height. First, the total PV ratio drops gradually, from 107% to 46%, with the energy generation from 44.7% to 39.8%. The benchmark of BENG 3 is reached for a total PV area to usable surface around 46% corresponding to at around half of the total usable floor area. Afterwards, in a second stage, the fast decrease of BENG 3 down to 31.7% occurs between ratios of 46% to 40%. Lastly, the slower rate decrease in the remaining height that appears to become constant occurs between ratios in between 40% and 35%.

In fact, the roof layer presents more efficiency in energy generation than the facades as long as it provides a total surface area of PV panels greater than the total usable area. However, according to the floor level reached, it has a greater potential up to the 12th floor where its exposure to the sun altitude is more efficient due to lower sun angle position in the winter period. Its performance becomes less significant after this level.

Regarding the regulations, the required total energy generation of BENG 3 above 40% is only satisfied until the 8th floor (level of 26.4 meters) with a total energy of 40.2%. Above this height, the benchmark is crossed, with a drop in the energy generation down to 31%. Thus, in the case of this study, the regulations have only been satisfied in the first zone of the high-rise, where the 26.4 meters reached can not be defined as a high-rise yet at this stage.

For the indicator BENG 2, similarly to BENG 1, a growing trend from the bottom to the top floor is observed (Graph 48). The primary energy usage presents lower value at the bottom of the high-rise, with 31.4 kWh/m2 at the 2nd floor, and gradually reaching the highest value of 69.4 kWh/m2 at the last floor, indicating a 55% decrease of performance of the indicator with floor addition.

The primary energy usage accounts for the cooling, heating, lighting and ventilation loads. The previous results of the heating loads are partly responsible for the decrease of its performance. In regard to the lighting loads, under the implemented low-rise context, the results show a usage around an average of 9.80 kWh/m2 for all the floors (Graph 50), with a drop in the upper zone 4, where the absolute difference is only of 0.20 kWh/m2.

However, due to the constraint of the plug-in, the dynamic shading is not affecting those results, which are expected to be higher under the shutting of the blinds. When the indoor temperature and solar radiation reach their setpoints, the shading system is shut, and in result, the amount of daylight entering the space is obstructed by the blind layer. Thus, by interfering with the visual comfort, a higher dependence on artificial lighting is needed to make up for the lack of daylight into the space. In this case, the illuminance threshold of 300 lux is not satisfied at all times of the day during occupancy. Also, under a smaller glazing ratio (20%) and the presence of the shading layer, the demand can reach higher loads.

Concerning the ventilation, referring to the Diagram 17 and Table 34, the total allowable hours of natural ventilation NV decreases from 645 to 186 hours respectively between the lower zone 5th floor and the upper zone 41th floor. This decrease is due to the higher wind speed that occurs in altitude. In response, the total amount of mechanical ventilation MV increases from 8115 to 8574 hours respectively at the 5th floor and 41th floor. Thus, the ventilation usage adapts to the micro-climate conditions, where there is a higher consumption of energy for the mechanical ventilation as the floors add up in the building.
Lastly, the share of renewable energy of BENG 3 is subtracted from the total of BENG 2. The decrease in the energy generation in parallel to height is reflected in the increase of the outcome of BENG 2.

According to the regulations, the second constraint to the design of the high-rise is reached at the 16th floor (level of 52.8 meters) when the total primary energy usage in BENG 2 reaches a total of 49.25 kWh/m2 being at proximity of its benchmark (< 50 kWh/m2). Above this height, the requirement is not met anymore, where the total energy increases considerably until the top of the high-rise.

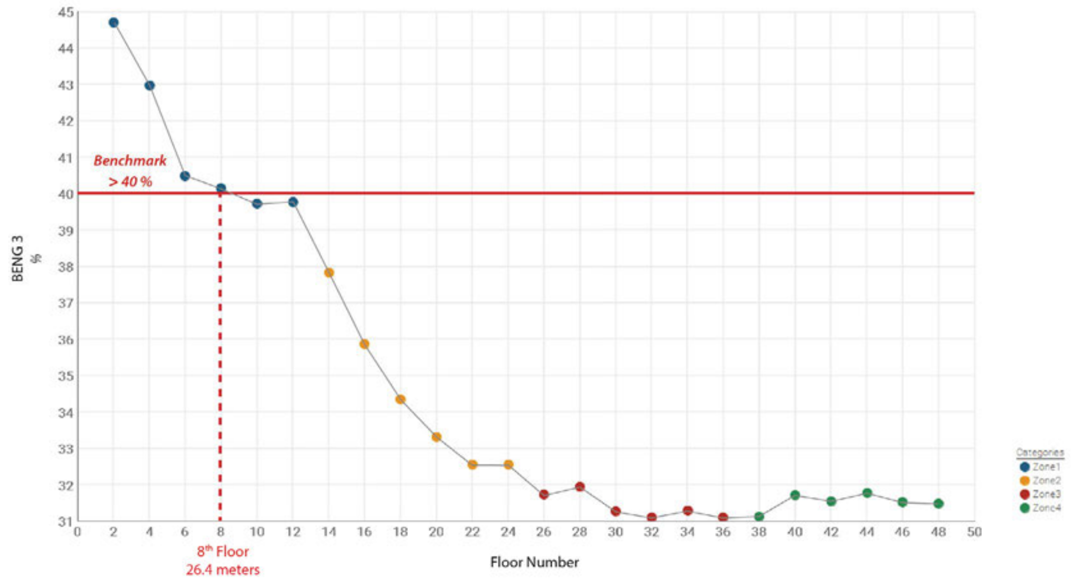

Graph 46 *Relationship between the gradual floor increment of the high-rise and the total renewable energy of BENG 3 regarding its benchmark*

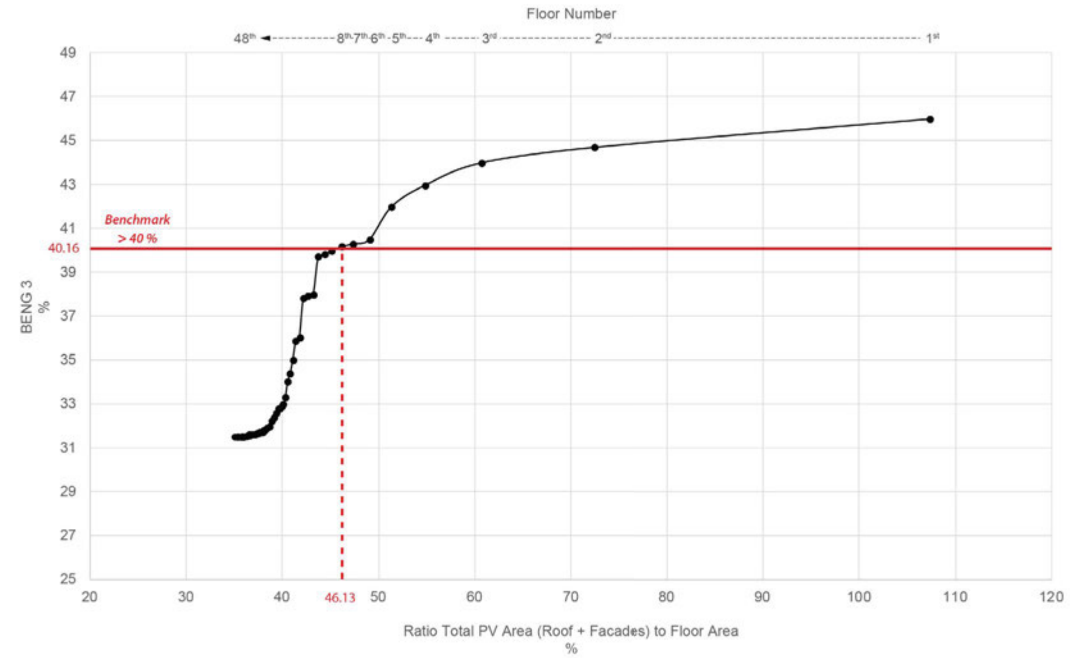

Graph 47 *Relationship between the gradual floor increment of the high-rise, BENG 3 and the ratio of the total area of PV on the roof and facade to the total usable floor area*

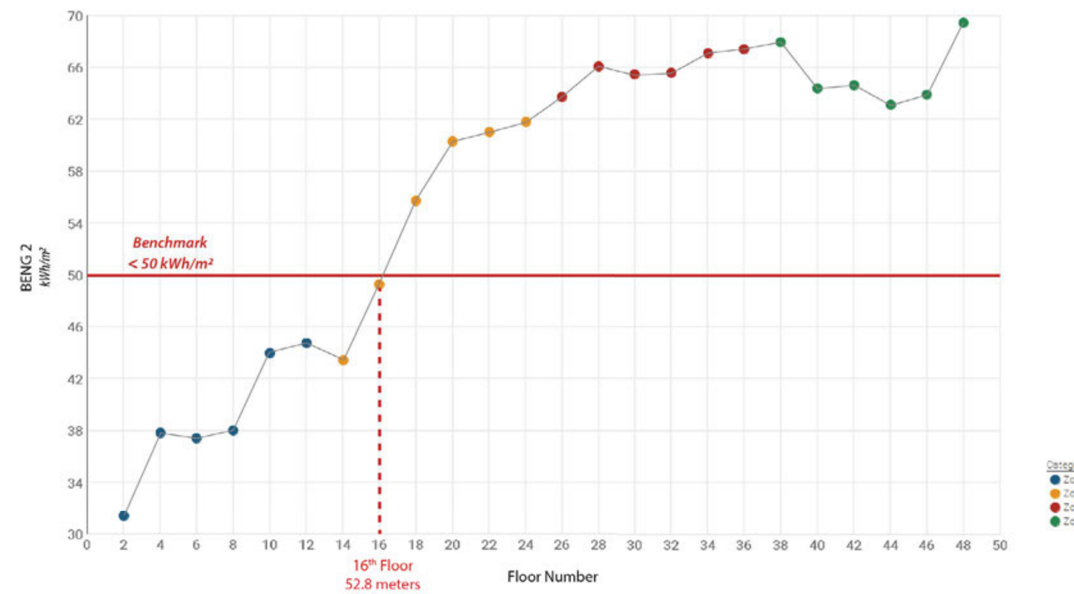

Graph 48 *Relationship between the gradual floor increment of the high-rise and the primary energy usage of BENG 2 regarding its benchmark*

Moreover, along the height increment, the user's comfort is determined for the annual period calculated for 8760 hours. The maximum indoor temperature recorded for the 4 different zones are extracted to verify the TOjuli limiting to 26 °C.

The total comfort presents larger fluctuations in the lower floors in zone 1, between 85.5% and 89.3%. At this zone, the maximum indoor temperature recorded is 28.2°C which exceeds the TOjuli of 26°C. The increase in satisfaction for the first floors is due to the presence of the low-rise surroundings that acts as a barrier from the sun during summer. However, the outdoor air temperatures are higher in the bottom of the high-rise which leads to more risk of overheating during warm periods.

Followingly, the comfort fluctuates less strongly in the zone 2, between 86% to 87%, where the indoor temperature reaches a maximum of 26.7 °C, also exceeding the TOjuli. Similarly, in zone 3 the comfort is between 86.7% and 87.7%, with a maximum temperature of 26.2 °C. Lastly, in zone 4, the comfort becomes more constant, between 87% to 87.7%, with a lower maximum temperature of 25.5 °C that is under the limit of the TOjuli in this case. However, the comfort level should be above 90%, which is not reached at any given height of the high-rise.

The difference in the micro-climate conditions and surroundings have a different impact on the high-rise when treating the facade. The drop in the temperature has resulted with a decrease in the maximum indoor temperature recorded for the different height.

However, the TOjuli of 26°C is exceeded for most of the floors, which is due to the cooling set point that is defined to 26°C in the workflow setting. In this case, when the indoor temperature increases, the set point will be crossed as between the time of activation of the cooling systems and the amount of time required to regulate the indoor temperature can lead to overheating. Thus, the set point should be fixed at a lower temperature, of 24°C, to provide a buffer time to prevent reaching the TOjuli limit.

Additionally, both of the cooling and heating set points are fixed at similar values for all the floors. Considering that the micro-climates change with height, it is assumed that different settings regarding the embedded systems should be considered between the lower floors, compared to the upper floors. Also, in the optimization phase of the zones, the objectives were more focused on satisfying the BENG requirement as a priority to the comfort level, which highlights the constraints of the possibility to satisfy both of the regulations and a comfortable indoor environment all together.

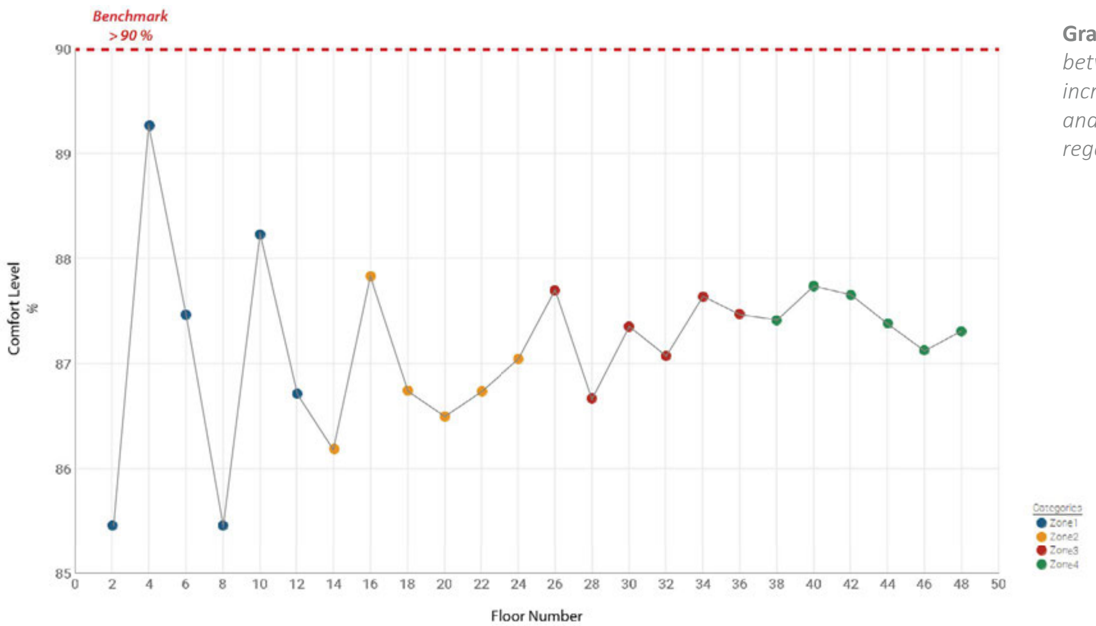

Graph 49 *Relationship between the gradual floor increment of the high-rise and the user comfort level regarding its benchmark*

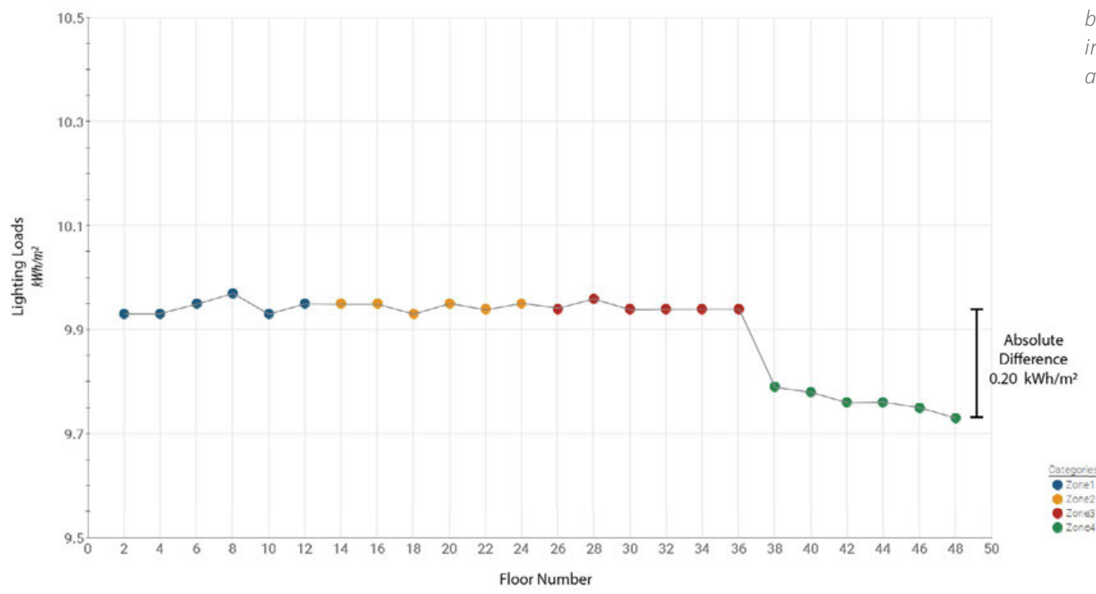

Graph 50 *Relationship between the gradual floor increment of the high-rise and the lighting loads*

	Mechanical Ventilation *Hours*	Natural Ventilation *Hours*
Zone 4 41th Floor 135.3 meters	8574	186
Zone 3 29th Floor 95.7 meters	8490	270
Zone 2 17th Floor 56.1 meters	8398	362
Zone 1 5th Floor 16.5 meters	8115	645

Table 34 *Results of the total annual MV and NV hours by zone level*

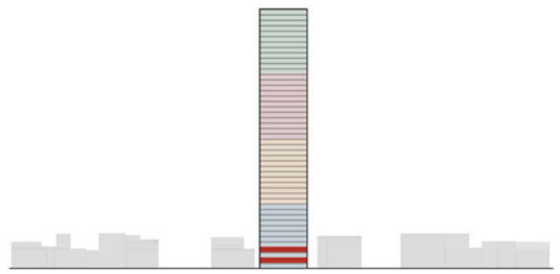

Diagram 30 *Position of the 2nd and 4th floors in relation to the surrounding building*

5 Guidelines Proposal and Amendment

The following guidelines proposed serve as a set of recommendations for designers and architects in the decision making concerning the design of a residential high-rise in the temperate climate of the Netherlands. Based on computational optimization and exploration, the most influential parameters related to the BENG 2020 regulations and the comfort level are extracted regarding the early design stage of the building for the orientation and compactness, as well as the influence of the surrounding context. In addition, the facade related parameters are presented with the WWR, the glazing type properties and shading systems. The implementation of PV panels on the envelope of the building is also included in order to provide a share of renewable energy.

The suggested guidelines have been established on a conceptual design of a residential apartment high-rise, in which high efficiency parameters have been incorporated regarding the envelope insulation that is highly airtight (0.15 ACH), with external walls R-value of 4.5 m2K/W and roof layer of 6.0 m2K/W, and the glazing type (U-value, g-value, VLT). Additionally, high efficiency building systems are implemented, with cooling EER of 15, heating COP of 3.6, heat recovery efficiency of 95% and PV efficiency of 20% (Table 35).

Envelope Properties		Building System Efficiency	
Highly Airtight	**0.15** [ACH]	Cooling EER	**15**
External Walls R-value	**4.5** [m²K/W]	Heating COP	**3.6**
Roof Layer R-value	**6.0** [m²K/W]	Heat Recovery Efficiency	**95%**
Glazing Type		PV Efficiency	**20%**
U-value	**0.6** [W/m²K]		
g-Value	**0.5**		

Table 35 *Energy-efficient parameters of the envelope and building systems properties applied in the study*

Under the current regulations, achieving a 160 meters tall residential high-rise does not present an obstacle in the total energy demand of BENG 1, under the benchmark of 65 kWh/m2. As it consists of the sum of the cooling and heating loads, passive design strategies serve as solutions in minimizing both demand.

In the temperate climate of the Netherlands, with moderate winter, heating presents a larger share of the consumption in the households compared to cooling. Prioritizing a reduction of heat loss through the facade can be implemented with a higher compactness of the geometry (smaller shape factor). It diminishes the total envelope surface area exposure to the external environment, and thus, all things being equal, reduces the total amount of heat gains during summer and heat loss during winter. In results, less cooling and heating is needed which contributes to a reduction of both the energy demand of BENG 1, as well as the primary fossil energy use of BENG 2 (Diagram 31).

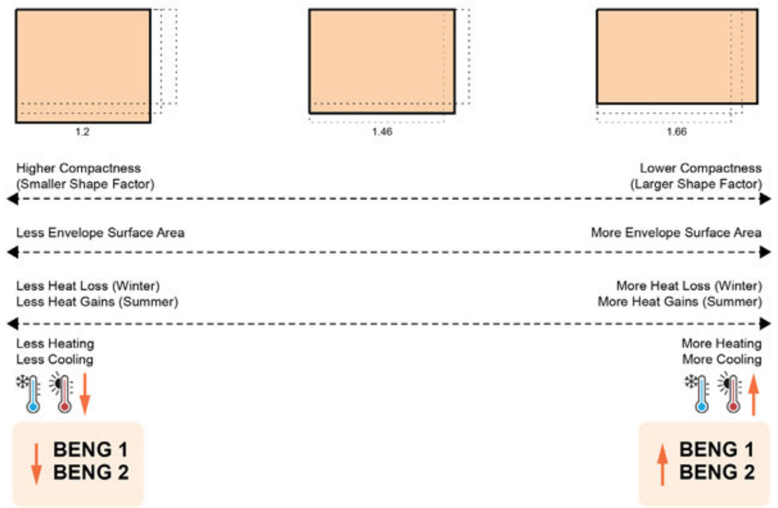

Diagram 31 *Guidelines regarding the geometry compactness*

Additionally, depending on the geometry of the design, the building can adjust to passive solar heating by shifting the main axis from the North-South. In the case of a more squarish plan shape (equal length/width) aiming for a 45° orientation exposes more than only 3 facades to sun loads. Thus, all of the spaces around the envelope perimeter will take advantage of the sun requiring a lower heating demand in winter (Diagram 32). However, for the summer period, the implementation of a proper shading system can prevent the risk of overheating. In the case of a longitudinal shape (rectangular plan), the longest facades should be prioritized to face the South-West, with orientation angle in between 0° and 90°. (Diagram 33)

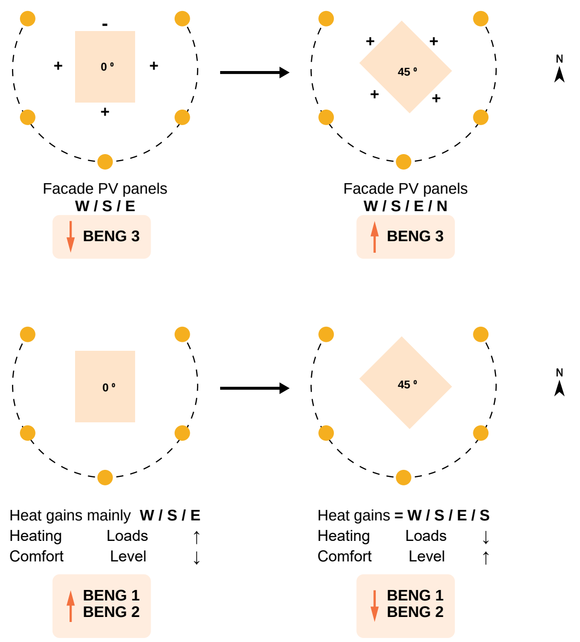

Diagram 32 *Guidelines regarding the orientation of a squarish plan from the North axis*

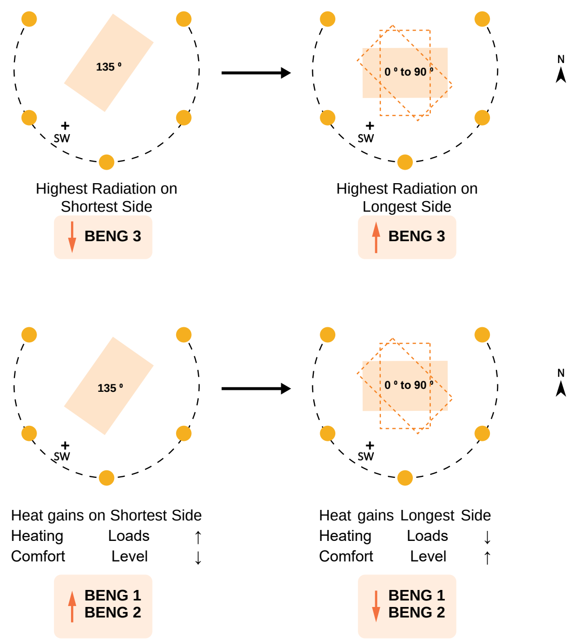

Diagram 33 *Guidelines regarding the orientation of a rectangular plan from the North axis*

Preventing overheating for the requirement of the TOjuli and minimizing the cooling loads, can be done though the selection of a shading system to control the solar gains. An externally controlled system blocks the solar radiation at an earlier stage of the envelope layer, and thus, reduces transfer of heat gains to the internal space.

As part of the envelope parameters, and in adaptation with the window-to-wall ratio, the selection of the glazing type should be based on minimizing heat losses in winter and gains in summer. By opting for a low U-value, in the case of this research around 0.6 W/m2K, indoor temperature can be conserved. Additionally, the g-value can counteract overheating from decisions regarding the building orientation, where a lower value around 0.5 in this case, can prevent heat gain from the solar radiation in summer (Diagram 34) and be more favorable for the TOjuli. By prioritizing a non-heating dominant design strategy, the outcome ensures a reduction in BENG 1 and BENG 2, in addition to the higher comfort level provided for the occupants.

Diagram 34 *Guidelines regarding the glazing properties (transparent parts)*

However, the selection of the glazing types properties is affected by the window-to-wall ratio (Diagram 34). First, a proper distribution of the ratios should be adapted to the orientation of each facade. The East, South and West should be prioritized with less glazing, as they are more sun oriented, and thus less heat transfer occurs on these facades in addition to prevent risk of overheating. In this case, the smaller ratio can allow for a higher U-value if required. As for the North, unless the orientation of the building exposes it to the sun, a proper balance with the amount of daylight can be more advantageous to increase the visual comfort (Diagram 35). Thus, prioritizing the larger ratio on this facade should be accordingly with a lower U-value.

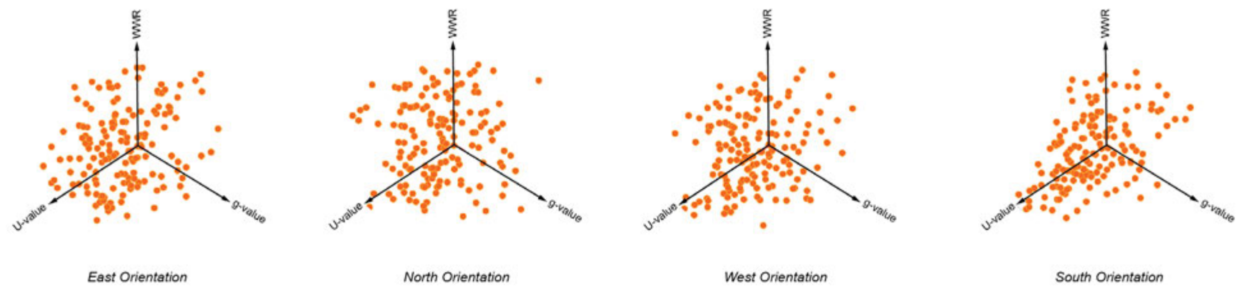

Diagram 35 *Guidelines for the glazing properties (transparent parts) according to the facade orientation*

From the building perspective, generating renewable energy from solar ressources is only advantageous and efficient when the ratio of the total PV area, from the roof and the facade, to the total floor area of the building is above 50%, representing more than half of the usable area. For the roof layer, its efficiency decreases with the height due to the lack of access of the sun radiation from its lower angle position. By increasing the height, the 40% threshold of BENG 3 is crossed at a given level in the high-rise. However, the implementation of design strategies allows to maintain a closer ranking to the regulations with the following decisions.

First, the orientation of the geometry determines the amount of facade exposed to sun radiation. For squarish shapes, shifting the main axis from the North-South axis, toward 45°, exposes more than 3 out of 4 facades to sun radiation and increases the energy generated from the mounted PV (Diagram 32). In the case of a rectangular plan, at least one of the longest sides should be oriented towards the South-West direction where the sun exposure is the highest.
However, the PV implementation on the facade comes hand in hand with the window-to-wall ratio. Those 2 factors are inversely proportional, thus a reduction of the WWR provides a greater available area for applying PV or BIPV.

In the case of the primary energy use of BENG 2, the limit in height is reached further in this study. The determination of BENG 2 adds up the cooling, heating, lighting and ventilation loads. Similarly to BENG 1 for cooling and heating, the decisions regarding the geometry and facades parameters allow to overcome challenges of BENG 2 to a certain extent. For the lighting, enlarging the WWR reduces the artificial light dependence. However, as the heating loads will tend to increase, it is more advantageous to prioritize a WWR that minimizes the surface of heat loss to the exterior with a reduction of the U-value, but also, a lower g-value. The thermal comfort of the user is more satisfied than the visual comfort under small ratios. Therefore, depending on the goal of the designer, and the space function, the decisions should balance between the thermal and visual comfort.

Amendment Proposal to the Current Regulations

According to the aforementioned guidelines, the design ranking is improved regarding the regulations benchmark. Along the height increment, the indicator of BENG 1 increased consistently, while remaining under the required 65 kWh/m2. However, both of BENG 2 and BENG 3 benchmarks have turned into limitations to the design of the target height at levels of 52.8 meters (16th floor) and 26.4 meters (8th floor) respectively. According to the literature review, a building is considered a high-rise in the Netherlands for a height above 70 meters (21 floors). Considering both limitations that occured in this study, the BENG indicators present constraints to the design of the high-rise typology according to the country's own definition (Diagram 36).

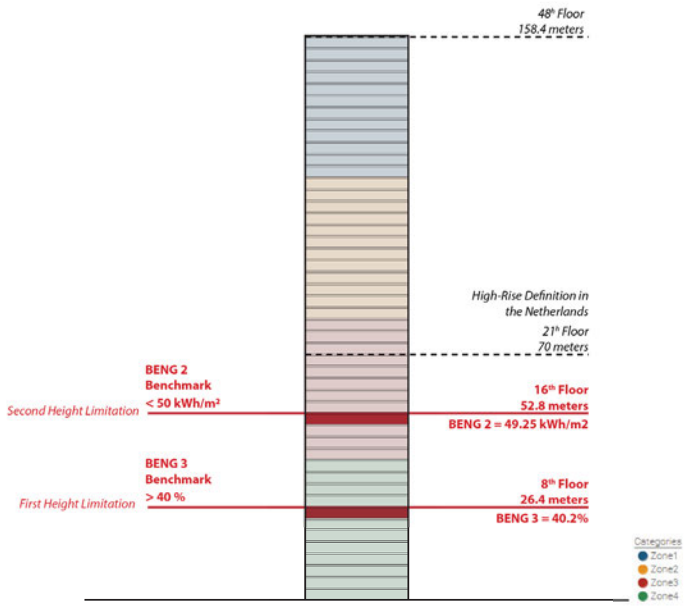

Diagram 36 *High-rise floor levels regarding the limitation of the BENG indicators*

Nevertheless, despite the optimization and the implementation of the guidelines, above both limits reached, the design of a residential high-rise necessitates amendment regarding BENG.

To do so, an index is used to establish a connection between the high-rise geometry and its height, and relate it to the energy performance of the indicators. Thus, the ratio of the volume to the loss surface of the envelope (Als) is determined at the different levels of the building (Appendix F, Table 8). As the height increases, the loss surface of the geometry expands gradually with more volume. In result, a larger amount of heat is lost through the envelope, although maximizing the available surface for PV implementation.

Amendment to BENG 3

The relationship between the volume and the envelope surface of the building geometry (Graph 51) indicates similar trends to the performance of BENG 3 in regard to the height (Graph 46). The higher the building, the more envelope area is provided for energy generation from the PV implementation. However, the total surface area does not seem to be enough until a certain height, indicated by the index ratio of V/Als = 5.60.

In fact, for V/Als < 5.60, the ratio is declining from 3.0 to 5.60, with an absolute difference in between consecutive floors greater than 0.10. At this stage, the energy generation is above the current benchmark of 40%, and gradually decreases by reaching the height level of 39.6 meters (12th floor). The decline in between the 2nd and the 12th floors indicates that the roof presents more potential in the energy generation until the 12th floor. Taking into account that the PVs are positioned with a 0° tilt angle on the roof surface, the sunlight only hits their surface when the sun altitude is higher at midday and during summer season.

Further in height, once the benchmark threshold is crossed, the ratio is declining at a faster rate for values between 5.60<V/Als<6.15, with absolute difference of 0.02 between consecutive floors. Consecutively, for a height level between 39.6 (12th floor) and 92.4 meters (28th floor), the renewable energy decreases at a fast rate, from 40% to a maximum share of 32%.

Taking into account that the roof layer has reached its maximal efficiency, the parallel decline of both the ratio index and BENG 3 highlights the potential of the facades in the energy generation. The available area for mounting PVs becomes less efficient in respect to the increasing usable surface (m2) under more volume. In this case, a revision of the benchmark from the current 40% to 32% would represent an allowable margin of 11%.

Lastly, for a ratio index of V/Als > 6.15, with the continuous enlargement of the volume of the building and the usable surface area (m2), the total envelope area reaches a stage where the amount of energy that can be generated from the facade is inefficient to supply the energy demand. Thus, the index above a height of 95.7 meters (29th floor) indicates an insignificant decrease that reaches a constant stage, with absolute difference between consecutive floors of less than 0.01. Followingly, the energy generation reaches a plateau maintained above 30% indicating neither an improvement or a regression in the amount of energy that can be generated from the facade, but rather a constant supply. With the last floor moving higher in altitude, the access to sunlight decreases mainly during the winter season where the sun position is at a lower angle. In this case, the amendment of the benchmark from the previous 32% to 30%, can qualify all floors for BENG 3 along the remaining height of the residential high-rise.

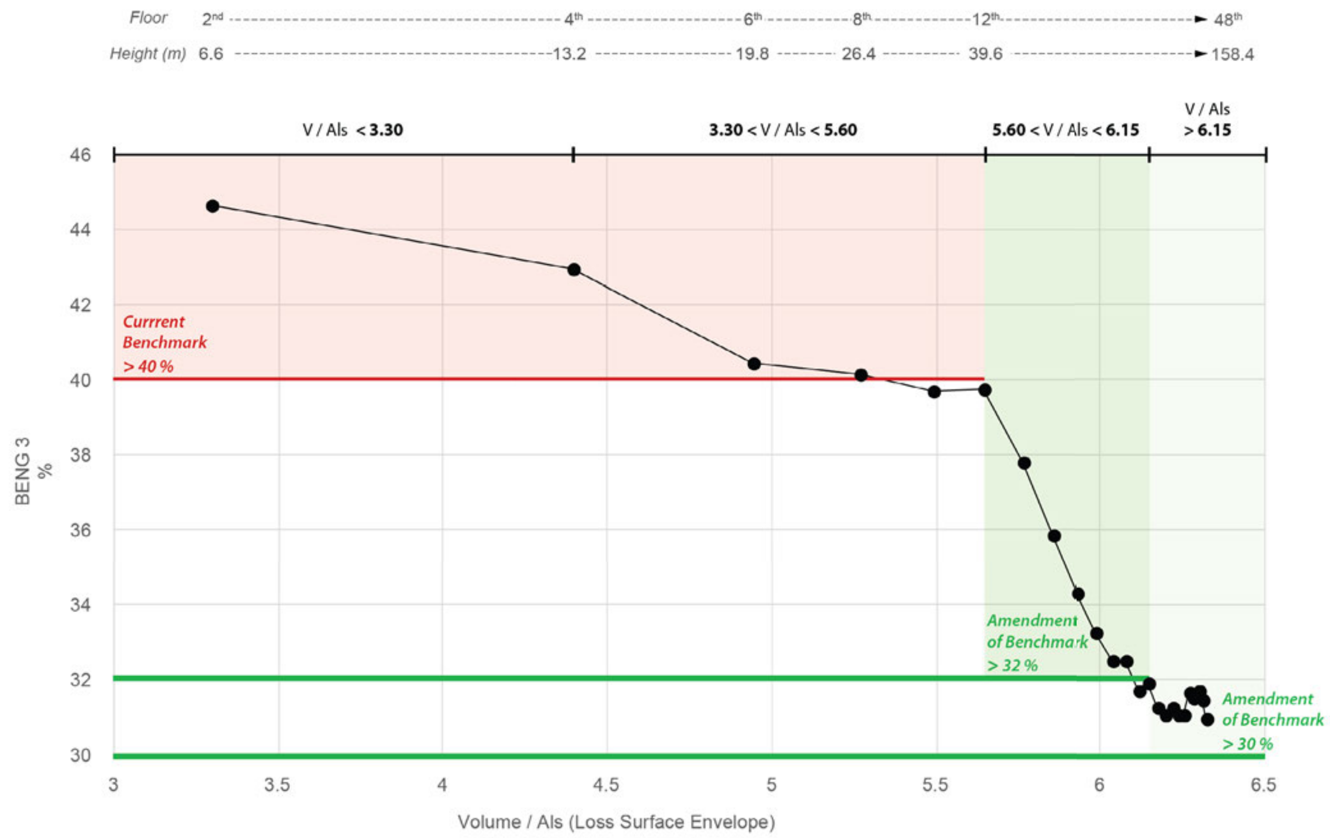

Graph 51 *Proposal of amendment for BENG 3 benchmark regarding the building volume and height*

Amendment to BENG 2

As the building expands in altitude, its energy consumption tends to increase gradually. In fact, with the addition of floors, the expansion of the volume in greater altitude exposes a larger amount of the envelope surface to the changing micro-climates where more heat loss occurs. Thus, the household demand for heating increases, in addition to the ventilation systems that become more necessary under unfavorable external conditions.

For the ratio index of V/Als < 5.65, up to a level of 39.6 meters (12th floor), the indicator of BENG 2 increases at a slower rate up to 45 kWh/m2 under which the micro-climate conditions are more constant (constant dry-bulb temperature and wind speed up to 4.7 m/s) (Graph 9 and Diagram 10). In this case, the amount of heat transfer through the surface area presents a gradual impact on the energy demand. Thus, the amendment of the current benchmark from 50 kWh/m2 to 45 kWh/m2 adapts to the volume to surface area ratio, and the amount of energy consumption required (Graph 52).

Followingly, for a ratio index of 5.65 < V/Als < 6.0, and levels between 42.9 (13th floor) and 66.0 meters (20th floor), the fossil energy of BENG 2 increases at a faster rate. In fact, the micro-climate conditions are less favorable at this stage, with an acceleration of the wind speed from 4.7 m/s to 6.7 m/s, and a drop in the outdoor air temperature from a minimum of -5.2°C to -6.0°C. Thus, at the considered floor levels, the rate of heat loss is higher through the loss surface area that expands with the height. In addition, as previously observed, the efficiency of renewable energy has decreased considerably which is reflected in BENG 2 as it is subtracted from the primary fossil use. In this case, a reassessment of the benchmark from 45 to 60 kWh/m2 corresponds to the considered floors and would represent an allowable 14% margin.

Above a height of 69.3 meters (21th floor), for an index of V/Als > 6.0, the increase of BENG 2 is at a slower rate with value close to proximity between 60 kWh/m2 and 70 kWh/m2. In fact, regarding the micro-climate, the floors are exposed to stronger wind speed above 7.0 m/s, and lower outdoor air temperature recorded with a minimum -11.8°C. Thus, with more volume and envelope area, there is a greater amount of heat loss with altitude. Also, the slower rate is partly due to the constant efficiency of the PV panels in BENG 3 at the similar floor levels, which is reflected in the final primary fossil usage. Therefore, for the target height reached, a reassessment of the benchmark at 70 kWh/m2 adapts to the volume of the high-rise in relation to the height.

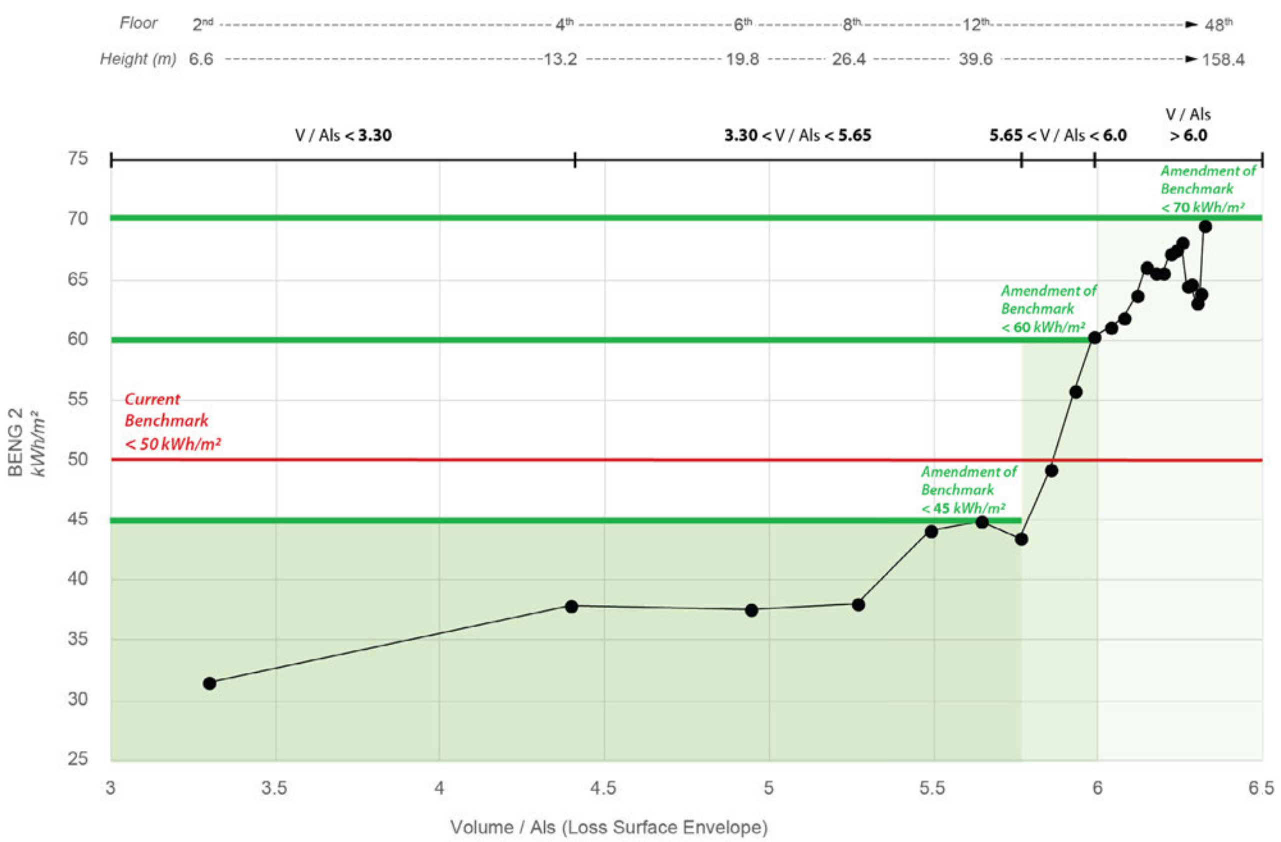

Graph 52 *Proposal of amendment for BENG 2 benchmark regarding the building volume and height*

The proposed amendments are based on the optimized design of his study. Although the ratio index is established for a link between the building volume and height, the final performance assessment can be affected by other factors such as the glazing ratio, the material selection of both the opaque components and the transparent parts, but also, the compactness and orientation that can affect both BENG 2 and BENG 3.

Urban scale and Context

The performance of a high-rise is highly related to the canopy layer of the context (Diagram 37). As a starting point, if the regulation benchmarks are not met in the floors at the bottom of the building, it presents an obstacle in progressing further to the target height. In the case of this study, and according to the current regulations, the low-rise scenario is more advantageous in reaching a closer ranking to the indicators.

However, the overall performance of the building is altered if changes occur in the neighborhood or if prone to obstruction. In this case, the access to natural ventilation, daylight and sun radiation is restricted. Thus, the energy generation of BENG 3 from the facade is less efficient. Subsequently, with a reduction of sun exposure, an increase in heating and lighting loads affects the performance of BENG 1 and BENG 2, as well as the thermal and visual comfort of the user.

Therefore, from the regulations side, within the urban layout, buildings should be arranged to avoid overshading each other, and ensure a better energy performance.

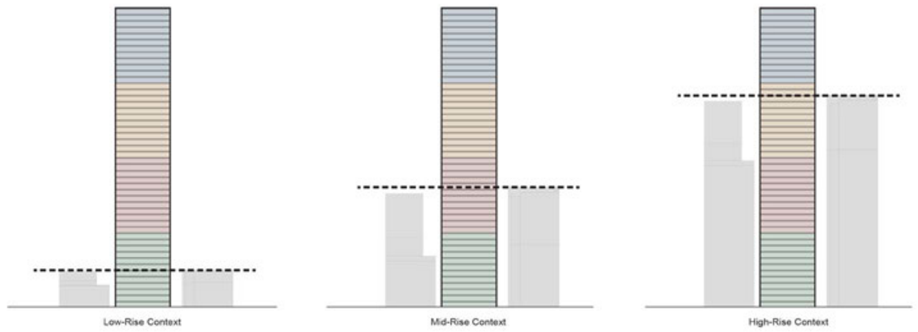

Diagram 37 *Impact of the surrounding buildings on the high-rise geometry at different levels*

Referring to the Integrated workflow

The high-rise performance depends on the design features selected for the geometry and facade, with a greater range of parameters to include. There is not a single optimal solution that suits all designs, but rather a proper combination of different parameters that should be assessed together. Being all interrelated, a change in one variable affects the efficiency of other factors, which presents a larger complexity to capture all the data set of the design space. Additionally, priorities have to be done from the designer regarding the objectives, as a solution can present advantages in improving BENG indicators, while being a constraint to the user's indoor thermal and visual comfort.

In order to check correlations between parameters and their relevance to the energy performance, it is suggested to refer to the provided integrated parametric workflow, in a digital platform where all data is stored, to have a preliminary overview of the design and the different choices that should be evaluated.

6 Discussion

Limitations

Along the application process of this research, the study was conducted on the 4 middle floors of the zone division. Although this method provides higher accuracy, proceeding with the optimization of all the parameters for each of the 4 floors at specific height is time-demanding, and turned into a limitation during the research. For the phase 3 and 4, the facade parameters were optimized separately. In addition, the selection of the glazing type and shading system was based on the results of the first zone, which might have led to different optimal solutions in other floors. For the time provided, a division of the total high-rise geometry into 2 or 3, rather than 4, would be more adapted to this type of research.

Although proceeding with the optimization in several phases speeds the research process, the resulting design space does not cover its entire width. In fact, with the current applied methodology, some parameters variables are left out at the end of a phase, and therefore will not have a probability to be combined with the design variables of the next phase. On the contrary, evaluating all of the parameters merged into a single phase does not disregard combinations, and might have provided a better performance. However, a longer period of time is needed for the calculation.

Also, the micro-climatic data are only related to the analyzed floor. As the wind speed increases and the temperature drops gradually, the design of the 48 floors based on the averages of only 4 floors might lead to results different from the realistic case. In fact, those factors affect the conditions of the natural ventilation and mechanical system activation that can result in different total hours allowed for each, but also, the facade parameters can be impacted by the temperature drop that necessitates lower U-value.

Moreover, in the simulation conducted by the plug-ins Honeybee and Ladybug in Grasshopper, some limitations occured in the workflow. Those platforms do not take into account the presence of obstacles and surrounding buildings around the high-rise geometry in the calculation of the wind speed for the natural ventilation. On the contrary, for the daylight analysis, all elements presenting obstruction are integrated with the exception of the dynamic shading devices. This is due to the fact that the daylight and energy simulation are calculated prior to the implementation of the shading systems in the workflow to determine its operating conditions of the indoor temperature and the solar radiation (Diagram 39). The lighting load is then calculated within the daylight simulation already, and is not recalculated based on the shading positions as it will result in a loop in the workflow. Therefore, the analysis of the visible transmittance VT of the glazing properties could not be evaluated.

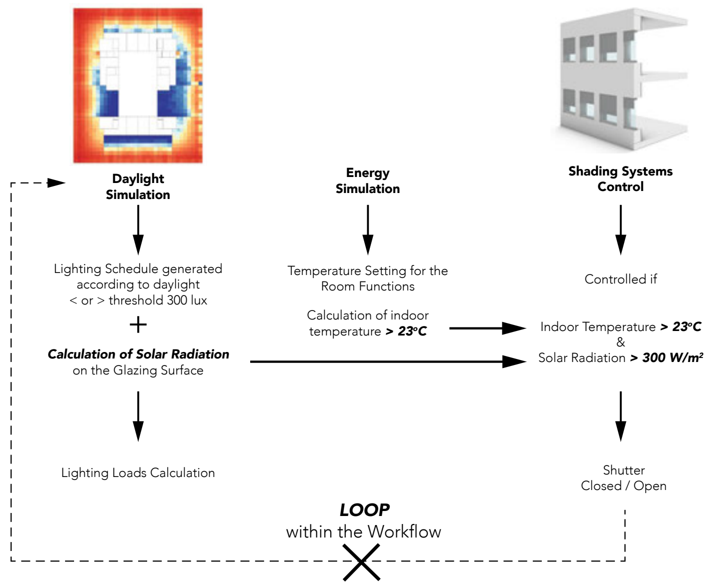

Diagram 39 *Limitation in the integrated workflow for the dynamic shading control with Honeybee*

Also, in this study, the window parameters that are evaluated includes the U-value and the g-value of the glazing part without its frame. With the component provided by Honeybee plug-in "Energy Plus Window Material" the created material has no mass, and is supposed to represent the entire window inclusive of the glass and the frame. Therefore, the accuracy can be affected considering that the mass is not calculated. In this case, the material should be adapted in the workflow by calculating the U-value of the total window with its frame.

From the outputs extracted in this study, the results are calculated based on the total floor loads rather than a breakdown of the results per each single room. This limitation of OpenStudio presents a constraint in the analysis and comparison of design results. The way around is to take each room and apply the entirety of the script to it which demands an intensive amount of time to calculate one single apartment that will be multiplied by the amount of rooms in the plan layout. Additionally, data of ventilation loads separately from the heating and cooling could not be extracted, and would be advantageous to analyze the micro-climate impact on the floor level and the energy demand.

rom the literature study, the estimated domestic hot water for 20 persons on the floor is 445300 litres/year. With Honeybee, the calculated 506422 litres/year is higher, contributing partly to the heating consumption. It is not possible to manually enter the exact number of litre usage required, but rather the plug-in uses its own standardized values. Also, a COP of 3.6 is used for the hot water, and as it is a higher range of temperature than the indoor heating, a lower COP value could have been used in this case.

6.1. Future Research and Development

This study can serve as a starting point for further studies. In this regard, the selection of other parameters and variables can be tested in the optimization and lead to improvement:

- Include a range of variables to the U-value for the insulation materials of the enclosed part of the envelope that are used as fixed values in this research.
- Investigate the effect on the final energy performance with different cooling and heating temperature set points, set back and buffer.
- Investigate the impact on the lighting load and visual comfort of the glazing ratio, with its position on the facade according to the room and the breakup distance between openings.
- Evaluate the energy generation from the facade with a higher efficiency of the PV panels.
- Analyze the impact on energy performance of different occupancy and usage schedules to observe the relationship with user's behavior, and relate the role and awareness of the target occupant in the energy performance aside from the building design.
- Implement the variation in the plan layout of upper floors in the high-rise where the usable space decreased due to structural principles.

6.2. Potential use of the integrated workflow

The workflow developed within the scope of this research can serve architects, facade designers, engineers, climate consultants and product companies for different potential usage. The computational integration facilitates the analysis and manipulation of a combination of different parameters which speed the time for achieving tasks and evaluating different solutions for decision taking.

For that, basic understanding of the Grasshopper workspace is required to be able to manipulate, adjust or apply changes to the workflow. Additionally, for modeFRONTIER, some knowledge is needed for the simulation and the optimization tool provided.

Initially for this study, the workflow incorporates the representative weather file of Amsterdam. It assists professional users in the Netherlands to assess the energy performance of a design for a given height in order to revise its compliance with the BENG regulations, according to the Dutch building decree. For the several weather files available in the Netherlands, it is possible to adapt the workflow to another site location, where its climatic data are simulated to evaluate the design under the given environment.

Additionally, the implementation of the surrounding buildings geometry can be adjusted to another site location. This feature serves facade designers and climate consultants to determine the amount of solar radiation exposure on the facades orientation, and identify potential areas for the implementation of PV panels for renewable energy, according to the glazing ratio and floor level, in order to be as cost-effective as possible.

With the flexibility of the workflow, a larger field of typologies can be explored other than residential apartments. In this case, the input values should be adjusted regarding the occupancy schedule, the integrated HVAC system, the ventilation rates, the equipment and lighting loads, and more.

More specifically, architects and products companies can compare and observe the efficiency of facade components where material properties of the glazing type, the PV panel or shading system can be inserted. Thus, it facilitates the task in selecting a product over another for greater performance.

7 Conclusion

This research investigates the extent to which the BENG 2020 regulations present a constraint to the height increment of the residential high-rise typology, in the temperate climate of the Netherlands. Based on the computational optimization of the high-rise, proposals of amendments to the current regulations are suggested to adapt the 160 meters target height to the energy performance.

Within the scope of this study, an integrated digital workflow is developed as the main tool to assess the performance of the different combination of design parameters in the high-rise, and reach energy-saving, near-optimal, solutions. According to the defined objectives and constraints of the optimization, the energy demand (BENG 1) and the mean primary fossil usage (BENG 2) are minimized, the energy generated (BENG 3) is maximized, and the thermal comfort serves as a constraint to evaluate the user's indoor environment.

Based on the results, the optimization of the geometry and facade parameters contribute to the improvement of the overall performance of the residential high-rise. However, under the changing micro-climate conditions with altitude, the efficiency of high-rise in parallel to the progressive floor addition is marked by several trends in the decrease of its performance.

First, the energy demand (BENG 1) increases gradually reaching a total mean of 48.62 kWh/m2, being below the maximum benchmark of 65 kWh/m2, and indicating an overall 39% decrease in performance. In fact, the heating demand increased by 40% between the lowest and upper floor due to the higher wind speed and the drop of temperature with altitude, where more heat loss occurs, and makes up for the largest share of the total energy demand.

However, the challenges to the height increment occurs for both of the indicators of BENG 2 and BENG 3. The first limit in the height increment occurs in the renewable energy of BENG 3 indicator, which performance declines by 30% when reaching the last floor. Its requirement is satisfied up to the 8th floor, at a level of 26.4 meters, when the share of renewable energy reaches a total of 40.2%, right above the minimum benchmark of 40%. While the roof layer provides a higher potential for the mounted PV than the facades, its performance becomes inefficient above this limit.
Further in height, the second limit is marked at the 16th floor, level of 52.8 meters, with a primary energy use of BENG 2 of 49.25 kWh/m2 being at proximity of its 50 kWh/m2 maximum benchmark.Its performance decreases by 55% in total along the high-rise. On one hand, the reduction of the share of renewable energy of BENG 3 in parallel to the height is reflected in the rise of BENG 2. On the other hand, there is a greater dependence on heating and mechanical ventilation with altitude in order to adapt to the changing micro-climates.

Despite the optimization of the final design and the implementation of energy-efficient systems, the final design of the residential high-rise has not reached the 160 meters target height. Additionally, both height limits marked at levels of 52.8 meters and 26.4 meters, respectively with BENG 2 and BENG 3, are not acknowledged as a high-rise according to the standard definition of 70 meters in the Netherlands.

To serve the residential high-rise typology, amendments are suggested to the BENG regulations with additional design guidelines to assist the designer in reaching a closer ranking to the indicators. The revision of the benchmarks of BENG 2 and BENG 3 are established according to the relationship between the high-rise volume to the loss surface area ratio (V/Als) and the energy performance of the optimized design as presented in Table 36 :

	BENG 1 Energy Demand kWh/m2.yr		BENG 2 Primary Fossil Energy Use kWh/m2.yr		BENG 3 Share of Renewable Energy %	
	Als/Ag		V/Als	BENG 2	V/Als	BENG 3
Residential Function	Als/Ag ≤ 1.83	≤ 65	V/Als < 5.65	≤ 45	V/Als < 5.60	≥ 40
			5.65 ≤ V/Als ≤ 6.0	≤ 60	5.60 ≤ V/Als ≤ 6.15	≥ 32
			V/Als > 6.0	≤ 70	V/Als > 6.15	≥ 30

Table 36 *Proposal of the amendments to BENG 2 and BENG 3 indicators for the residential function*

With the extension in height, more volume adds up that expands the envelope surface. Despite the additional surface area provided for mounting PV, on one hand, the roof position is displaced according to the designated last floor level, and on the other hand, the upper floors are exposed to the different microclimates.

For the energy generation of BENG 3, when the index is V/Als < 5.60, the energy generation is above the current benchmark of 40% where the roof supply is at its foremost potential alongside the facade area of the resulting volume. Followingly, for the index between 5.60 < V/Als < 6.15, as the maximal efficiency of the PV mounted on the envelope has been crossed, the energy generation decreases within a fast transition between the 40% and its adjusted benchmarks of 32%. Lastly, above an index of V/Als > 6.15, the amount of energy that can be generated from the facade neither improves or reduces, but rather becomes constant above the assessed benchmark of 30% on the remaining of the height.

For the primary fossil usage BENG 2, for the index V/Als < 5.65, the floors are located at levels of constant temperature and wind speed, and are designed for a benchmark of 45 kWh/m2, below the current 50 kWh/m2. Consecutively, between 5.65 < V/Als < 6.0, under less favorable micro-climates, with an acceleration in the wind speed and a drop of the air temperature, the rate of heat loss is higher through the enlarged loss surface area at the considered floor levels. At this stage, the design can respond to the maximum benchmarks of 60 kWh/m2. At greater altitude, with an index V/Als > 6.0, the rate of heat loss becomes faster, with above average wind speeds, and considerable decrease in the outdoor temperature. In addition, at the levels reached, the renewable energy share does not provide additional supply of energy from BENG 3 to subtract from the final primary fossil usage. To assist the target height of the high-rise, the benchmark is revised to the maximum value of 70 kWh/m2.

Regarding the user's comfort, the required level of 90% is not satisfied at any given floor of the high-rise. In this study, the shift of focus in the objectives is led on prioritizing the improvement of BENG 2 and 3 in the optimization, which highlights the constraint of balancing between saving too much energy while designing a highly comfortable indoor environment under the changing micro-climate conditions. Also, the cooling set point is fixed at a high value of 26°C, that should be lowered to at least 24°C.

Based on the results of the optimization, design guidelines are established for the early stage design and facade parameters to assist overcoming the challenges of BENG within a closer range to the benchmarks, while providing a better indoor comfort. It is advised to opt for the most compact geometry to minimize the loss surface area and reduce the heat transfer through the facade. Depending on the final building shape, whether rectangular or squarish, the orientation angle from the North axis determines the amount of exposure of each facade to the sun. For a square plan, toward a 45° angle, the design performance is enhanced as less facade is facing directly the North or the South which implies a better distribution of the sun among all facades that can lower the heating demand, but also maximize energy generation of all PV mounted on facades. In the case of rectangular shapes, the largest facade should be oriented towards the South-West. The openings are advised to be designed with lower WWR toward South, East and West (up to 40%), and larger ratio for North (between 40 and 60%).

Lastly, the properties of the glazing types perform better with lower U-value that minimizes heat loss in winter and heat gains in summer, along with a low g-value to prevent heat gains from solar radiation. This can also be done by implementing a shading system, preferable to be externally controlled, as it prevents heat gains from direct sun at an early stage. Overall, prioritizing a cooling dominant design over a heating dominant saves more energy in a temperate climate where heating makes up for most of the energy consumption in households. Nevertheless, considering additional facades parameters and energy generating sources such as off-site strategy is advised as BENG 2 is partly related to the amount of renewable energy of BENG 3 that is subtracted from it, and since the implementation of PVs on their own have shown to not be sufficient.

Nevertheless, the context selection of the high-rise location affects the high-rise performance that decreases under higher neighboring buildings. More obstruction of the facades results in less access to direct sun and daylight. In the case of this study, out of the 3 indicators, only BENG 1 is satisfied, where BENG 2 and 3 are too far from reaching the requirement presenting substantial challenges. Also, if the design is verified to meet BENG indicators at a given time, a change in the urban surroundings leaves a question mark on the consequence of this certification.

Due to the time-intensive simulations, the results are based on only 4 floors at different levels out of 48. Also, the optimization process was divided into phases between the WWR, and glazing types with shading systems. If evaluating them simultaneously with additional height levels, the final results could lead to improvement in the performance of the final design. The variation of the WWR in parallel to the height increment has not indicated improvement in regards to the performance, with only constant range from the bottom to the upper floors, whereas the variation by orientation resulted in more efficiency.

Compared to low-rises, high-rises serve as a solution to provide large amounts of accommodations for less land exploitation. However, the energy consumption with height increases which can have a greater environmental impact. The developed workflow in this research assists architects and designers in finding the balance to those challenges by evaluating the performance of the residential high-rise in the temperate climate. A greater range of parameters and variables can be integrated to verify their impact on the design according to the regulations, and achieve a better indoor environment for the occupants.

8 References

AEA. (2010). Green Public Procurement: Thermal Insulation Technical Background Report. Harwell. Retrieved from https://ec.europa.eu/environment/gpp/pdf/thermal_insulation_GPP_%20background_report.pdf

Al-Waeli, A. H., Bin Sopian, K., Kazem, H. A., & Chaichan, M. T. (2017). Photovoltaic Thermal PV/T systems: A review. International Journal of Computation and Applied Sciences 2(2):62-67. Retrieved from https://www.researchgate.net/publication/318333960_Photovoltaic_Thermal_PVT_systems_A_review

Al-Waeli, A. H. A., Sopian, K., Kazem, H. A., & Chaichan, M. T. (2017). Photovoltaic/Thermal (PV/T) systems: Status and future prospects. Retrieved from https://www.sciencedirect.com/science/article/pii/S136403211730463X

ASHRAE. (2016). ANSI/ASHRAE Standard 62.2-2016 - Standard for Ventilation and ACceptable Indoor Air Quality in Residential Buildings. Atlanta: American Society of Heating, Refrigerating and Air-Conditioning Engineers, Inc. Retrieved from https://ashrae.iwrapper.com/ViewOnline/Standard_62.2-2016

BPIE. (2015). Indoor Air Quality, Thermal Comfort and Daylight: Analysis of Residential Building Regulations in Eight EU Member States. Retrieved from http://bpie.eu/wp-content/uploads/2015/10/BPIE__IndoorAirQuality2015.pdf

Bouwbesluit Online. (2012). (n.d.). Retrieved from https://rijksoverheid.bouwbesluit.com/

Bouwbesluit Online. (2012). (n.d.). Retrieved from https://rijksoverheid.bouwbesluit.com/Inhoud/docs/wet/bb2012/hfd2/afd2-14/art2-128

Bouwbesluit Online. (2012). (n.d.). Retrieved from https://rijksoverheid.bouwbesluit.com/Inhoud/docs/wet/bb2003/hfd2/afd2-23/art2-208

CBS. (2019). StatLine - Energy balance sheet; supply and consumption, sector. Retrieved from https://opendata.cbs.nl/statline/#/CBS/en/dataset/83989ENG/table?ts=1578650763988

Chen, X., Yang, H., & Sun, K. (2016). A holistic passive design approach to optimize indoor environmental quality of a typical residential building in Hong Kong. Retrieved from https://www.sciencedirect.com/science/article/abs/pii/S0360544216309823#abs0015

Ching, F. D. K. (2014). Building Structures Illustrated: Patterns, Systems, and Design (Second Edition). John Wiley & Sons.

Chartered Institute of Building Services Engineers (CIBSE). (2006). Guide A: Environmental design. London: Author.

CTBUH. (2019). Retrieved from http://www.skyscrapercenter.com/

CTBUH. (n.d.). CTBUH Height Criteria. Retrieved from https://www.ctbuh.org/resource/height

Davies, N., & Jokiniemi, E. (2008). Dictionary of Architecture and Building Construction. Amsterdam: Elsevier/Architectural Press.

De minister van Binnenlandse Zaken en Koninkrijksrelaties (Ministry of the Interior and Kingdom Relations) (2019). Letter to Parliament on the draft decision amending the 2012 Building Decree on nearly energy-neutral new construction, to the chairman of the House of Representatives of the States General. Den Haag. Retrieved from https://www.rijksoverheid.nl/documenten/kamerstukken/2019/06/11/kamerbrief-bij-voorhang-van-het-ontwerpbesluit-houdende-wijziging-van-het-bouwbesluit-2012-inzake-bijna-energieneutrale-nieuwbouw

Designing Buildings Wiki. (2019). Building Height. Retrieved from https://www.designingbuildings.co.uk/wiki/Building_height

Designing Buildings Wiki. (2019). Solar transmittance through building fabric (gtot). Retrieved from https://www.designingbuildings.co.uk/wiki/Solar_transmittance_through_building_fabric_(gtot)

Lente-akkoord. (2019). Eerste inzichten uit Lente-akkoord onderzoek BENG-eisen. Retrieved from https://www.lente-akkoord.nl/eerste-inzichten-uit-lente-akkoord-onderzoek-beng-eisen/

Ekici, B. F., Kazanasmaz, R. F., Turrin, M. F., Tasgetiren, M. F., & Sariyildiz, S. F. (2019). A Methodology for daylight optimization of high-rise buildings in the dense urban district using overhang length and glazing type variables with surrogate modelling. Retrieved from https://www.researchgate.net/publication/335715852

Ellis, P. G., & Torcellini, P. A. (2005). Simulating tall buildings using EnergyPlus. Proceedings of IBPSA International Conference, Montreal, Canada.

EN 15251 (2006). Indoor environmental input parameters for design and assessment of energy performance of buildings addressing indoor air quality, thermal environment, lighting and acoustics (English Version). CEN, Brussels. Retrieved from http://www.cres.gr/greenbuilding/PDF/prend/set4/WI_31_Pre-FV_version_prEN_15251_Indoor_Environment.pdf

EnergySage. (2019). Thin Film Solar Panels: Do They Make Sense?. Retrieved from https://news.energysage.com/thin-film-solar-panels-make-sense/

Engineering ToolBox. (2003). U.S. Standard Atmosphere. Retrieved from https://www.engineeringtoolbox.com/standard-atmosphere-d_604.html

Eurima. (2019). EURIMA - Trias Energetica. Retrieved from https://www.eurima.org/energy-efficiency-in-buildings/trias-energetica

European Commission. (2020). Nearly zero-energy buildings - Energy European Commission. Retrieved from https://ec.europa.eu/energy/en/topics/energy-efficiency/energy-performance-of-buildings/nearly-zero-energy-buildings

European Environment Agency. (2012). Energy consumption by end uses per dwelling. Retrieved from https://www.eea.europa.eu/data-and-maps/figures/households-energy-consumption-by-end-uses-3

Fédération de l'Industrie du Verre FIV. (2013). Un autre regard sur les vitrages et leurs fonctions (2nd Edition). Retrieved from https://www.vgi-fiv.be/wp-content/uploads/2012/11/Un-autre-regard-sur-les-vitrages-et-leurs-fonctions-2e-edition-Fr.pdf

Green, M. A., Hishikawa, Y., Dunlop, E. D., Levi, D. H., Hohl-Ebinger, J., Yoshita, M., & Ho-Baillie, A. W. Y. (2018, December 25). Solar cell efficiency tables (Version 53). Retrieved from https://onlinelibrary.wiley.com/doi/10.1002/pip.3102

Godoy-Shimizu, D., Steadman, P., Hamilton, I., Donn, M., Evans, S., Moreno, G. and Shayesteh, H. (2018). Energy use and height in office buildings. Building Research & Information, 46(8), pp.845-863. Retrieved from https://doi.org/10.1080/09613218.2018.1479927

Google. (2020). Rotterdam. Retrieved from https://goo.gl/maps/4Eq9J7PLWTw55Ezu8

Guerra-Santin, O., Bosch, H., Budde, P., Konstantinou, T., Boess, S., Klein, T., & Silvester, S. (2018). Considering user profiles and occupants' behaviour on a zero energy renovation strategy for multi-family housing in the Netherlands. Energy Efficiency (online). https://doi.org/10.1007/s12053-018-9626-8

Hachem, C., Athienitis, A., & Fazio, P. (2013, December 8). Energy performance enhancement in multistory residential buildings. Applied Energy, 116, 9-19. Retrieved from https://doi.org/10.1016/j.apenergy.2013.11.018

Hunter Douglas Architectural. (2020). Roller Blinds | Fabrics. Retrieved from https://www.hunterdouglasarchitectural.eu/en-RS/windowcoverings/roller-blind-fabrics/index.jsp

Industrial Heat Pumps. (2020). COP warmtepomp. Retrieved from https://industrialheatpumps.nl/nl/techniek/cop_warmtepomp/
International Passive House Association. (2019). Passive House Guidelines. Retrieved from https://passivehouse-international.org/index.php?page_id=80&level1_id=78

Jacobs, A. (2012). Radiance Tutorials. Retrieved from http://www.jaloxa.eu/resources/radiance/documentation/docs/radiance_tutorial.pdf

Konstantinou, T. (2014). Facade Refurbishment Toolbox: Supporting the Design of Residential Energy Upgrades. TU Delft, Architecture and the Built Environment.

Konstantinou, T., Ćuković Ignjatović, N., & Zbašnik-Senegačnik, M. (Eds.) (2018). Energy: resources and building performance. (Reviews of Sustainability and Resilience of the Built Environment for Education, Research and Design; Vol. 4). Delft: TU Delft Open. http://resolver.tudelft.nl/uuid:320f4b29-235d-4355-913f-2b07f0d5d44c

LenteAkkoord. (2019). BENG én ook nog MPG, is bouwen nog wel mogelijk? Retrieved from https://www.lente-akkoord.nl/beng-en-ook-nog-mpg-is-bouwen-nog-wel-mogelijk/

LenteAkkoord. (2019). Temperatuur tapwater en legionella. Retrieved from https://www.lente-akkoord.nl/temperatuur-tapwater-en-legionella/

Looman, R. (2017). Climate-responsive design: A framework for an energy concept design-decision support tool for architects using principles of climate-responsive design. A+BE | Architecture and the BuiltEnvironment. https://doi.org/10.7480/abe.2017.1
Lyons, A. (2010). Materials for Architects and Builders (Fourth Edition). Elsevier Science

Mackey, C. (2013). Honeybee plug-in for Grasshopper (Version 0.0.65) [Windows]

Mandalaki, M. and Tsoutsos, T., 2020. Solar Shading Systems: Design, Performance, And Integrated Photovoltaics. SpringerBriefs in Energy. Retrieved from https://link-springer-com.tudelft.idm.oclc.org/book/10.1007%2F978-3-030-11617-0

Marginean, C. M. (2019). Optimized facade design towards nearly zero-energy residential high-rises: Facade Design Assessment Criteria for Residential High-Rise Buildings in the NL. Master Thesis. TU Delft

Marugg, C. (2018). Vertical Forests: The Impact of Green Balconies on the Microclimate by Solar Shading, Evapotranspiration and Wind Flow Change. TU Delft, Civil Engineering and Geosciences.

Ministerie van Algemene Zaken. (2015). Basics on Dutch housing. Retrieved from https://www.government.nl/topics/investing-in-dutch-housing/basics-dutch-housing

Ministerie van Algemene Zaken. (2015). Investing in the rental market. Retrieved from https://www.government.nl/topics/investing-in-dutch-housing/investing-in-rental-market

Mlecnik, E. (2013). Innovation development for highly energy-efficient housing: Opportunities and challenges related to the adoption of passive houses. TU Delft. https://doi.org/10.4233/uuid:82884adb-e990-4b8a-accc-d9440e52253d

Mobius Consult. (2017). Ventilation in BENG requirement 1. Retrieved from https://www.rvo.nl/sites/default/files/2019/05/EinddrapportVentilatie in BENG1 Mobius.pdf

Nash, S. (2013). Impact of mechanical ventilation systems on the indoor-air quality in highly energy-efficient houses. Default journal. Retrieved from https://www.co2indicator.nl/documentatie/EES-2013-169T_SabrinaNash.pdf

National Weather Service. (2019). Climate Prediction Center. Retrieved from https://www.weather.gov/

Nederlands Vlaamse Bouwfysica Vereniging. (2018). Handboek Bouwfysische Kwaliteit Gebouwen (Version 2.30).

Nicol, F., Humphreys, M. & Roaf, S. (2012). Adaptive Thermal Comfort: Principles and Practice. Routledge. Retrieved from https://ebookcentral-proquest-com.tudelft.idm.oclc.org/lib/delft/reader.action?docID=956913&ppg=32

Nieman. (2020). Eisen Luchtdichtbouwen. Retrieved from www.nieman.nl/specialismen/bouwtechniek-en-praktijk/luchtdicht-bouwen/eisen/

NREL. (2017). Current Status of Concentrator Photovoltaic (CPV) Technology. Retrieved from https://www.ise.fraunhofer.de/content/dam/ise/de/documents/publications/studies/cpv-report-ise-nrel.pdf

Odysee. (2020). Netherlands profile. Retrieved from https://www.odyssee-mure.eu/publications/efficiency-trends-policies-profiles/netherlands.html#buildings

Office of Energy Efficiency & Renewable Energy. (n.d.). Choosing and Installing Geothermal Heat Pumps. Retrieved from https://www.energy.gov/energysaver/choosing-and-installing-geothermal-heat-pumps

OneBuilding. (2020). Repository of free climate data for building performance simulation. Retrieved form http://climate.onebuilding.org/WMO_Region_6_Europe/NLD_Netherlands/index.html

Ramesh, T., Prakash, R., & Shukla, K. K. (2010). Life cycle energy analysis of buildings: An overview. Energy and Buildings, 42(10), 1592–1600. https://doi.org/10.1016/j.enbuild.2010.05.007

Raji, B., Tenpierik, M. J., Bokel, R. & van den Dobbelsteen, A. (2019). Natural summer ventilation strategies for energy-saving in high-rise buildings: A case study in the Netherlands. The International Journal of Ventilation. Retrieved from http://resolver.tudelft.nl/uuid:d9dbf3f2-05e5-4938-a852-1f73a87f6d2b

Rijksoverheid. (2012). Bouwbesluit 2012. Retrieved from https://rijksoverheid.bouwbesluit.com/Inhoud/docs/wet/bb2012/hfd3/afd3-6/par3-6-1

Rijksoverheid. (2012). Bouwbesluit 2012. Retrieved from https://rijksoverheid.bouwbesluit.com/Inhoud/docs/wet/bb2012_nvt/artikelsgewijs/hfd4/afd4-1

RVO. (2013). Referentie-Woningen Nieuwbouw 2013. Retrieved from https://www.rvo.nl/sites/default/files/2013/09/Referentiewoningen.pdf

RVO. (2020). Warmtepompen en warmte- en koudeopslag (categorie 8a). Retrieved from https://www.rvo.nl/subsidies-regelingen/regeling-groenprojecten/voorwaarden/projectcategorie%C3%ABn/energiebesparing/warmtekoudeopslag

Passive House Institute. (2015). Passive House requirements. Retrieved from http://passiv.de/en/02_informations/02_passive-house-requirements/02_passive-house-requirements.htm

Pellegrini, M., Bloemendal, M., Hoekstra, N., Spaak, G., Gallego, A. A., Comins, J. R., ... Steeman, H. J. (2019). Low carbon heating and cooling by combining various technologies with Aquifer Thermal Energy Storage. Science of The Total Environment. Retrieved from https://www.sciencedirect.com/science/article/pii/S0048969719301524

Peutz. (2018). Influence of building geometry on the BENG indicators. Retrieved from https://www.rvo.nl/sites/default/files/2019/05/Eindrapport Geometrie Peutz.pdf

Sadeghipour Roudsari, M., & Mackey, C. (2013). Ladybug Plug-in for Grasshopper (Version 0.0.68) [Windows]

Sapa Solar BIPV. (2008). Sapa Building System. Retrieved from https://www.sapabuildingsystem.com/globalassets/sapa-building-systems-ab/pictures/brochures/solar_bipv_low.pdf?ts=636316455108630000

Saroglou, T., Meir, I., & Theodosiou, T. (2017). Quantifying Energy Consumption in Skyscrapers of Various Heights. Procedia Environmental Sciences, 38, 314–321. doi: 10.1016/j.proenv.2017.03.085

Schittich, C. (2006). In Detail: Building Skins: New Enlarged Edition. Basel: Birkhäuser - Publishers for architecture.

Sherman, M. H., Chan, R. (2004). Building Airtightness: Research and Practice. Retreived from https://www.researchgate.net/publication/238573993_Building_Airtightness_Research_and_Practice/stats

Solar Heat Gain Coefficient (SHGC) (2018). Efficient Windows Collaborative. Retrieved from https://www.efficientwindows.org/shgc.php

U-Values Explained - What does U-value mean? (2018). Energlaze. Retrieved from https://www.energlaze.ie/u-values-explained/

UCL Energy Institute. (2019). UCL-Energy 'High-Rise Buildings: Energy and Density' research project results. [online] Available at: https://www.ucl.ac.uk/bartlett/energy/news/2017/jun/ucl-energy-high-rise-buildings-energy-and-density-research-project-results

Urban Land Institute. (2008). Getting Density Right: Tools for Creating Vibrant Compact Development; National Multi Housing Council, Urban Land Institute: Washington, DC, USA, 2008

Van der Linden, A.C., Boerstra, A.C., Raue, A.K., Kurvers, S.R. and De Dear, R.J. (2006). Adaptive temperature limits: A new guideline in The Netherlands - a new approach for the assessment of building performance with respect to thermal indoor climate in Energy and Buildings, vol. 38, issue 1. Retreived from https://www.sciencedirect.com/science/article/pii/S0378778805000460

Velux. (2020). Data Sheet VELUX INTEGRA Roller Blind. Retrieved from https://velcdn.azureedge.net/~/media/marketing/ch/fachleute/vms/downloads/technische-datenblaetter/roller%20blind%20-%20velux%20integra.pdf

Vewin. (2016). Watergebruik Thuis 2016. Retrieved from https://www.vewin.nl/SiteCollectionDocuments/Publicaties/Cijfers/Watergebruik-Thuis-2016.pdf

Visible Transmittance. (2019). Commercial Windows. Retrieved from https://www.commercialwindows.org/vt.php

Wood A. & Salib R. (2012).Guide To Natural Ventilation in High Rise Office Buildings (Ctbuh Technical Guide), Routledge, Chicago.

Wortmann, T. (2019). Architectural Design Optimization-Results from a User Survey. KnE Social Sciences. doi:10.18502/kss.v3i27.5550

Wortmann, T. (2017). Opossum: Introducing and Evaluating a Model-based Optimization Tool for Grasshopper. Proceedings of the 22nd International Conference of the Association for Computer-Aided Architectural Design Research in Asia (CAADRIA) 2017 (283-293). Retrieved from https://pdfs.semanticscholar.org/05be/09aea9c60fa1e82db028a9976c0a267fd762.pdf

Xiang, X., Zhao, K., Liu, X. & Jiang, Y. (2020). Cooling Performance Comparison Of Radiant Floor System And All-Air System With Solar Radiation. Retrieved from https://www.sciencedirect.com/science/article/pii/S1876610215021189

Xin, Q. (2014). Optimization techniques in diesel engine system design. Retrieved from https://www.sciencedirect.com/science/article/pii/B9781845697150500030

9 Appendices

Appendix A *Climatic Data*

WEATHER DATA SUMMARY													
LOCATION:	AMSTERDAM, -, NLD												
Latitude/Longitude:	52.3° North, 4.77° East, **Time Zone from Greenwich** 1												
Data Source:	IWEC Data 062400 WMO Station Number, **Elevation** -2 m												
MONTHLY MEANS	**JAN**	**FEB**	**MAR**	**APR**	**MAY**	**JUN**	**JUL**	**AUG**	**SEP**	**OCT**	**NOV**	**DEC**	
Global Horiz Radiation (Avg Hourly)	79	142	211	248	309	299	307	281	219	151	96	61	Wh/sq.m
Direct Normal Radiation (Avg Hourly)	95	164	204	159	190	181	205	170	154	109	96	65	Wh/sq.m
Diffuse Radiation (Avg Hourly)	57	87	116	152	184	174	164	171	137	108	68	47	Wh/sq.m
Global Horiz Radiation (Max Hourly)	279	439	661	776	824	861	858	794	654	445	322	219	Wh/sq.m
Direct Normal Radiation (Max Hourly)	608	780	859	851	826	850	813	755	746	640	549	565	Wh/sq.m
Diffuse Radiation (Max Hourly)	164	287	339	384	441	441	439	395	336	308	163	135	Wh/sq.m
Global Horiz Radiation (Avg Daily Total)	639	1362	2476	3430	4812	4927	4934	4065	2720	1551	824	463	Wh/sq.m
Direct Normal Radiation (Avg Daily Total)	762	1564	2380	2219	2962	2980	3295	2467	1897	1104	824	493	Wh/sq.m
Diffuse Radiation (Avg Daily Total)	460	830	1363	2092	2866	2874	2631	2461	1716	1119	589	360	Wh/sq.m
Global Horiz Illumination (Avg Hourly)	8644	15478	23029	27288	34075	33268	34140	31162	24249	16639	10497	6732	lux
Direct Normal Illumination (Avg Hourly)	7111	14402	19175	15345	18314	17435	19537	15971	14236	9600	7706	4632	lux
Dry Bulb Temperature (Avg Monthly)	4	3	5	8	12	15	16	17	14	10	6	4	degrees C
Dew Point Temperature (Avg Monthly)	2	1	2	6	7	10	14	13	11	7	4	2	degrees C
Relative Humidity (Avg Monthly)	87	87	82	86	73	74	84	79	84	83	89	89	percent
Wind Direction (Monthly Mode)	170	310	210	240	350	330	210	210	260	210	80	210	degrees
Wind Speed (Avg Monthly)	7	6	5	6	4	4	4	4	4	6	4	6	m/s
Ground Temperature (Avg Monthly of 3 Depths)	7	6	5	5	6	9	11	13	14	14	12	10	degrees C

Table 1 *Weather data from the Amsterdam weather file of 2018 (source: Climate Consultant 6.0)*

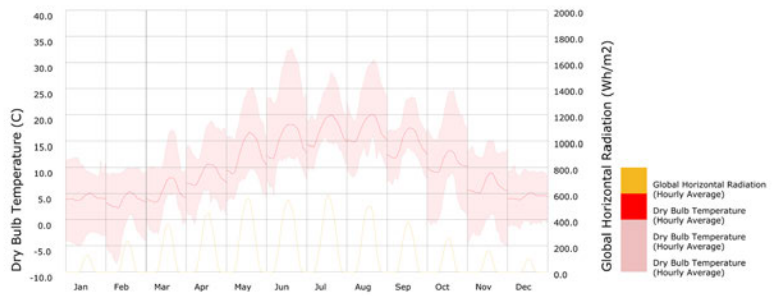

Diagram 1 *Monthly mean minimum and maximum temperature in parallel to the total horizontal radiation (Source: Honeybee / Ladybug)*

Function	Kitchen/Living Room		Bedrooms		WC / Bathroom		Storage		Hall	
	Weekday / Weekend		*Weekday / Weekend*		*Weekday / Weekend*		*Weekday / Weekend*		*Weekday / Weekend*	
Hour	Occupancy	Equipments	Occupancy	Equipments	Occupancy	Equipments	Occupancy	Equipments	Occupancy	Equipments
0	0	0.1	1	0	0	0	0	0	0	0
1	0	0.1	1	0	0	0	0	0	0	0
2	0	0.1	1	0	0	0	0	0	0	0
3	0	0.1	1	0	0	0	0	0	0	0
4	0	0.1	1	0	0	0	0	0	0	0
5	0	0.1	1	0	0	0	0	0	0	0
6	0.8	0.5	1	0	0.3	0	0	0	0.05	0
7	1	1	0.8	0.1	0.5	0.2	0	0	0.1	0
8	1	1	0.5	0.1	0.8	0.2	0	0	0.1	0
9	0.8	0.5	0.2	0.1	0	0	0	0	0.1	0
10	0.5	0.2	0.2	0.2	0	0	0	0	0.05	0
11	0.2	0.2	0.2	0.2	0.1	0	0	0	0.05	0
12	0.3	0.8	0.2	0	0.1	0	0	0	0.1	0
13	0.3	0.5	0.1	0	0.2	0	0	0	0.1	0
14	0.5	0.3	0.1	0	0	0	0	0	0.05	0
15	0.5	0.1	0.2	0.1	0	0	0	0	0.05	0
16	0.8	0.3	0.5	0.1	0	0	0	0	0.05	0
17	0.8	0.3	0.5	0.1	0	0	0	0	0.05	0
18	1	0.8	0.5	0.1	0.1	0	1	1	0.05	0
19	1	1	0.8	0.5	0.2	0	0	0	0.1	0
20	1	1	0.8	0.5	0.3	0.2	0	0	0.1	0
21	0.8	0.5	1	0.1	0.2	0	0	0	0.1	0
22	0.3	0.2	1	0.1	0	0	0	0	0.05	0
23	0.1	0.1	1	0	0	0	0	0	0.05	0

Table 2 *Schedule of Occupancy and Equipment Usage for each Zone/Room*

Diagram 2 *Schedule of Occupancy and Equipment Usage for each Zone/Room*

	Hot Water			
	Showering	Dishwasher	Washing	Total
Litre per day per person	45	3	13	61
Litre per Year per person	16425	1095	4745	22265
Litre per Year for 20 persons	328500	21900	94900	445300

Table 3 *Domestic hot water consumption (Vewin, 2016)*

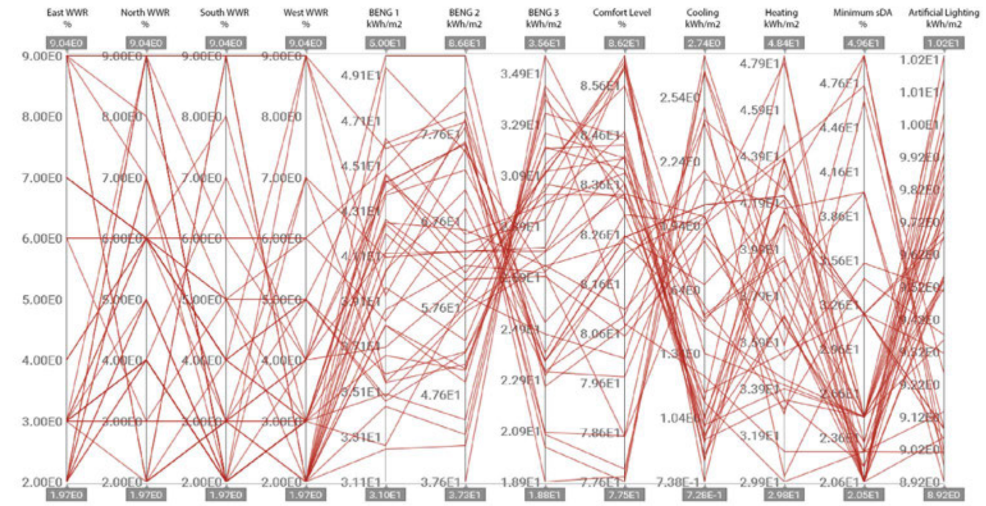

Graph 1 *Parallel coordinates chart of the final results of WWR with low-rises surroundings*

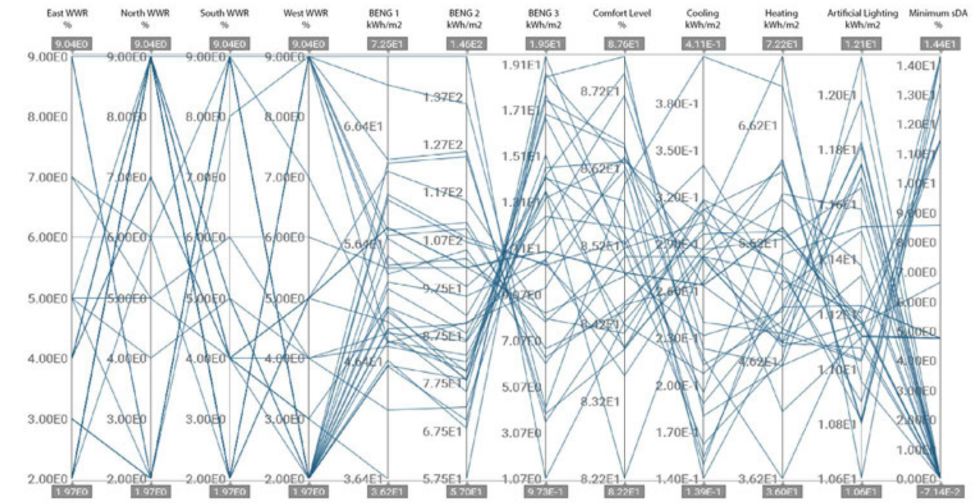

Graph 2 *Parallel coordinates chart of the final results of WWR with mid-rises surroundings*

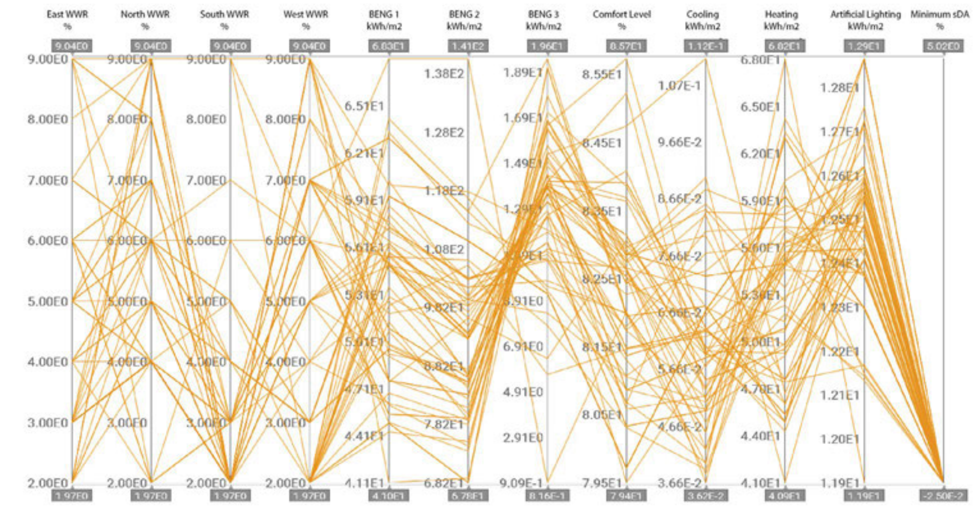

Graph 3 *Parallel coordinates chart of the final results of WWR with mid-rises surroundings*

	< 65	< 50	> 40					
WWR	BENG 1 kWh/m2	BENG 2 kWh/m2	BENG 3 %	Cooling kWh/m2	Heating kWh/m2	Lighting kWh/m2	Comfort %	min_SDA %
20%	34.5	41.5	35.3	0.74	32.96	10.23	87.7	20.62
30%	34.86	46	33	1.13	33.36	9.69	86.18	31.96
40%	35.42	51.88	30.2	1.54	33.94	9.37	84.58	39.18
50%	36.07	58.34	27.08	1.95	34.3	9.17	83.21	47.42
60%	37.7	65.1	23.7	2.37	35.46	9.01	81.84	49.48
70%	39.7	71.95	20.12	2.8	36.41	8.89	80.67	56.7
80%	44.04	78.84	16.32	3.2	37.66	8.83	79.58	62.92
90%	46.39	85.79	12.29	3.6	39.54	8.81	78.68	63.92

Table 4 *Results of the BENG indicators and energy performance under constants WWR on all facades*

Zone 2 Results

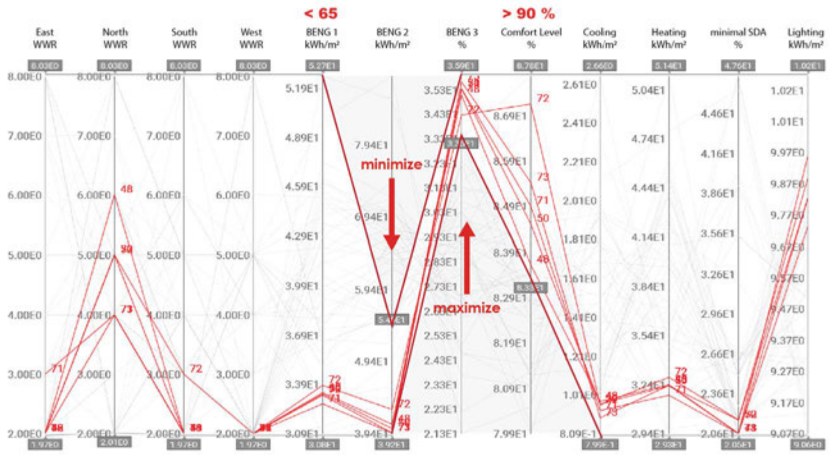

Graph 4 *Parallel coordinates chart of the design iteration selection for zone 2 by adjusting the range toward the objectives (source: modeFRONTIER2019R3)*

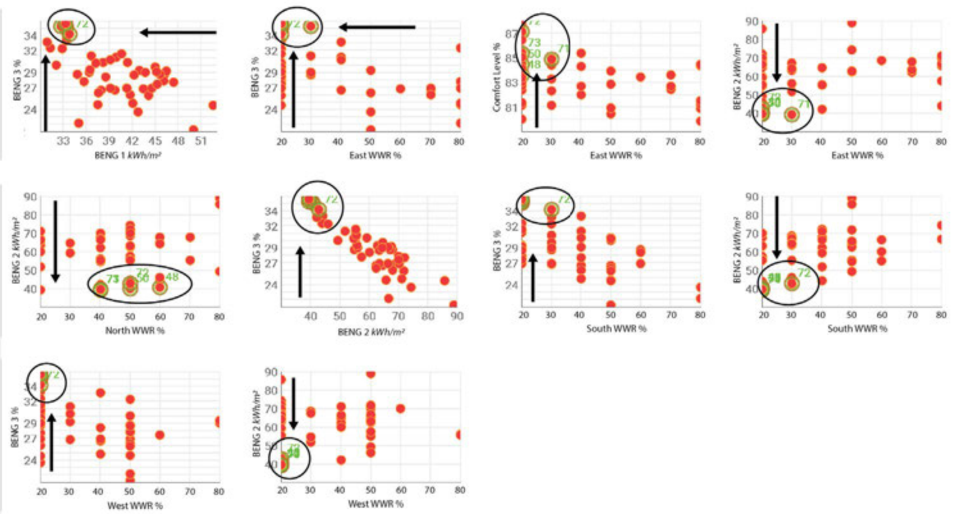

Graph 5 *Scatter diagram representing the proximity of the design iterations WWR of zone 2 regarding energy indicators and comfort level*

Graph 6 *Scatter matrix of the correlation between the WWR, BENG indicators and the energy outputs at the Zone 2 (source: modeFRONTIER2019R3)*

Zone 3 Results

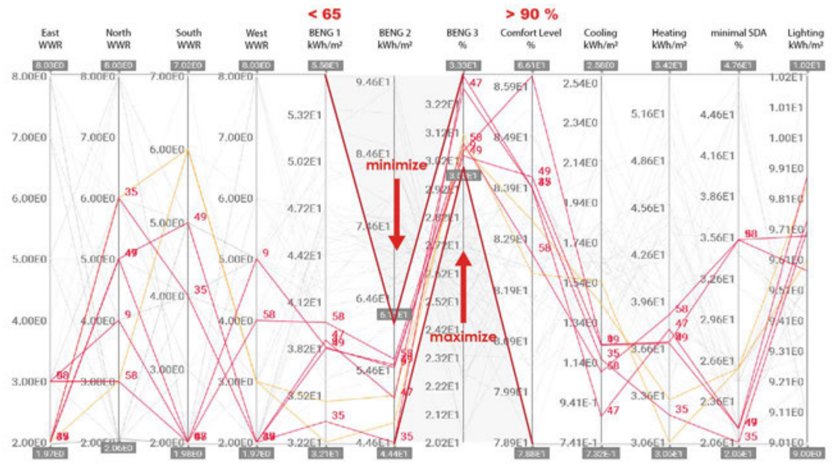

Graph 7 *Parallel coordinates chart of the design iteration selection for zone 3 by adjusting the range toward the objectives (source: modeFRONTIER2019R3)*

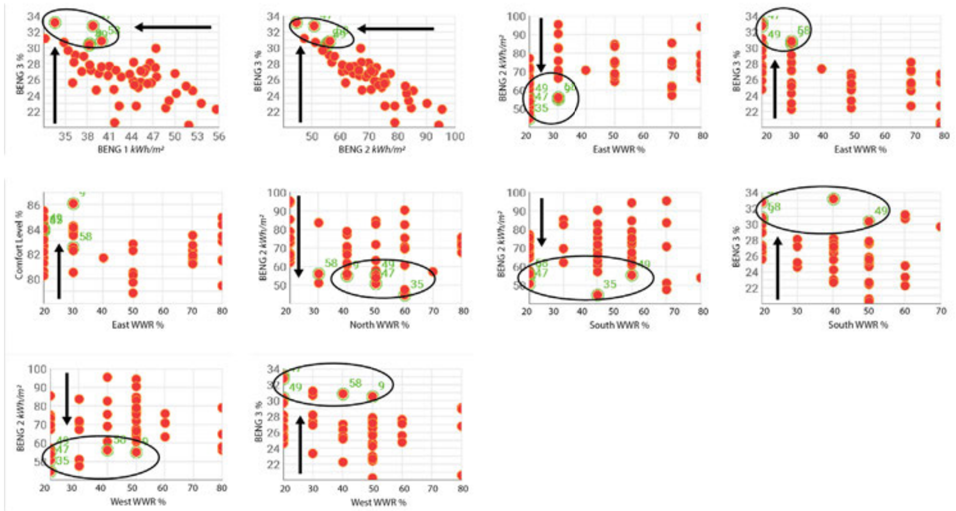

Graph 8 *Scatter diagram representing the proximity of the design iterations WWR of zone 3 regarding energy indicators and comfort level*

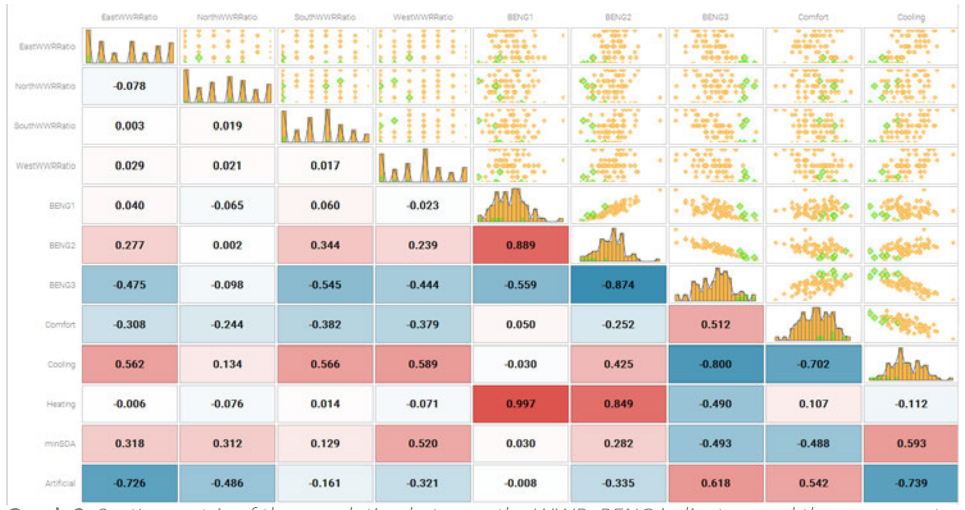

Graph 9 *Scatter matrix of the correlation between the WWR, BENG indicators and the energy outputs at the Zone 3 (source: modeFRONTIER2019R3)*

Zone 4 Results

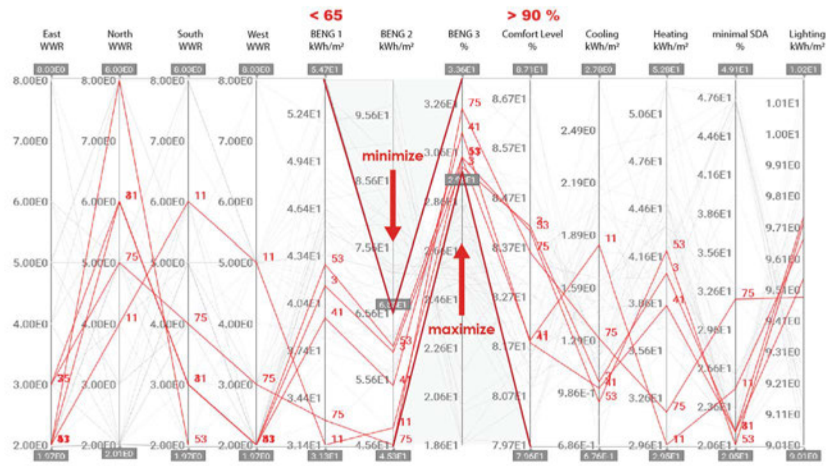

Graph 10 *Parallel coordinates chart of the design iteration selection for zone 4 by adjusting the range toward the objectives (source: modeFRONTIER2019R3)*

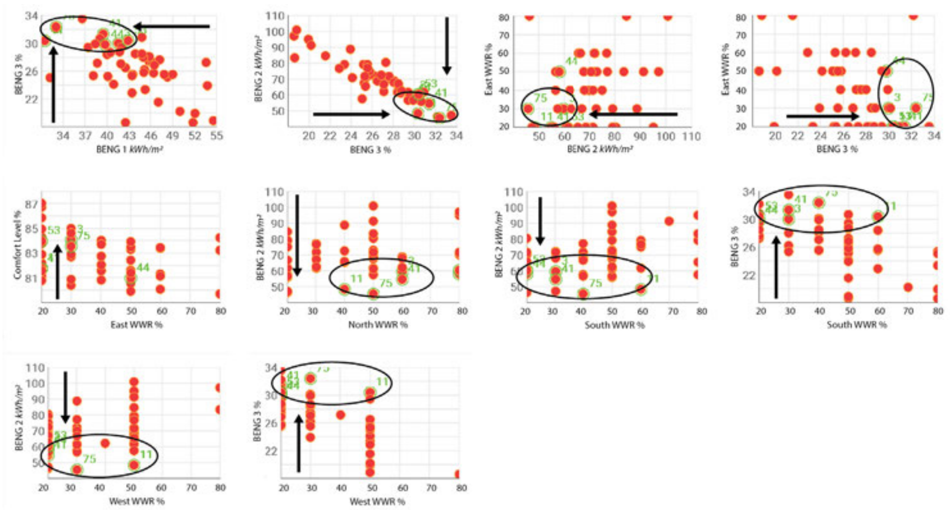

Graph 11 *Scatter diagram representing the proximity of the design iterations WWR of zone 4 regarding energy indicators and comfort level*

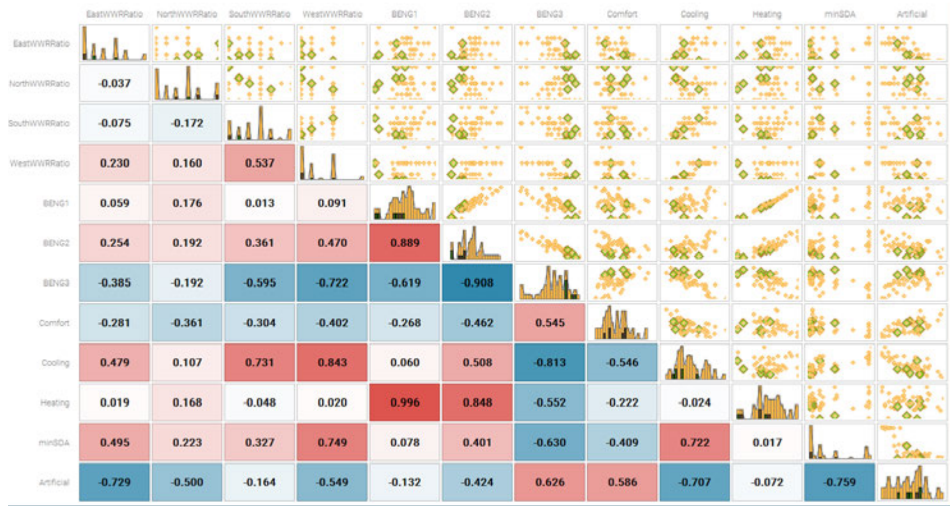

Graph 12 *Scatter matrix of the correlation between the WWR, BENG indicators and the energy outputs at the Zone 4 (source: modeFRONTIER2019R3)*

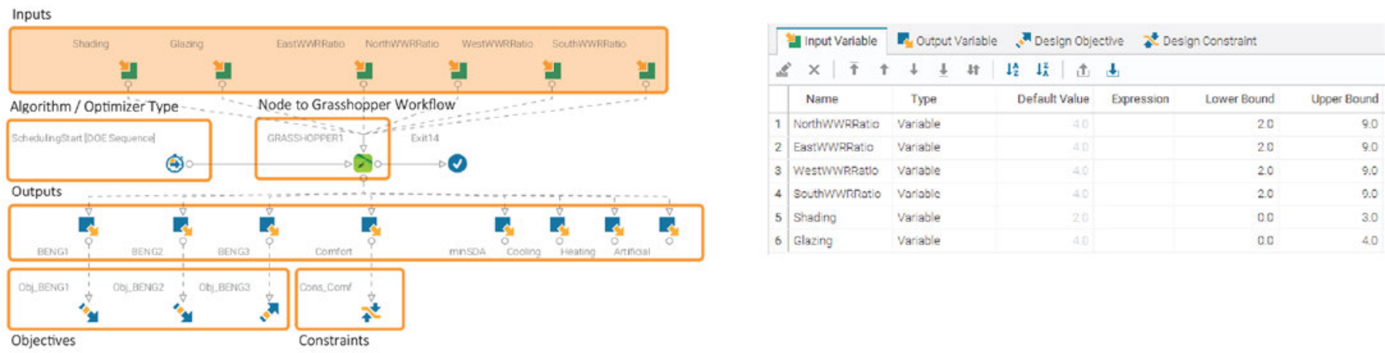

Diagram 3 *Inputs setting in the ModeFrontier workflow*

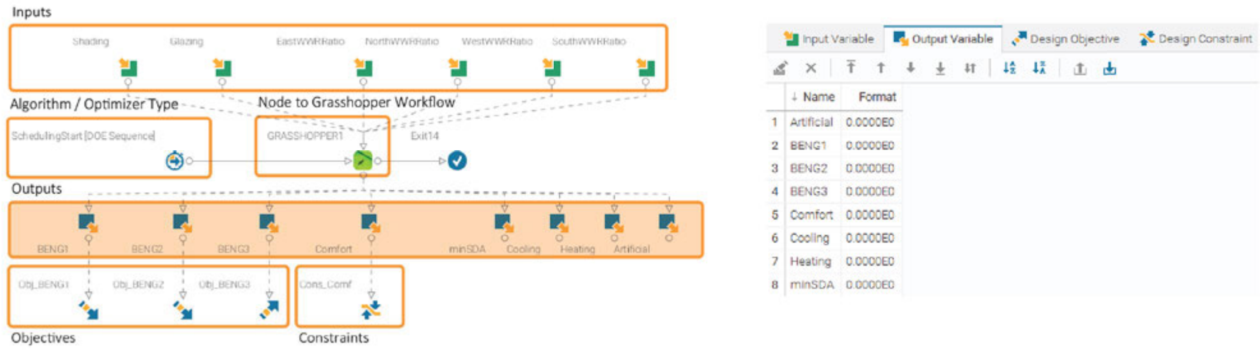

Diagram 4 *Outputs setting in the ModeFrontier workflow*

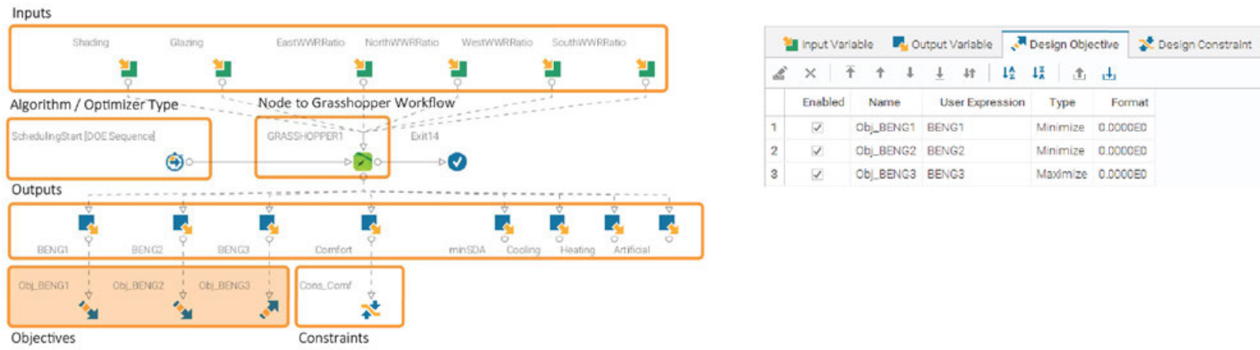

Diagram 5 *Objectives setting in the ModeFrontier workflow*

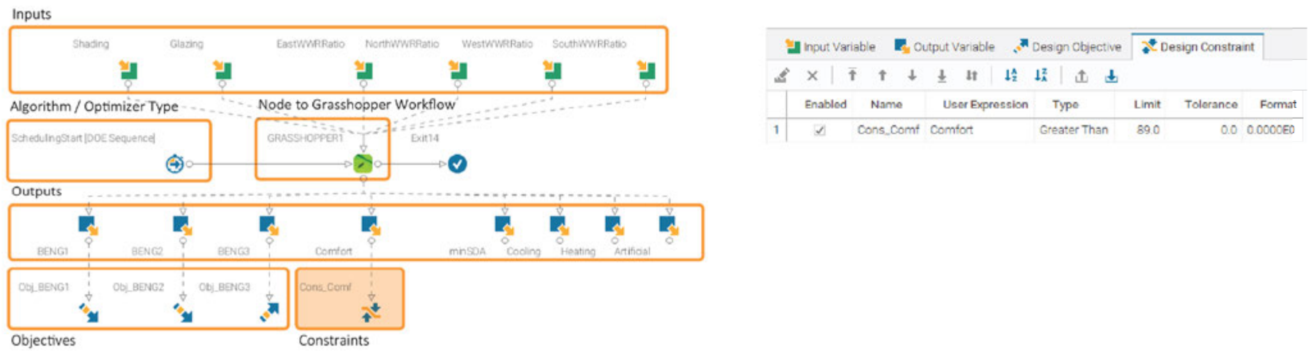

Diagram 6 *Constraints setting in the ModeFrontier workflow*

ID	Zone	Floor	BENG1	BENG2	BENG3	Comfort	Cooling	Heating	Artificial	minSDA
0	Zone1	2.0000E0	2.9460E1	3.1390E1	4.4700E1	8.5460E1	7.2000E-1	2.8800E1	9.9300E0	2.0620E1
1	Zone1	4.0000E0	3.2900E1	3.7830E1	4.2980E1	8.9270E1	7.6000E-1	3.2520E1	9.9300E0	2.0620E1
2	Zone1	6.0000E0	3.2560E1	3.7420E1	4.0490E1	8.7470E1	1.0800E0	3.2020E1	9.9500E0	2.0620E1
3	Zone1	8.0000E0	3.2850E1	3.8010E1	4.0160E1	8.5460E1	1.0700E0	3.2310E1	9.9700E0	2.1650E1
4	Zone1	1.0000E1	3.5830E1	4.3970E1	3.9720E1	8.8230E1	1.1000E0	3.5280E1	9.9300E0	2.0620E1
5	Zone1	1.2000E1	3.6980E1	4.4760E1	3.9780E1	8.6720E1	1.0500E0	3.5300E1	9.9500E0	2.1650E1
6	Zone2	1.4000E1	3.5490E1	4.3420E1	3.7830E1	8.6190E1	1.2000E0	3.4890E1	9.9500E0	2.0770E1
7	Zone2	1.6000E1	3.8400E1	4.9250E1	3.5870E1	8.7830E1	1.2000E0	3.7800E1	9.9500E0	2.0880E1
8	Zone2	1.8000E1	4.1610E1	5.5720E1	3.4360E1	8.6750E1	1.1200E0	4.1050E1	9.9300E0	2.0960E1
9	Zone2	2.0000E1	4.3990E1	6.0290E1	3.3310E1	8.6500E1	1.1000E0	4.3430E1	9.9500E0	2.0960E1
10	Zone2	2.2000E1	4.4350E1	6.1010E1	3.2560E1	8.6740E1	1.1000E0	4.3800E1	9.9400E0	2.0620E1
11	Zone2	2.4000E1	4.4730E1	6.1790E1	3.2560E1	8.7050E1	1.0700E0	4.4200E1	9.9500E0	2.1090E1
12	Zone3	2.6000E1	4.5740E1	6.3740E1	3.1740E1	8.7700E1	1.0400E0	4.5220E1	9.9400E0	2.0830E1
13	Zone3	2.8000E1	4.6890E1	6.6080E1	3.1950E1	8.6670E1	1.0700E0	4.6350E1	9.9600E0	2.1030E1
14	Zone3	3.0000E1	4.6610E1	6.5490E1	3.1280E1	8.7360E1	1.0400E0	4.6090E1	9.9400E0	2.0880E1
15	Zone3	3.2000E1	4.6650E1	6.5590E1	3.1100E1	8.7080E1	1.0900E0	4.6100E1	9.9400E0	2.0620E1
16	Zone3	3.4000E1	4.7410E1	6.7080E1	3.1290E1	8.7640E1	1.0400E0	4.6880E1	9.9400E0	2.0620E1
17	Zone3	3.6000E1	4.7590E1	6.7410E1	3.1110E1	8.7480E1	1.0200E0	4.7070E1	9.9400E0	2.0620E1
18	Zone4	3.8000E1	4.7860E1	6.7980E1	3.1120E1	8.7420E1	1.0400E0	4.7340E1	9.7900E0	2.5620E1
19	Zone4	4.0000E1	4.6070E1	6.4400E1	3.1720E1	8.7740E1	1.0400E0	4.5550E1	9.7800E0	2.5470E1
20	Zone4	4.2000E1	4.6170E1	6.4610E1	3.1550E1	8.7660E1	1.0400E0	4.5650E1	9.7600E0	2.5140E1
21	Zone4	4.4000E1	4.5410E1	6.3110E1	3.1770E1	8.7390E1	1.0400E0	4.4890E1	9.7600E0	2.5120E1
22	Zone4	4.6000E1	4.5820E1	6.3890E1	3.1520E1	8.7130E1	1.0400E0	4.5300E1	9.7500E0	2.4970E1
23	Zone4	4.8000E1	4.8620E1	6.9440E1	3.1490E1	8.7310E1	1.0000E0	4.8120E1	9.7300E0	2.4580E1

Table 5 *Results of phase 5, for the increment of height with floor addition, regarding the BENG indicators, the cooling and heating loads and the comfort level*

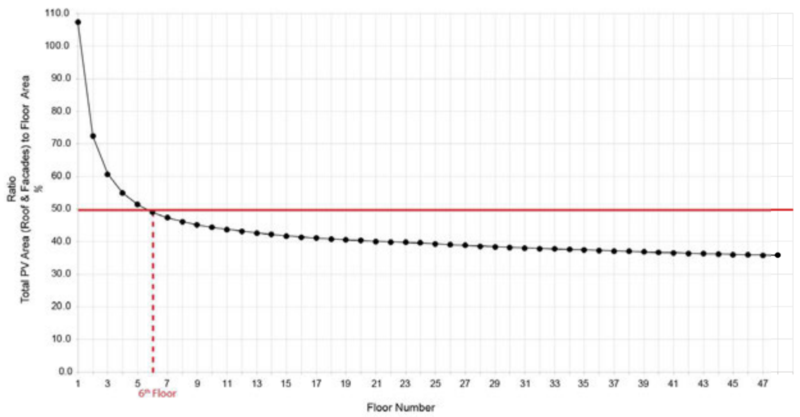

Graph 13 *Relationship between the gradual floor increment of the high-rise and the ratio of the total area of PV on the roof and facade to the total usable floor area*

	Number of Floor	Height of Floor (m)	Total Floor Area (m2)	Total PV Area Façade (m2)	PV Area Roof + Façade (m2)	Ratio Roof to Floor Area (%)	BENG 3	BENG Limit
Zone 1	1	3.3	698	260.9	749.5	107.38		
	2	6.6	1396	521.8	1010.4	72.38	44.7	
	3	9.9	2094	782.8	1271.4	60.72		
	4	13.2	2792	1043.7	1532.3	54.88	43.0	
	5	16.5	3490	1304.6	1793.2	51.38		
	6	19.80	4188.00	1565.55	2054.15	49.05	40.5	
	7	23.1	4886	1826.5	2315.1	47.38		
	8	**26.4**	**5584**	**2087.4**	**2576.0**	**46.13**	**40.16**	**BENG 3 Limitation**
	9	29.7	6282	2348.3	2836.9	45.16		
	10	33	6980	2609.2	3097.8	44.38	39.7	
	11	36.3	7678	2870.2	3358.8	43.75		
	12	39.6	8376	3131.1	3619.7	43.22	39.8	
Zone 2	13	42.9	9074	3382.5	3871.1	42.66		
	14	46.2	9772	3633.9	4122.5	42.19	37.8	
	15	49.5	10470	3885.3	4373.9	41.78		
	16	52.8	11168	4136.6	4625.2	41.42	35.9	
	17	56.1	11866	4388.0	4876.6	41.10		
	18	59.4	12564	4639.4	5128.0	40.82	34.4	
	19	62.7	13262	4890.8	5379.4	40.56		
	20	66	13960	5142.2	5630.8	40.34	33.3	
	21	69.3	14658	5393.6	5882.2	40.13		
	22	72.6	15356	5645.0	6133.6	39.94	32.6	
	23	75.9	16054	5896.4	6385.0	39.77		
	24	79.2	16752	6147.7	6636.3	39.62	32.6	
Zone 3	25	82.5	17450	6376.8	6865.4	39.34		
	26	85.8	18148	6605.9	7094.5	39.09	31.7	
	27	89.1	18846	6835.0	7323.6	38.86		
	28	92.4	19544	7064.0	7552.6	38.64	32.0	
	29	95.7	20242	7293.1	7781.7	38.44		
	30	99	20940	7522.2	8010.8	38.26	31.3	
	31	102.3	21638	7751.3	8239.9	38.08		
	32	105.6	22336	7980.3	8468.9	37.92	31.1	
	33	108.9	23034	8209.4	8698.0	37.76		
	34	112.2	23732	8438.5	8927.1	37.62	31.29	
	35	115.5	24430	8667.5	9156.1	37.48		
	36	118.8	25128	8896.6	9385.2	37.35	31.1	
Zone 4	37	122.1	25826	9113.0	9601.6	37.18		
	38	125.4	26524	9329.4	9818.0	37.02	31.1	
	39	128.7	27222	9545.8	10034.4	36.86		
	40	132	27920	9762.2	10250.8	36.71	31.7	
	41	135.3	28618	9978.6	10467.2	36.58		
	42	138.6	29316	10194.9	10683.5	36.44	31.6	
	43	141.9	30014	10411.3	10899.9	36.32		
	44	145.2	30712	10627.7	11116.3	36.20	31.8	
	45	148.5	31410	10844.1	11332.7	36.08		
	46	151.8	32108	11060.5	11549.1	35.97	31.5	
	47	155.1	32806	11276.9	11765.5	35.86		
	48	158.4	33504	11493.3	11981.9	35.76	31.5	

Table 6 *Data for the ratio of the total PV area to the total floor area, regarding BENG 3 indicator*

Floors	Ag Usable Floor Area m2	Als Loss Surface Area (including Roof) m2	Als / Ag (including Roof)
1	698	1048	1.50
2	1396	1398	1.00
3	2094	1748	0.83
4	2792	2098	0.75
5	3490	2448	0.70
6	4188	2798	0.67
7	4886	3148	0.64
8	5584	3498	0.63
9	6282	3848	0.61
10	6980	4198	0.60
11	7678	4548	0.59
12	8376	4898	0.58
13	9074	5248	0.58
14	9772	5598	0.57
15	10470	5948	0.57
16	11168	6298	0.56
17	11866	6648	0.56
18	12564	6998	0.56
19	13262	7348	0.55
20	13960	7698	0.55
21	14658	8048	0.55
22	15356	8398	0.55
23	16054	8748	0.54
24	16752	9098	0.54
25	17450	9448	0.54
26	18148	9798	0.54
27	18846	10148	0.54
28	19544	10498	0.54
29	20242	10848	0.54
30	20940	11198	0.53
31	21638	11548	0.53
32	22336	11898	0.53
33	23034	12248	0.53
34	23732	12598	0.53
35	24430	12948	0.53
36	25128	13298	0.53
37	25826	13648	0.53
38	26524	13998	0.53
39	27222	14348	0.53
40	27920	14698	0.53
41	28618	15048	0.53
42	29316	15398	0.53
43	30014	15748	0.52
44	30712	16098	0.52
45	31410	16448	0.52
46	32108	16798	0.52
47	32806	17148	0.52
48	33504	17498	0.52

Table 7 *Calculation of the ratio Als/Ag for the total height of the building*

Floor	Height	Als Loss Surface Area (including Roof) m2	Volume m3	Volume / Als	Volume / Als Absolute Difference between consecutive floors
1	3.3	1048	2303	2.20	
2	6.6	1398	4607	3.30	1.10
3	9.9	1748	6910	3.95	0.66
4	13.2	2098	9214	4.39	0.44
5	16.5	2448	11517	4.70	0.31
6	19.8	2798	13820	4.94	0.23
7	23.1	3148	16124	5.12	0.18
8	26.4	3498	18427	5.27	0.15
9	29.7	3848	20731	5.39	0.12
10	33	4198	23034	5.49	0.10
11	36.3	4548	25337	5.57	0.08
12	39.6	4898	27641	5.64	0.07
13	42.9	5248	29944	5.71	0.06
14	46.2	5598	32248	5.76	0.05
15	49.5	5948	34551	5.81	0.05
16	52.8	6298	36854	5.85	0.04
17	56.1	6648	39158	5.89	0.04
18	59.4	6998	41461	5.92	0.03
19	62.7	7348	43765	5.96	0.03
20	66	7698	46068	5.98	0.03
21	69.3	8048	48371	6.01	0.03
22	72.6	8398	50675	6.03	0.02
23	75.9	8748	52978	6.06	0.02
24	79.2	9098	55282	6.08	0.02
25	82.5	9448	57585	6.09	0.02
26	85.8	9798	59888	6.11	0.02
27	89.1	10148	62192	6.13	0.02
28	92.4	10498	64495	6.14	0.02
29	95.7	10848	66799	6.16	0.01
30	99	11198	69102	6.17	0.01
31	102.3	11548	71405	6.18	0.01
32	105.6	11898	73709	6.20	0.01
33	108.9	12248	76012	6.21	0.01
34	112.2	12598	78316	6.22	0.01
35	115.5	12948	80619	6.23	0.01
36	118.8	13298	82922	6.24	0.01
37	122.1	13648	85226	6.24	0.01
38	125.4	13998	87529	6.25	0.01
39	128.7	14348	89833	6.26	0.01
40	132	14698	92136	6.27	0.01
41	135.3	15048	94439	6.28	0.01
42	138.6	15398	96743	6.28	0.01
43	141.9	15748	99046	6.29	0.01
44	145.2	16098	101350	6.30	0.01
45	148.5	16448	103653	6.30	0.01
46	151.8	16798	105956	6.31	0.01
47	155.1	17148	108260	6.31	0.01
48	158.4	17498	110563	6.32	0.01

Table 8 *Calculation of the ratio Volume/Als for the total height of the building*

Appendix G *Results Validation of Phase 1*

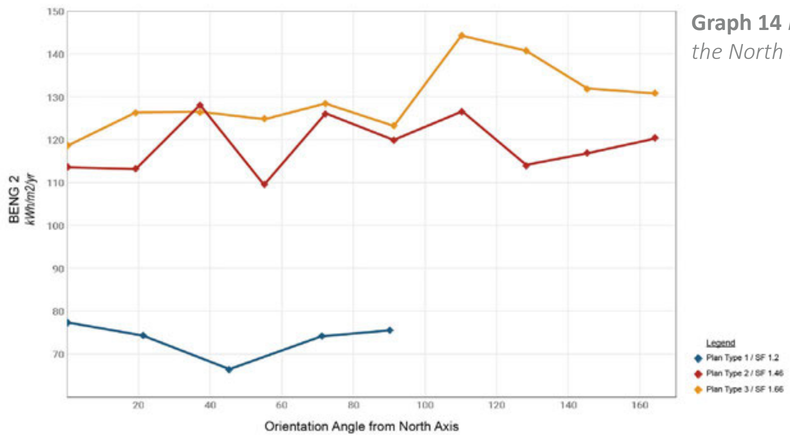

Graph 14 *Results of BENG 2 regarding the orientation angle from the North axis for the 3 types of plan*

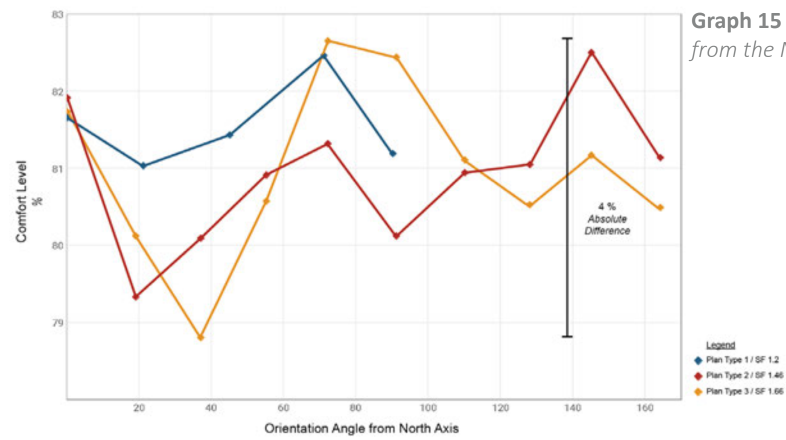

Graph 15 *Results of comfort level regarding the orientation angle from the North axis for the 3 types of plan*

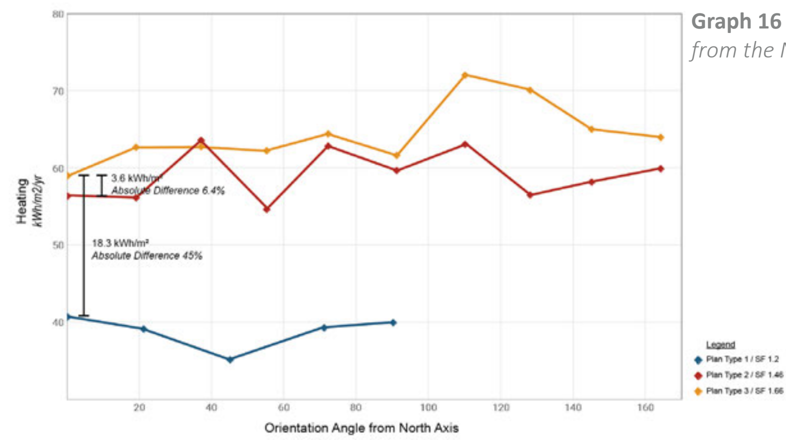

Graph 16 *Results of heating loads regarding the orientation angle from the North axis for the 3 types of plan*

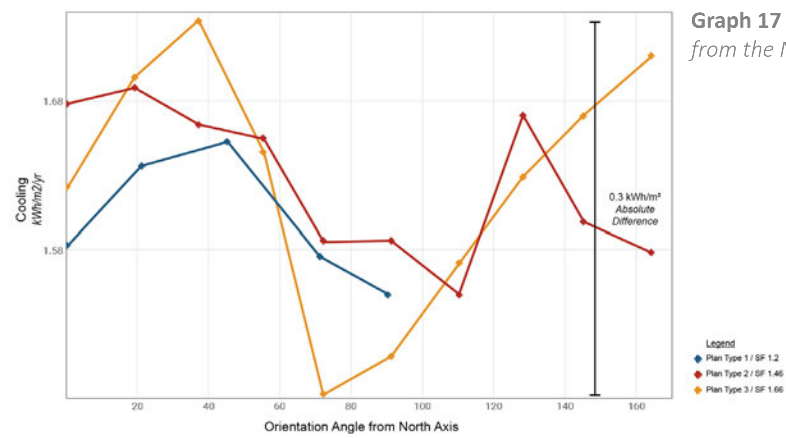

Graph 17 *Results of cooling loads regarding the orientation angle from the North axis for the 3 types of plan*

Appendix H *Context Location*

Figure 1 *Screenshot of the used site location from the city of Rotterdam (source: Google Maps, 2020)*

Appendix I *Research Variables Matrix*

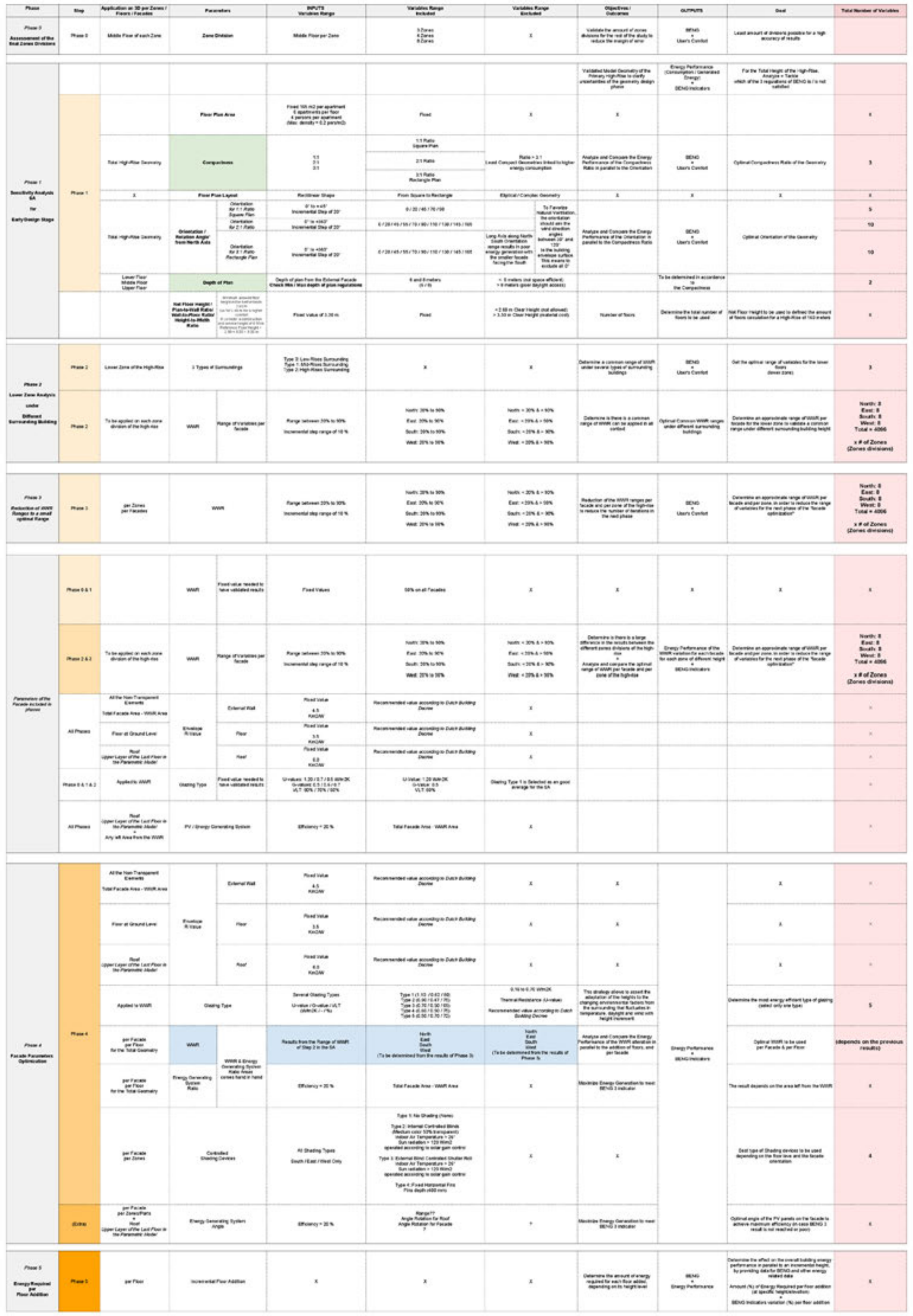

Table 9 *Table of the steps for the processing of the research detailed by its inputs parameters, variables, goals and outcomes*